The strong N–H acid
bis[bis(pentafluoroethyl)phosphinyl]imide,
$H[\{(C_2F_5)_2P(O)\}_2N]$
Salts and ionic liquids

Thesis submitted to the Faculty of Mathematics and Natural Sciences
Bergische Universität Wuppertal
for the Degree of Doctor of Natural Sciences
– Dr. rerum naturalium –

by

Dana Bejan

November, 2010

Die Dissertation kann wie folgt zitiert werden:

urn:nbn:de:hbz:468-20111129-145657-9
[http://nbn-resolving.de/urn/resolver.pl?urn=urn%3Anbn%3Ade%3Ahbz%3A468-20111129-145657-9]

The work described in this thesis was carried out in the Department of Inorganic Chemistry, University of Wuppertal, under the scientific supervision of Prof. Dr. H. Willner, during the period of February 2006 – November 2010.

Referee:	Prof. Dr. H. Willner
Co-referee:	Prof. Dr. F. Mohr

Cu dragoste, soțului meu
şi
părinților mei

I would like to express my sincere gratitude to Prof. Dr. Helge Willner for the opportunity of doing this PhD in his research group and for his continuous guidance and fruitful advices. I will always be indebted to him for the rigorous guidance into the science.

I am also deeply grateful to Dr. Nikolai Ignat'ev for his helpful assistance and his insight to resolve problems during all the stages of the research.

Furthermore, I thank Prof. Dr. Fabian Mohr for evaluating my thesis as co-referee as well as Prof. Dr. Hans-Josef Altenbach and Prof. Dr. Michael W. Tausch for their acceptance as members of my thesis examination committee.

A special recognition to Priv.-Doz. Dr. Eduard Bernardt and Prof. Dr. Christian W. Lehmann for X-ray structural determinations included in my thesis. All thanks to Prof. Dr. Eujen Reint and Priv.-Doz. Dr. Helmut Beckers for fruitful discussions and suggestions.

Dr. Andriy Kucheryna is acknowledged for his help at begin of my research work.

I am very thankful to Dr. Jane Hübner for part of analytical measurements, to Mrs. Anja Amman for the conductivity and the cyclic voltammetry measurements, to Dr. Peter Barthen for the elemental analysis, to Mr. Andreas Siebert for NMR and to Mrs. Melanie Dausend for MS measurements.

My special thanks to Mrs. Marion Litz and Dipl. Ing. Erwin Petrauskas for their help for solving administrative and technical problems.

The present and past colleagues (André, Markus, Xiaoqing, Lücker, Waldemar, Simone, Torsten, Tamara) are special in my heart for their friendship and assistance. I thank all the members of Departament of Inorganic Chemistry for the support.

The financial support of the Merck KGaA is gratefully acknowledged.

My deepest gratitude goes to my family for their support throughout my life.

I owe my loving thanks to my husband Iustinian. Without his love, encouragement and understanding it would have been imposibble for me to finish this work.

Abstract

This work was developed in the course of a cooperation project with the Merck KGaA Company (Darmstadt) on weakly coordinating anions and their applications. The main target was the preparation of the new strong N-H acids bis[bis(perfluoroalkyl)-phosphinyl]imides (HFPI), bis(pentafluoroethyl)phosphinyl–(trifluoromethyl)sulfonyl-imide (HPSI), their salts and ionic liquids as well as the study of their catalytic properties. Most of the compounds were analysed by NMR, IR and Raman spectroscopy, mass spectrometry and elemental analysis and in some cases by single crystal X-ray diffraction. The new ionic liquids were characterized by measuring their viscosity, density, melting point, thermal properties, electrochemical stability, conductivity, water and ionic impurities.

The first chapter describes improved syntheses of the precursors of HFPI. By selective hydrolysing $(C_nF_{2n+1})_3PF_2$ (n = 2, 4) pure bis(perfluoroalkyl)phosphinic, $(C_nF_{2n+1})_2P(O)OH$, and perfluoroalkylphosphonic, $C_nF_{2n+1}P(O)(OH)_2$, acids have been obtained. $PhPCl_4$ was found to be a suitable reagent to convert the acids into acid chlorides.

In chapter 2 formation of $(C_2F_5)_2P(O)NH_2$ by treatment of $(C_2F_5)_3PO$ with NH_3 at low temperature is described. Both precursors $(C_2F_5)_2P(O)Cl$ and $(C_2F_5)_2P(O)NH_2$ were reacted in the presence of Et_3N to form the salt $[Et_3NH][\{(C_2F_5)_2P(O)\}_2N]$. The free acid was obtained by heating the salt in 100 % H_2SO_4 in vacuum. Its acidity was determined by different methods.

In chapter 3 the preparation of new MFPI salts (M = Li, Na, K, Cs, Ag, Mg, Zn, La, Eu, Ce, and Yb) is described. LiFPI can be used as an electrolyte for lithium ion batteries. One important application of lanthanide salts are their use as Lewis acid catalysts.

HFPI and the Na and K salts are suitable starting materials for the synthesis of new hydrophobic ionic liquids with the FPI anion as described in chapter 4. Relationships between their physico-chemical properties and their structures are discussed. FPI ionic liquids possess advanced properties such as: (i) melting points below 50 °C; (ii) hydrolytic stability in neutral aqueous solution up to 100 °C; (iii) thermal stability up to 280 °C; (iv) low viscosity; (v) high electrochemical stability; and (vi) they can be synthesized from industrially available materials.

In the fifth chapter another strong N–H acid (HPSI) and new ionic liquids with the PSI anion are presented. The properties of a series of ionic liquids with asymmetrical perfluoroanions, such as PSI anion, are reported here. The asymmetric species have significant lower melting points than the corresponding symmetric ionic liquids. Further properties of these PSI derivatives were also investigated and compared with related FPI and TFSI derivatives. Furthermore, [Et_3NH][PSI] was characterized by X-ray crystallography.

The catalytic activity of the HFPI acid and some of its salts were investigated for acylation reactions of various compounds (with –OH, –NH, –SH functional groups) and the results are shown in chapter 6.

Finally, the last chapter presents the synthesis and characterization of new bis(pentafluoroethyl)phosphinic acid amides and hydrazides.

Zusammenfassung

Die vorliegende Arbeit entstand im Rahmen eines Kooperationsprojekts mit der Firma Merck KGaA (Darmstadt) über schwach koordinierende Anionen und ihre Anwendungen. Das wichtigste Ziel bestand in der Synthese der starken N-H Brønsted Säuren Bis[bis(perfluoralkyl)-phosphinyl]imid (HFPI), Bis(pentafluorethyl)phosphinyl–(trifluormethyl)sulfonyl-imid (HPSI), ihrer Salze und ionischen Flüssigkeiten wie auch das Studium ihrer katalytischen Eigenschaften. Die meisten der synthetisierten Verbindungen wurden durch NMR, IR und Raman Spektroskopie, Massenspektrometrie, Elementaranalysen, und in einigen Fällen auch durch Einkristallstrukturanalysen untersucht. Die neuen ionischen Flüssigkeiten wurden durch Messung ihrer Viskosität, Dichte, Schmelzpunkte, thermischen Eigenschaften, elektrochemischen Stabilitäten, Leitfähigkeit und ihres Wasser- und Fremdionen-Gehalts charakterisiert.

Im ersten Kapitel sind die Synthesen der Ausgangsverbindungen für die HFPI Herstellung beschrieben. Durch selektive Hydrolyse von $(C_nF_{2n+1})_3PF_2$ (n = 2, 4) konnten die reinen Bis(perfluoroalkyl)phosphin-, $(C_nF_{2n+1})_2P(O)OH$, und Perfluoralkylphosphon-Säuren, $C_nF_{2n+1}P(O)(OH)_2$, erhalten werden. $PhPCl_4$ erwies sich als nützliches Reagenz, um die Säuren in Säurechloride zu überführen.

In Kapitel 2 ist die Bildung von $(C_2F_5)_2P(O)NH_2$ durch Umsetzung von $(C_2F_5)_3PO$ mit NH_3 bei tiefen Temperaturen beschrieben. Beide Vorläufer $(C_2F_5)_2P(O)Cl$ und $(C_2F_5)_2P(O)NH_2$ ließen sich in Gegenwart von Et_3N zum Salz $[Et_3NH][\{(C_2F_5)_2P(O)\}_2N]$ verknüpfen. Die freie Säure konnte schließlich durch Erhitzen des Salzes in 100 % H_2SO_4 im Vakuum erhalten werden. Ihre Säurestärke ließ sich mit verschiedenen Methoden ermitteln.

In Kapitel 3 werden die neuen MFPI Salze (M = Li, Na, K, Cs, Ag, Mg, Zn, La, Eu, Ce, und Yb) beschrieben. LiFPI kann für Elektrolyte in Lithiumionen Batterien verwendet werden. Eine wichtige Anwendung der Lanthanoid Salze besteht in ihrer katalytischen Aktivität.

HFPI und die Na und K Salze sind nützliche Ausgangs-materialien für die Synthese von neuen hydrophoben ionischen Flüssigkeiten mit dem FPI Anion wie in Kapitel 4 beschrieben. Beziehungen zwischen ihren physikalisch-chemischen Eigenschaften und ihren Strukturen werden diskutiert. FPI ionische Flüssigkeiten besitzen fortschrittliche Eigenschaften wie: (i) Schmelzpunkte unter 50 °C; (ii)

hydrolytische Stabilität in neutraler wässeriger Lösung bis 100 °C; (iii) thermische Stabilität bis 280 °C; (iv) niedrige Viskosität; (v) hohe elektrochemische Stabilität; und (vi) sie lassen sich aus industriell verfügbaren Ausgangsmaterialien herstellen.

Im fünften Kapitel wird eine andere starke N–H Säure (HPSI) und ihre ionischen Flüssigkeiten vorgestellt. Über die Eigenschaften einer Serie ionischer Flüssigkeiten mit asymmetrischen Perfluoranionen, wie das PSI Anion, wird berichtet. Sie weisen signifikant niedrigere Schmelzpunkte auf als die entsprechenden symmetrischen ionischen Flüssigkeiten. Zudem wurden Eigenschaften dieser PSI Derivate untersucht und mit verwandten FPI und TFSI Derivaten verglichen. Weiterhin wurde $[Et_3NH][PSI]$ auch durch Röntgenstrahlbeugung am Einkristall charakterisiert.

In Kapitel 6 wird die katalytische Aktivität der HFPI Säure und einiger ihrer Salze für Acylierungsreaktionen an verschiedenen Verbindungen (mit –OH, –NH, –SH funktionellen Gruppen) beschrieben.

Schließlich wird im letzten Kapitel die Synthese und Charakterisierung von neuen Bis(pentafluorethyl)phoshin-Säure-amiden und -hydraziden behandelt.

Content

Compounds synthesized in this thesis

Compound name, formula, abbreviation (number)

Chapter 1:

Bis(pentafluoroethyl)phosphinic acid, $(C_2F_5)_2P(O)OH$ (**1a)**
Calcium bis(pentafluoroethyl)phosphinate dihydrate, $Ca[(C_2F_5)_2PO_2]_2\cdot 2H_2O$ (**2a**)
Bis(nonafluorobutyl)phosphinic acid, $(C_4F_9)_2P(O)OH$ (**3a**)
Oxonium bis(nonafluorobutyl)phosphinate, $[H_3O][(C_4F_9)_2PO_2]$ (**4a**)
Pentafluoroethylphosphonic acid, $C_2F_5P(O)(OH)_2$ (**5a**)
Nonafluorobutylphosphonic acid, $C_4F_9P(O)(OH)_2$ (**6a**)
Phenyltetrachlorophosphorane, $PhPCl_4$ (**7a**)
Bis(pentafluoroethyl)phosphinic acid chloride, $(C_2F_5)_2P(O)Cl$ (**8a**)
Bis(nonafluorobutyl)phosphinic acid chloride, $(C_4F_9)_2P(O)Cl$ (**9a**)
Pentafluoroethylphosphonic acid dichloride, $C_2F_5P(O)Cl_2$ (**10a**)
Nonafluorobutylphosphonic acid dichloride, $C_4F_9P(O)Cl_2$ (**11a**)

Chapter 2:

Bis(pentafluoroethyl)phosphinyl amide, $(C_2F_5)_2P(O)NH_2$ (**1b**)
Ammonium bis[bis(pentafluoroethyl)phosphinyl]imide, $[NH_4][\{(C_2F_5)_2P(O)\}_2N]$ (**2b**)
Ammonium bis(pentafluoroethyl)phosphinate $[NH_4][(C_2F_5)_2PO_2]$ (**3b**)
Pentafluoroethylphosphonic diamide, $C_2F_5P(O)(NH_2)_2$ (**4b**)
Triethylammonium bis[bis(pentafluoroethyl)phosphinyl]imide, $[Et_3NH][\{(C_2F_5)_2P(O)\}_2N]$ (**5b**)
Bis[bis(pentafluoroethyl)phosphinyl]imide, HFPI (**6b**)
N-(trimethyl-silyl) bis(pentafluoroethyl)phosphinyl amide, $(C_2F_5)_2P(O)NHSiMe_3$ **(7b)**
Mesityl oxide, $Me_2CCHC(O)Me$ (**8b**)

Chapter 3:

Lithium bis[bis(pentafluoroethyl)phosphinyl]imide, Li FPI (**1c**)
Sodium bis[bis(pentafluoroethyl)phosphinyl]imide, NaFPI (**2c**)
Potassium bis[bis(pentafluoroethyl)phosphinyl]imide, KFPI (**3c**)
Cesium bis[bis(pentafluoroethyl)phosphinyl]imide, CsFPI (**4c)**
Silver bis[bis(pentafluoroethyl)phosphinyl]imide, AgFPI (**5c**)
Magnesium bis[bis(pentafluoroethyl)phosphinyl]imide, $Mg(FPI)_2$ (**6c**)
Zinc bis[bis(pentafluoroethyl)phosphinyl]imide, $Zn(FPI)_2$ (**7c**)
Lanthanum bis[bis(pentafluoroethyl)phosphinyl]imide, $La(FPI)_3$ (**8c**)
Cerium bis[bis(pentafluoroethyl)phosphinyl]imide, $Ce(FPI)_3$ (**9c**)

Europium bis[bis(pentafluoroethyl)phosphinyl]imide, Eu(FPI)$_3$ (**10c**)
Ytterbium bis[bis(pentafluoroethyl)phosphinyl]imide, Yb(FPI)$_3$ (**11c**)

Chapter 4:

1-Ethyl-3-methylimidazolium bis[bis(pentafluoroethyl)phosphinyl]imide, [emim]FPI (**1d**)
1-Butyl-3-methylimidazolium bis[bis(pentafluoroethyl)phosphinyl]imide, [bmim]FPI (**2d**)
1-Hexyl-3-methylimidazolium bis[bis(pentafluoroethyl)phosphinyl]imide, [hmim]FPI (**3d**)
1-Decyl-3-methylimidazolium bis[bis(pentafluoroethyl)phosphinyl]imide, [dmim]FPI (**4d**)
1-Octadecyl-3-methylimidazolim bis[bis(pentafluoroethyl)phosphinyl]imide, [omim]FPI (**5d**)
1-Allyl-3-methylimidazolium bromide, [allylmim]Br (**6d**)
1-Allyl-3-methylimidazolium bis[bis(pentafluoroethyl)phosphinyl]imide, [allylmim]FPI (**7d)**
1-*n*-Butyl-2,3-dimethylimidazolium bis[bis(pentafluoroethyl)phosphinyl]imide, [C_4dmim]FPI (**8d**)
1-*n*-Butylpyridinium bis[bis(pentafluoroethyl)phosphinyl]imide, [C_4Py]FPI (**9d**)
1-*n*-Butyl-3,5-dimethylpyridinium bis[bis(pentafluoroethyl)phosphinyl]imide, [C_4dmPy]FPI (**10d**)
Tetramethyl ammonium bis[bis(pentafluoroethyl)phosphinyl]imide, [Me_4N]FPI (**11d**)
Tetraethyl ammonium bis[bis(pentafluoroethyl)phosphinyl]imide, [Et_4N]FPI (**12d**)
Tetra(*n*-butyl)ammonium bis[bis(pentafluoroethyl)phosphinyl]imide, [Bu_4N]FPI (**13d**)
1-*n*-Butyl-1-methylpyrrolidinium bis[bis(pentafluoroethyl)phosphinyl]imide, [bmpl]FPI (**14d**)
N-(2-hydroxyethyl)-N-methylpyrrolidinium bis[bis(pentafluoroethyl)phosphinyl]imide, [$HOCH_2CH_2$pyrr]FPI (**15d**)
N-(3-ethoxy-3-oxopropyl)-N-methylpyrrolidinium bis[bis(pentafluoroethyl)phosphinyl]imide, [$C_{10}H_{20}NO_2$]FPI (**16d**)
Guanidinium bis[bis(pentafluoroethyl)phosphinyl]imide, [$C(NH_2)_3$]FPI (**17d**)
Tetra(*n*-butyl)phosphonium bis[bis(pentafluoroethyl)phosphinyl]imide, [Bu_4P]FPI (**18d**)
Benzyl(triphenyl)phosphonium bis[bis(pentafluoroethyl)phosphinyl]imide, [$(C_6H_5)_3P(CH_2C_6H_5)$]FPI (**19d**)
Trihexyl(tetradecyl)phosphonium bis[bis(pentafluoroethyl)phosphinyl]imide, [p(h3)te3]FPI (**20d**)
N-ethylbenzothiazolium bis[bis(pentafluoroethyl)phosphinyl]imide, [$(C_6H_4)SCHNC_2H_5$]FPI (**21d**)

Chapter 5:

Triethylammonium [bis(pentafluoroethyl)phosphinyl–(trifluoromethyl)sulfonyl)]imide, [Et_3NH]PSI (**1e**)
Bis[(pentafluoroethyl)phosphinyl–(trifluoromethyl)sulfonyl]imide, HPSI (**2e**)

1–Ethyl–3–methylimidazolium [bis(pentafluoroethyl)phosphinyl–(trifluoromethyl)sulfonyl)] imide, [emim]PSI (**3e**)

1–*n*–Butyl–1–methylpyrrolidinium [bis(pentafluoroethyl)phosphinyl–(trifluoromethyl)sulfonyl)] imide, [bmpl]PSI (**4e**)

Trihexyl(tetradecyl)phosphonium [bis(pentafluoroethyl)phosphinyl–(trifluoromethyl)sulfonyl)] imide, [p(h3)te3]PSI (**5e**)

Benzyl(triphenyl)phosphonium [bis(pentafluoroethyl)phosphinyl–(trifluoromethyl)sulfonyl)] imide, $[(C_6H_5)_3P(CH_2C_6H_5)]$PSI (**6e**)

Tetra(*n*–butyl)phosphonium [bis(pentafluoroethyl)phosphinyl–(trifluoromethyl)sulfonyl)]imide, $[Bu_4P]$PSI (**7e**)

Tetra(n–butyl)ammonium [bis(pentafluoroethyl)phosphinyl–(trifluoromethyl)sulfonyl)]imide, $[Bu_4N]$PSI (**8e**)

Chapter 6:

1–Naphtyl acetate (**1f**)

2–Naphtyl acetate (**2f**)

Pyrocatechol diacetate (**3f**)

4–Nitrophenol acetate (**4f)**

4–Methoxyphenyl acetate (**5f**)

N–Phenyl–acetamide (**6f**)

N–Benzyl–acetamide (**7f**)

N–Phenethyl–acetamide (**8f)**

N–(4–bromophenyl)–acetamide (**9f**)

S–Phenyl–thioacetate (**10f**)

S–Octyl–thioacetate (**11f**)

Chapter 7:

Bis(pentafluoroethyl)phosphinyl–N–(benzyl)amide, $(C_2F_5)_2P(O)NHCH_2C_6H_5$ (**1g**)

Bis(pentafluoroethyl)phosphinyl–N–(2–phenyl–ethyl)amide, $(C_2F_5)_2P(O)NH(CH_2)_2C_6H_5$ (**2g**)

Bis(pentafluoroethyl)phosphinyl–N–(2–ethylhexyl)amide, $(C_2F_5)_2P(O)NHCH_2CH(C_2H_5)(CH_2)_3CH_3$ (**3g**)

Bis(pentafluoroethyl)phosphinyl–N–(methyl)hydrazide, $(C_2F_5)_2P(O)NHNHCH_3$ (**4g**)

Bis(pentafluoroethyl)phosphinyl–N–(phenyl)hydrazide, $(C_2F_5)_2P(O)NHNHC_6H_5$ (**5g**)

Bis(pentafluoroethyl)phosphinyl–N,N–di(methyl)hydrazide, $(C_2F_5)_2P(O)NHNH(CH_3)_2$ (**6g**)

Chapter 1

1. Synthesis and characterization of precursors for the synthesis of bis[bis(pentafluoroethyl)phosphinyl]imide (FPI) derivatives

Bis(pentafluoroethyl)phosphinic acid and bis(pentafluoroethyl)phosphinic acid chloride are very attractive precursors for the synthesis of new FPI derivatives such as: HFPI , FPI salts and ionic liquids. Therefore, we were interested to develop much simpler and less expensive synthetic routes, superior to the reported ones. In this chapter, new procedures are described for the synthesis of the precursors.

1.1 Bis(perfluoroalkyl)phosphinic, $(C_nF_{2n+1})_2P(O)OH$ and perfluoroalkylphosphonic, $C_nF_{2n+1}P(O)(OH)_2$ acids

Since the first synthesis of trifluoromethylphosphonic acid, $CF_3P(O)(OH)_2$, performed by Bennett *et al.* (1954) [1], this class of compounds have gained considerable interest. There are several reports on the preparation and application of different perfluoroalkyl phosphorus compounds. Their use as surfactants [2], catalysts in organic chemistry (Chapter 7) or as components of proton–conducting membranes [3] makes them of interest from laboratory research to industrial use.

Examples of such type of derivatives are presented below.

$(C_nF_{2n+1})_2P(O)OH$	$C_nF_{2n+1}PO(OH)_2$
bis(perfluoroalkyl)phosphinic acid	perfluoroalkylphosphonic acid
n= 1, 2, 3, 4, 6, 7, 8.	

The diprotic acid, trifluoromethylphosphonic acid $CF_3P(O)(OH)_2$, was first synthesized by Bennett *et al*. (1954) via oxidative hydrolysis of CF_3PX_2 and $(CF_3)_2PX$ (X = Cl or I) or by controlled hydrolysis of $(CF_3)_3P$ followed by oxidation [1]. The monoprotic acid, $(CF_3)_2P(O)OH$ was synthesized by hydrolysis of $(CF_3)_2PCl_3$ [4] as well as by hydrolysis of $(CF_3)_3PO$ [5].

The heptafluoropropyl derivatives, $(C_3F_7)_2P(O)OH$ and $C_3F_7P(O)(OH)_2$, were synthesized by Emeleus and Smith (1959) [6]. Reaction of C_3F_7I with red phosphorous in an autoclave at 220 – 230 °C resulted in a mixture of $C_3F_7PI_2$ and $(C_3F_7)_2PI$. After trap to trap distillation, separated $(C_3F_7)_2PI$ was treated with AgCl in a sealed tube, for 11 days, yielding $(C_3F_7)_2PCl$. After chlorination, the resultant $(C_3F_7)_2PCl_3$ was hydrolyzed into the acid. These procedures are quite complex and only small quantities of $(C_3F_7)_2P(O)OH$ were obtained.

Later, $(C_4F_9)_2P(O)OH$ was synthesized near to quantitative yield by heating of $(C_4F_9)_3PO$ with water at 44 °C (equation 1.1) [7]. $(C_4F_9)_2P(O)OH$ can be further hydrolyzed to $(C_4F_9)_2P(O)OH$ at higher temperatures (150 °C) for 36 hours.

$$(C_4F_9)_3PO + H_2O \xrightarrow[36\ h]{44\ °C} (C_4F_9)_2P(O)OH + C_4F_9H\uparrow \qquad (1.1)$$

Another route to perfluoroalkylphosphonic acids (n = 2, 3, 4) is described by Kovaleva *et al*. (1989) [8]. The reaction of $(C_nF_{2n+1})_3PF_2$ with 20% aqueous NaOH solution results in the sodium salt, $Na_2[C_nF_{2n+1}PO_3]$. The free acid was isolated by treatment with concentrated HCl. The protocol describes a two steps procedure with difficulties in separation of the side product (NaCl). Recently this method was modified by using $Ba(OH)_2\cdot 8H_2O$, instead of NaOH. In that case the free acid was obtained by treatment of the reaction mixture with H_2SO_4 followed by filtration of insoluble $BaSO_4$ [9]. However, still some disadvantages as the application of toxic $Ba(OH)_2\cdot 8H_2O$ and the two step procedure make this technique not attractive.

Recently, a new synthesis of $(C_nF_{2n+1})_2P(O)OH$ (equation 1.2) was developed by hydrolysis of tris(perfluoroalkyl)trifluorophosphoric acid, $H[(C_nF_{2n+1})_3PF_3]\cdot nH_2O$

(shortly named HFAP). The two step procedure and the use of concentrated, harmful HF make the reaction not convenient [10, 11] for laboratory application.

$$\begin{aligned}(C_nF_{2n+1})_3PF_2 + 5\,H_2O + HF &\xrightarrow{\text{ice}} H[(C_nF_{2n+1})_3PF_3]\cdot 5H_2O \xrightarrow{\Delta} \\ &\xrightarrow{\Delta} (C_nF_{2n+1})_2P(O)OH + C_nF_{2n+1}H\uparrow + 3\,HF + 3\,H_2O \qquad (1.2)\end{aligned}$$

n = 2, 4.

The acids formation by hydrolysis of the corresponding anhydrides is another interesting method as presented in equation 1.3. The anhydrides were synthesised by oxidation of $(C_nF_{2n+1})_2PI$ with NO_2 [12]. Bis(perfluoroalkyl)phosphinic acids can be also obtained by hydrolysis of bis(perfluoroalkyl)phosphinyl acid chlorides (equation 1.4). In the following the different routes of bis(perfluoroalkyl)phosphinic acids formation are summarized:

$$\begin{tikzcd} 2\,(C_nF_{2n+1})_2PI + 3\,NO_2 \arrow[r, "-196\,^\circ C", "22\,^\circ C"'] & (C_nF_{2n+1})_2P(O)OP(O)(C_nF_{2n+1})_2 + I_2 + 3\,NO \arrow[d, "+\,H_2O"] \\ & 2\,(C_nF_{2n+1})_2P(O)OH \end{tikzcd} \qquad (1.3)$$

n = 6, 7, 8.

$$(C_nF_{2n+1})_2P(O)Cl + H_2O \longrightarrow (C_nF_{2n+1})_2P(O)OH + HCl \qquad (1.4)$$

Our main interest was to simplify the synthesis of the monoprotic $(C_nF_{2n+1})_2P(O)OH$ and diprotic acids $C_nF_{2n+1}PO(OH)_2$, in particular for n = 2 and 4 [13]. Finally, it was found that industrially available phosphoranes $(C_nF_{2n+1})_3PF_2$ [14] can be simply hydrolyzed in water at different temperatures, depending on the reactivity of the phosphoranes. The hydrolyses were carried out in PFA (perfluoroalkyl–perfluoralkoxycopolymer) or PTFE (polytetrafluoroethylene) flasks. The product formation was followed by NMR spectroscopy (equation 1.5).

$$(C_nF_{2n+1})_3PF_2 + 2\,H_2O \xrightarrow{\Delta} (C_nF_{2n+1})_2P(O)OH + C_nF_{2n+1}H\uparrow + 2\,HF \qquad (1.5)$$

n = 2 and 4.

This new synthesis of pure $(C_2F_5)_2P(O)OH$ (**1a**) is most convenient and can be performed in big scale. $(C_2F_5)_3PF_2$ is added to an excess of water under vigorous stirring at room temperature. The obtained mixture is then refluxed at 120 °C for 24 hours. The aqueous HF is distilled off and then acid (**1a**) is distilled at reduced pressure. Unexpectedly, after long storage of acid aqueous solution (**1a**), small crystals of $Ca[(C_2F_5)_2PO_2]_2 \cdot 2H_2O$ (**2a**) were obtained from presence of traces of Ca^{2+} ions in water. A suitable crystal of (**2a**) was subjected of X–ray diffraction investigation (Section 1.3).

The preparation of $(C_4F_9)_2P(O)OH$ acid (**3a**) requires higher reaction temperatures. $(C_4F_9)_3PF_2$ was slowly added to hot water (90 – 100 °C) and then refluxed at 120 °C. According to the ^{19}F and ^{31}P NMR spectra, the reaction was finished in one hour; despite of the longer perfluoroalkyl chain length. The aqueous HF obtained in the reaction was distilled off and the residue has been dried at reduced pressure. The acid (**3a**) is a white solid at room temperature. A suitable crystal for single crystal X–ray diffraction of the oxonium salt $[H_3O][(C_4F_9)_2PO_2]$ (**4a**) was obtained by slow crystallization from a concentrated aqueous solution of **3a** at room temperature (Section 1.3).

A mechanism for the formation of $(C_nF_{2n+1})_2P(O)OH$ is proposed in Figure 1.1. The tris(pentafluoroethyl)trifluorophosphoric acid (HFAP) is a side product and is the less reactiv. The intermediates formation was investigated by NMR spectroscopy. For example, after addition of $(C_2F_5)_3PF_2$ into hot water the molar ratio between HFAP and $(C_2F_5)_2P(O)OH$ was 2:1 and after refluxing at 120 °C for one day, the total conversion of the phosphorane was observed.

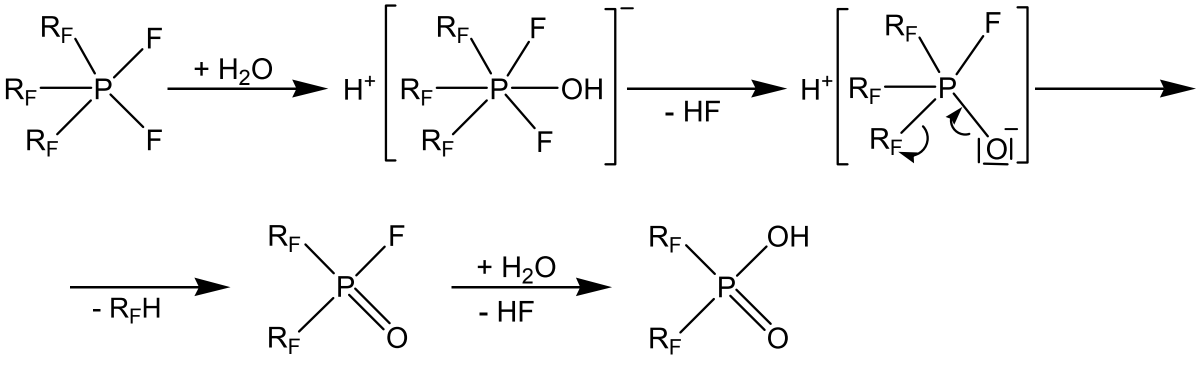

Figure 1.1 Reaction mechanism proposed for the $(C_nF_{2n+1})_2P(O)OH$ formation by hydrolysis of $(C_nF_{2n+1})_3PF_2$.

The corresponding diprotic acids were obtained via hydrolysis of tris(perfluoroalkyl)difluorophosphoranes with hot water by refluxing at high temperature (120 – 130 °C) (equation 1.6) and in longer reaction time. Different reaction times were necessary for diprotic acids formation: $C_2F_5P(O)(OH)_2$ (**5a**) – 14 days and for $C_4F_9P(O)(OH)_2$ (**6a**) – 4 days. The conversion ratio and reaction time depend on both the concentration of HF remaining in the reaction mixture and the temperature, respectively.

$$(C_nF_{2n+1})_3PF_2 + 3\ H_2O \xrightarrow{\Delta} C_nF_{2n+1}P(O)(OH)_2 + 2\ C_nF_{2n+1}H\uparrow + 2\ HF \qquad (1.6)$$

n = 2 and 4.

As example, the conversion of bis(nonafluorobutyl)phosphinic acid into nonafluorobutylphosphonic acid is shown in the ^{31}P NMR spectra in Figure 1.2. The relative signal intensities of the two phosphorous species allow the monitoring of the reaction process.

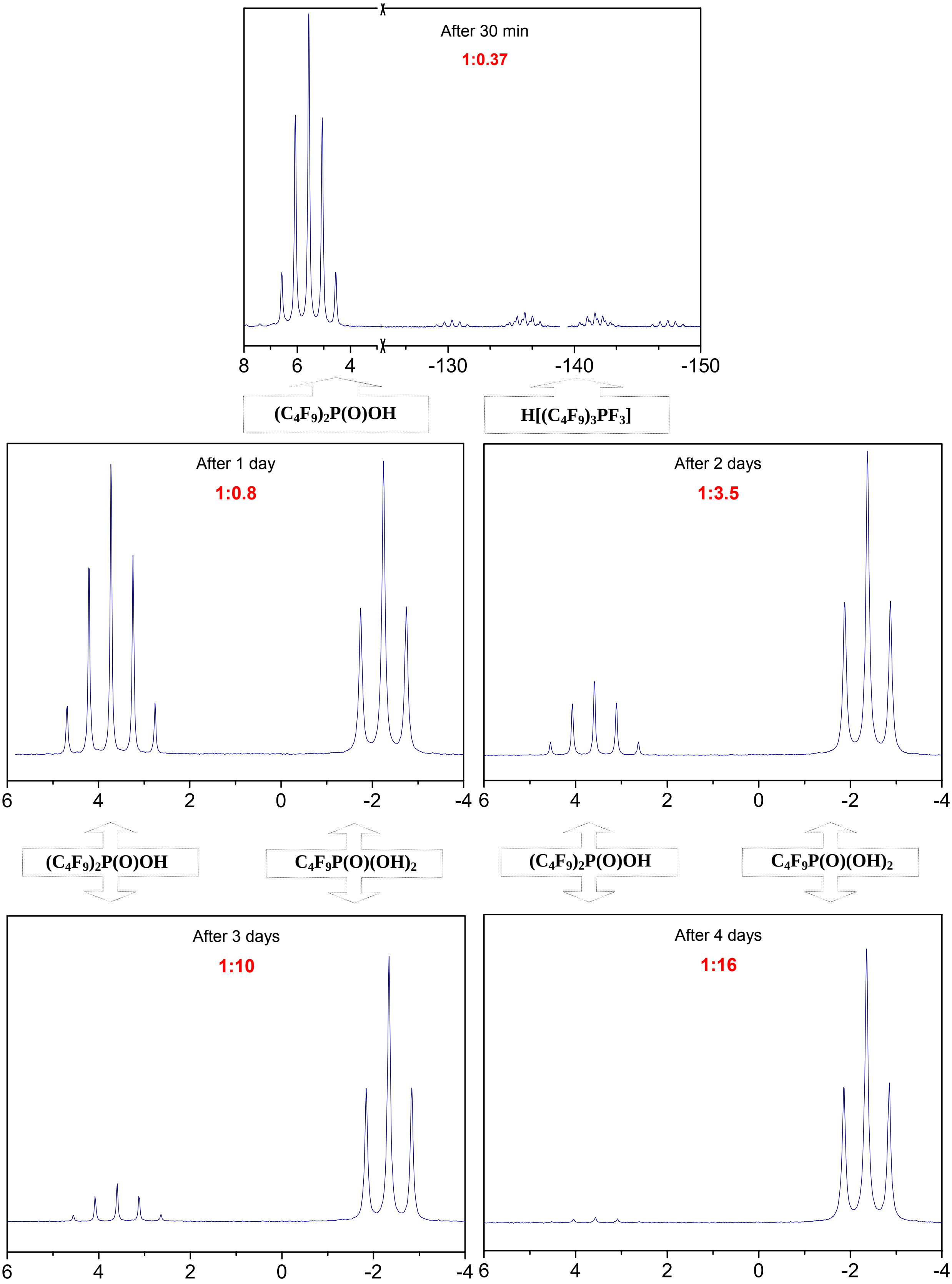

Figure 1.2 Decrease of the ^{31}P NMR signal (ppm) of $(C_4F_9)_2P(O)OH$ and increase of the ^{31}P NMR signal of $(C_4F_9)P(O)(OH)_2$ with increasing reaction time.

1.2 Bis(perfluoroalkyl)phosphinic acid chlorides, $(C_nF_{2n+1})_2P(O)Cl$ and perfluoroalkylphosphonic acid chlorides, $C_nF_{2n+1}P(O)Cl_2$

The phosphonic acid (phosphonyl) halides and phosphinic acid (phosphinyl) halides are very useful compounds. They can be applied for preparation of different types of phosphorus derivatives such as: (i) cyclic boron–phosphorus compounds, e.g. $(Ph_2P{-}BH_2)_3$ [15, 16]; (ii) tetrafluorophosphoranes, e.g. RPF_4 [16]; (iii) thiohalide, e.g. $RPSCl_2$ and (iv) P–N derivatives (e.g. phosphinic acid amides, phosphonic acid diamides, phosphinic acid hydrazides and phosphonic dihydrazides) (equation 1.7, 1.8 and 1.9) [16]. The preparation of P–N derivatives received more attention in our studies (Chapter 7).

$$Ph_2P(O)Cl + NaBH_4 \longrightarrow 1/3\,(Ph_2P{-}BH_2)_3 + NaCl + H_2O \quad (1.7)$$

$$RP(O)Cl_2 + SF_4 \longrightarrow RPF_4 + SOCl_2 \quad (1.8)$$

$$10\,RP(O)Cl_2 + P_4S_{10} \longrightarrow 10\,RPSCl_2 + P_4O_{10} \quad (1.9)$$

The synthesis of $CF_3P(O)Cl_2$ was pioneered by Griffiths (1968) [17]. Two decades later Yagupol'skii *et al.* (1984) reported the synthesis of $(C_3F_7)_2P(O)Cl$ [18]. Subsequently, Mahmmod and Shreeve (1986) described the preparation of $(C_2F_5)_2P(O)Cl$ and $C_2F_5P(O)Cl_2$ by oxidation of $(C_2F_5)_2PCl$ and $C_2F_5PCl_2$ with NO_2 according to the equation 1.10 and 1.11 [7].

$$(C_2F_5)_2PCl + NO_2 \xrightarrow{-20\ ^{\circ}C} (C_2F_5)_2P(O)Cl + NO \quad (1.10)$$

$$C_2F_5PCl_2 + NO_2 \xrightarrow{-48\ ^{\circ}C} C_2F_5P(O)Cl_2 + NO \quad (1.11)$$

A recently reported, synthesis of $(C_2F_5)_2P(O)Cl$ was based on the treatment of the corresponding acid with PCl_5 [19]. However, the small difference of the boiling points of the product and of $POCl_3$, made the purification of the acid chloride difficult. Therefore $C_6H_5PCl_4$ (**7a**) was used in the place of PCl_5, because $C_6H_5P(O)Cl_2$ has a much higher boiling point (258 °C) than $POCl_3$ (104 °C). $C_6H_5PCl_4$ is easily prepared from commercially available $C_6H_5PCl_2$ with chlorine according to the equation 1.12 [20,21,22].

$C_6H_5PCl_2 + Cl_2 \longrightarrow C_6H_5PCl_4$ (1.12)

The reactions of the acids with $C_6H_5PCl_4$ were carried out mainly at room temperature by slowly addition of the acid to $C_6H_5PCl_4$ [23]. The reaction is completed when HCl gas evolution is accomplished. $(C_nF_{2n+1})_2P(O)Cl$ and $C_nF_{2n+1}POCl_2$ (n = 4) are isolated by distillation.

$(C_nF_{2n+1})_2P(O)OH + C_6H_5PCl_4 \longrightarrow (C_nF_{2n+1})_2P(O)Cl + C_6H_5P(O)Cl_2 + HCl$ (1.13)
for n = 2, $(C_2F_5)_2P(O)Cl$ (**8a**) and for n = 4, $(C_4F_9)_2P(O)Cl$ (**9a**).

$C_nF_{2n+1}P(O)(OH)_2 + 2\ C_6H_5PCl_4 \longrightarrow$
$\longrightarrow C_nF_{2n+1}P(O)Cl_2 + 2\ C_6H_5P(O)Cl_2 + 2\ HCl$ (1.14)
for n = 2, $C_2F_5P(O)Cl_2$ (**10a**) and for n = 4, $C_4F_9P(O)Cl_2$ (**11a**).

$(C_nF_{2n+1})_2P(O)Cl$ and $C_nF_{2n+1}POCl_2$ (n = 2 and 4) are colourless liquids which can be stored without decomposition at room temperature in a glass container equipped with a Young (London) valve under an inert gas atmosphere.

1.3 Crystal structures of $Ca[(C_2F_5)_2PO_2]_2{\cdot}2H_2O$ and $[H_3O][(C_4F_9)_2PO_2]$

Crystals of $Ca[(C_2F_5)_2PO_2]_2{\cdot}2H_2O$ (**2a**) and $[H_3O][(C_4F_9)_2PO_2]$ (**4a**) suitable for X-ray diffraction were obtained from a concentrated aqueous solution at room temperature. A **Gemini E Ultra –Diffractometer** (Oxford) was used for measurements at 150 K and 140 K, respectively, with Mo–Kα radiation (λ = 0.717073 Å). The crystal structures were solved by direct methods using SHELXS–97. Full–matrix least–squares of refinement on F^2 was perfomed with WinGX V1.6405 (SHELXL–97). The hydrogen atoms were found on the difference maps and refined isotropically.

The following parameters obtained for **2a** are listed in Table 1.2 and the angles and distances in Appendix 1. Figure 1.3 shows a part of the structure within the unit cell. The Ca^{+2} ions are sixfold coordinated by oxygen atoms. Two times by water molecules (Ca–O: 2.356 Å) and four times by the bridging two dentate $[(C_2F_5)_2PO_2]^-$ anion (Ca–O: 2.290 Å). The anions are linked by the cations to infinitive chains. The anion exhibit local C_2 symmetry and the Ca^{+2} sixfold coordinated with O atoms exhibit D_2 symmetry.

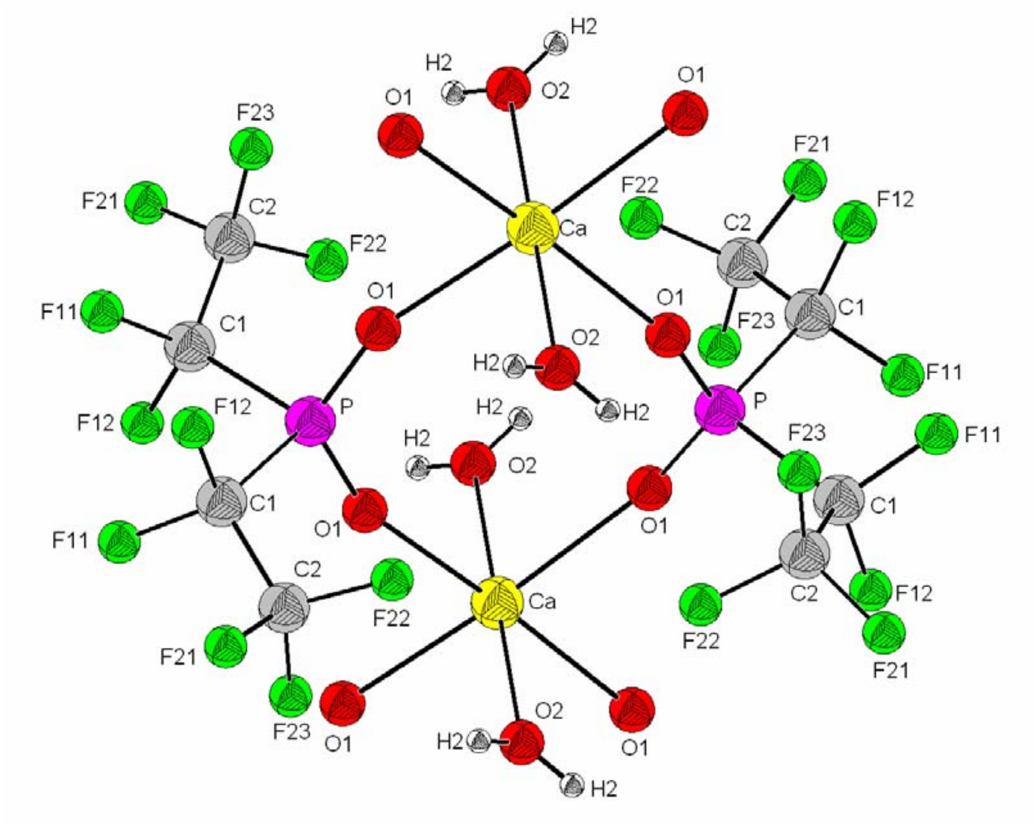

Figure 1.3 Part of the crystal structure of $Ca[(C_2F_5)_2PO_2]_2 \cdot 2H_2O$ in the solid state.

Single crystals of $[H_3O][(C_4F_9)_2PO_2]$ (**3a**) were grown by slow evaporation of a concentrated aqueous solution at room temperature. The crystal structure is stabilized by hydrogen bonds involving the $[(C_4F_9)_2PO_2]$ anions and the oxonium cations (Figure 1.4). The two O atoms of the phosphinic acid group are nearly identical, as indicated by the lengths of the bond $P–O_1$ (1.485 Å) and $P–O_2$ (1.499 Å), respectively. The P–O lengths agree within the error limits of similar bonds in phosphinate compounds P–O (1.49 Å) [24]. The P–C and C–C are typical for such reported bonds. The coordination around the P atom departs significantly from regular tetrahedral. The angels are varying from C–P–C (102.41°) to O–P–O (120.6°), that agrees well with values found in α-aminomethyl(methyl)phosphinic acid ($H_3N^+–CH_2–PCH_3O_2^-$) [25]. The hydrogen bondings between the anion and H of cation are very strong (H–O: 1.767 Å; 1.763 Å; 1.631 Å; 1.781 Å). The H atoms were refined at the same displacements and for 6 restrains of bonding lengths O–H it was find 0.85(2) Å. All angles and distances are presented in Appendix I.

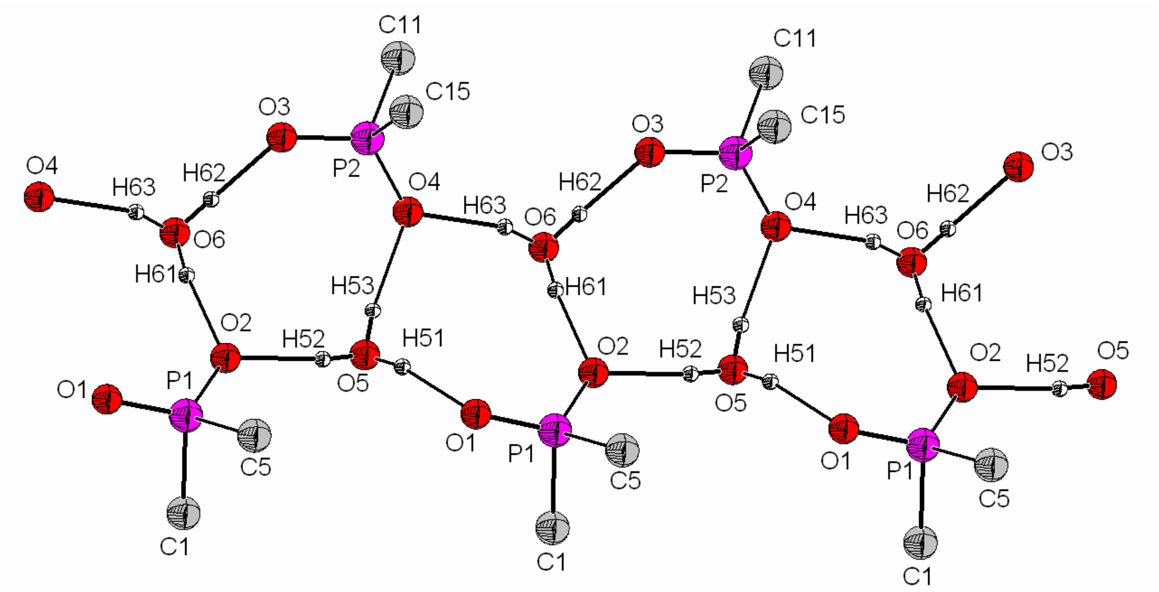

Figure 1.4 Part of the crystal structure of $[H_3O][(C_4F_9)_2PO_2]$ in the solid state and the intermolecular interaction in the crystal dominated by hydrogen bonding.

Table 1.2 Crystalographic and refinement data for (**2a**) and (**4a**).

Crystalographic data	$Ca[(C_2F_5)_2PO_2]_2 \cdot 2H_2O$ (**2a**)	$[H_3O][(C_4F_9)_2PO_2]$ (**4a**)
Empirical formula	$C_8H_4O_6F_{20}P_2Ca$	$C_8H_3O_3F_{18}P$
Colour	Colourless	Colourless
Formula weight	678.13 $g \cdot mol^{-1}$	520.05 $g \cdot mol^{-1}$
Temperature	150 K	140 K
Wavelength	0.71073 Å	0.71073 Å
Crystal system	Tetragonal	Triclinic
Space group	$P4_12_12$	P-1 (No. 2)
Unit cell dimensions	a = 13.7296(2) Å α = 90° b = 13.7296(2) Å β = 90° c = 5.74524(14) Å γ = 90°	a = 6.4447(3) Å α = 107.509° b = 13.5217(8) Å β = 92.056(4)° c = 20.0884(11) Å γ = 91.355(4)°
Volume	1082.99(4) $Å^3$	1667.30(16) $Å^3$
Z	2	4
Density (calculated)	2.080 $mg \cdot m^{-3}$	2.0 $mg \cdot m^{-3}$
Absorption coefficient	0.633 mm^{-1}	0.359 mm^{-1}
F(000)	660 e	968 e
Crystal size	0.60 x 0.15 x 0.1 mm^3	0.3 x 0.5 x 1.0 mm^3
θ range for data collection	2.97 to 29.02°	3.63 to 28.15°
Index ranges	$-17 \leq h \leq 17, -18 \leq k \leq 17, -7 \leq l \leq 7$	$--8 \leq h \leq 8, -17 \leq k \leq 17, -26 \leq l \leq 25$
Reflections collected	13976	23043
Independent reflections	1363 [R_{int} = 0.0392]	7545 [R_{int} = 0.0436]
Completeness to	(= 29.02°) 95.8 %	(= 26.4°) 99.7 %
Absorption correction	None	Numerical
Refinement method	Full–matrix least–squares on F^2	Full–matrix least–squares on F^2
Data/restraints/parameters	1363/0/91	7545/6/580
Goodness–of–fit on F^2	0.997	1.031
Final R indices [$I>2\sigma(I)$][a]	R_1 = 0.0305 wR^2 = 0.0720	R_1 = 0.0975 wR^2 = 0.2598
R indices (all data)[b]	R_1 = 0.0417 wR^2 = 0.0748	R_1 = 0.1266 wR^2 = 0.2807
Largest diff. peak and hole	0.341 and -0.254 e $Å^{-3}$	1.059 and -0.785 e $Å^{-3}$

1.4 Experimental part

Bis(pentafluoroethyl)phosphinic acid, $(C_2F_5)_2P(O)OH$ (1a)

86 g (4.78 mol) of deionized water was placed in a three–neck PFA flask equipped with a reflux condenser and a PFA funnel. Under vigorous stirring, 250 g (0.58 mol) of $(C_2F_5)_3PF_2$ was slowly added at room temperature. The resulting solution was refluxed at 120 °C (temperature in oil–bath) for 24 hours and then aqueous HF was distilled off. The residue was distilled under reduced pressure ($6\cdot10^{-1}$ mbar). 133 g of a colourless transparent liquid was obtained. Yield: 76 %. Bp: 54 – 56 °C at $6\cdot10^{-1}$ mbar (literature value: 63 – 64 °C at 1.25 mbar [10]).

NMR spectra were measured using an FEP tube with an acetonitrile–D_3 film as external lock:

^{1}H NMR (400 MHz), δ, ppm: 12.6 s (OH).

^{19}F NMR (376.4 MHz), δ, ppm: –81.9 m ($2CF_3$); –127 d ($2CF_2$); $^2J_{P,F}$ = 85 Hz.

^{31}P NMR (161.9 MHz), δ, ppm: 6.7 quin; $^2J_{P,F}$ = 84 Hz.

Calcium bis(pentafluoroethyl)phosphinate, $Ca[(C_2F_5)_2PO_2]_2\cdot2H_2O$ (2a)

^{19}F NMR (lock/solvent D_2O, 376.4 MHz), δ, ppm: –80.9 m ($4CF_3$); –126.1 d ($4CF_2$); $^2J_{P,F}$ = 76 Hz.

^{31}P NMR (lock/solvent D_2O, 161.9 MHz), δ, ppm: 3.4 quin (2P); $^2J_{P,F}$ = 76 Hz.

Bis(nonafluorobutyl)phosphinic acid, $(C_4F_9)_2P(O)OH$ (3a)

Using the same PFA installation, 117 g (0.16 mol) of $(C_4F_9)_3PF_2$ was slowly added (within 30 min) under vigorous stirring to 55 g (3.06 mol) of deionized water, which was heated at 90 – 100 °C (temperature in oil–bath). The resulting solution was refluxed for 1 hour at 120 °C (temperature in oil–bath) and then aqueous HF was distilled off. The residue was dried under reduced pressure ($5\cdot10^{-2}$ mbar) within 18 hours at 50 °C (temperature in oil–bath). 76 g of a transparent solid was obtained. Yield: 94 %. Mp: 113 °C.

^{1}H NMR (lock/solvent CD_3CN, 400 MHz), δ, ppm: 12.1 s (OH).

^{19}F NMR (lock/solvent CD_3CN, 376.4 MHz), δ, ppm: –82.4 t,m ($2CF_3$); –121.8 br.s ($2CF_2$); –122.4 d ($2CF_2$); –127 m ($2CF_2$); $^2J_{P,F}$ = 85 Hz; $^4J_{F,F}$ = 10 Hz.

^{31}P NMR (lock/solvent CD_3CN, 161.9 MHz), δ, ppm: 3.9 quin; $^2J_{P,F}$ = 85 Hz.

Pentafluoroethylphosphonic acid, $C_2F_5P(O)(OH)_2$ (5a)

Using the same PFA installation, 222 g (0.52 mol) of $(C_2F_5)_3PF_2$ was slowly added (within 30 min) under vigorous stirring to 120 g (6.67 mol) of heated deionized water at 95 – 100 °C (temperature in oil–bath). The resulting solution was refluxed at 120 – 130 °C (temperature in oil–bath) for 14 days and then aqueous HF was distilled off. The residue was dried under reduced pressure 10 hours at 60 – 70 °C (temperature in oil–bath). 103 g of a transparent liquid was obtained. Yield: 99 %.

NMR spectra were measured using an FEP tube with an acetonitrile–D_3 film as external lock:

^{1}H NMR (400 MHz), δ, ppm: 11.3 s (2OH).

^{19}F NMR (376.4 MHz), δ, ppm: –82.8 br.s (CF_3), –128.4 d (CF_2), $^2J_{P,F}$ = 89 Hz.

^{31}P NMR (161.9 MHz), δ, ppm: –1.3 t, $^2J_{P,F}$ = 89 Hz.

Nonafluorobutylphosphonic acid, $C_4F_9P(O)(OH)_2$ (6a)

Using the same PFA installation, 115 g (0.16 mol) of $(C_4F_9)_3PF_2$ was slowly added (within 30 min) under vigorous stirring to 60 g (3.33 mol) of water heated to 90 – 96 °C (temperature in oil–bath). The resulting solution was refluxed at 130 °C (temperature in oil–bath) for 4 days and then the aqueous HF was distilled off. The residue was dried under reduced pressure ($5 \cdot 10^{-2}$ mbar) for 18 hours at 60 °C. 47 g of a transparent liquid, which slowly crystallized, was obtained. Yield: 99 %. Mp: 101 °C.

^{1}H NMR (lock/solvent CD_3CN, 400 MHz), δ, ppm: 11.1 s (2OH).

^{19}F NMR (lock/solvent CD_3CN, 376.4 MHz), δ, ppm: –82.4 t,m (CF_3), –122.5 m (CF_2), –124.8 d,t,m (CF_2), –127.1 t,m (CF_2), $^2J_{P,F}$ = 88 Hz, $^4J_{F,F}$ = 14 Hz, $^4J_{F,F}$ = 11 Hz.

^{31}P NMR (lock/solvent CD_3CN, 161.9 MHz), δ, ppm: –1.1 t, $^2J_{P,F}$ = 90 Hz.

Phenyltetrachlorophosphorane, $C_6H_5PCl_4$ (7a)

30.1 g (0.168 mol) of $C_6H_5PCl_2$ dissolved in 130 cm^3 of dry $CHCl_3$ was placed in a 500 ml round bottom flask, equipped with a reflux condenser, magnetic stirring bar, gas dispersion tube and a thermometer. Below 10 °C excess of chlorine gas was bubbled through the reaction mixture until the solution became yellow (about 20 min).

After evaporation of the solvent, 40.7 g of a white solid was obtained. Yield: 97%. Mp: 73 – 74 °C (literature value: 73 °C [21]).

^{31}P NMR (lock solvent $CDCl_3$, 161.9 MHz), δ, ppm: – 42.6 m.

Bis(pentafluoroethyl)phosphinic acid chloride, $(C_2F_5)_2P(O)Cl$ (8a)

20.2 g (80 mmol) of $C_6H_5PCl_4$ was placed in a two–neck round–bottom flask, equipped with a magnetic stirring bar, drying tube and dropping funnel. 21.7 g (72 mmol) of $(C_2F_5)_2P(O)OH$ was slowly added at room temperature. The reaction mixture was kept stirring for 4 hours at room temperature until two liquid layers were formed. The lower layer, $(C_2F_5)_2P(O)Cl$ was isolated from the reaction mixture by distillation at atmospheric pressure. 18.1 g of a colourless liquid was obtained. Yield: 78 %. Bp: 86 – 88 °C.

NMR spectra were measured using an FEP tube with an acetonitrile–D_3 film as external lock:

^{19}F NMR (376.4 MHz), δ, ppm: –81.9 s ($2CF_3$); –120.1 d,d ($2CF_a$); –124.3 d,d ($2CF_b$); $^2J_{P,Fa}$ = 89 Hz; $^2J_{P,Fb}$ = 101 Hz; $^2J_{Fa,Fb}$ = 320 Hz.

^{31}P NMR (161.9 MHz), δ, ppm: 20.8 quin; $^2J_{P,F}$ = 96 Hz

FT–IR (4 mbar) ν/cm^{-1}: 1332 (vs); 1306 (vs); 1241 (vs); 1163 (vs); 995 (vs); 758 (m); 639 (m); 602 (s); 582 (s); 560 (m); 537 (w); 495 (s); 477 (s); 437 (w).

Raman (liquid): 1331(w); 1302 (w); 1224 (w); 1165 (w); 994 (w); 756(vs); 640 (w); 610 (w); 584 (w); 562 (w); 539 (w); 438 (s); 399 (w); 364 (s); 327 (s); 299 (w); 284 (w); 263 (s); 247 (w); 214 (w); 179 (w); 150 (s).

Bis(nonafluorobutyl)phosphinic acid chloride, $(C_4F_9)_2P(O)Cl$ (9a)

2.5 g (4.9 mmol) of $(C_4F_9)_2P(O)OH$ was placed in a two–neck round–bottom flask, equipped with a magnetic stirring bar, drying tube and dropping funnel. 1.5 g (6.0 mmol) of $C_6H_5PCl_4$ diluted in 3 cm^3 of dry $CHCl_3$ was added. The reaction mixture was kept stirring for 30 minutes at room temperature. $(C_4F_9)_2P(O)Cl$ was isolated from the reaction mixture by distillation at atmospheric pressure. 1.6 g of a colourless liquid was obtained. Yield: 63 %. Bp: 158 – 160 °C.

NMR spectra were measured using an FEP tube with an acetonitrile–D_3 film as external lock:

^{19}F NMR (376.4 MHz), δ, ppm: –84 t,m ($2CF_3$); –115.4 d,d ($2F_a$); –119.7 d,d ($2F_b$); –121.5 m ($2CF_2$); –128.6 m ($2CF_2$); $^2J_{P,Fa}$ = 95 Hz; $^2J_{P,Fb}$ = 102 Hz; $^2J_{Fa,Fb}$ = 324 Hz, $^4J_{F,F}$ = 9.6 Hz.

^{31}P NMR (161.9 MHz), δ, ppm: 21.7 quin,m; $^2J_{P,F}$ = 98 Hz

Pentafluoroethylphosphonic acid dichloride, $C_2F_5P(O)Cl_2$ (10a)

19.3 g (77 mmol) of $C_6H_5PCl_4$ was placed in a two–necked round–bottom flask, equipped with a magnetic stirring bar, drying tube and dropping funnel. 6.4 g (32 mmol) of $C_2F_5P(O)(OH)_2$ was slowly added at 0 °C. The reaction mixture was kept stirring for 2 hours at room temperature. $C_2F_5P(O)Cl_2$ was distilled off at atmospheric pressure. 4.6 g of a colourless liquid was obtained. Yield: 61 %. Bp: 77 – 79 °C.

NMR spectra were measured using an FEP tube with an acetonitrile–D_3 film as external lock:

^{19}F NMR (376.4 MHz), δ, ppm: –81 m (CF_3); –122.5 d,m (CF_2); $^2J_{P,F}$ = 110 Hz.

^{31}P NMR (161.9 MHz), δ, ppm: 17.7 t; $^2J_{P,F}$ = 109 Hz

Nonafluorobutylphosphonic acid dichloride, $C_4F_9P(O)Cl_2$ (11a)

A mixture of $C_4F_9P(O)(OH)_2$ (6.0 g, 20 mmol) and 13.0 g (52 mmol) of $C_6H_5PCl_4$ was placed in a round–bottom flask, equipped with a magnetic stirring bar and drying tube. The mixture was stirred 4 hours at room temperature until all the solid acid was reacted and the contents consisted of two liquid layers. $C_4F_9P(O)Cl_2$ was isolated from the reaction mixture by distillation at atmospheric pressure. 5.7 g of a colourless liquid was obtained. Yield: 85 %. Bp: 124 – 126 °C.

NMR spectra were measured using an FEP tube with an acetonitrile–D_3 film as external lock:

^{19}F NMR (376.4 MHz), δ, ppm: –83.8 m (CF_3), –118.5 d,t,m (CF_2), –121.3 m (CF_2),–128 m (CF_2), $^2J_{P,F}$ = 113 Hz, $^4J_{F,F}$ = 14 Hz.

^{31}P NMR (161.9 MHz), δ, ppm: 17.7 t, $^2J_{P,F}$ = 113 Hz.

Chapter 2

2. Bis[bis(pentafluoroethyl)phosphinyl]imide, $H[\{(C_2F_5)_2P(O)\}_2N]$ – HFPI

2.1 Introduction

In the past 20 years, a lot of efforts have been directed towards discovering new molecular superacids. As a result of these efforts, new HNR_2 and HCR_3 compounds have been synthesized and found to be a versatile class of acids. Their NH or CH–Brønsted acidity is highly dependent on the nature of the substituent R. If R is strongly electron–withdrawing group, then the resulting imides are strong acids [26, 27]. Prominent examples are bis(perfluoroalkylsulfonyl)imides [28, 29, 30, 31], in particular bis[(trifluoromethyl)sulfonyl]imide, $(CF_3SO_2)_2NH$ (TFSI) which was first reported by Foropoulos and DesMarteau (1984) [32].

The anion bis[(trifluoromethyl)sulfonyl]imide (TFSI) also called NTf_2^-, received most attention in the last decades [32, 33, 34]. Salts containing this anion are used as electrolytes in batteries [35, 36, 37], room temperature ionic liquids [38, 39], Lewis acid catalysts [40, 41, 42, 43] as well as in spectroscopic investigations [33, 34, 44, 45] and structural studies [46].

$(R_FSO_2)_2N^-$ anions are chemically very robust and therefore they undergo slow degradation in the environment. As more environmental friendly compounds bis[bis(perfluoroalkyl)phosphinyl]imides, $[(R_F)_2P(O)]_2N^-$ can be considered.

2.2 Synthesis of HFPI

The first perfluorinated–phosphinyl imide and its derivatives were reported by Pavlenko *et al.* (1985) [47]. According to this procedure, the preparation of $H[\{(C_3F_7)_2P(O)\}_2N]$ requires a multi step procedure and the total yield was quite low (32 to 39 %). Recently, a similar synthesis of $H[\{(C_2F_5)_2P(O)\}_2N]$ was reported [19]. However, this method also requires three steps and the total yield was less than 42 %. In the first step the amide was prepared and isolated according to equation 2.1:

$$(C_2F_5)_2P(O)Cl + 2\ NH_3 \longrightarrow (C_2F_5)_2P(O)NH_2 + NH_4Cl\downarrow \qquad (2.1)$$

In a second step, the imide was formed under strong basic conditions (equation 2.2). Finally, the pure acid was isolated by heating the imide with sulphuric acid (100 %) in vacuum (equation 2.3).

$$\begin{aligned}&(C_2F_5)_2P(O)NH_2 + (C_2F_5)_2P(O)Cl + 2\ Et_3N \longrightarrow \\ &\qquad \longrightarrow [Et_3NH][\{(C_2F_5)_2P(O)\}_2N] + [Et_3NH]Cl\downarrow \qquad (2.2)\end{aligned}$$

$$[Et_3NH][\{(C_2F_5)_2P(O)\}_2N] + H_2SO_4 \longrightarrow H[\{(C_2F_5)_2P(O)\}_2N] + [Et_3NH]HSO_4 \quad (2.3)$$

In this work an improved synthesis of the $H[\{(C_2F_5)_2P(O)\}_2N]$ was developed.

2.2.1 *Synthesis of the HFPI from $(C_2F_5)_2P(O)Cl$*

In this new procedure a one pot reaction was applied resulting of increasing yield up to 80 % [48]. In a pre–reaction, $(C_2F_5)_2P(O)Cl$ diluted in diethyl ether was treated with 2 equivalents of ammonia at –78 °C. After warming up at room temperature, the mixture was stirred for 4 hours and a solid material precipitate. According to the NMR spectra the reaction mixture contains following products: $(C_2F_5)_2P(O)NH_2$ (**1b**), $[NH_4][\{(C_2F_5)_2P(O)\}_2N]$ (**2b**), $[NH_4][(C_2F_5)_2PO_2]$ (**3b**), and traces of $C_2F_5P(O)(NH_2)_2$ (**4b**) (Table 2.1).

Table 2.1 NMR data of related C_2F_5–P compounds.

Compound	δ(^{1}H) [ppm]	δ(^{19}F$_A$) [ppm] CF_2	δ(^{19}F$_B$) [ppm] CF_2	δ(^{31}P) [ppm]	$^2J_{P,FA}$ [Hz] PCF_2	$^2J_{P,FB}$ [Hz] PCF_2	$^2J_{FA,FB}$ [Hz] PCF_2	δ(^{19}F) [ppm] CF_3
$(C_2F_5)_2P(O)Cl$	–	–120.1 (m)	–124.4 (m)	+20.8 (quin)	89	101	320	–81.9
$(C_2F_5)_2P(O)NH_2$	5.3 (s br)	–124.9 (m)	–127.7 (m)	+12.9 (quin,m)	79	84	335	–81.2
$C_2F_5P(O)(NH_2)_2$	4.03 (s br)	–127.7 (d)		10.8 (t)	77			–81.7
$[NH_4]^+$ $[(C_2F_5)_2PO_2]^-$	6.53 (s br)	–126.7 (d)		–0.5 (quin)	69			–82.0
$[NH_4]^+$ $[(C_2F_5)_2P(O)]_2N^-$	3.15 (m)	–124.4 (m)	–127.1 (m)	–5.9 (quin,m)	79	89	333	–81.7
$[Et_3NH]^+$ $[(C_2F_5)_2P(O)]_2N^-$	3.12(q) 1.22(t)	–123.7 (m)	–126.8 (m)	–8.1 (quin,m)	78	85	316	–81.1

Previously unknown, $[NH_4][\{(C_2F_5)_2P(O)\}_2N]$ (**2b**) was easy converted to $[Et_3NH][\{(C_2F_5)_2P(O)\}_2N]$ (**5b**) under action of Et_3N. Compound $(C_2F_5)_2P(O)NH_2$ (**1b**) was also converted into (**5b**), by addition of $(C_2F_5)_2P(O)Cl$ (**8a**), at 0 °C in the presence of Et_3N or pyridine. Both compounds $(C_2F_5)_2P(O)NH_2$ (**1b**) and $[NH_4][\{(C_2F_5)_2P(O)\}_2N]$ (**2b**) were not isolated, but were identified in the reaction mixture by NMR spectroscopy. The processes are described by the equations 2.4 and 2.5.

$$3\ (C_2F_5)_2P(O)Cl + 6\ NH_3 \xrightarrow[-78\ ^\circ C]{Et_2O} \left\{ \begin{array}{l} (C_2F_5)_2P(O)NH_2\ (\mathbf{1b}) \\ [NH_4][\{(C_2F_5)_2P(O)\}_2N]\ (\mathbf{2b}) \\ 3\ NH_4Cl + \text{traces products}\ (\mathbf{3b+4b}) \end{array} \right. \qquad (2.4)$$

$$[NH_4][\{(C_2F_5)_2P(O)\}_2N] + Et_3N \longrightarrow \underset{(\mathbf{5b})}{[Et_3NH][\{(C_2F_5)_2P(O)\}_2N]} + NH_3\uparrow \qquad (2.5)$$

After warming up of the reaction mixture (equation 2.4 and 2.5), the deposit of NH_4Cl and $[Et_3NH]Cl$ was filtered off. A white solid of **5b** was obtained after removing the solvent under vacuum. The free acid (HFPI) (**6b**) was obtained according to the equation 2.3.

Excess of NH_3 can further react with $(C_2F_5)_2P(O)NH_2$ according to the equation 2.6. This undesired reaction, would reduce the yield considerably.

$$(C_2F_5)_2P(O)NH_2 + NH_3 \longrightarrow \underset{(\mathbf{4b})}{C_2F_5P(O)(NH_2)_2} + C_2F_5H\uparrow \qquad (2.6)$$

The products from several experiments were investigated by NMR spectroscopy and the data are listed in the Table 2.2. As it can be seen in Table 2.2, NH_3 in dioxane shows quite good conversion into products only at low temperature. The optimal temperature is in the range of –60 to –78 °C. Increasing of temperature is leading to formation of undesired products, in particular of $C_2F_5P(O)(NH_2)_2$ (**4b**). The best results have been obtained using Et_2O as a solvent. Traces of water hydrolysed $(C_2F_5)_2P(O)Cl$ (**8a**), that decrease considerably the yield of the products. This process seems to be nearly unavoidable and leads to the formation of traces of undesired product $[NH_4][(C_2F_5)_2PO_2]$ (**3b**) even if excess of NH_3 is used.

The best conditions for the preparation of HFPI are: (i) low temperature, (ii) very dry reagents and (iii) molar ratio between $(C_2F_5)_2P(O)Cl$ and NH_3 of 1:2.

Table 2.2 Composition of products identified by NMR spectroscopy at different conditions in the reaction 2.4.

NR.	**Reagent A**	**NH_3**	**Solvent**	**T(°C)**	**Products (% yield)**						**Ratio A:NH_3**
					A	**(1b)**	**(2b)**	**(3b)**	**(4b)**	**Others[a]**	
1.	$(C_2F_5)_2P(O)Cl$	in dioxan (0.5 mol/L)	dioxan	–60 °C	4	8	47	37	4	**1**	1:2
2.	$(C_2F_5)_2P(O)Cl$	in dioxan (0.5 mol/L)	Et_2O	–20 °C	–	31	29	37	3	–	1:2
3.	$(C_2F_5)_2P(O)Cl$	in dioxan (0.5 mol/L)	Et_2O	–70 °C	–	–	64	26	7	**3**	1:2
4.	$(C_2F_5)_2P(O)Cl$	gas	Et_2O	–40 °C	–	–	49	23	25	**3**	1:2
5.	$(C_2F_5)_2P(O)Cl$	gas	Et_2O	–78 °C	9	24	49	15	3	–	1:2
6.	$(C_2F_5)_2P(O)Cl$	gas	Et_2O	–60 °C	2	22	55	13	8	–	2:3
7.	$(C_2F_5)_2P(O)Cl$	gas	Et_2O	–70 °C	–	–	55	8	37	–	excess NH_3
8.*	**$(C_2F_5)_2P(O)Cl$**	**gas–dry**	**Et_2O**	**–70 °C**	**6**	**45**	**49**		**–**	**–**	**1:2**
9.	$(C_2F_5)_3PO$	in dioxan (0.5 mol/L)	–	–40 °C	21	67	–	12	–	–	1:1
10.	$(C_2F_5)_3PO$	gas	Et_2O	ice	–	–	–	50	30	20	excess NH_3
11.	$(C_2F_5)_3PO$	in dioxan (0.5 mol/L)	DME	RT	–	23	–	77	–	–	1:1
12.	**$(C_2F_5)_3PO$**	**gas**	**–**	**–35 °C**	**14**	**86**	**–**	**–**	**–**	**–**	**excess NH_3**

[a] Other compounds not identified. * In closed system at a vacuum line.

2.2.2 *Synthesis of the HFPI from $(C_2F_5)_3PO$*

$(C_2F_5)_3PO$ is also a possible precursor for the synthesis of HFPI. It can be obtained from $(C_2F_5)_3PF_2$ much easier than $(C_2F_5)_2P(O)Cl$ (**8a)** [49]. The equation 2.7 presents the reaction of $(C_2F_5)_3PO$ with excess of NH_3 at –35 °C. Unfortunatly expected formation of HFPI was not observed in this case.

$$(C_2F_5)_3PO + \underset{\text{(excess)}}{NH_3} \xrightarrow[\text{-35 °C}]{\text{without solv.}} \underset{(\mathbf{1b})}{(C_2F_5)_2P(O)NH_2} + C_2F_5H\uparrow \tag{2.7}$$

Product (**1b**) was isolated in 86 % yield without additional purification. The absence of any solvent makes this process very efficient. As can be seen in Table 2.2, the best results were obtained by using of NH_3 in excess, in the absence of the solvents at low temperature –35 °C (experiment 12).

The process (equation 2.7) requires a continuous control of the temperature. Increase of temperature over the –25 °C (due to the exothermic process) lead to formation of $C_2F_5P(O)(NH_2)_2$ (**4b**) and decreasing in the yield of desired product. After removing the volatile compounds and unreacted $(C_2F_5)_3PO$ (traces), the white solid $(C_2F_5)_2P(O)NH_2$ can be used in the next step, according to equation 2.2 without further purification.

The amide $(C_2F_5)_2P(O)NH_2$ (**1b**) is stable in dry conditions, very soluble in organic solvents (acetonitrile, acetone, chloroform), low soluble in benzene, hexane and undergo fast hydrolysis in water.

The described procedure can be applied for large scale preparation of HFPI. The synthesis of HFPI using $(C_2F_5)_3PO$ instead of $(C_2F_5)_2P(O)Cl$ is prefered, due to the low costs of this reagent. Another advantage is the suppress hydrolysis during that process. The detailed characterization of $(C_2F_5)_2P(O)NH_2$ (**1b**) together with other amides will be presented in Section 7.1.

2.2.3 Synthesis of the HFPI from $[(C_2F_5)_2P(O)]_2O$

A third route for the synthesis of HFPI was attempted using $[(C_2F_5)_2P(O)]_2O$ in excess of ammonia. The reaction proceeded according to equation 2.8 in a closed system starting from –78 °C by slowly warming up to room temperature. According to the NMR spectra the products $(C_2F_5)_2P(O)NH_2$ (**1b**), $[NH_4][(C_2F_5)_2PO_2]$ (**3b**) and traces of $C_2F_5P(O)(NH_2)_2$ (**4b**) are formed. The yield of amide $(C_2F_5)_2P(O)NH_2$ (**1b**) is low and compound $[NH_4][(C_2F_5)_2PO_2]$ (**3b**) is formed in parallel as a product of ammonolysis process. After removing the volatile compounds, a white solid mixture of the products was obtained. The amide (**1b**) was used in the second step for the preparation of HFPI, according to the equation 2.2.

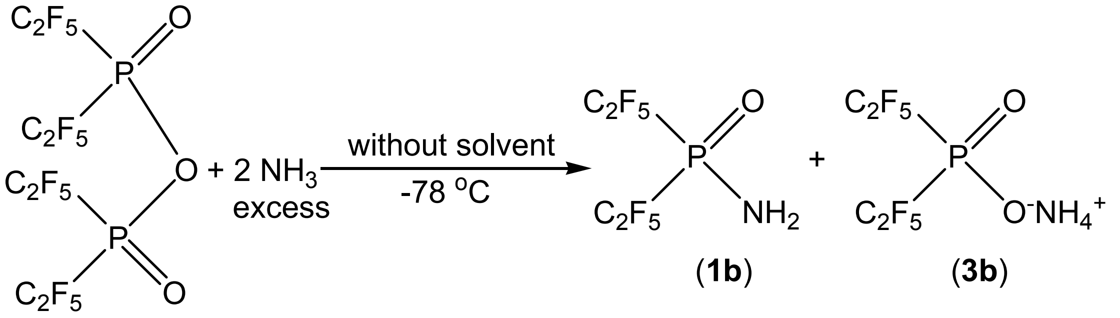

(2.8)

Suitable crystals for single crystal X–ray diffraction of $(C_2F_5)_2P(O)NH_2$ (**1b**) were obtained from the reaction mixture. The crystals were formed on the wall of the flask during evaporation of volatile compounds at low pressure. Crystallographic data of **1b** will be presented in detail in the chapter 7.

Treatment of $(C_2F_5)_2P(O)OMe$ or $(C_2F_5)_2P(O)OSiMe_3$ with ammonia failed to provide the desired product (**1b**). Attempts to prepare $(C_2F_5)_2P(O)NHSiMe_3$ (**7b**) result in very small yield (^{31}P NMR, δ, ppm: –38.5 quin and ^{19}F NMR, δ, ppm: –81 s; –126 m). Reaction of $(Me_3Si)_2NH$ with $(C_2F_5)_3PO$, within five days, at 80 °C, resulting in the formation of a brown mixture of products. Further reaction of $(C_2F_5)_2P(O)NHSiMe_3$ (**7b**) with $(C_2F_5)_2P(O)Cl$ lead to the $(C_2F_5)_2P(O)NH_2$ and HFPI.

In conclusion, the synthesis of HFPI can be prepared in good yields using $(C_2F_5)_3PO$ as precursor which is not so expensive as $(C_2F_5)_2P(O)Cl$.

2.3 Properties of HFPI

2.3.1 Acidity

Acidity constant in aqueous solution

The acid, $H[\{(C_2F_5)_2P(O)\}_2N]$ (HFPI) is a colourless hygroscopic solid. It is hydrolytically stable in aqueous solution at room temperature for at least five months. However, at 100 °C, after 2 hours in water, signals of $(C_2F_5)_2P(O)OH$ and $C_2F_5P(O)(OH)_2$ were observed in the ^{19}F NMR spectrum. In other solvents like DMSO and ethanol (or methanol) at room temperature the acid is stable for more then 5 days.

Acidity of HFPI was determined by titration with KOH, $pK_a = 1.9$ (Figure 2.1). This value is close to the $pK_a = 1.7$ for $HN(SO_2CF_3)_2$ reported by Foropoulos and DesMarteau (1984) [32].

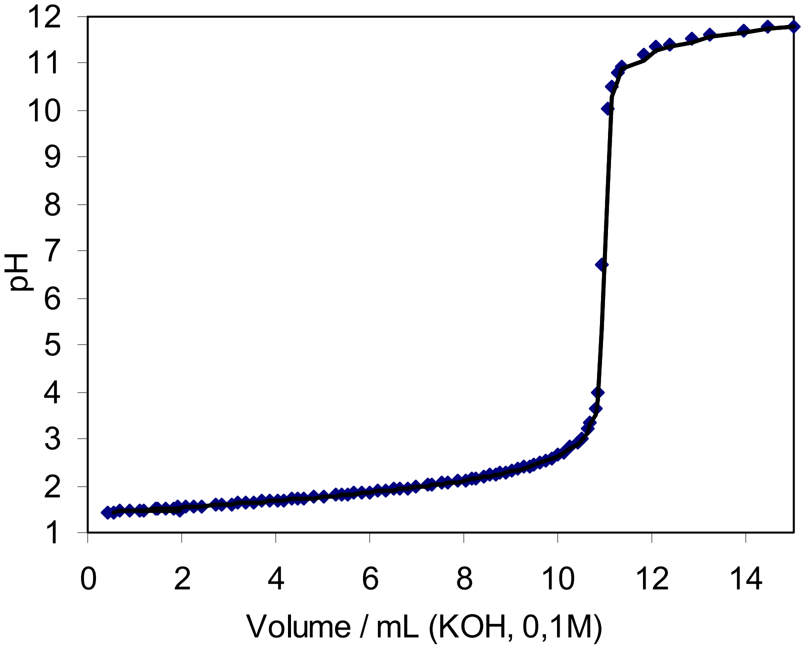

Figure 2.1 Titration curves of $H[\{(C_2F_5)_2P(O)\}_2N]$ (0.1 M) with KOH (0.1 M).

Acidity measurements by NMR spectroscopy

To gain more information about the acidity of HFPI, the ^{13}C NMR method reported by Farcasiu and Ghenciu (1991) was applied [50]. The method is based on difference in the ^{13}C NMR chemical shift between C_α and C_β atoms of mesityl oxide and its protonated form (**8b**). As solvent, liquid SO_2 is used due to its low basicity and relative high dielectric constant.

The protonation of 4–methyl–3–pentene–2–one (mesityl oxide) is described by equation 2.9. A consequence of protonation is an increase of the positive charge of C_β that causes a shift of the signal to higher frequency. The difference between the chemical shifts of C_α and C_β, noticed as $\Delta\delta$, is correlated with the acidity of the acid participating in the protonation process. The larger $\Delta\delta$ indicate the stronger acid.

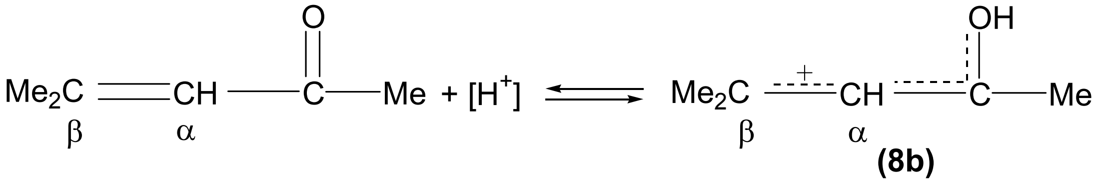

$$\underset{\beta}{\mathrm{Me_2C}}{=}\underset{\alpha}{\mathrm{CH}}{-}\overset{\mathrm{O}}{\overset{\|}{\mathrm{C}}}{-}\mathrm{Me} + [\mathrm{H}^+] \rightleftharpoons \underset{\beta}{\mathrm{Me_2C}} \overset{+}{\cdots} \underset{\alpha}{\mathrm{CH}} \cdots \overset{\mathrm{OH}}{\overset{\vdots}{\mathrm{C}}}{-}\mathrm{Me} \qquad (2.9)$$

(8b)

The ^{13}C NMR chemical shifts of pure mesityl oxide in SO_2, of C_β 158.39 ppm and C_α 126.02 ppm, are identical with data reported by Farcasiu and Ghenciu (1991) [50]. According to Figure 2.2 the ^{13}C NMR chemical shift difference ($\Delta\delta$) is 81.8 ppm in the case of $H[\{(C_2F_5)_2P(O)\}_2N]$; higher than of $HN(SO_2CF_3)_2$ ($\Delta\delta$ = 72.0 ppm) [51]. However, the acidity of $H[\{(C_2F_5)_2P(O)\}_2N]$ is lower than that of carborane acids ($\Delta\delta \approx$ 84 ppm). For example, for $H(CHB_{11}H_5Cl_6)$ is $\Delta\delta$ = 83.8 ppm and for $H(CHB_{11}H_5I_6)$ is $\Delta\delta$ = 83.3 ppm [50-52].

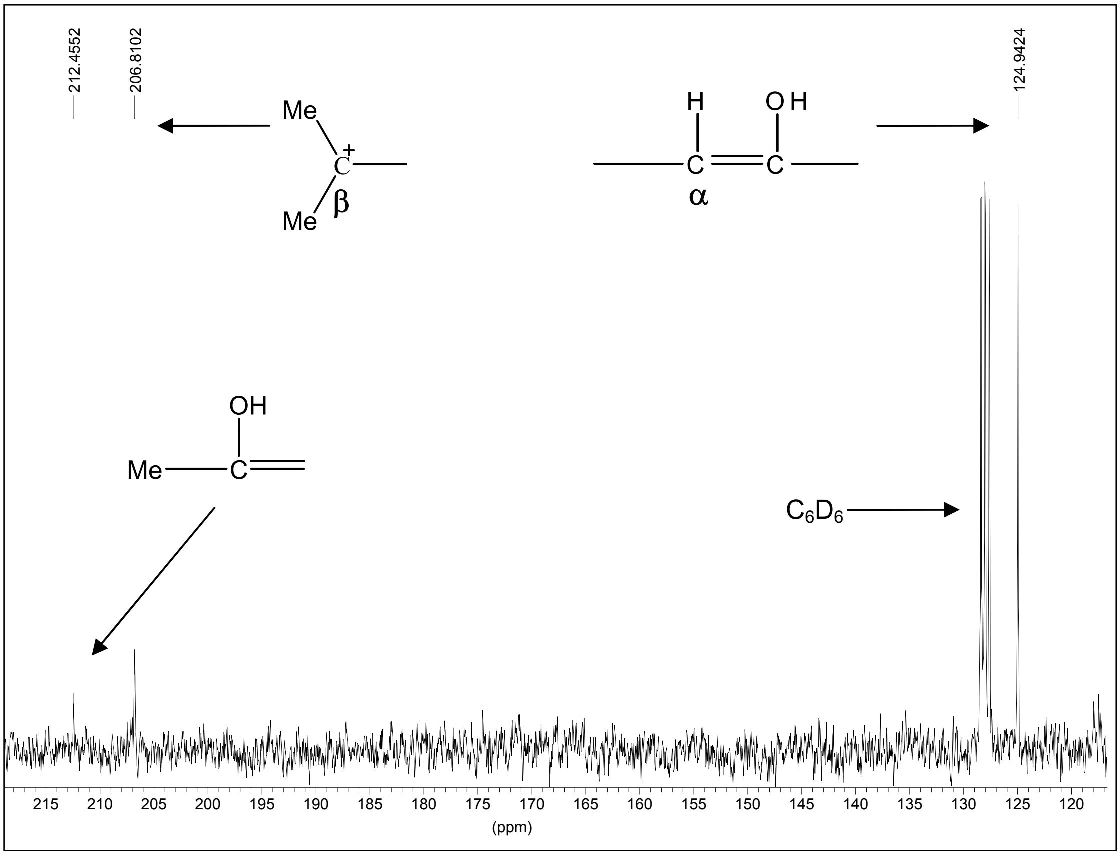

Figure 2.2 ^{13}C NMR spectrum of mesityl oxide protonated with $H[\{(C_2F_5)_2P(O)\}_2N]$ in SO_2.

The disadvantages of this method are: (i) NMR spectroscopy is less sensitive than UV – visible spectroscopy and requires a higher concentration of the substrate and (ii) mesityl oxide can decompose easily.

Acidity measurements by IR spectroscopy

IR spectroscopy was also used as an additional method to measure the relative acidity of $H[\{(C_2F_5)_2P(O)\}_2N]$. This qualitative method was well developed to measure the high acidities of the different carborane acids [51, 53, 54].

The method is based on measuring ν(N–H) frequencies for $octyl_3NH^+A^-$ (tri–*n*–octylammonium salts) dissolved in CCl_4 or $ClCH_2CH_2Cl$. The basicity of A^- determines the hydrogen bond strength in the ion contact pair $[NH\cdots A^-]$. Low basicity results in a high ν(N–H) frequency.

The measurements were performed in dilute solution of CCl_4 (0.01 – 0.008 mol/L) to avoid the concentration's dependence. For the contact ion pair:

$(C_2H_{17})_3N^+ — H\cdots\cdots N[P(O)(C_2F_5)_2]_2^-$

the ν(N–H) frequency is 3081 cm^{-1} (Figure 2.3). This frequency is a little lower than in the case of $HN(SO_2CF_3)_2$ [55]. Own measurements with $HN(SO_2CF_3)_2$ under the same condition gave a ν(N–H) frequency of 3090 cm^{-1}, close to the reported data. Furthermore, the same data of ν(N–H) frequency (3081 cm^{-1}) was obtained using the $Cs[\{(C_2F_5)_2P(O)\}_2N]$ as precursor for the synthesis of ionic liquid ($[octyl_3NH]^+[\{(C_2F_5)_2P(O)\}_2N]^-$).

The ν(N–H) frequency was also measured for neat compound ($[octyl_3NH]^+[\{(C_2F_5)_2P(O)\}_2N]^-$) placed between Si windows. The value of ν(N–H) in this case was 3029 cm^{-1} (Figure 2.3).

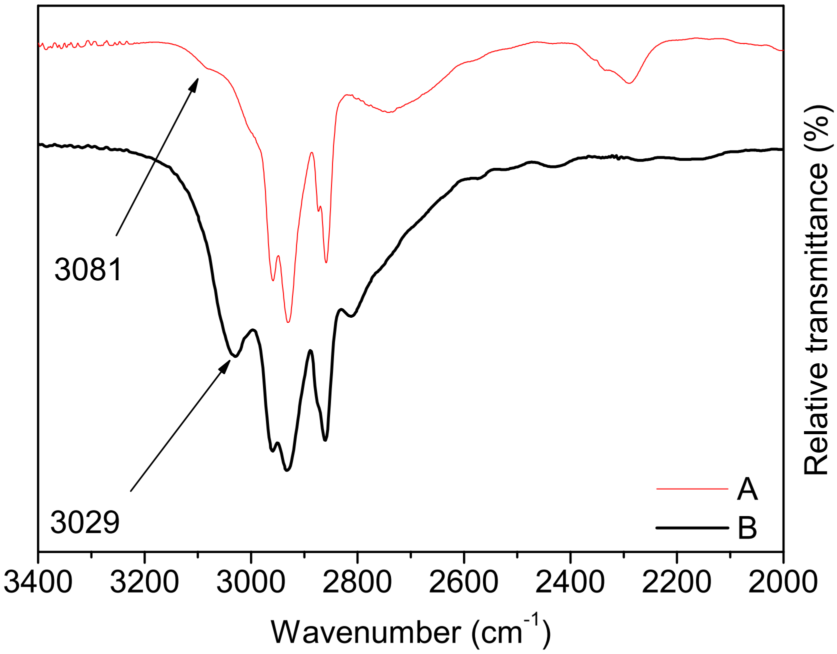

Figure 2.3 ν(N–H) frequencies of tri–*n*–octylammonium FPI in CCl_4 (A) and as neat compound in Si windows (B).

These results confirm that the conjugated acid of the FPI anion is a strong Brønsted acid and can be used to protonate very weak basic molecules. The IR method ranks the basicity of weekly coordinating anions, while ^{13}C NMR method ranks the acidity strength according to the protonation of weak ketone bases in dilute solutions.

2.3.2 Vibrational spectroscopy

The vibrational spectra of $H[\{(C_2F_5)_2P(O)\}_2N]$ are quite similar to that of salts with the FPI anion. Additional bands at 1392 (broad band) and 735 cm^{-1} were observed for free acid. The infrared and Raman spectra of $Cs[\{(C_2F_5)_2P(O)\}_2N]$ presented here, were recorded at room temperature, using ATR–IR spectrometer (**HARRICK, MVP Star^{TM}**) with a diamond as the ATR crystal and on Bruker (**EQUINOX 55**) FT Raman spectrometer (Figure 2.4).

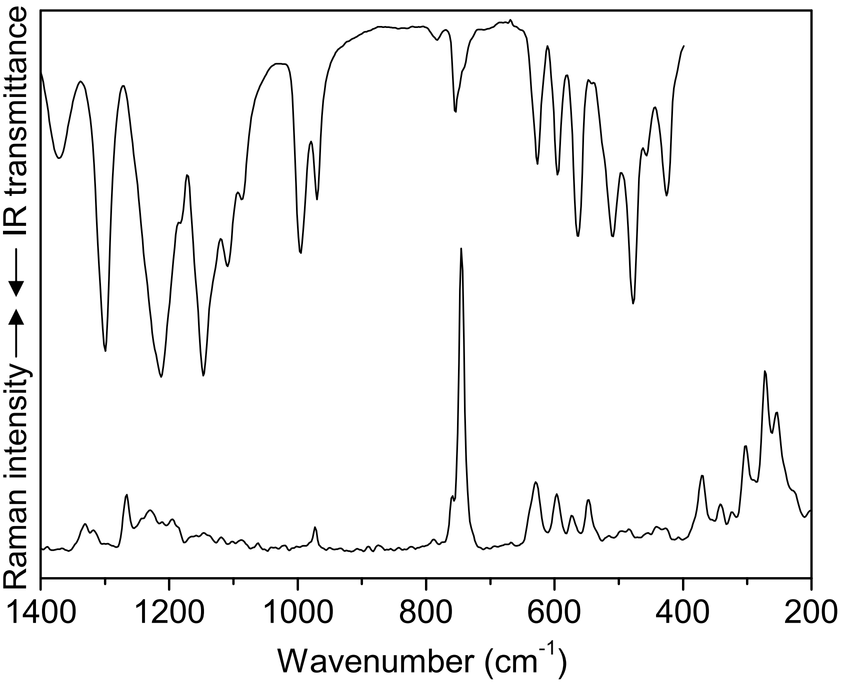

Figure 2.4 Infrared and Raman spectra recorded for neat solid $Cs[\{(C_2F_5)_2P(O)\}_2N]$.

The spectra are complicated due to the low symmetry and high numbers of atoms present in the anion (93 fundamentals are in principle allowed). Additionaly, several rotamers (P=O/P=O *cis* or *trans* and different C_2F_5 orientations) are possible. Each of them has different vibrational characteristics displayed in the spectrum. However, the signals from several C_2F_5 groups and some of stretching modes are overlapping as it can be seen from comparison of observed and calculated band positions listed in Table 2.3. The highest mode is attributed to the ν_{as} P–N–P stretch, followed by C–C, P=O, C–F stretches, and deformations modes with the frequencies below 1000 cm^{-1}. The strongest Raman band at 746 cm^{-1} is attributed to the symmetric CF_3 deformations. Altogether, the vibrational spectra are suitable for fingerprint identification of FPI anion. The possible rotamers could be identified by recording of the spectra at different temperatures, but that is not the aim of the work.

Table 2.3 Observed and calculated band positions (cm^{-1}) and infrared band intensities of the $[(C_2F_5)_2P(O)]_2N^-$anion.

IR[a]	Raman[b]	$\nu_{calcd.}$[c]	Assignment
1371 vs	1331 m	1370 (1000)	ν_1 $\nu(PNP)$
1301 vs	1317 m	1307 (440)	ν_2/ν_3 $\nu(CC)$
–	1268 s	1295(600)	ν_4/ν_5 $\nu(CC)$
–	1230 s	1255 (280)	ν_6 $\nu_s(PO)$
1215 vs	1212 w	1215 (800)	$\nu_7/\nu_8/\nu_9$ $\nu_{as}(CF_3)$
1184 s	1196 w	1186 (250)	$\nu_{10} - \nu_{15}$ $\nu_{as}(CF_3)/\nu_s(PO)$
1147 vs	1147 w	1142 (900)	ν_{16} $\nu_s(CF_2)$
1110 vs	1119 w	1134 (500)	$\nu_{17} - \nu_{18}$ $\nu(PC)$
1086 s	1064 w	1100 (330)	$\nu_{19} - \nu_{23}$ $\nu(CF_2)$
996 vs	–	965 (250)	$\nu_{24} - \nu_{26}$ $\nu(PC)$
971 s	973 s	950 (100)	ν_{27} $\nu(PC)$
784 m	760 m	750 (10)	ν_{28} $\nu_s(PNP)$
755 w	746 vs	730 (25)	$\nu_{29} - \nu_{32}$ $\delta(CF_3)$
627 s	629 m	620 (30)	$\nu_{33} - \nu_{35}$
595 s	597 m	596 (50)	$\nu_{36} - \nu_{37}$
564 s	574 w	580 (40)	$\nu_{38} - \nu_{39}$
545 w	548 m	575 (0.5)	ν_{40}
–	–	550 (200)	ν_{41}/ν_{42}
512 vs	–	520 (150)	$\nu_{43} - \nu_{46}$
479 s	–	472 (130)	ν_{47}/ν_{48}
458 m	–	430 (20)	$\nu_{49} - \nu_{50}$
427 s	425 w	435 (50)	$\nu_{51} - \nu_{52}$
–	370 m	360 (10)	$\nu_{53} - \nu_{56}$
–	340 w	340 (3)	ν_{57}
–	303 m	300 (4)	$\nu_{58} - \nu_{61}$
–	272 s	272 (4)	$\nu_{62} - \nu_{63}$
–	255 s	250 (7)	$\nu_{64} - \nu_{65}$

[a] Solid/[b] Solid neat compound; s = strong, m = medium, w = weak, v = very.
[c] B3LYP/6–31+G(d), IR intensities in parentheses (km·mol^{-1}).

2.3.3 NMR spectroscopy

The NMR spectra of $H[\{(C_2F_5)_2P(O)\}_2N]$ were measured in dry CD_3CN solution. A broad singlet between 9 – 12 ppm in the ^{1}H NMR spectrum corresponds to the N–H proton. The ^{19}F NMR spectrum of the C_2F_5 group shows a singlet at –81 and a multiplet at –125 ppm in a relative ratio of 3:2 as depicted in Figure 2.5.

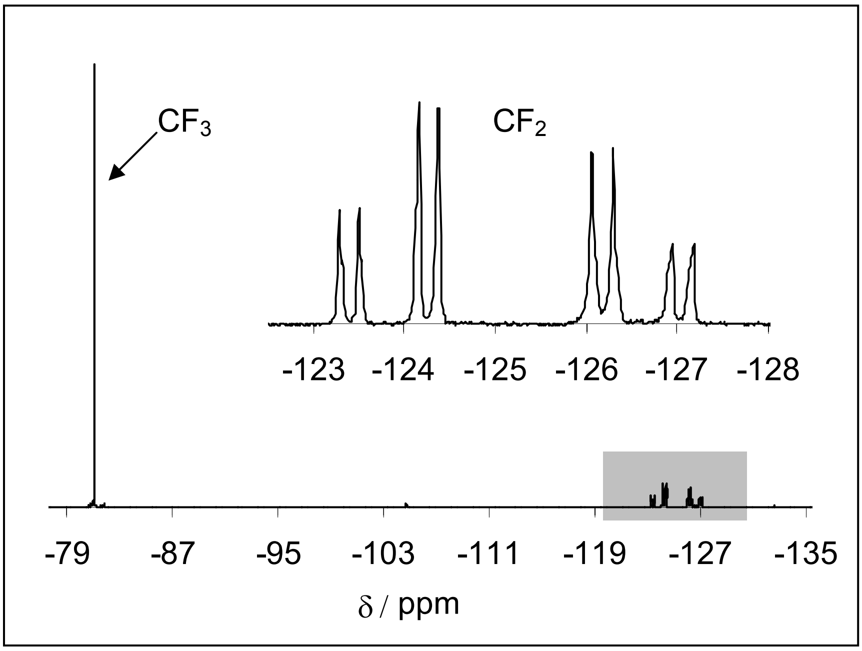

Figure 2.5 Spectrum of the CF_3 and CF_2 resonance in acetonitrile–D_3.

The sharp singlet at –81 ppm indicates that F atoms of the CF_3 group does not couple with the F atoms of the CF_2–group, but the ^{13}C satellites ($^1J_{CF}$ = 95 Hz) are split by coupling with the CF_2 group. The free FPI anion exhibits no symmetry. As a consequence the F atoms in the CF_2 group are not equivalent and the $–CF_2–P$ moiety forms an AA'X spin system.

A theoretical NMR spectrum can be calculated from the equations 2.10 and 2.11. The chemical shift, δ and coupling constant, $J_{AA'}$, from experimental NMR spectrum are corrected and compared in Table 2.4 and Figure 2.6.

$$J_1 = \frac{1}{2}\left(J_1^m + J_2^m\right) + \frac{1}{2}n\left(J_1^m - J_2^m\right); \; J_2 = \frac{1}{2}\left(J_1^m + J_2^m\right) + \frac{1}{2}n\left(J_2^m - J_1^m\right) \qquad (2.10)$$

$$n = \frac{\sqrt{\Delta^2 + J^2}}{|\Delta|} \qquad (2.11)$$

Table 2.4 Corrected (**gNMR 4.1**) experimental ^{19}F chemical shift and coupling constants for $H[\{(C_2F_5)_2P(O)\}_2N]$.

Compound	**$\delta(^{19}F_A)$ [ppm] CF_2**	**$\delta(^{19}F_B)$ [ppm] CF_2**	**$^2J_{P,FA}$ [Hz] PCF_2**	**$^2J_{P,FB}$ [Hz] PCF_2**	**$^2J_{FA,FB}$ [Hz] PCF_2**
$H[\{(C_2F_5)_2P(O)\}_2N]^a$	–123.75 (m)	–126.4 (m)	82.4	88.5	330

The experimental ^{19}F NMR parameters have been used as input for simulation of the ^{19}F NMR spectrum of $[(C_2F_5)_2P(O)]_2N^-$ anion as a AA'X spin system. The observed and simulated, by mean of **gNMR 4.1** program, AA' part of the ^{19}F NMR spectrum is depicted in Figure 2.6. The additional unresolved splitting in the experimental spectrum may be due to different rotameres of the anion.

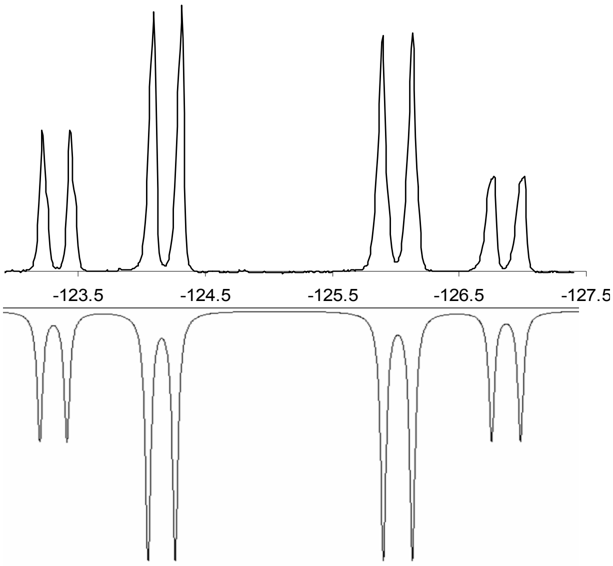

Figure 2.6 Observed (top) and simulated (bottom) spectrum of the CF_2 resonances in $[(C_2F_5)_2P(O)]_2N^-$ anion.

In the ^{31}P NMR spectrum only one broad quintet is observed at 7.8 ppm due to coupling with the four nearly identical ^{19}F nuclear of the two CF_2 groups (Figure 2.7).

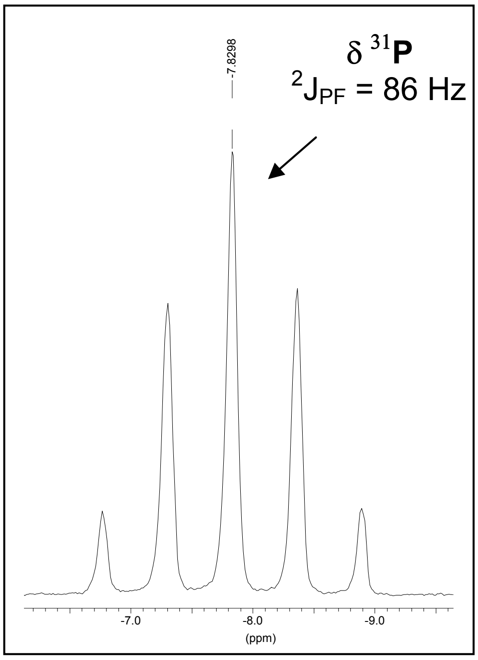

Figure 2.7 ^{31}P NMR spectrum of $H[\{(C_2F_5)_2P(O)\}_2N]$ in acetonitrile–D_3.

2.3.4 Thermal properties

The thermal behaviour of $H[\{(C_2F_5)_2P(O)\}_2N]$ was characterized by DSC and TG measurements. The sample was heated in inert atmosphere (N_2) at a rate of 10 $°C \cdot min^{-1}$. The decomposition curves of HFPI showed a continuous mass loss between 100 and 300 °C. The melting point is 49 °C. The thermal degradation curve showed an endothermic process at approximately 149 °C. Above 400 °C the mass loss was more than 90%. The thermal decomposition products of the HFPI were not investigated.

2.4 Experimental part

Bis[bis(pentafluoroethyl)phosphinyl]imide, $H[\{(C_2F_5)_2P(O)\}_2N]$ (6b)

A solution of 45 g (140 mmol) of $(C_2F_5)_2P(O)Cl$ in 40 mL of dry Et_2O was placed in a 250 mL flask equipped with a glass valve with PTFE piston (Young, London) and cooled to –78 °C (dry ice/ethanol bath). A 250 mL container charged with 4.7 g (276 mmol) of liquid ammonia was connected to the reactor and then the ammonia slowly added. The mixture was stirred and allowed to warm up to room temperature within 4 hour. A white deposit was formed and the solution was examined by ^{31}P NMR spectroscopy: $(C_2F_5)_2P(O)Cl$ (9%), $(C_2F_5)_2P(O)NH_2$ (24%), $C_2F_5P(O)(NH_2)_2$ (3%), $[NH_4][(C_2F_5)_2PO_2]$ (15%) and $[NH_4][\{(C_2F_5)_2P(O)\}_2N]$ (49%). Subsequently, 12 g (37 mmol) $(C_2F_5)_2P(O)Cl$ and 10 g (99 mmol) triethylamine were added to the reaction mixture within 30 min at 0 °C. After an additional 30 min stirring, the deposit of NH_4Cl was filtered off and washed three times with 20 mL of dry diethyl ether. After removing the solvent under vacuum, the white solid was dissolved in 2–propanol and then, by addition of water, pure $[Et_3NH][\{(C_2F_5)_2P(O)\}_2N]$ (**5b**) precipitated. After drying under vacuum, 50 g of a white solid was obtained. Yield: 79%. Mp: 106 – 107 °C. The decomposition curves of $[Et_3NH][\{(C_2F_5)_2P(O)\}_2N]$ showed an exothermic onset temperature at 215 °C.

^{1}H NMR (lock/solvent CD_3CN, 400 MHz), δ, ppm: 3.12 q (CH_2); 1.22 t (CH_3, $^3J_{H,H}$ = 7.3 Hz).

^{19}F NMR (lock/solvent CD_3CN, 376.4 MHz), δ, ppm: –81.1 s ($4CF_3$); –123.7 m ($4CF_a$); –126.8 m ($4CF_b$); $^2J_{P,Fa}$ = 78 Hz; $^2J_{P,Fb}$ = 85.4 Hz; $^2J_{Fa,Fb}$ = 316 Hz.

^{31}P NMR (lock/solvent CD_3CN, 161.9 MHz), δ, ppm: –8.1 quin,m (2P, $^2J_{P,F}$ = 80 Hz).

MS for $[Et_3NH][N\{P(O)(C_2F_5)_2\}_2]$: m/z = 686 ($M^+$), m/z = 787 ($M^+$+ $(C_2H_5)_3N$)

Sulphuric acid (35 mL/100 %) was added to the salt and the mixture was heated under vacuum (< 10^{-2} mbar) to 120–135 °C. The product sublimed through an ascending glass tube. The white solid $H[\{(C_2F_5)_2P(O)\}_2N]$ (**6b**) (41.7 g) was collected in a bulb at 0 °C. It is very hygroscopic and must be handled under dry nitrogen. Yield: 97.8 %. Mp: 47 °C.

^{1}H NMR (lock/solvent CD_3CN, 400 MHz), δ, ppm: 9–12 br. s (NH).

^{19}F NMR (lock/solvent CD_3CN, 376.4 MHz), δ, ppm: –81.2 s ($4CF_3$); –123.8 m ($4CF_a$); –126.6 m ($4CF_b$); $^2J_{P,Fa}$ = 79 Hz; $^2J_{P,Fb}$ = 87 Hz; $^2J_{Fa,Fb}$ = 332 Hz.
^{31}P NMR (lock/solvent CD_3CN, 161.9 MHz), δ, ppm: –7.8 quin,m (2P, $^2J_{P,F}$ = 86 Hz).
Elemental analysis calcd. (%) for $C_8HF_{20}NO_2P_2$ (M = 585.01 g/mol): C 16.42, H 0.17, N 2.39; found: C 16.07, H 0.11, N 2.47.
MS for $H[\{(C_2F_5)_2P(O)\}_2N]$: m/z = 467 $[(C_2F_5)_2P(O)NHP(O)C_2F_5]$, m/z = 585 ($M^+$).

Bis(pentafluoroethyl)phosphinyl amide, $(C_2F_5)_2P(O)NH_2$ (1b)

35.9 g (0.089 mol) of $(C_2F_5)_3PO$ was placed in a 250 ml round bottom flask, equipped with a cooler condenser (dry ice/ethanol), magnetic stirring bar, gas dispersion tube and a thermometer. Excess of ammonia gas was bubbled through the $(C_2F_5)_3PO$ for about 20 min. The reaction mixture was kept at temperatures between –30 to –35 °C (dry ice/ethanol bath). The reaction end was visually estimated when the resulting white product was formed. To complete the reaction, the mixture was kept at –30 °C for 10 minutes and then all volatile products were removed under vacuum (10^{-3} mbar). 23.1 g of a white solid was obtained. Yield 86 %. Mp: 96 – 98 °C.
^{1}H NMR (solvent CD_3CN, 400 MHz), δ, ppm: 5.3 br. s (NH_2).
^{19}F NMR (solvent CD_3CN, 376.4 MHz), δ, ppm: –81.2 s ($2CF_3$); –124.9 m ($2CF_a$); –127.7 m ($4CF_b$); $^2J_{P,Fa}$ = 79 Hz; $^2J_{P,Fb}$ = 84 Hz; $^2J_{Fa,Fb}$ = 335 Hz.
^{31}P NMR (solvent CD_3CN, 161.9 MHz), δ, ppm: 12.9 quin,m (P, $^2J_{P,F}$ = 86 Hz).

NMR measurements with mesityloxide

23.4 mg (0.039 mmol) of $H[\{(C_2F_5)_2P(O)\}_2N]$ was placed in a glass tube (l 20 cm and ∅ 0.4 cm) under Ar atmosphere in a glove box ($O_2 < 2$ ppm, $H_2O < 2$ ppm) together with 2.9 mg (0.03 mmol ~ 0.76 equiv.) of mesityloxide. Ca. 750 mg of dry SO_2 was condensed at –196 °C into the tube and flame sealed. After shacking to homogenize the solution, the tube was placed into a NMR tube containing benzene–D_6 as external lock and reference. ^{13}C NMR spectrum was recorded at 25 °C on a Bruker Avance 250 MHz spectrometer.

IR measurements with trioctylamine

The IR spectra were recorded with an adjustable path length IR cell (**Glenrothes RIIK**) with KRS-5 windows.

a. In a typical experiment 201 mg (0.34 mmol) of $H[\{(C_2F_5)_2P(O)\}_2N]$ was placed in a flask equipped with a Young valve, with 122 mg (0.34 mmol) of trioctylamine. The mixture was allowed to stir one hour and the ionic liquid $octyl_3NH^+FPI^-$ was obtained. Infrared spectrum of neat compound measured in Si windows is shown in Figure 2.2.

b. The ionic liquid, $octyl_3NH^+FPI^-$ was placed in a flask equipped with a Young valve and dry CCl_4 was condensed as solvent. The CCl_4 was dried over 4A molecular sieves before use. Characteristic spectrum of $octyl_3NH^+FPI^-$ was recorded in the CCl_4 at the concentration 0.008 mol/L and is shown in Figure 2.2.

c. 14 mg (0.02 mmol) of $Cs[\{(C_2F_5)_2P(O)\}_2N]$ and 7 mg (0.02 mmol) of trioctylamine were placed in a flask equipped with a Young valve. Dry CH_2Cl_2 was condensed as solvent. The mixture was cooled to –70 °C and HCl was added slowly making sure that the CsCl was precipitate. The solvent and excess of HCl was pump off and a mixture of $octyl_3NH^+FPI^-$ and CsCl was isolated. CCl_4 was condensed to this mixture and characteristic spectrum of $octyl_3NH^+FPI^-$ indicate ν(N–H) frequencies value at 3081 cm^{-1}.

d. A solution of $HN(SO_2CF_3)_2$ (1.03 g, 3.66 mmol) in 5 mL of water was added at room temperature to trioctylamine (1.28 g, 3.61 mmol). The mixture was left stirring over night. The water insoluble material was extracted with CH_2Cl_2 and washed few times with water. After evaporation of CH_2Cl_2 the residue was dried 24 h in vacuum at 70 °C. A liquid material (2.1 g) was obtained and the yield was 92%. The solution of $octyl_3NH^+TFSI^-$ (0.008 mol/L) in CCl_4 was prepared using the same procedure described above. Characteristic spectra of $octyl_3NH^+TFSI^-$ indicate ν(N–H) frequencies value at 3090 cm^{-1}.

Chapter 3

3. Bis[bis(pentafluoroethyl)phosphinyl]imide salts, $M[\{(C_2F_5)_2P(O)\}_2N]_n$, M = Li, Na, K, Cs, Ag, Mg, Zn and lanthanoides

The bis(pentafluoroethyl)phosphinyl group is a strong electron–withdrawing group and charge delocalizing and as a consequence of that the acidity of HFPI is high. The synthesis of some salts of bis[bis(perfluoroalkyl)phosphinyl]imide and their properties are described in this work. The salts with FPI anion was intensively studied for several possible applications: (i) the lithium salt can be used as electrolyte for lithium ion batteries; (ii) K, Na, Ag salts are possible precursors for ILs (Chapter 4); and (iii) lanthanide salts can be used as Lewis acid catalysts, for example, in acylation reaction (Chapter 6).

3.1 $M[\{(C_2F_5)_2P(O)\}_2N]_n$, M = Li, Na, K, Cs, Ag, Mg, Zn

The imide salts were obtained by neutralization of an aqueous solution of HFPI with the corresponding metal oxide, carbonate and hydroxide or by reaction with metals. The reactions have been carried out mostly at 0 °C or at room temperature. After completion of the reaction, the water was evaporated, and the solid residue was dried in vacuum at 60 – 80 °C for about 12 hours to give the pure metal imide. The reactions proceed almost quantitatively in all cases.

The salts are hygroscopic. The neutral aqueous solutions are hydrolytically stable, but under basic conditions they decompose rapidly with evolution of C_2F_5H. In the solid state they are stable up to 200 °C. The FPI salts (exception is AgFPI) display a high affinity to organic solvents having O and N donor's centre.

Lithium salts with large anions exhibit generally low lattice energies due to its anion size and extended delocalization of the negative charge. Specially, Li[TFSI] solutions possess high conductivity [35]. Thus, the first goal was to prepare LiFPI as an electrolyte for lithium ion batteries. LiFPI (**1c**) was prepared by reacting Li_2CO_3 with HFPI in water at 0 °C in good yields ca. 96% (equation 3.1). The extremely hygroscopic colourless compound was dried only by azeotropic distillation with $(MeO)_2CO$. The procedure was repeated three times and then the salt was dried in vacuum at 40 °C for 2 days. The water content detected by Karl–Fischer titration was 160 ppm. An undesired by–product $(C_2F_5)_2P(O)OLi$ (< 10 %) was also observed during the reaction between LiH and HFPI, in different solvents (dimethoxyethan, CH_2Cl_2 or water) at room temperature.

Conductivity of LiFPI has been investigated using a **703 Conductometer (Knick)** in the range at – 20 °C to 80 °C. Figure 3.1 shows how the conductivity of the LiFPI solution varies with temperature.

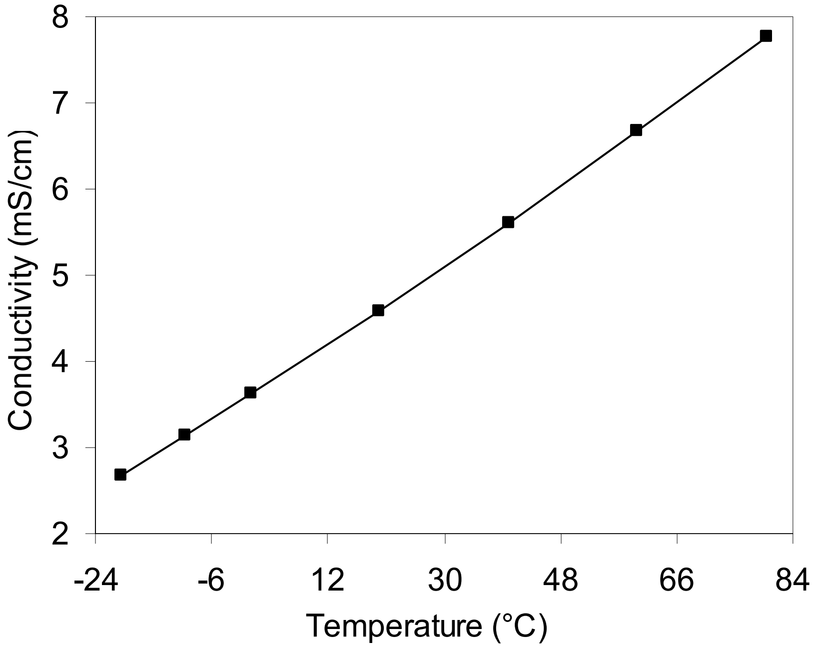

Figure 3.1 The conductivity curve for LiFPI (■) in acetonitrile solution (conc 0.3 mol/L).

Table 3.1 presents the conductivity data of different Li salts. The conductivity of LiFAP and $LiPF_6$ are higher than the conductivity of LiFPI [56]. This can be probably due to the huge size of the FPI anion. Large size anions lead to lower ion mobility which results in a lower conductivity.

Table 3.1 Conductivities of various salts in solvent system.

Conductivity (mS/cm) / Temp.	**– 20 °C**	**0 °C**	**20 °C**	**40 °C**	**60 °C**
LiFAP[a]	0.75	2.01	3.87	6.23	9.08
$LiPF_6$[b]	3.2	6.4	10.5	15.2	19.8
LiFPI[c]	2.68	3.63	4.58	5.60	6.67

[a] $Li[(C_2F_5)_3PF_3]$ in propylene carbonate (conc. 0.5 mol/L); [b] $LiPF_6$ in ethylene carbonate: dimethyl carbonate (1:1; conc. 1 mol/L) [56]; [c] LiFPI in acetonitrile (conc 0.3 mol/L).

Figure 3.2 shows the electrochemical window for LiFPI. The potential window of LiFPI was over 5 V. The irreversible reduction starts at about -2.5 V versus Fc^+/Fc and oxidation at about 2.6 V.

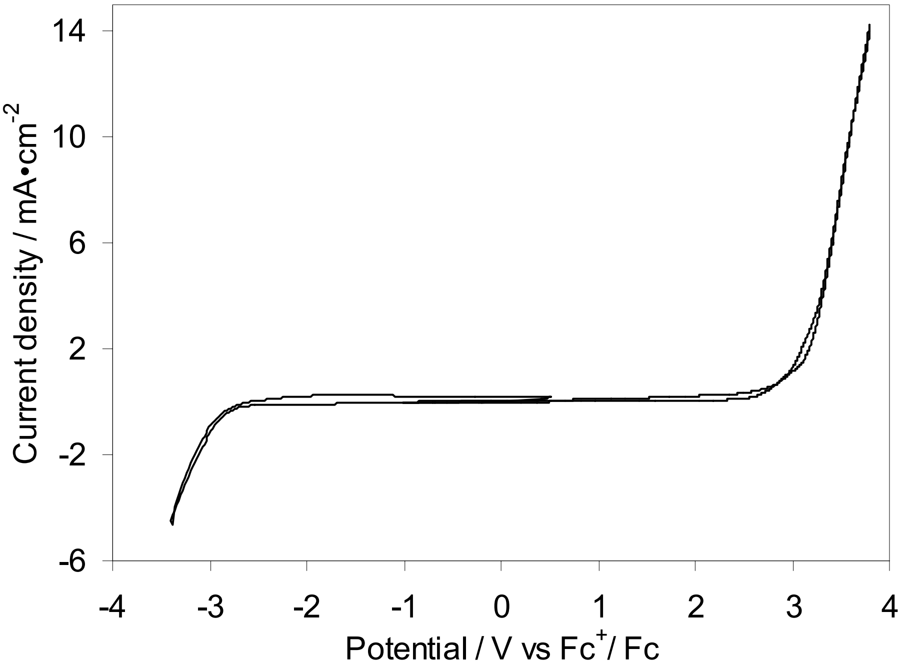

Figure 3.2 Cyclic voltammogram of LiFPI (**1c**).

NaFPI (**2c**) and CsFPI (**4c**) were synthesized by neutralization of an aqueous solution of HFPI with a solution of NaOH or $CsOH \cdot H_2O$, respectively, in equimolar ratio. For instance, an aqueous solution of K_2CO_3 was added slowly to the solution of the HFPI acid. The pH should not exceed 7 – 8 to avoid the decomposition. Silver carbonate (powder) reacts with an aqueous solution of HFPI to form AgFPI (**5c**) (equation 3.1). In all cases the pH value of the solutions was controlled (equation 3.2).

$$M_2CO_{3(s)} + 2\,H[\{(C_2F_5)_2P(O)\}_2N]_{(aq)} \longrightarrow$$
$$\longrightarrow 2\,M[\{(C_2F_5)_2P(O)\}_2N]_{(s)} + CO_{2(g)} + H_2O_{(l)} \qquad (3.1)$$

M = Li, K, Ag

$$MOH_{(aq)} + H[\{(C_2F_5)_2P(O)\}_2N]_{(aq)} \longrightarrow M[\{(C_2F_5)_2P(O)\}_2N]_{(s)} + H_2O_{(l)} \qquad (3.2)$$

M = Na, Cs

$Mg(FPI)_2$ (**6c**) and $Zn(FPI)_2$ (**7c**) salts were prepared by the reaction of HFPI with metals Mg or Zn, correspondigly (equation 3.3). These reactions proceed slowly. It can be accelerated by warming up of the reaction mixture.

$$M_{(s)} + 2\,H[\{(C_2F_5)_2P(O)\}_2N]_{(aq)} \longrightarrow M[\{(C_2F_5)_2P(O)\}_2N]_{2(s)} + H_{2(g)} \qquad (3.3)$$

M = Mg, Zn.

Additionally, $Mg(FPI)_2$ (**6c**) was also prepared from metal oxide, according to the equation 3.4. The solid MgO was added to the HFPI acid solution in water. After 4 hours mixing, the **6c** was isolated in near to quantitative yield.

$$MgO_{(s)} + 2\,H[\{(C_2F_5)_2P(O)\}_2N]_{(aq)} \longrightarrow Mg[\{(C_2F_5)_2P(O)\}_2N]_{2(s)} + H_2O_{(l)} \qquad (3.4)$$

The melting point of the FPI metal salts increase in the following order: LiFPI (44 °C) < CsFPI (107 °C) < KFPI (223 °C) < NaFPI (230 °C) according to increasing in the lattice energy. AgFPI (Mp = 211 °C) does not fit in this series because Ag^+ is more covalently bonded to FPI anion The salts with divalent cations exhibit a melting point of 112 °C for $Mg(FPI)_2$ and 98 °C for $Zn(FPI)_2$.

The thermal stability (T_{onset}, TGA) of the salts dependens on the strength of the cation – anion interaction: CsFPI (380 °C) > KFPI (250 °C) > NaFPI (230 °C). Again AgFPI (220 °C) and LiFPI (300 °C) does not fit in this series. For $Mg(FPI)_2$ and $Zn(FPI)_2$ a sharp weight loss was observed at about 180 °C.

The thermal behaviour and stability of the metal salts have been investigated by DSC and TGA, as presented, for example, in the Figure 3.3 for NaFPI (**2c**). The visually measured melting points are in agreement with the data presented above from DSC measurements.

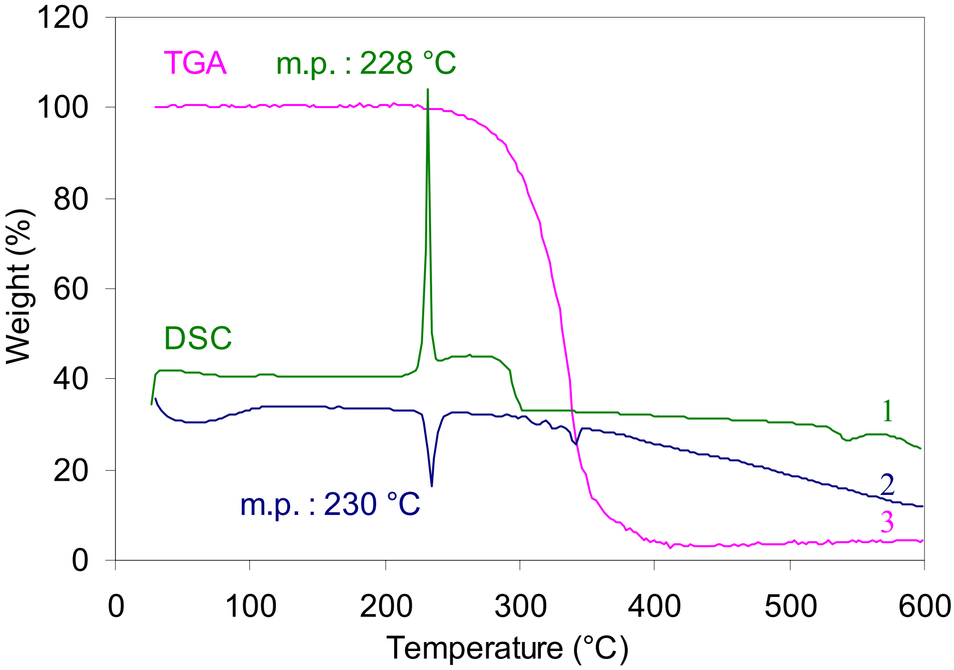

Figure 3.3 The thermal behaviour of NaFPI: 1 – measured with Netzsch DSC (204) instrument and 2, 3 – measured with Netzsch STA (409) instrument.

All salts are soluble in water, acetonitrile, acetone and Et_2O but insoluble in chloroform and hexane.

3.2 $Ln[\{(C_2F_5)_2P(O)\}_2N]_3$, Ln = La, Eu, Ce, Yb

The interest on rare earth compounds as catalysts in organic chemistry has grown considerably during the past twenty years. Lanthanide trifluoromethanesulfonate – $Ln(OTf)_3$ and lanthanide bis(perfluoroalkyl)sulfonyl amide – ($Ln(NTf_2)_3$) have been described as strong Lewis acids and as very efficient catalysts in Diels–Alder [57, 58], Michael [59], Friedel–Crafts [60, 61] and Mukaiyama reactions [62].

The lanthanide bis[bis(pentafluoroethyl)phosphinyl]imides (Ln(FPI)$_3$): Ce (FPI)$_3$ (**7c**), Eu (FPI)$_3$ (**8c**), Yb(FPI)$_3$ (**9c**), La(FPI)$_3$ (**10c**) were prepared from HFPI acid with metal oxides or carbonates in water, according to equations 3.5 and 3.6. After slow evaporation of the water on a rotary evaporator, the salts can be isolated and dried at elevated temperature under high vacuum. It should be noted that, using La_2CO_3 or $LaCl_3$ in aqueous solution, formation of $La[(C_2F_5)_2PO_2]_3$ as a by–product was observed. The activation of P=O bond and nucleophilic attack on the P atom can be the reason of $La[(C_2F_5)_2PO_2]_3$ formation.

$$Ln_2O_{3(s)} + 6\ H[\{(C_2F_5)_2P(O)\}_2N]_{(aq)} \longrightarrow$$
$$\longrightarrow 2\ Ln[\{(C_2F_5)_2P(O)\}_2N]_{3(s)} + 3\ H_2O_{(l)} \qquad (3.5)$$

Ln = La, Eu.

$$Ln_2(CO_3)_{3(s)} + 6\ H[\{(C_2F_5)_2P(O)\}_2N]_{(aq)} \longrightarrow$$
$$\longrightarrow 2\ Ln[\{(C_2F_5)_2P(O)\}_2N]_{3(s)} + 3\ CO_{2(g)} + 3\ H_2O_{(l)} \qquad (3.6)$$

Ln = Ce, Yb.

The lanthanide salts with FPI anion are colourless stable solids at room temperature. Almost all of them are hygroscopic. For example, La(FPI)$_3$ takes up to 7 % of water after 2 months exposure to air. Several attempts to grow crystals led to the formation of only amorphous precipitates. Slow removal of water/solvents, accomplished in desiccator under a nitrogen atmosphere by using P_4O_{10} as a drying agent, gave only colourless powder with more than 2000 ppm of water. It was impossible to isolate suitable single crystals for an X–ray diffraction analysis.

Ln(FPI)$_3$ are soluble in acetonitrile, acetone and Et_2O but insoluble in chloroform and hexane. Thermogravimetric analysis was used to characterize the thermal stability of the Ln(FPI)$_3$ salts. After drying in high vacuum at 60 °C, small portions (ca. 15 – 20 mg) of four different lanthanide salts were used for TG and DSC measurements. TG studies indicate that the decomposition of Ln(FPI)$_3$ occurr in two steps. The first stage relates to the dehydration (near 8 % mass lost), followed by the decomposition of Ln(FPI)$_3$ at 160 – 210 °C.

The study of catalytic activity of some FPI salts is presented in chapter 7.

3.3 Experimental part

General procedure:

The salts were prepared by reacting aqueous solutions of $HN[P(O)(C_2F_5)_2]_2$ at 0 °C with equal molar amounts of carbonate, oxide or hydroxide solutions in water. The vigorous stirring of the reaction mixture is important to prevent local basic conditions, to avoid the anion decomposition under formation of C_2F_5H. Neutral aqueous solution was evaporated and the solid residue was dried under vacuum ($<10^{-2}$ mbar) at 60 – 80 °C for 12 hours.

The NMR spectra of all salts are almost identical:

^{19}F NMR (lock/solvent CD_3CN, 376.4 MHz), δ, ppm: –81.1 s ($4CF_3$); –123.7 m ($4CF_a$); –126.8 m ($4CF_b$); $^2J_{P,Fa}$ = 76 Hz; $^2J_{P,Fb}$ = 84 Hz; $^2J_{Fa,Fb}$ = 322 Hz.

^{31}P NMR (lock/solvent CD_3CN, 161.9 MHz), δ, ppm: –7.8 quin,m (2P, $^2J_{P,F}$ = 80 Hz).

Lithium bis[bis(pentafluoroethyl)phosphinyl]imide, $Li[\{(C_2F_5)_2P(O)\}_2N]$ (1c)

Under vigorous stirring, 0.702 g (9.4 mmol) of Li_2CO_3 powder was slowly added to the aqueous solution of $HN[P(O)(C_2F_5)_2]_2$ (11 g, 18.8 mmol, in 20 mL of H_2O) cooled at 0 °C. The resulting neutral solution was left stirring over night to ensure complete reaction (checked pH = 7.1). The water was removed on a rotary evaporator and 20 mL of $(MeO)_2CO$ was added. After 2 hours stirring, the solvent/water mixture was distilled off at 90 °C. The procedure was repeated 3 times. After drying for 48 hours in vacuum at 40 °C, 10.6 g of a very hygroscopic white solid was obtained (160 ppm of residual water). Yield: 96%. Mp: 44 °C.

Sodium bis[bis(pentafluoroethyl)phosphinyl]imide, $Na[\{(C_2F_5)_2P(O)\}_2N]$ (2c)

A solution 0.086 g (2.1 mmol) of NaOH in 3 mL of H_2O was slowly added to a solution of $HN[P(O)(C_2F_5)_2]_2$ (1.260 g, 2.1 mmol) in 3 mL of H_2O, by stirring at 0 °C. The resulting neutral solution was evaporated and dried in vacuum, yielding 1.250 g of **2c** as a hygroscopic microcrystalline solid. Yield: 96%. Mp: 230 °C.

Elemental analysis calcd. (%) for $C_8F_{20}NO_2P_2Na$ (M = 607.0 g/mol): C 15.83, N 2.31; found: C 15.76, N 2.40.

IR (KBr pellet): ν (cm^{-1}) = 1357 (vs); 1312 (vs); 1302 (vs); 1224 (vs); 1157 (vs); 1110 (vs); 1003 (vs); 976 (s); 758 (m); 752 (w); 631 (s); 599 (s); 569 (s); 516 (s); 477 (s); 424 (m).

Potassium bis[bis(pentafluoroethyl)phosphinyl]imide, $K[\{(C_2F_5)_2P(O)\}_2N]$ (3c)

0.33 g (2.3 mmol) of K_2CO_3 in H_2O (3 mL) was added to the solution of 2.80 g (2.3 mmol) of $HN[P(O)(C_2F_5)_2]_2$ in H_2O (5 mL). Reaction mixture was stirred as described above. The resulting solution was concentrated by rotary evaporator and dried in vacuum (<10^{-2} mbar) at 60 °C overnight. This yielded 2.95 g (98%) of the white, hygroscopic (**3c**) compound. Mp: 223 °C.

Elemental analysis calcd. (%) for $C_8F_{20}NO_2P_2K$ (*M* = 623.1 g/mol): C 15.42, N 2.25; found: C 15.29, N 2.34.

MS – CI for $K^+[(C_2F_5)_2P(O)]_2N^-$: m/z 69 (CF_3); 623 (M^+).

Cesium bis[bis(pentafluoroethyl)phosphinyl]imide, $Cs[\{(C_2F_5)_2P(O)\}_2N]$ (4c)

The solution of 0.72 g (4.2 mmol) of $CsOH{\cdot}H_2O$ in 5 mL of H_2O was added to 2.5 g (4.2 mmol) $HN[P(O)(C_2F_5)_2]_2$ in 5 mL of H_2O as described above. The resulting neutral solution was evaporated and dried in vacuum. 2.90 g of **4c** as a microcrystalline solid was obtained. Yield: 94 %. Mp: 107 °C.

Elemental analysis calcd. (%) for $C_8F_{20}NO_2P_2Cs$ (*M* = 716.9 g/mol): C 13.40, N 1.95; found: C 13.51, N 2.10.

Silver bis[bis(pentafluoroethyl)phosphinyl]imide, $Ag[\{(C_2F_5)_2P(O)\}_2N]$ (5c)

0.55 g (2 mmol) of solid Ag_2CO_3 was added to 2.04 g (3.5 mmol) of $HN[P(O)(C_2F_5)_2]_2$ dissolved in 10 mL of H_2O. The suspension was stirred at room temperature for 1 hour in darkness. Filtration, evaporation and drying in vacuum (<10^{-2} mbar) gave 2.17 g of **5c**. Yield: 90 %. Mp: 212 – 214 °C.

Elemental analysis calcd. (%) for $C_8F_{20}NO_2P_2Ag$ (*M* = 691.8 g/mol): C 13.89, N 2.02; found: C 13.96, N 2.24.

Magnesium bis[bis(pentafluoroethyl)phosphinyl]imide, Mg[{(C$_2$F$_5$)$_2$P(O)}$_2$N]$_2$ (6c)

A. Mg powder (0.035 g, 1.44 mmol) was added to the solution of HN[P(O)(C$_2$F$_5$)$_2$]$_2$ (1.370 g, 2.3 mmol) in 5 mL of water. The mixture was stirred at room temperature for 1 day. After filtration, the water was evaporated on a rotary evaporator. The white hygroscopic powder (**6c**) was obtained by drying in vacuum at 70 °C for 1 day. Yield: 96 %. Mp: 112 °C.

B. MgO (0.1 g, 2.4 mmol, excess) was added to the solution of HN[P(O)(C$_2$F$_5$)$_2$]$_2$ (2.0 g, 3.4 mmol) in 10 mL of water. The mixture was stirred at room temperature for 4 hours. After filtration, water was evaporated by rotary evaporator. The white powder was obtained by drying in vacuum at 70 °C for 1 day. Yield: 98 %. Mp: 112 °C.

Elemental analysis calcd. (%) for $C_{16}F_{40}N_2O_4P_4Mg$ (M = 1192.3 g/mol): C 16.12, N 2.35; found: C 15.81, N 2.62.

Zinc bis[bis(pentafluoroethyl)phosphinyl]imide, Zn[{(C$_2$F$_5$)$_2$P(O)}$_2$N]$_2$ (7c)

Zn (dust) was activated with 2% aqueous HCl solution, filtered and washed again with water. Finally, Zn was washed with acetone and ether (the solvents were removed each time by filtration). After drying in vacuum, Zn (0.24 g, 3.6 mmol) was added slowly to the solution of HN[P(O)(C$_2$F$_5$)$_2$]$_2$ (1.72 g, 2.9 mmol) in H_2O (5 mL). The reaction mixture was stirred at room temperature for 5 h. Filtration, evaporation and drying in vacuum (<10^{-2} mbar) gave 1.7 g of **7c**. Yield: 95 %. Mp: 87 °C.

Elemental analysis calcd. (%) for $C_{16}F_{40}N_2O_4P_4Zn$ (M = 1233.4 g/mol): C 15.58, N 2.27; found: C 15.58, N 2.30.

^{31}P NMR (lock/solvent CD$_3$CN, 161.9 MHz), δ, ppm: –8.4 quin,m (2P, $^2J_{P,F}$ = 81 Hz).

Cerium bis[bis(pentafluoroethyl)phosphinyl]imide, Ce[{(C$_2$F$_5$)$_2$P(O)}$_2$N]$_3$ (8c)

$Ce_2(CO_3)_3 \cdot xH_2O$ (0.1 g, excess) was added to the solution of HN[P(O)(C$_2$F$_5$)$_2$]$_2$ (0.6 g, 1.02 mmol) in H_2O (5 mL) and the reaction mixture was stirred at room temperature for 4 hours. Filtration, evaporation and drying in vacuum (<10^{-2} mbar) gave 0.61 g of hygroscopic **9c**. Yield: 95%.

^{31}P NMR (lock/solvent CD$_3$CN, 161.9 MHz), δ, ppm: 8.1 m (2P).

Elemental analysis calcd. (%) for $C_{24}F_{60}N_3O_6P_6Ce$ (M = 1892.1 g/mol): C 15.23, N 2.22; found: C 14.65, N 2.28.

Europium bis[bis(pentafluoroethyl)phosphinyl]imide, Eu[{(C_2F_5)$_2$P(O)}$_2$N]$_3$ (9c)

Eu_2O_3 (0.1 g, 0.28 mmol) was added to the solution of HN[P(O)(C_2F_5)$_2$]$_2$ (1.0 g, 1.7 mmol) in H_2O (5 mL). The reaction mixture was stirred at room temperature for 12 hours. The solution was concentrated by rotary evaporator and then dried in vacuum ($<10^{-2}$ mbar) at 60 °C overnight. Yield: 94%.

^{31}P NMR (lock/solvent CD_3CN, 161.9 MHz), δ, ppm: – 45.6 m (2P).

Elemental analysis calcd. (%) for $C_{24}F_{60}N_3O_6P_6Eu$ (*M* = 1903.9 g/mol): C 15.14, N 2.21; found: C 14.92, N 2.32.

Ytterbium bis[bis(pentafluoroethyl)phosphinyl]imide, Yb[{(C_2F_5)$_2$P(O)}$_2$N]$_3$ (10c)

Yb_2O_3 powder (0.25 g, 0.63 mmol) was added to the solution of HN[P(O)(C_2F_5)$_2$]$_2$ (1.87 g, 3.1 mmol) in H_2O (8 mL). The reaction mixture was stirred at 43 °C for 2 days. After filtration, water was evaporated at rotary evaporator and residue was dried in vacuum ($<10^{-2}$ mbar) at 30 °C overnight. Yield: 98%.

^{31}P NMR (lock/solvent CD_3CN, 161.9 MHz), δ, ppm: – 16.1 quin,m (2P, $^2J_{P,F}$ = 83 Hz).

Elemental analysis calcd. (%) for $C_{24}F_{60}N_3O_6P_6Yb$ (*M* = 1925.0 g/mol): C 14.97, N 2.18; found: C 14.81, N 2.04.

Lanthanum bis[bis(pentafluoroethyl)phosphinyl]imide, La[{(C_2F_5)$_2$P(O)}$_2$N]$_3$ (11c)

La_2O_3 powder (0.14 g, 0.42 mmol) was added to the solution of HN[P(O)(C_2F_5)$_2$]$_2$ (1.32 g, 2.2 mmol) in 10 mL of H_2O. The mixture was stirred at room temperature for 1 day. A viscous liquid phase was formed on the bottom of the flask. After filtration under vacuum, the aqueous phase was separated from the mixture. The residue (the organic layer) was concentrated under vacuum and dried in vacuum ($<10^{-2}$ mbar) at 40 °C overnight.

^{31}P NMR (lock/solvent CD_3CN, 161.9 MHz), δ, ppm: – 3.4 quin, m (2P, $^2J_{P,F}$ = 87 Hz).

Elemental analysis calcd. (%) for $C_{24}F_{60}N_3O_6P_6La$ (*M* = 1890.6 g/mol): C 14.24, N 2.22; found: C 15.02, N 2.20.

Chapter 4

4. Ionic liquids with the FPI anion

Ionic liquids (ILs) are very promising class of innovative compounds which attracted much attention in the last decade. The huge number of papers and patents currently being published reflects both academic and industrial interest in using ILs in diverse areas. This interest is due to unique properties of ionic liquids: negligible vapour pressure, thermal and electrochemical stability, conductivity, miscibilities with water and other solvents, ability to dissolve organic, inorganic and polymeric materials.

In the following chapter the synthesis and properties of ILs with the bis[bis(pentafluoroethyl)phosphinyl]imide – anion are described. New low melting and hydrophobic ILs containing the FPI anion and imidazolium, ammonium, pyrrolidinium, pyridinium, phosphonium or benzothiazolium cations were prepared and characterized. Density, viscosity, melting point, glass transition temperature, decomposition temperature and conductivity were measured for these new materials.

4.1 Introduction in ionic liquids (ILs)

Ionic liquids are defined as materials containing only ions without any neutral compounds and having a low melting point, usually less then 100 °C [63]. Over time the term of ionic liquids is now generally associated with the salts having weakly coordinating anions and which are liquid at room temperature.

The discovery of ionic liquids can be dated to the last century. The synthesis of nitrite salts of ethylamine, dimethylamine and trimethylamine were reported in 1911, which, however, were not stable [64]. Later, in 1914, the synthesis of first stable room temperature IL, ethylammonium nitrate, $[EtNH_3][NO_3]$ (Mp = 12 °C), as a “red oil” was described [65]. In 1951, the $AlCl_3$–based ILs were developed by Hurley and Wier Jr. at Rice Institute in Texas [66]. The research groups of the U.S. Air Force Academy became interested in that work and investigated the spectroscopic and electrochemical properties of these ILs [66, 67]. In 1967 the liquid salt based on tetrahexyl ammonium benzoate was reported [68]. Hussey and Laher used for the first time tetraalkylpyridinium tetrahalidoaluminate, $[Rpy][AlCl_3X]$ as solvents [69].

The first generation of ILs, chloroaluminates–ILs, are very hygroscopic, air–sensitive compounds, and therefore difficult to handle. A few years later, these problems were solved when new air/water stable ILs were prepared, e.q. 1–ethyl–3–metylimidazolium tetrafluoroborate, $[emim][BF_4]$, 1–ethyl–3–metylimidazolium hexafluorophosphate, $[emim][PF_6]$ and 1–ethyl–3–metylimidazolium trifluoracetate, $[emim][CF_3CO_2]$ [70].

Afterwards, the number of new ILs reported has exploded. Many different ILs have been prepared by choosing different combination of ions, or by modifying the chemical structures of the constituent ions (Table 4.1). The organic cations are mainly derivatives of imidazolium, pyridinium, pyrrolidinium, thiazolium, oxazolium, ammonium, phosphonium and sulfonium. Typical inorganic anions are e.g. tetrachloroaluminates, hexafluorophosphate and tetrafluoroborate. Typical organic anions are perfluoroalkylfluorophosphate, alkylsulfate, alkylsulfonate, bis[(trifluoromethyl)sulfonyl]imide, p–toluenesulfonate (tosylate) and trifluoroacetate. Some of ILs have a zwitterionic structure, in which both cation and anion are covalently bounded.

Table 4.1 Examples of common cations and anions used for the synthesis of ILs.

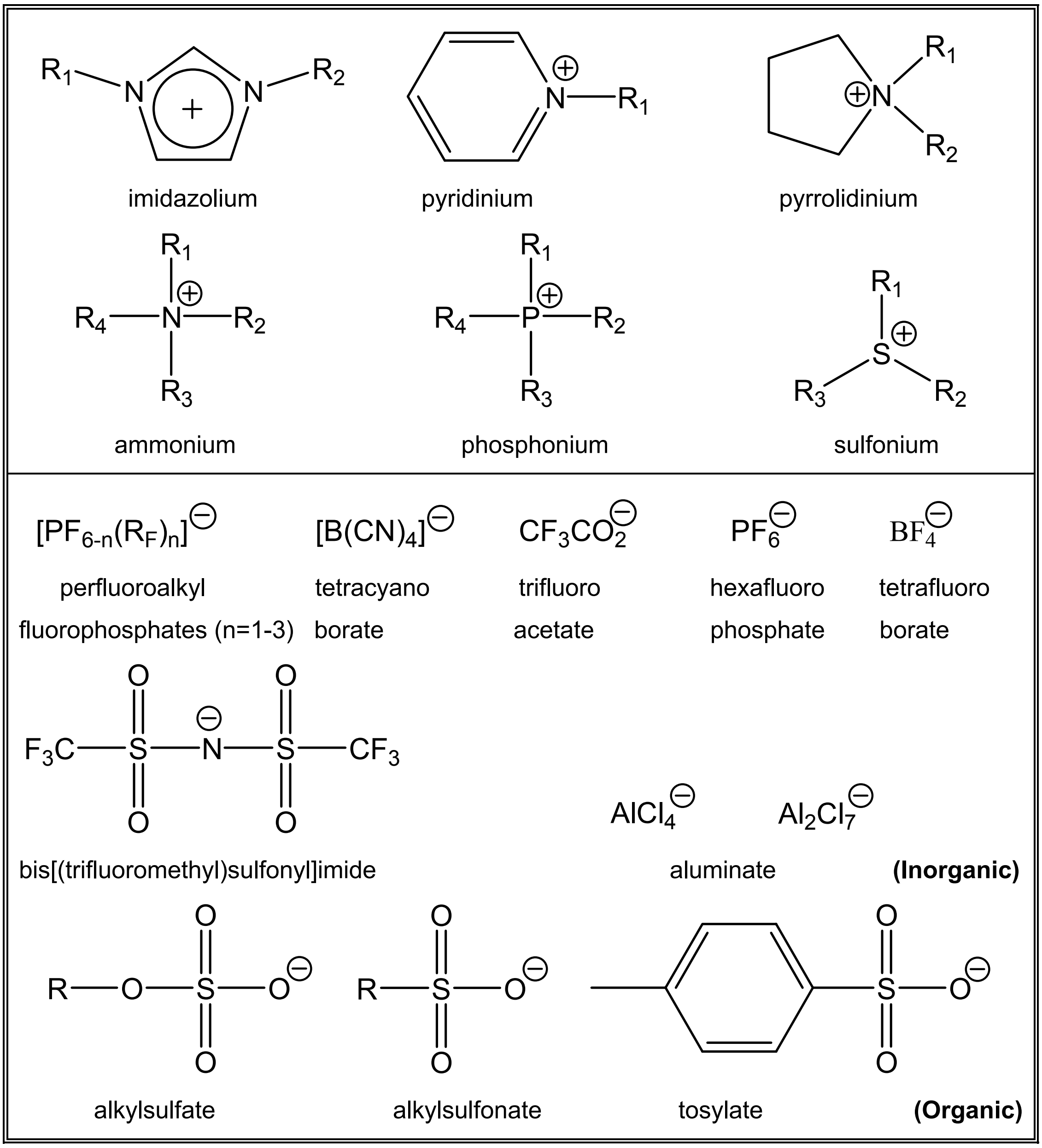

General method to prepare ILs is based on quaternization of an amine, a phosphine or a heterocyclic N–ring with an alkylating reagent ($R'X$). The synthesis of ILs can be performed in two steps: formation of the desired cation, e.g. imidazolium, pyridinium, ammonium, phosphonium followed by anion exchange as it is presented in Figure 4.1. The direct quaternization process is the preferred method for the production of ILs. The preparation of some ILs under microwave irradiation was also developed [71, 72]. But, if IL with desired anion–cation combination can not be formed by direct synthesis, an anion exchange reaction is needed. This complementary route is the most used method in this work. The metathesis reaction represents an interesting and potentially feasible alternative in the synthesis of a "task–specific" IL [73]. Commonly used ILs can be purchased from several sources: Merck KGaA, Sigma–Aldrich, Fluka, Acros Organics, BASF, IoLiTec.

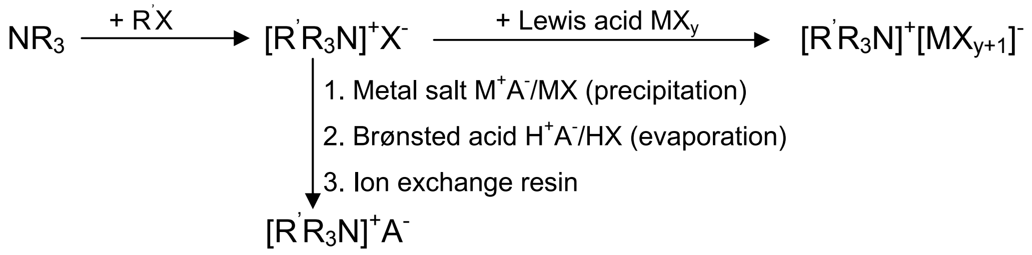

Figure 4.1 Synthetic routes for preparation of ILs with ammonium cations.

The unique properties and potential utilities as functional liquids make ionic liquids very attractive for the following applications:

(i) as "designer solvents" (new alternatives for the chemical industry to replace the volatile organic compounds) [74, 75, 76];

(ii) in catalysis: Diels–Alder reaction [77]; Friedel–Crafts reaction [78, 79] and ester formation [80]. The transition metal catalyzed reactions, e.g. hydrogenations [81], Heck reaction [82, 83], and oxidations [84], are the major class of catalytic chemical reactions carried out in ILs [85, 86];

(iii) in biocatalysis [87, 88];

(iv) in analytical application, e.g. as stationary phase in gas chromatography [89, 90], as additives for the mobile phase in high performance liquid chromatography [91] or as electrolytes in capillary electrophoresis [92, 93].

Figure 4.2 summarizes important properties of ILs and their wide range of applications (Sigma – Aldrich) [94].

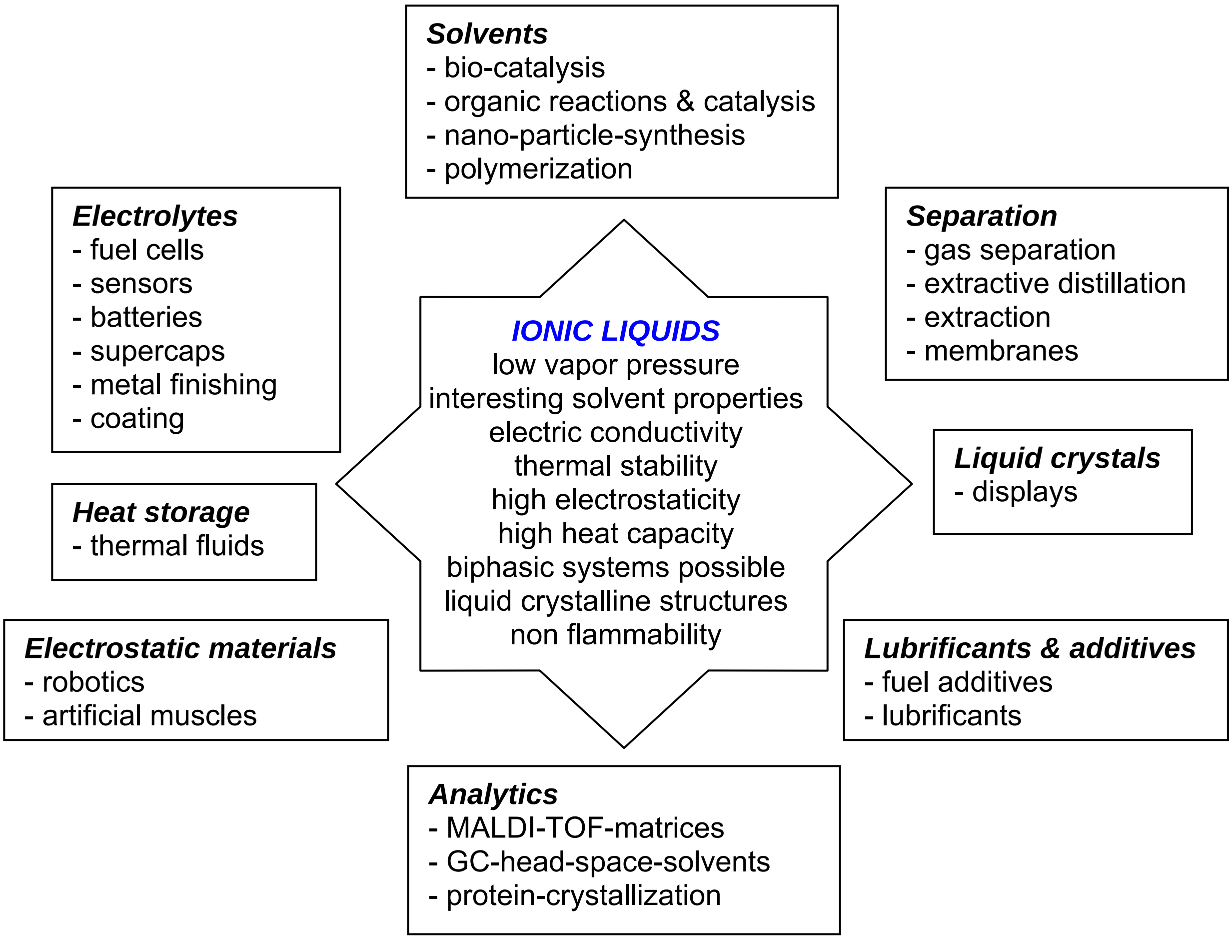

Figure 4.2 Important properties and applications of ionic liquids.

4.2 Synthesis of new ionic liquids with the FPI anion

The syntheses of ILs with the FPI anion were carried out by metathesis reactions, similar as it is shown in Figure 4.1, path 1 and 2. The general procedure was as followed: the acid (HFPI) or salt MFPI (M = Na, K) and Cat^+A^- were dissolved separately in a minimum quantity of water (some reactions required organic solvents). Both aqueous solutions were then mixed together and stirred at room temperature (equation 4.1). The obtained FPI ILs are insoluble and stable in water and precipitate as a dense bottom phase in the reactions flask. Vigorous stirring is essential for the reaction to proceed quantitatively. The bottom phase was separated; if necessary extracted with CH_2Cl_2, and washed several times with water. If a solid material is formed, it can be filtered and also washed with water until the test for chloride (bromide) with $AgNO_3$ is negative. To avoid any excess of the FPI – acid in the IL, the washing water should contain some K_2CO_3.

$$\mathrm{Cat^{+}A^{-}} + \mathrm{H[\{(C_2F_5)_2P(O)\}_2N]} \longrightarrow \mathrm{Cat^{+}[(C_2F_5)_2P(O)]_2N^{-}} + \mathrm{HA} \qquad (4.1)$$

A = Cl, Br, OH
Cat^+ = cation (will be further presented).

4.2.1 ILs with imidazolium cations

Imidazolium [Im] cations are probably the most used cations in the preparation of ILs. The positive charge in imidazolium cation is well delocalized. That supports good chemical stability of ILs with this cation. The imidazolium system can be easy derivatized to vary the properties of ILs.

The [Im] ILs with FPI anion, [$C_n$mim]FPI for n = 2 (**1d**), n = 4 (**2d**), n = 6 (**3d**), n = 10 (**4d**), n = 18 (**5d**), were prepared in good yield using commercially available [Im]chloride. By exchanging of halide with the FPI anion, new hydrophobic [Im][FPI ILs possessing low viscosity were prepared. The impurities, e.g. organic halide salts, halide residues, acid residues, were easily removed from FPI ionic liquids by washing with deionized water or with water containing small amount of K_2CO_3.

Introduction of the FPI anion into ILs can be carried out with the metal salts (MFPI, where M = K, Na) by metathesis reaction (route 1). For example, the [emim]FPI (**1d**) was synthesized by stirring equimol amounts of [emim]Cl with MFPI in water at room temperature. The resulting ILs are immiscible with water and forms a bottom phase which can be easily separated and purified by washing with water.

[emim]FPI (**1d**) was also prepared from ionic liquid with the bis(pentafluoroethyl)phosphinate anion $[(C_2F_5)_2P(O)O]^-$. The starting materials were dissolved in water and mixed together at room temperature with HFPI (equation 4.2). After separation of bottom phase the corresponding FPI IL was obtained in nearly quantitative yield.

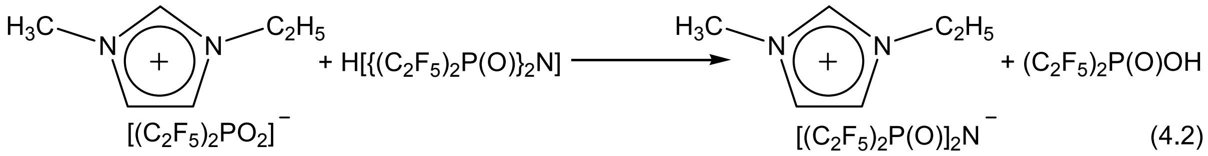

(4.2)

Instead of HFPI the MFPI (M = Na, K) can be used in this synthesis (equation 4.3).

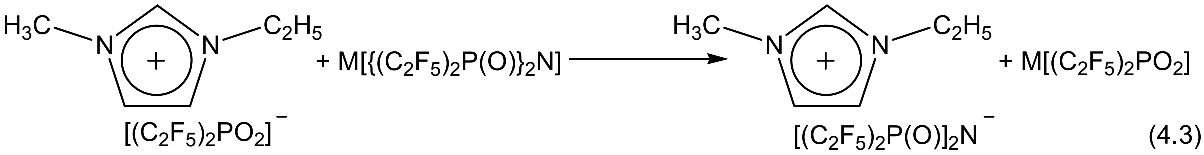

(4.3)

M = Na, K

Alkenyl or alkynyl functional groups can be easily introduced into the imidazole ring using the quaternization methods [95, 96, 97]. ILs with such imidazolium cations are often less viscous than their saturated counterparts and they can be further functionalized via addition reactions across the unsaturated bond. 1–allyl–3–methylimidazolium bromide (**6d),** was prepared by alkylation of 1–methyl imidazole with $BrCH_2CH=CH_2$ according to the published procedure [98]. The yield of the yellow viscous liquid (**6d**) was 95%. The new low viscosity IL, 1–allyl–3–methylimidazolium FPI (**7d**), was synthesized in good yield via metathesis reaction starting from **6d**. The viscosity of **7d** (127 mPa·s) is less then that of [emim]FPI (**2d**) (172 mPa·s).

Trisubstituted [Im] derivative, 1–n–butyl–2,3–dimethylimidazolium FPI (**8d**), was prepared using the same procedure. The properties of IL **8d** confirm that increasing the chain lengths and the molecular weight lead to higher melting point and higher viscosity. The advantage of such type of ILs is their high thermal stability [99].

4.2.2 ILs with pyridinium cations

The synthesis of pyridinium ILs was pioneered by Carpio, (1979) [100]. Two pyridinium FPI ILs were synthesized by metathesis reaction in water from N–alkylpyridinium chloride with HFPI: 1–n–butyl pyridinium FPI (**9d**) and 1–n–butyl–3,5–dimethyl pyridinium FPI (**10d**). The IL **9d** is a solid with a melting point of 49 °C. The IL **10d** is liquid at room temperature probably due to the hindrances in the crystal packing caused by CH_3 groups. IL **10d** shows high thermal stability (300 °C).

4.2.3 ILs with quaternary ammonium cations

Quaternary ammonium, $[NR_3R^{'}]$ (R, R’ = alkyl), ILs are more electrochemically stable that the corresponding [Im] ILs. Furthermore, it was demonstrates that such ILs with “robust” anions, such as TFSI and BF_4^- are resistant against oxidation and reduction

[101, 102]. Simple preparation and low cost of these type of ILs make them attractive for possible industrial applications [103, 104].

In this work different FPI alkylammonium salts were prepared by metathesis reactions. Structures and yields are depicted in Table 4.2. The asymmetrical salt (**5b**) was already described in chapter 2.

Table 4.2 Structures and yields of quaternary ammonium FPI ILs.

	Compound	R_1	R	yield, %
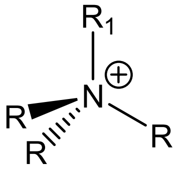	**5b**	H	C_2H_5	79
	11d	CH_3	CH_3	93
	12d	C_2H_5	C_2H_5	94
	13d	C_4H_9	C_4H_9	85

Pyrrolidinium ILs, in particular TFSI ILs, are useful materials for many applications due to low melting points, low viscosities and high electrochemical stabilities [105]. Recently, ILs with pyrrolidinium cations were investigated as surface active agents [106]. Burrell *et al.* (2007) reported a simple method for producing high quality of ILs in large scale using Na^+A^- (where A^-= BF_4, TFSI) [107]. That is the reason for our interest to prepare FPI ILs with pyrrolidinium cation. 1–n–butyl–1–methylpyrrolidinium FPI (**14d**) was synthesised in good yield (84 %) reacting HFPI with 1–butyl–3–methylpyrrolidinium chloride.

In an attempt to gain more information about the properties of ILs with the FPI anion, the syntheses of ILs with other functional groups attached to the pyrrolidinium cation was investigated. The reaction according to equation 4.4 was carried out at room temperature in deionized water. The mixture was stirred for some minutes until a bottom liquid phase was formed. Then, it was separated and washed two times with deionized water. During this procedure a solid product was formed. According to NMR spectroscopy and X–ray diffraction, the ester group was hydrolyzed during the synthesis, resulting in the formation of **15d**. The hydroxyl functional group can provide the possibility for further derivatisation [108].

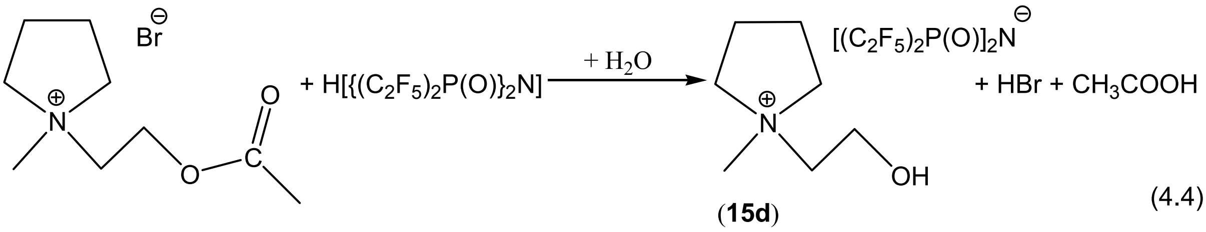

(**15d**) (4.4)

Recently, Lee *et al.* (2006) showed that the introduction of an ester functional group into the cations of ILs significantly improved their thermal and electrochemical properties [109]. Therefore, N–(3–ethoxy–3-oxopropy)–N–methyl pyrrolidinium FPI (**16d**) was prepared according to equation 4.5 (yield 72%). The very viscous liquid, **16d** exhibits a high thermal stability (300 °C).

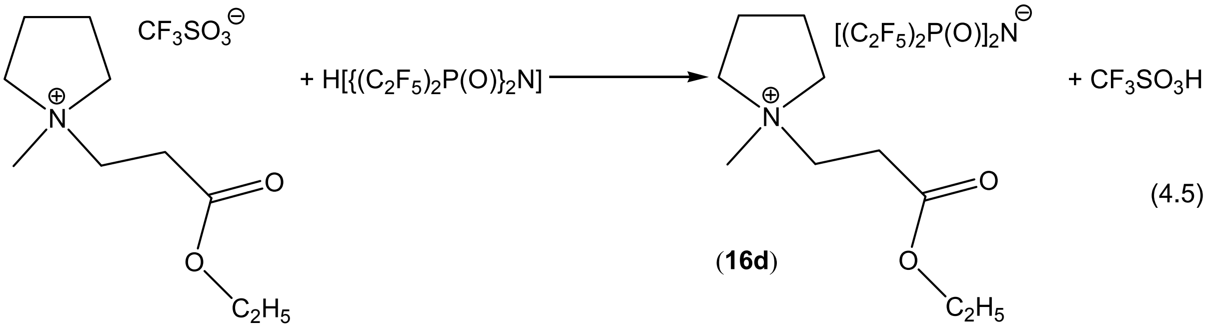

(**16d**) (4.5)

Guanidinium is another type of cation which was used in preparation of guanidinium FPI (**17d**) ionic liquid (equation 4.6). The IL **17d** is a very hygroscopic solid with a melting point of 47 °C.

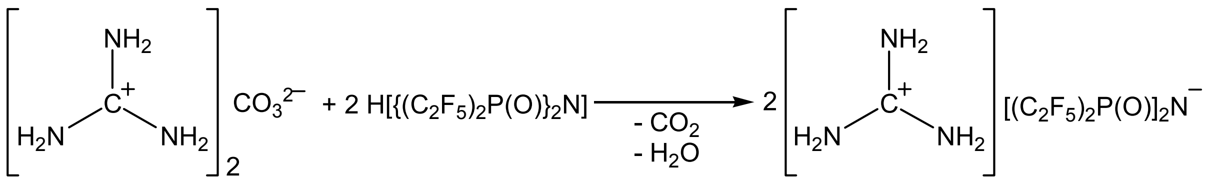

(**17d**) (4.6)

4.2.4 ILs with quaternary phosphonium cations

In the last years it was demonstrated that the imidazolium cation can degrade under basic condition (i.e. by action of Grignard, organolithium and amide – reagents) [110] and is susceptible to aromatic substitution reactions [111]. As a consequence, in the last years, phosphonium $[R_3R'P]$ ILs are more and more investigated [112, 113, 114]. Many publications devoted to study of these ILs and their properties are reported, by the reason that they are: (i) less expensive than those based on imidazolium cation ; (ii) can be used as recyclable media for Pd–mediated cross–coupling reaction [115, 116]; (iii) thermally very stable [112, 117]; (iv) stable towards strong basic reagents [110] and (v) commercially available in a big scale and at low cost (www.aldrich.com) [94].

In this work, the $[R_3R'P]$FPI ILs were synthesized and their properties were investigated.

Table 4.3 Structures and yields of quaternary phosphonium FPI ILs.

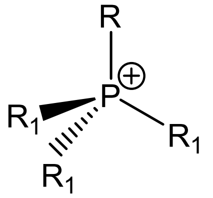	**Compound**	**R_1**	**R**	**yield, %**
	18d	C_4H_9	C_4H_9	86
	19d	C_6H_5	$CH_2C_6H_5$	75
	20d	C_6H_{13}	$C_{14}H_{29}$	86

4.2.5 *ILs with other cations*

Benzothiazolium salt with the FPI anion (**21d**) was obtained as a light yellow powder in good yield (78 %) by reaction of the benzothiazolium bromide with HFPI in water at low temperature (0 °C).

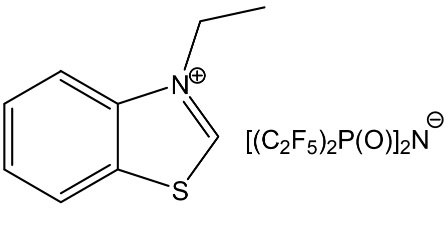

(**21d**)

4.3 Quality aspects of ILs

The presence of impurities influence essentialy the properties of ILs. Major impurities are organic salts, halide and acid residues. They are the result of incomplete reactions. Usually, the main impurity in [Im] ILs is methylimidazole, which is quite difficult to remove from the product. Organic impurities can be removed by distillation or extraction with diethyl ether, dichloromethane, dioxane or ethyl acetate. Halides are probably the most common impurities of ILs. They are strongly solvated in ILs making them difficult to remove completely. Halide impurities have a detrimental effect on transition– metal catalyzed reactions, e.g. hydrogenation [118, 119] or Heck type reactions [82]. Amount of residue of water depends on the nature of the ILs. Some of them require a special drying procedure and/or handling only in a glove box.

The presence of impurities affect the properties of ILs (e.q.: Mp, viscosity or colour) [120] and some applications (e.g. rate of catalytic reactions, corrosive effects) [121, 122]. For example, for [emim]BF_4 of different purity five different melting points are reported: 15 °C [70], 5.8 °C [123], 12.5 °C [124], 11 °C [125], 14.6 °C [126] and for [emim]TFSI three different melting points: –17°C [127], –15 °C [128], –21°C [38].

In conclusion, the quality of ILs must be checked prior to use by different analytical methods: NMR [129, 130], LC/MS (ESI^+ and ESI^-) [92, 131], IR and elemental analysis. The chloride content can be detected by titration with $AgNO_3$ [132], by ion chromatography [133] or by chloride–sensitive electrodes [134]. Small amounts of water, which cannot be detected by ^{1}H NMR, can be measured by Karl – Fisher titration.

All ILs presented in this work were analysed by ^{1}H, ^{19}F, ^{31}P NMR. For some ILs also ^{13}C NMR. Spectra were recorded on a **Brucker 400** and **600 MHz** spectrometer in CD_3CN or $CDCl_3$ as solvent and lock. The chemical shifts are reported in ppm on the δ scale calculated from internal standard (see experimental part).

ILs with the FPI anion were also identified using elemental analysis and some of them were analyzed with electrospray ionization mass spectrometry (ESI–MS). In all cases the strong peaks appear belongs to the parent cation and anion.

ILs with the FPI anion may content (i) halide impurities (ii) water and (iii) traces of other ionic impurities, in particular the HFPI acid from incomplete metathesis reaction.

Halide contents higher than 50 ppm were determined by titration with $AgNO_3$. Ion cromatography was used to measure low concentration of halide impurities in ILs. The content of chloride or bromide in all synthesized ILs was below 50 ppm, namely (halide/ppm): **1d** (5); **2d** (30); **3d** (7); **4d** (3); **5d** (19); **7d** (7); **8d** (9); **9d** (9); **10d** (13); **11d** (3); **12d** (3); **13d** (7); **14d** (9); **15d** (5); **16d** (5); **17d** (5); **18d** (45); **19d** (7); **20d** (14); **21d** (5).

Almost all FPI ILs are hydrophobic and their water content was reduced by drying at elevated temperature, in vacuum, for at least 12 h. The temperature should not exceed 80 °C. Higher temperature can cause a colourization of ILs. The water content of FPI ILs was in ppm: **1d** (20); **2d** (40); **3d** (45); **4d** (48); **5d** (13); **7d** (32); **8d** (42); **10d** (43); **14d** (42); **15d** (48); **17d** (28); **20d** (30).

Solid FPI ILs contain water typically between 20 to 1000 ppm (0.002 to 0.1 mass %) after drying. An efficient procedure to reduce the water content in these ILs is to dissolve the solid in dry dioxan or ethanol and then to distill off the solvent. The procedure can be repeated several times. In this manner, for example, the water content in [Et$_4$N]FPI was reduced from 1280 ppm to 12 ppm.

Some of FPI ILs are hygroscopic. For example, [emim]FPI takes up 8780 ppm of water after 3 weeks at air exposure.

Recently it was shown that IR spectroscopy can provide detailed information on the nature of the interaction between water and ILs [135]. As it can be seen in Figure 4.3, the broad asymmetric/symmetric stretching bands of water are found in the 3300 – 3700 cm^{-1} region. The position and intensity of these bands depend on water concentration in ILs.

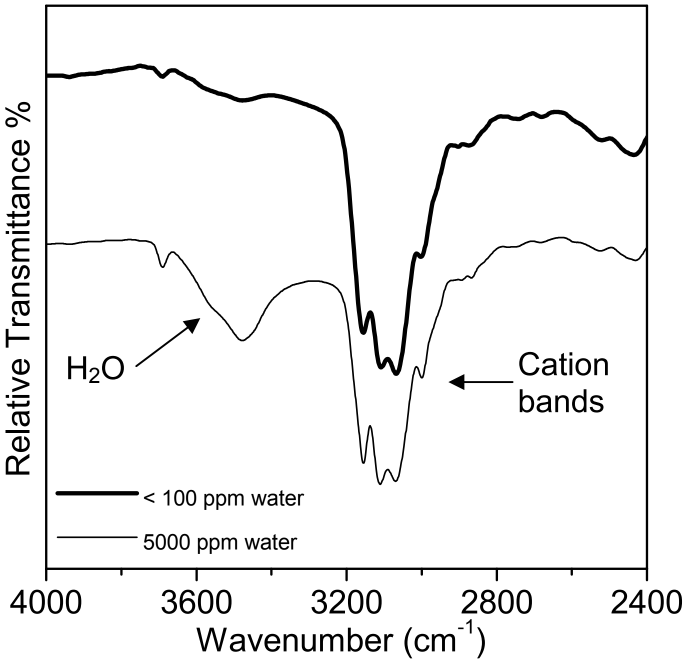

Figure 4.3 The IR spectrum of [emim]FPI showing the two stretching frequencies of water.

Table 4.4 presents the vibrational frequencies of the [hmim]Cl, [hmim]FPI and for comparison HFPI. The IR spectra for [hmim] cation coincide well with the results obtained by Berg *et al.*, (2005) [136]: the C–H vibrations of the ring occur at 3142 and 3062 cm^{-1} in the chloride salt. In our measurements these bands are shifted to 3139 and 3045 cm^{-1} for [hmim]Cl and to 3156 and 3057 cm^{-1} for [hmim]FPI. The peak positions and relative band intensities are influenced by hydrogen bonding between anion and hydrogen atoms of imidazolium ring. The corresponding spectra are shown in Figure 4.4.

Table 4.4 Experimental spectra bands of the [hmim]Cl, [hmim]FPI and HFPI.

Compound (Method)	**ν/cm^{-1}**
[hmim]Cl (ATR^{a})	3139 (m); 3045 (br. s); 2956 (s); 2932 (vs); 2859 (s); 2741 (w); 1643 (w); 1568 (s); 1462 (s); 1432 (br. m); 1379 (m); 1336 (m); 1304 (br. w); 1170 (vs); 1121 (w); 1093 (w); 1021 (w); 889 (m); 831 (m); 794 (m); 765 (m); 735 (m); 698 (w); 653 (s); 624 (vs); 599 (vw); 502 (w); 417 (vw).
[hmim]FPI (ATR^{a})	3156 (w); 3057 (br. w); 2965 (w); 2939 (w); 2872 (br. w); 1575 (m); 1387 (s); 1302 (s); 1265 (vs); 1212 (vs); 1142 (vs); 983 (s); 885 (br. w); 832 (w); 749 (m); 699 (vw); 627 (m); 595 (m); 562 (s); 507 (s); 476 (s); 427 (m).
HFPI (ATR^{b})	1388 (br. m); 1301 (s); 1215 (vs); 1144 (vs); 1125 (br. m); 998 (m); 978 (m); 780 (m); 757 (w); 733 (w); 639 (m); 621 (br. w); 597 (m); 565 (s); 507 (br. s); 493 (br. s); 475 (br. s); 427 (m).

^{a} Liquid/^{b} Solid - neat compound; s = strong, m = medium, w = weak, v = very, br. = broad.

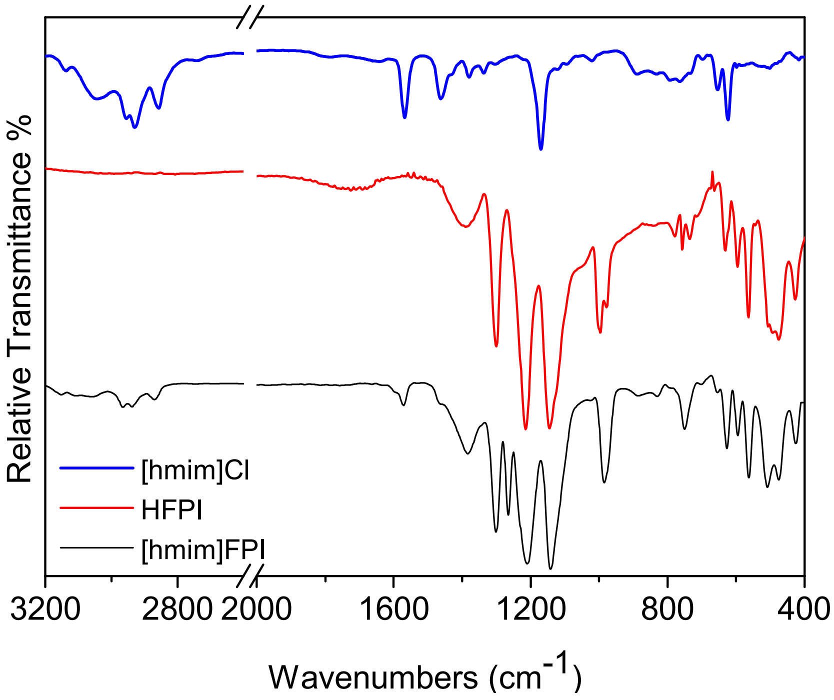

Figure 4.4 ATR–IR spectra of [hmim]Cl, HFPI and [hmim]FPI measured with an **HARRICK, MVP Star^{TM}** with a diamond as the ATR crystal.

Almost all ILs with the FPI anion are colourless compounds. Some of them are yellowish due to impurities in the precursors. Decolourization of FPI ILs can be achieved with active charcoal, similar to the procedure decribed in the literature [107]. Typically, the FPI IL is dissolved in ethanol and small amounts of active charcoal are added. The mixture left stirred and heated at 60 °C. After one day, the solution is cooled down to room temperature, filtered and the solvent is evaporated. If necessary, the decolorizing process is repeated.

4.4 Physical and chemical properties of ionic liquids with the FPI anion

4.4.1 Hydrolytic stability of FPI ionic liquids

The FPI ILs are stable against hydrolysis in water at room temperature for more than two months. However, after keeping an aqueous solution of [emim]FPI (**1d**) for 5 days at 100 °C a small signal belongs to the bis(pentafluoroethyl)phosphinate can be observed in the ^{19}F NMR spectrum of this solution.

Under basic conditions (6% aqueous KOH) at room temperature the hydrolysis of [emim]FPI proceeds much faster. Within 10 days about 40% of the IL is hydrolyzed to the phosphinate.

4.4.2 Viscosity and density

The viscosity is an important property of ILs, because it strongly influences the diffusion of species, which are dissolved or dispersed in the IL. This is especially important for electrochemical applications. In general, the viscosities of ILs are much higher than the viscosity of common organic solvents and are strongly influenced by cation–anion interactions, hydrogen bonding, as well as by the coordinating ability and symmetry of the ions [137].

It should be mentioned that the presence of water or other impurities (organic solvents) reduces the viscosity of ionic liquids substantially. Therefore, the water content in all FPI ILs are carefully controlled by Karl–Fischer titration prior to viscosity measurement, as discussed in Section 4.3. In all studied ionic liquids the water content was below 50 ppm which should not have a substantial influence on the viscosity. To avoid the influence of the halide impurities, all ILs were purified as described above, until the halide content was less that 30 ppm, controlled by ion chromatography.

ILs with the FPI anion possess kinematic viscosities which are comparable to the viscosities of ILs with the FAP anion or other phosphate anions [138]. For example, the viscosities data of [hmim] ILs with different anions are presented in Table 4.5. Anyway, all ILs having pefluoroalkyl groups bonded to phosphorus ILs show low kinematic viscosities in comparison to [hmim]PF_6 despite of their bulky molecule. Hence, the viscosity of ILs is dominated by the nature of the anion, in particular on its coordination ability.

Table 4.5 Viscosity and density data for some ILs with different anions.

[hmim]X	**Kinematic viscosity mm^2/s (at 20 °C)**	**Density g/cm^3**
[hmim]Cl	7453	1.05
[hmim][PF_6]	548	1.30
[hmim][BF_4]	195	1.15
[hmim][$(C_3F_7)_3PF_3$]	227	1.62
[hmim][$\{(C_2F_5)_2P(O)\}_2N$]	**103**	**1.54**
[hmim][$(C_2F_5)_3PF_3$]	74	1.56
[hmim][$(C_2F_5)_2PF_4$]	61	1.47
[hmim][$C_2F_5PF_5$]	74	1.40
[hmim][$(CF_3SO_2)_2N$]	44	1.37

In the series [$C_n$mim]FPI with different alkyl groups (n = 2, 4, 6) the viscosities (in mPa·s) are very similar: [emim]FPI (**1d**) has a viscosity of 171, [bmim]FPI (**2d**) 151, and [hmim]FPI (**3d**) 159 (Figure 4.5) [139]. For these three ionic liquids the influence of the cation size on the viscosity is minimal, because the bulky FPI anion occupies the major volume in the ionic liquid and carries the largest part of the molar mass (Table 4.6**)**. The viscosity also decreases with introduction of unsaturated groups into side chain of alkyl-imidazolium cation: e.g. 1–allyl–3–methylimidazolium FPI (**7d**) has 127 mPa·s, less than of [emim]FPI (**1d**).

Table 4.6 Dynamic and kinematic viscosity and density of ILs with the FPI anion.

Ionic liquid	**M.W.**	**Part of FPI anion in the molecular weigh of IL %**	**Dynamic viscosity η/mPa·s (20 °C)**	**Kinematic viscosity ν/mm^2·s^{-1} (20 °C)**	**Density ρ/g·cm^{-3}**
[emim]FPI	695.17	84.0	171	102	1.68
[bmim]FPI	723.22	80.7	151	95	1.59
[hmim]FPI	751.28	77.7	159	103	1.54
[dmim]FPI	807.38	72.3	199	137	1.45
[omim]FPI	919.60	63.5	376	285	1.32
[bmpl]FPI	726.27	80.4	325	206	1.58
[p(h3)t]FPI	1061.82	55.0	536	443	1.21

Recently it was shown that there is a strong relationship between the molecular volume V_m of ILs and their viscosity, conductivity and density [140]. According to equation 4.7 the volume of the FPI anion is estimated to be 0.467 nm^3 by using V_m = 0.58 nm^3 (available from single crystal X–ray diffraction) of $[(CH_3)_4N][\{(C_2F_5)_2P(O)\}_2N]$ and the volume for the $[(CH_3)_4N]^+$ cation $V_{ion}(C^+)$ = 0.113 nm^3 [141]. This anion volume is double than that of $[TFSI]^-$ (0.232 nm^3) [142]. The large size of the FPI anion influences the viscosity of ILs with this anion (Table 4.6).

$$V_m = V_{ion}(A^-) + V_{ion}(C^+) \qquad (4.7)$$

Figure 4.5 presents the viscosity of different FPI ILs plotted as a function of temperature. The difference in the viscosities of FPI ILs with various cations becomes very small at 80 °C. It looks that above 80 °C the weak interactions between FPI anion and organic cations are completely broken and the viscosity of FPI ILs practically doesn't depend on the size of the cation anymore. In this critical point (above 80 °C) the viscosities of different ILs become very similar.

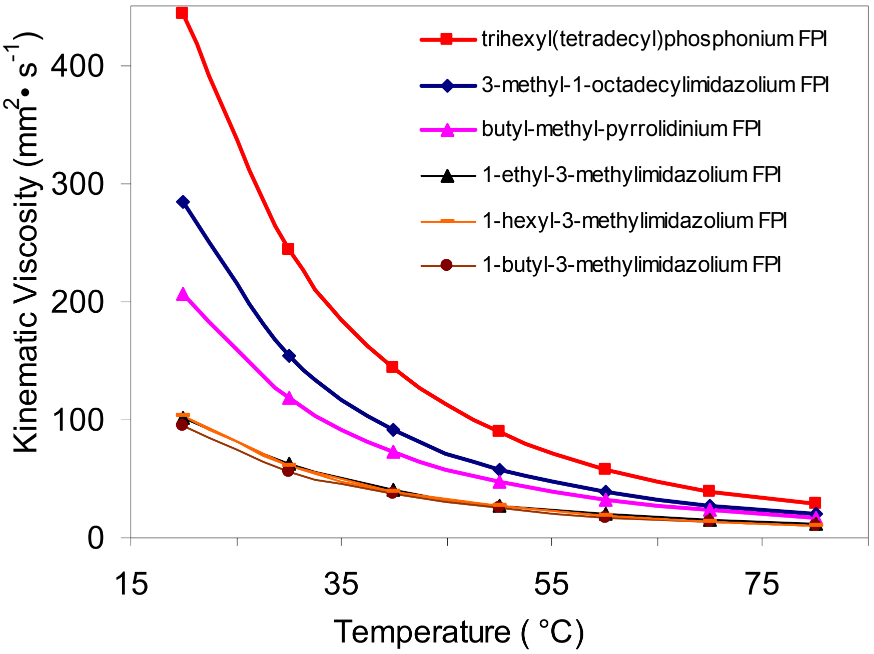

Figure 4.5 Viscosity of a series of FPI ILs as a function of temperature.

The density of FPI ILs decreases slowly with increasing the length of the alkyl chain (Table 4.6**)**. In general, the density of ILs depends on molar mass. ILs with heavier atoms tend to be more dense than those with lighter atoms (Table 4.5). Again the dominant influence of the bulky and heavy FPI anion on the density of ILs with this anion is evident (Table 4.6).

4.4.3 Melting point and glass transition temperature

Measurements of phase–transition temperatures and heat capacities were carried out with a **Netzsch DSC**, model **204** and a **Netzsch STA** thermal gravimetric analyzer, model **409**. The data were evaluated using the **Netzsch Protens 4.2** software. A temperature range between –120 and 600 °C with a heating rate of 10 °C/min under dry N_2 was employed. The glass transition temperature was determined to be a midpoint of a heat capacity range, whereas the melting and crystallization temperature were determined as the onset of the transition. For visual determinations of the melting point a **SMP 10 STUART** instrument was used.

The melting points for some FPI ILs are presented in Table 4.7. It is evident that by reducing the symmetry of the cations, an ionic liquid with a low melting point can be obtained. Also, presence of the functional group in the alkyl chain can influence the melting point: e.g. for N–(2–hydroxyethyl)–N–methylpyrrolidinium FPI (**15d**) mp =

77 °C and N–(3–ethoxy–3-oxopropy)–N–methylpyrrolidinium FPI (**16d**) mp = 13 °C were observed. Small differences in the melting point measured by means of these three different instruments were notable, but not higher than ± 2 °C. Figure 4.6 shows characteristic DSC curves for three different ILs with the FPI anion.

Table 4.7 The melting points (T_m) for some solid salts with the FPI anion.

Compound	**DSC[a]** **(T_{onset}/°C)**	**DSC[b]** **(T_{onset}/°C)**	**Visual** **(T_m/°C)**
$[Me_4N]$FPI (**11d**)	100	103	100
$[Et_3NH]$FPI (**5b**)	106	104	106
$[Et_4N]$FPI (**12d**)	–	–	46 – 47
$[Bu_4N]$FPI (**13d**)	151	151	150 – 151
$[Bu_4P]$FPI (**18d**)	143	145	144 – 145
$[(C_6H_5)_3P(CH_2C_6H_5)]$FPI(**19d**)	108	108	109 – 110
$[C(NH_2)_3]$FPI (**17d**)	–	–	52
$[C_4Py]$FPI (**9d**)	49	49	49
$[C_4dmim]$FPI (**8d**)	42	42	42
$[HOCH_2CH_2pyrr]$FPI (**15d**)	–	77	77

[a] Measured with Netzsch DSC (204) instrument.
[b] Measured with Netzsch STA (409) instrument.

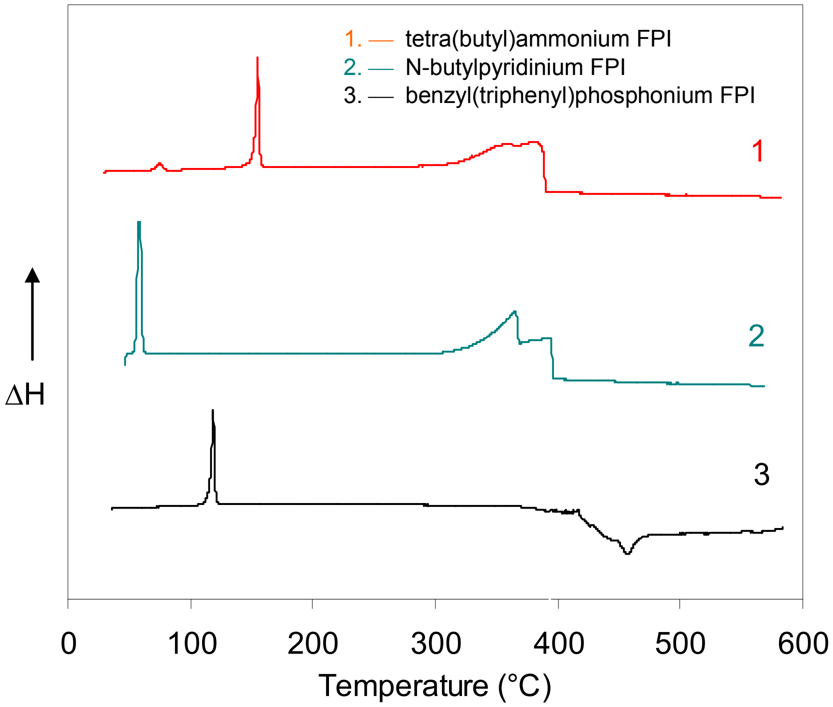

Figure 4.6 DSC curve for three FPI salts: $[Bu_4N]$FPI (T_m = 151 °C), $[C_4Py]$FPI (T_m = 49 °C) and $[(C_6H_5)_3P(CH_2C_6H_5)]$FPI ($T_m$ = 108 °C).

As it was shown earlier, a relationship between the molecular structure and the melting point of ILs was observed [139]. Table 4.8 presents the melting point of three [emim] ILs. It can be seen that the symmetry of these weekly coordinating anions (which contain P) influences strongly the melting point [56].

Table 4.8 The influence of the symmetry on the melting point of [emim] ILs.

[emim]		
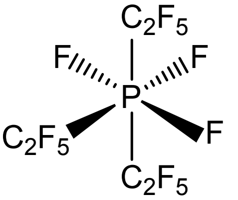	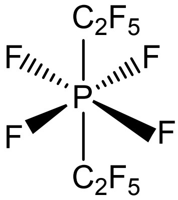	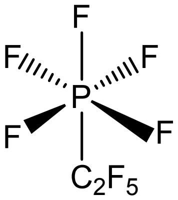
liquid at room temperature mp: –1 °C	**solid at room temperature** mp: 62 – 64 °C	**liquid at room temperature** mp: –2 °C

Not only the symmetry of anion or/and cation, but also interaction anion–cation strongly influences the melting points of organic salts (Table 4.9) [143].

Table 4.9 Melting points (T_m) of ammonium, phosphonium and pyridinium salts with different anions.

Cation	**Anion**	**T_m/ºC**	**Reference**
[Et_4N]	Cl	110	[144]
	TFSI	104	[128]
	FAP	95	[138]
	FPI	46–47	this work (**12d**)
[Bu_4P]	Cl	62–64	[145]
	TFSI	65	[146]
	FAP	74	[138]
	FPI	145	this work (**18d**)
[Bu_4N]	Cl	41	[147]
	TFSI	90	[145]
	FAP	62	[138]
	FPI	151	this work (**13d**)
[C_4Py]	Cl	103/162	[148, 149]
	TFSI	26	[150]
	FPI	49	this work (**9d**)

Beside the melting points, the crystallization and glass transition temperatures for ILs with the FPI anion have been also investigated (Table 4.10). A typical thermogram for [emim]FPI and [bmpl]FPI is shown in Figure 4.7. A glass transition temperature can be seen around –80 °C and one exothermic peak appears at around

–50 °C (–34 °C respectively). These peaks represent probably the crystallization of the supercooled liquid. In general FPI ILs show glass transition points at low temperature (Table 4.10). The subsequent endothermic peaks are attributed to the melting points.

The melting points of these ILs were also checked visually (Table 4.10). For some compounds only the glass state was observed by cooling at low temperature.

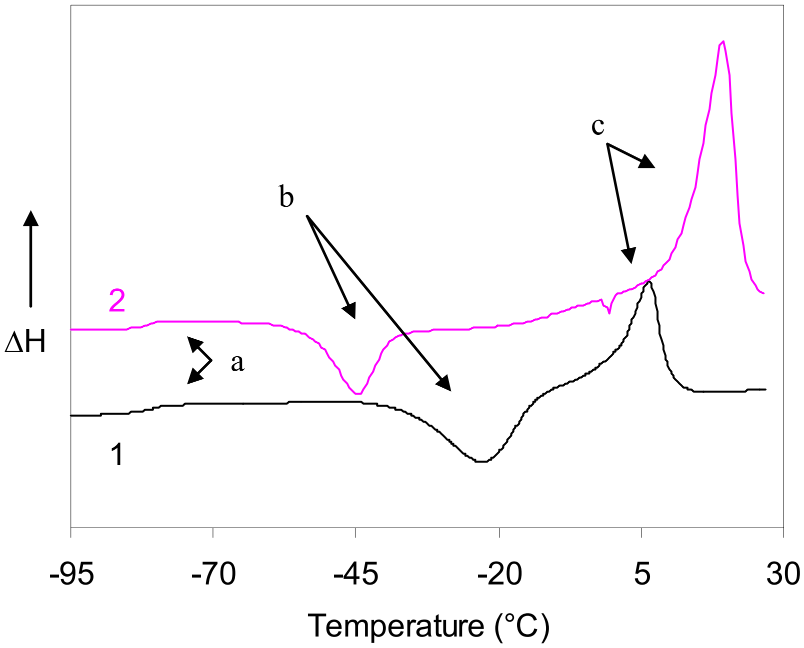

Figure 4.7 DSC curve for [bmpl]FPI (1) and [emim]FPI (2); (a) glass transition temperature (–80 °C); (b) crystallization temperature (–34 °C/ –50 °C); (c) melting point (7 °C/ 13 °C).

Table 4.10 The melting points (T_m), glass transition points (T_g) and crystallization peaks (T_{cc}) for ionic liquids containing the FPI – anion.

Compound	**DSC (T_m/°C)**	**Visual (T_m/°C)**	**T_{cc}/°C**	**T_g/°C**
[emim]FPI (**1d**)	+13	17–18	– 50	– 81[a]
[bmim]FPI (**2d**)	+ 7	[b]	–	– 82
[hmim]FPI (**3d**)	–	[b]	–	– 81
[dmim]FPI (**4d**)	+ 10 –15[a]	[b]	–	– 79
[omim]FPI (**5d**)	+ 14	16–17	–	–
[bmpl]FPI (**14d**)	+ 7	6–7	– 34	– 80[a]
[p(h3)te3]FPI (**20d**)	– 2[a]	[b]	–	– 81
[C_4dmPy]FPI (**10d**)	+ 19	21	– 31	– 67[a]

[a] In these cases the melting point and glass transition temperature peaks are week and the reported values are only approximate. [b] In these cases glass state and no melting point was observed.

4.4.4 Thermal stability

Figures 4.8 and 4.9 show characteristic TGA curves for FPI salts with organic cations. The samples were heated in an inert atmosphere (N_2) at the rate of 10 °C per min on the **TG STA 409** instrument.

The thoroughly dried compounds show no weight loss up to 280 °C. [Bu_4N]FPI (**13d**) is less thermally stable, while [Me_4N]FPI (**11d**) is the most stable one (Figure 4.8).

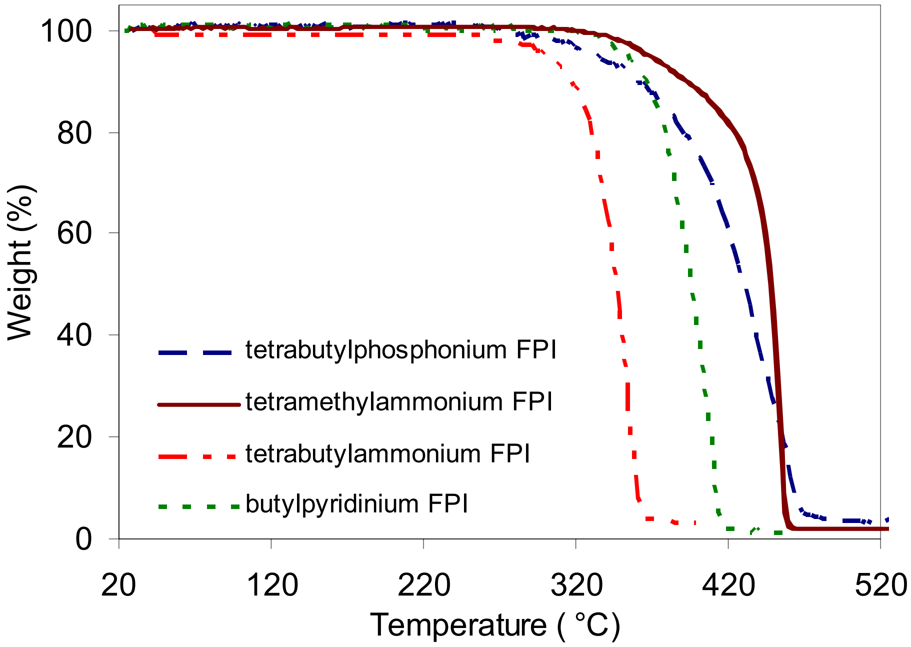

Figure 4.8 TGA for different solid salts with the FPI anion.

The TGA measurements indicate that liquid FPI ILs containing different imidazolium cations shows rather similar thermal behaviour with continuous mass loss between 300 °C and 400 °C (Figure 4.9). This behaviour is common for ILs with weakly coordinating fluoro - anions (Table 4.11).

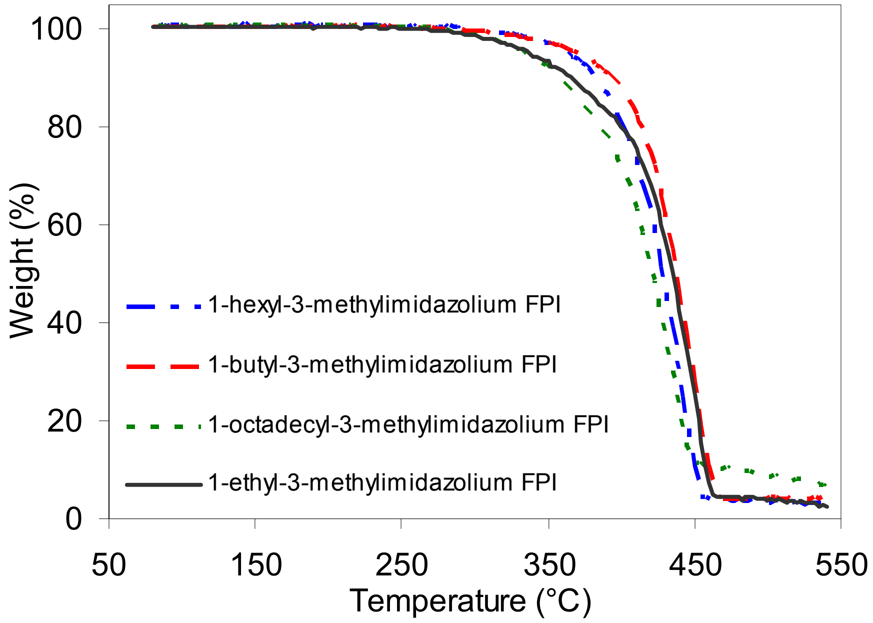

Figure 4.9 TGA for selected imidazolium ILs with the FPI anion.

The analysis of the TGA curves allowed to determine (i) the start temperature (T_{start}), the temperature at which decomposition of the sample begins (a measurable weigh loss, less than 2%) and (ii) the onset temperature (T_{onset}) – the intersection of the baseline from the beginning of the experiment and the tangent to the exothermic curve. This definition is important because many authors used the decomposition temperature as T_{start} or T_{onset} or the temperature at 10 % weight loss [150] or even 0.05% [151]. The relatively fast heating rate (10 °C/min) gives a T_{onset} of above 320 °C for FPI ILs. Moderation of the heating rate to 5 °C/min, for example for [emim]FPI, lowers T_{onset} by 40 °C. Above 450 °C the mass loss is significant for all ILs and the weight of the residue remained almost constant. The decomposition products of the FPI ILs were not investigated.

Table 4.11 Influence of some anions on degradation temperature of [emim] ILs.

[emim]X	T (decomp.)/°C	Reference
[emim]Cl	285 (pan:Al) 281 (pan:Al_2O_3)	[128]
[emim]Br	311 (pan:Al) 303 (pan:Al_2O_3)	[128]
[emim]BF_4	447 (TGA) 391 (TGA)	[152] [150]
[emim]PF_6	373 (pan:Al)	[128]

[emim]PF_6	481 (pan:Al_2O_3)	[128]
[emim]TFSI	455 (pan:Al) 453 (pan:Al_2O_3) 417 (TGA)	[128] [128] [150]
[emim]FAP	300 (TGA)	[138]
[emim]FPI	280 (TGA)	this work

It can be concluded that the thermal stability of ILs with the FPI anion are high and comparable to those ILs with other weekly coordinating anions, like TFSI or FAP anions. For example, [hmim]FAP is stable up to 290 °C and [hmim]TFSI to 302 °C at a heating rate of 10 °C/min [138, 151].

The general trend in thermal stability of ILs with different anions seems to be as follow [127, 128]:

$$\xrightarrow[\text{Decreasing thermal stability}]{(C_2F_5SO_2)_2N^- \quad (CF_3SO_2)_2N^- \quad PF_6 \quad BF_4 \quad (CF_3SO_2)_3C^- \quad AsF_6^- \quad I^- \quad Br^- \quad Cl^-}$$

4.4.5 Electrochemical stability

The electrochemical stability is another very important property of ILs. The potential windows of ILs with the FPI anion were measured using an **Autolab PGSTAT 30** instrument (Eco Chemie). Cyclic voltammograms (CV) were recorded for 0.1 mol/L solutions in CH_3CN, at glassy carbon disc (∅ 3 mm) electrode (surface area: 7.065×10^{-2} cm^2), at room temperature (23 °C) with a scan rate of 20 $mV\cdot s^{-1}$. Auxiliary Pt electrode and $Ag/AgNO_3$ (CH_3CN) as the reference electrode were used. The potential values were normalized to E° of ferrocene.

In the last decade, numerous investigations of the electrochemical properties of ILs demonstrate that $[R_3R'N]$ ILs, especially $[Et_4N]BF_4$, possess high electrochemical stability [153]. Therefore, in this work the electrochemical stability (oxidation and reduction) of two different ammonium salts have been investigated: $[Me_4N]$FPI (**11d**) and $[Bu_4N]$FPI (**13d**). The FPI ILs have an electrochemical window of about 7 V (Figure 4.10), higher than the reported value of 5.5 V for $[Me_3prN]$TFSI [154], but close to the value reported for $[Bu_4N]$FAP [138].

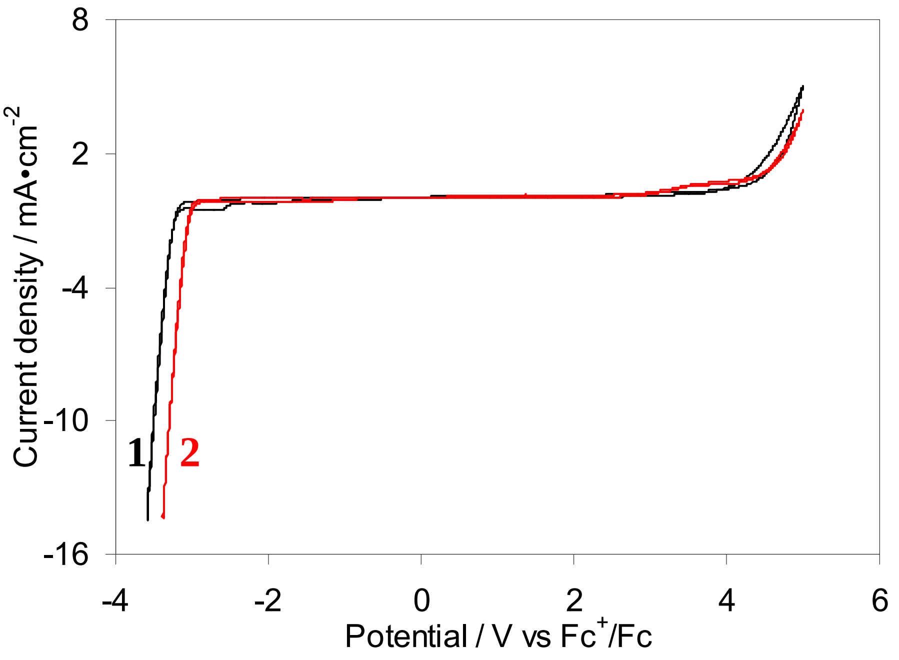

Figure 4.10 Cyclic voltammogram of [Bu$_4$N]FPI (1) and [Me$_4$N]FPI (2).

For [Bu$_4$N]FPI the irreversible reduction starts at about –3V versus F_C^+/F_C and irreversible oxidation appears at ca. 4 V.

In conclusion, the anodic stability of ILs with FPI anion is higher than for ILs with other anions: e.g. [BF$_4$] (2.2 V), [TFSI] (2.3 ÷ 2.5 V) [154], but close to FAP anion (4.0 V) [138], while the [R$_3$R'N] cations show almost the same cathodic stability, e.g. [Me$_3$BuN] (–3.3 V) or [Me$_3$N(CH$_2$OCH$_3$)] (–2.7 V) [154]. Anyway, salts with FPI anion are very attractive for electrochemical applications.

4.4.6 Conductivity

The conductivity was studied using a **703 Conductometer (Knick)** in the temperature range at –20 to +80 °C. The conductivity of 0.83 mol/L solution of [emim]FPI in acetonitrile increases linear with increasing of the temperature. The conductivity of [emim]FAP is higher than the conductivity of [emim]FPI, probably because the FAP anion is less bulky than the FPI anion.

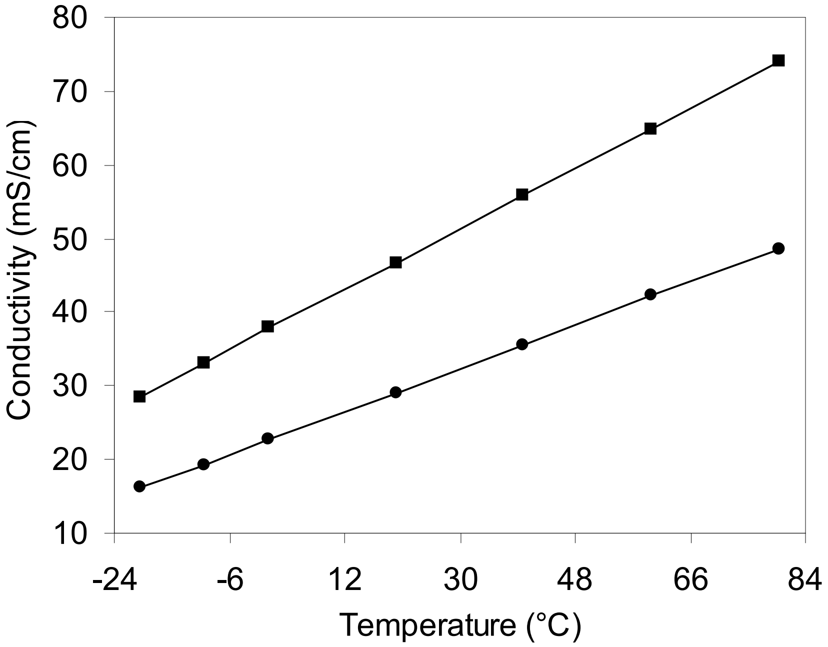

Figure 4.11 The conductivity curve for [emim]FAP (■) and for [emim]FPI (•) in acetonitrile solution (conc 0.83 mol/L).

In conclusion, ILs with FPI anion possess advanced properties as: (i) melting points below 50 °C; (ii) hydrolytic stability in neutral aqueous solution up to 100 °C; (iii) thermal stability up to 280 °C; (iv) low viscosity; (v) high electrochemical stability; and (vi) can be syntheses from industrially available materials.

4.5 Crystal structures of $[(CH_3)_4N]$FPI and $[C_7H_{16}NO]$FPI

Single crystals of $[Me_4N][\{(C_2F_5)_2P(O)\}_2N]$ suitable for X–ray diffractometry were obtained by recrystallization from an isopropanole/water solution. Single crystal diffraction data were collected at 100 K on a **Kappa CCD** diffractometer (**Bruker AXS**) using Mo–K_α radiation (λ = 0.71073 Å) and a graphite monochromator. The crystal structure of $[Me_4N][\{(C_2F_5)_2P(O)\}_2N]$ (**11d**) was solved by direct methods using SHELXS–97 and full–matrix least–squares refinement on F^2 was performed with SHELXL–97 [155]. Diffracted intensities were corrected for absorption based on indexed crystal faces, T_{min}, and T_{max}: 0.87 and 0.95. The crystal structure was determined in space group $P2_1/n$ with two independent formula units per unit cell, which are depicted in Figure 4.12.

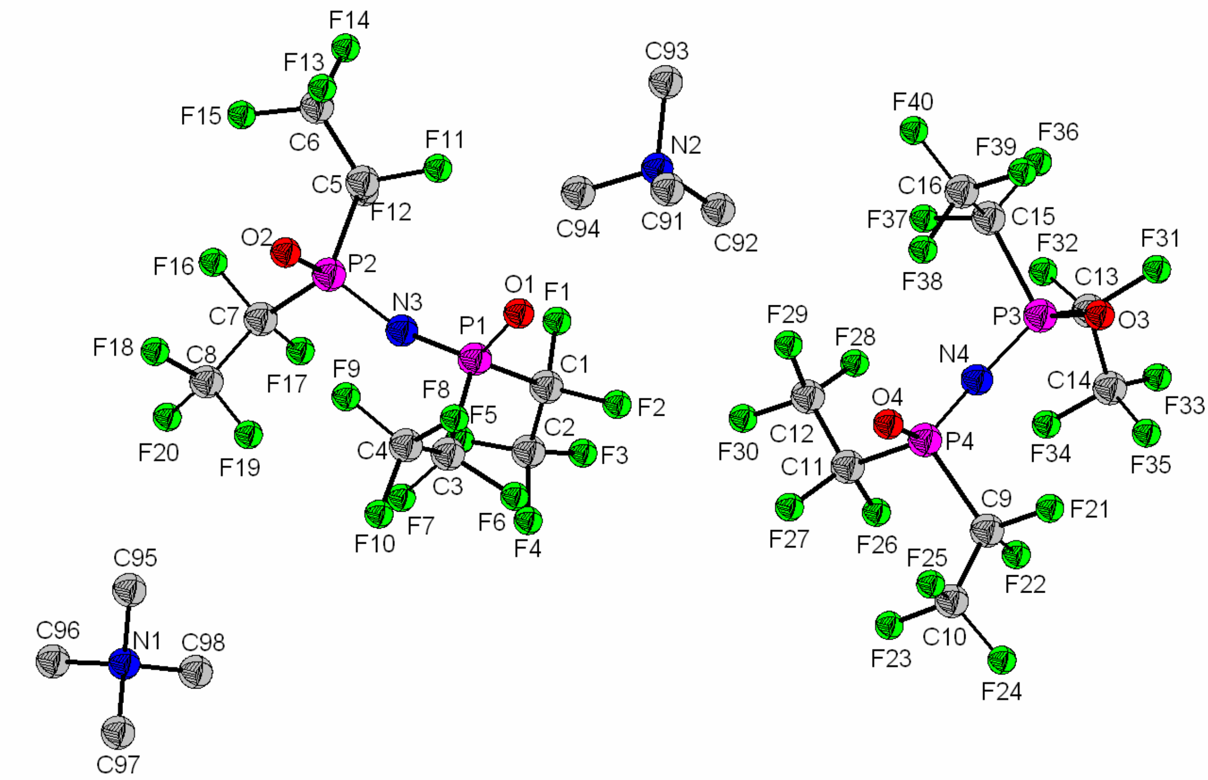

Figure 4.12 Molecular structure of two formula unit of $[Me_4N][\{(C_2F_5)_2P(O)\}_2N]$ in the unit cell.

The OPNPO skeleton of both $[(C_2F_5)_2P(O)]_2N^-$ anions shows approx. C_2 symmetry (rms 0.0624 Å) with the two P = O groups orientated *gauche* to each other *(dihedral angles of 59° and –51°)*. The C_2F_5 groups don't follow the local C_2 symmetry. Average values of selected bond lengths and angles for the anions are collected in Table 4.12 and are compared to the structural parameters of the free anion obtained from DFT calculations. The predicted and observed structural parameters are almost identical because there are no significant interionic contacts in the salt and the chosen basis set in the calculation is sufficient for this anion. The global minimum for the calculated gas–phase structure exhibits C_1 symmetry. The shortest distances between the cation and anion amount to 2.349, 2.382 and 2.392 Å for P=O…H contacts about 0.3 Å shorter than the sum of the van der Waals radii.

Table 4.12 Observed/calculated[a] average bond lengths (Å) and angles (deg.) for the $[(C_2F_5)_2P(O)]_2N^-$ anion in the $[Me_4N]FPI$ salts.

bond	obs./calc.	bond/angle	obs./calc.
CF_2–F	1.33/1.35	P=O	1.47/1.49
CF–F	1.36/1.37	P–N	1.56/1.59
C–C	1.53/1.55	P–C	1.88/1.92
		PNP	144/143

[a] B3LYP/6–31+G(d)

As input in the Gaussian 03W program (version 6.0, revision B.04) the averaged experimental geometric parameters of the anion (Figure 4.12) were used and then the structure was fully optimized at the B3LYP/6–31+G(d) level [156].

The P–N bond distances and the P–N–P angle of the FPI anion differ substantially from the related acid. The P–N bonds in FPI anion are significantly shortened 1.562(6) Å comparing to 1.670(1) Å in $iPr_2P(O)NHP(O)iPr_2$ [157] and the P–N–P angle is widened from 130.1° to 143.9(15)°. Equally long P–N distances and reduced P–N–X angles are observed from the crystal structures of other molecules containing the $R_2P(O)NR'_2$ fragment [an analysis of the CSD Ver. 5.29 (Cambridge Crystallographic Data Centre, Cambridge, U.K.) yields 1.65(2) Å for a sample consisting of 11 observations, and 126(3)° derived from 7 observations]. On the other hand there is no significant difference between the P=O distances of the FPI anion 1.471(3) Å and the HFPI acid, where this distances averages to 1.48(1) Å. The mesomeric structures rationalize this effect for the central bonds (Figure 4.13).

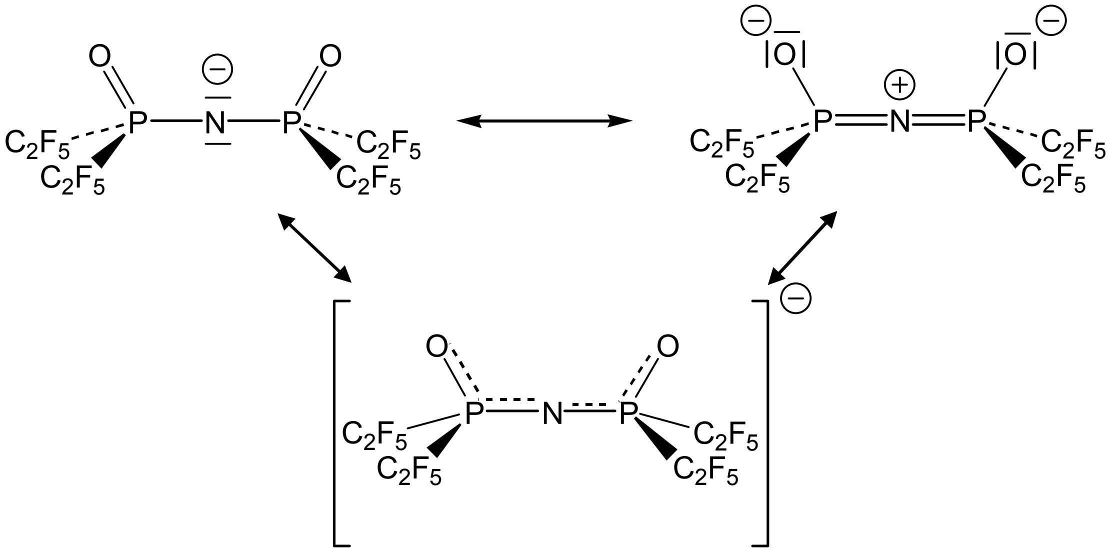

Figure 4.13 Mesomeric structures of $[(C_2F_5)_2P(O)]_2N^-$ anion.

Further analysis of the crystal structures of **11d** suggests a small but significant shortening of the C–F bonds of the terminal CF_3–groups (1.359(6) Å) compared to the CF_2–groups (1.327(5) Å) by 0.032(6) Å. At least in part, this will be due to the larger anisotropic displacement parameters of the terminal CF_3–groups, which causes an apparent reduction of the bond length [158]. This effect is also present – albeit less pronounced – in the optimized molecular structure obtained from DFT (Density Functional Theory) calculations.

Crystals of N–(2–hydroxyethyl) N–methylpyrrolidinium FPI (**15d**) suitable for X–ray diffraction were obtained from an ethanol–water solution at low temperature. A Gemini E Ultra –Diffractometer (Oxford) was used for measurements at 145 K with Mo–Kα radiation (λ = 0.717073 Å). The crystal structures were solved by direct methods using SHELXS–97 [155]. The full–matrix least–squares of refinement on F^2 was perfomed with WinGX V1.6405 (SHELXL–97). The hydrogen atoms were found on the difference maps and refined isotropically. The crystals are monoclinic (space group $P2_1$) with a = 9.2968(2), b = 10.0664(3), c= 27.2497(6) Å, and α = 90°, β = 95.379(2)°, γ = 90° as it is shown in Figure 4.14.

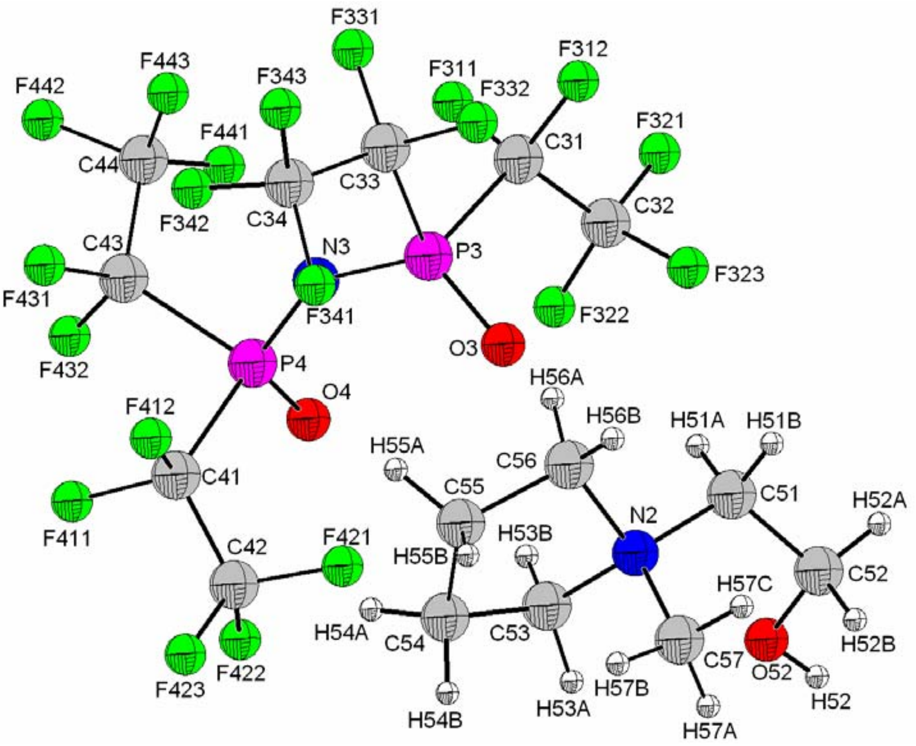

Figure 4.14 Part of the crystal structure of of $[C_7H_{16}NO]FPI$ (**15d**) in the unit cell.

In the solid–state structures of [$(CH_3)_4N$]FPI (**11d**) and [$C_7H_{16}NO$]FPI (**15d**) the parameters of the FPI anion are very similar despite of different cations. The pyrrolidinium ring in **15d** is planar. Slight differences between the pyrrolidinium ring in **15d** and [bmPyr][PF_6] can be appreciated (Table 4.13) [159]. There are no significant intermolecular contacts, but hydrogen bonding between the O donor from anion and the H acceptor from the cation is observed, shorter than usually (O…H 1.953 Å to 2.002 Å).

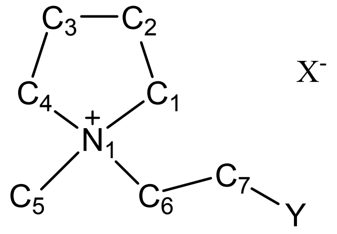

Y = OH, CH_3 and X = FPI, PF_6

Table 4.13 Observed average bond lengths (Å) and angles (deg.) for pyrrolidinium cation with different anions.

Bond/angle	[$C_7H_{16}NO$]FPI (15d)	[bmpyr][PF_6]^a
N(1) – C(5)	1.491(6)	1.496(6)
N(1) – C(6)	1.514(4)	1.509 (7)
N(1) – C(1)	1.490(6)	1.492(6)
N(1) – C(4)	1.501(4)	1.514(6)
C(1) – C(2)	1.589(7)	1.505(8)
C(3) – C(4)	1.504(6)	1.509(7)
C(2) – C(3)	1.507(8)	1.507(8)
C(5) – N(2) – C(6)	111.7(2)	108.9(4)
C(4) – N(2) – C(1)	102.9(3)	103.0(4)

[a] Ref. [159]

Table 4.14 Crystalographic and refinement data for (**11d**) and (**15d**).

Crystalographic data	$[(CH_3)_4N]$FPI (**11d**)	$[C_7H_{16}NO]$FPI (**15d**)
Empirical formula	$C_{12}H_{12}F_{20}N_2O_2P_2$	$C_{15}H_{16}F_{20}N_2O_3P_2$
Colour	colourless	colourless
Formula weight	658.18 $g \cdot mol^{-1}$	714.24 $g \cdot mol^{-1}$
Temperature	100 K	145 K
Wavelength	0.71073 Å	0.71073 Å
Crystal system	Monoclinic	Monoclinic
Space group	**$P2_1/n$, (no. 14)**	**$P2_1$, (no. 4)**
Unit cell dimensions	a = 15.7308(12) Å α= 90° b = 15.5515(13) Å β = 109.463(4)° c = 20.1328(14) Å γ = 90°	a = 9.2968(2) Å α= 90° b = 10.0664(3) Å β= 95.379(2)° c = 27.2497(6) Å γ = 90°
Volume	4643.8(6) $Å^3$	2538.95 $Å^3$
Z	8	4
Density (calculated)	1.883 $mg \cdot m^{-3}$	1.869 $mg \cdot m^{-3}$
Absorption coefficient	0.362 mm^{-1}	0.342 mm^{-1}
F(000)	2592 e	1416 e
Crystal size	0.10 x 0.02 x 0.01 mm^3	0.162 x 0.232 x 0.428 mm^3
θ range for data collection	2.91 to 31.01°	2.78 to 29.57°
Index ranges	$-22 \le h \le 22$, $-22 \le k \le 22$, $-29 \le l \le 27$	$-12 \le h \le 12$, $-13 \le k \le 12$, $-37 \le l \le 36$
Reflections collected	88109	34689
Independent reflections	14781 [R_{int} = 0.1325]	11627 [R_{int} = 0.0363]
Reflections with $I>2\sigma(I)$	6920	7203
Completeness to	(= 31.01°) 99.8 %	(= 26.4°) 89.7 %
Absorption correction	Empirical	Numerical
Max./min. transmission	0.75 and 0.49	0.905 and 0.954
Refinement method	Full-matrix least-squares on F^2	Full-matrix least-squares on F^2
Data/restraints/parameters	14781/0/693	11627/203/898
Goodness-of-fit on F^2	1.013	0.939
Final R indices $[I>2\sigma(I)]^a$	R_1 = 0.0775 wR^2 = 0.0970	R_1 = 0.0597 wR^2 = 0.1512
R indices (all data)^b	R_1 = 0.1966 wR^2 = 0.1226	R_1 = 0.0942 wR^2 = 0.1645
Largest diff. peak and hole	0.406 and -0.410 e $Å^{-3}$	0.665 and -0.350 $e \cdot Å^{-3}$

4.6 Experimental part

Chemicals were obtained from commercial suppliers and used without purifications. For all reactions deionized water was used.

1–Ethyl–3–methylimidazolium bis[bis(pentafluoroethyl)phosphinyl]imide, $[C_6H_{11}N_2][\{(C_2F_5)_2P(O)\}_2N]$ (1d)

A solution of $[C_6H_{11}N_2]Cl$ (2.49 g, 16.9 mmol) in 10 mL of water was added to the solution of $HN[P(O)(C_2F_5)_2]_2$ (9.93 g, 16.9 mmol) in 30 mL of water at room temperature. After 1 h stirring the water insoluble material was extracted with CH_2Cl_2 and washed several times with water containing of few mg of K_2CO_3. After evaporation of CH_2Cl_2, the residue was dried 24 h in vacuum at 70 °C. A liquid material (9.8 g) was obtained. Yield: 83%.
^{1}H NMR (lock/solvent CD_3CN, 400 MHz), δ, ppm: 8.46 s (CH); 7.38 s (CH); 7.32 s (CH); 4.15 q (CH_2, $^3J_{H,H}$ = 7.3 Hz); 3.80 s (CH_3); 1.44 t (CH_3, $^3J_{H,H}$ = 7.1 Hz).
^{19}F NMR (lock/solvent CD_3CN, 376.4 MHz), δ, ppm: –81.2 s ($4CF_3$); –123.7 m ($4CF_a$); –126.8 m ($4CF_b$); $^2J_{P,Fa}$ = 76 Hz; $^2J_{P,Fb}$ = 82 Hz; $^2J_{Fa,Fb}$ = 326 Hz.
^{31}P NMR (lock/solvent CD_3CN, 161.9 MHz), δ, ppm: –7.9 quin,m (2P; $^2J_{P,F}$ = 80 Hz).
Elemental analysis calcd. (%) for $C_{14}H_{11}F_{20}N_3O_2P_2$ (*M* = 695.17 g/mol): C 24.19, H 1.59, N 6.04; found: C 24.12, H 1.6, N 6.16.
% MS (ESI$^+$) {m/z calcd./m/z found [rel. int.(%)]}: [emim] {111.09/111.09 [100]}; $[C_4H_7N_2]$ {83.06/83.06 [21]}
% MS (ESI$^-$) {m/z calcd./m/z found [rel. int.(%)]}: [FPI] {583.90/583.90 [100]}.

1–Butyl–3–methylimidazolium bis[bis(pentafluoroethyl)phosphinyl]imide, $[C_8H_{15}N_2][\{(C_2F_5)_2P(O)\}_2N]$ (2d)

To the stirred solution of $[C_8H_{15}N_2]Cl$ (1.13 g, 6.4 mmol) in 5 mL of water, the solution of $HN[P(O)(C_2F_5)_2]_2$ (3.78 g, 6.4 mmol) in 10 mL of water was slowly added at room temperature. The mixture was left stirring for 30 min and the bottom liquid phase was extracted with CH_2Cl_2 and washed with water until the test for chloride was negative. After evaporation of CH_2Cl_2, the residue was dried 48 h at 70 ° C in vacuum. 3.65 g of the pure viscous liquid (**2d**) was obtained. Yield: 79%.

^{1}H NMR (lock/solvent CD_3CN, 400 MHz), δ, ppm: 8.42 s (CH); 7.35 s (CH); 7.31 s (CH); 4.1 t (CH_2, $^3J_{H,H}$ = 7.38 Hz); 3.80 s (CH_3); 1.79 quin (CH_2 ,$^3J_{H,H}$ = 7.4 Hz); 1.32 q,t (CH_2, $^3J_{H,H}$ = 7.4 Hz); 0.92 t (CH_3, $^3J_{H,H}$ = 7.4 Hz).

^{19}F NMR (lock/solvent CD_3CN, 376.4 MHz), δ, ppm: –81.2 s (4CF_3); –123.7 m (4CF_a); –126.8 m (4CF_b); $^2J_{P,Fa}$ = 76 Hz; $^2J_{P,Fb}$ = 85 Hz; $^2J_{Fa,Fb}$ = 330 Hz.

^{31}P NMR (lock/solvent CD_3CN, 161.9 MHz), δ, ppm: –8.1 quin,m (2P; $^2J_{P,F}$ = 80 Hz). Elemental analysis calcd. (%) for $C_{16}H_{15}F_{20}N_3O_2P_2$ (*M* = 723.22 g/mol): C 26.57, H 2.09, N 5.81; found: C 26.96, H 2.55, N 5.76.

1–Hexyl–3–methylimidazolium bis[bis(pentafluoroethyl)phosphinyl]imide, $[C_{10}H_{19}N_2][\{(C_2F_5)_2P(O)\}_2N]$ (3d)

To the stirred solution of $[C_{10}H_{19}N_2]Cl$ (2.8 g, 13.8 mmol) in 5 mL of water, a solution of $HN[P(O)(C_2F_5)_2]_2$ (8.1 g, 13.8 mmol) in 30 mL of water was slowly added at room temperature. After 1 h stirring the water insoluble material was extracted with CH_2Cl_2 and washed few times with water containing a few mg of K_2CO_3. After evaporation of CH_2Cl_2 and drying the residue 24 h in vacuum at 70 °C, 8.4 g of a liquid material was obtained. Yield: 81 %.

^{1}H NMR (lock/solvent CD_3CN, 400 MHz), δ, ppm: 8.42 s (CH); 7.35 s (CH); 7.31 s (CH); 4.09 t (CH_2, $^3J_{H,H}$ = 7.4 Hz); 3.80 s (CH_3); 1.80 t,t (CH_2, $^3J_{H,H}$ = 6.8 Hz); 1.30 m (3CH_2); 0.87 t (CH_3, $^3J_{H,H}$ = 6.4 Hz).

^{19}F NMR (lock/solvent CD_3CN, 376.4 MHz), δ, ppm: –81.2 s (4CF_3); –123.7 m (4CF_a); –126.8 m (4CF_b); $^2J_{P,Fa}$ = 76 Hz; $^2J_{P,Fb}$ = 85 Hz; $^2J_{Fa,Fb}$ = 330 Hz.

^{31}P NMR (lock/solvent CD_3CN, 161.9 MHz), δ, ppm: –8.0 quin,m (2P; $^2J_{P,F}$ = 80 Hz). Elemental analysis calcd. (%) for $C_{18}H_{19}F_{20}N_3O_2P_2$ (*M* = 751.28 g/mol): C 28.78, H 2.55, N 5.59; found: C 29.11, H 2.65, N 6.07.

1–Decyl–3–methylimidazolium bis[bis(pentafluoroethyl)phosphinyl]imide, $[C_{14}H_{27}N_2][\{(C_2F_5)_2P(O)\}_2N]$ (4d)

To the stirred solution of $[C_{14}H_{27}N_2]Cl$ (3.1 g, 11.9 mmol) in 15 mL of water a solution of $HN[P(O)(C_2F_5)_2]_2$ (7.0 g, 11.9 mmol) in 5 mL of water was slowly added at room temperature. After 30 min stirring, the water insoluble material was extracted with CH_2Cl_2 and washed several times with water containing a few mg of K_2CO_3. After evaporation of CH_2Cl_2, the residue was dried 16 h in vacuum at 60 °C. 8.98 g of a liquid material was obtained. Yield: 94%.

^{1}H NMR (lock/solvent CD_3CN, 400 MHz), δ, ppm: 8.45 s (CH); 7.36 s (CH); 7.32 s (CH); 4.09 t (CH_2, $^3J_{H,H}$ = 7.4 Hz); 3.80 s (CH_3); 1.26 s ($8CH_2$); 0.86 t (CH_3, $^3J_{H,H}$ = 6.4 Hz).

^{19}F NMR (lock/solvent CD_3CN, 376.4 MHz), δ, ppm: –81.2 s ($4CF_3$); –123.7 m ($4CF_a$); –126.8 m ($4CF_b$); $^2J_{P,Fa}$ = 73 Hz; $^2J_{P,Fb}$ = 82 Hz; $^2J_{Fa,Fb}$ = 327 Hz.

^{31}P NMR (lock/solvent CD_3CN, 161.9 MHz), δ, ppm: –7.9 quin,m (2P; $^2J_{P,F}$ = 80 Hz).

Elemental analysis calcd. (%) for $C_{22}H_{27}F_{20}N_3O_2P_2$ (*M* = 807.38 g/mol): C 32.73, H 3.37, N 5.20; found: C 32.17, H 3.32, N 5.08.

1–Octadecyl–3–methylimidazolim bis[bis(pentafluoroethylphosphinyl]imide, $[C_{22}H_{43}N_2][\{(C_2F_5)_2P(O)\}_2N]$ (5d)

A solution of $[C_{22}H_{43}N_2]Cl$ (3.25 g, 8.7 mmol) in 10 mL of ethanol was added at room temperature to the stirred solution of $HN[P(O)(C_2F_5)_2]_2$ (5.10 g, 8.7 mmol) in 10 mL of ethanol. The mixture was left stirring for 0.5 h. The solvent was removed in vacuum and the residue was washed with water until the test for chloride was negative. The obtained substance was dried 48 h at 60 °C in vacuum. 6.51 g of pure **5d** was obtained. Yield: 81%.

^{1}H NMR (lock/solvent CD_3CN, 400 MHz), δ, ppm: 8.43 s (CH); 7.35 m (CH); 7.32 m (CH); 4.09 t (CH_2, $^3J_{H,H}$ = 7.38 Hz); 3.80 s (CH_3); 1.80 q,t (CH_2, $^3J_{H,H}$ = 7.4 Hz); 1.26 m ($15CH_2$); 0.87 t (CH_3, $^3J_{H,H}$ = 6.8 Hz).

^{19}F NMR (lock/solvent CD_3CN, 376.4 MHz), δ, ppm: –81.1 s ($4CF_3$); –123.7 m ($4CF_a$); –126.2 m ($4CF_b$); $^2J_{P,F}$ = 74 Hz; $^2J_{P,F}$ = 86 Hz; $^2J_{Fa,Fb}$ = 317 Hz.

^{31}P NMR (lock/solvent CD_3CN, 161.9 MHz), δ, ppm: –7.9 quin,m (2P;$^2J_{P,F}$ = 80 Hz).

Elemental analysis calcd. (%) for $C_{30}H_{43}F_{20}N_3O_2P_2$ (*M* = 919.60 g/mol): C 39.18, H 4.71, N 4.57; found: C 40.19, H 5.38, N 4.57.

1–Allyl–3–methylimidazolium bromide $[C_7H_{11}N_2]Br$ (6d)

A mixture of fresh distilled 1-methyl imidazole (8.72 g, 0.106 mmol) and C_3H_5Br (12.86 g, 0.106 mmol) in 30 mL ethanol was stirred at room temperature for 6 days. Two phases were formed with viscous oil at the bottom. The phases were separated

and the pale yellow viscous liquid was washed with diethyl ether (3 x 100 mL). After drying under vacuum at 60 °C for one day, 20.92 g of **6d** was obtained. Yield: 97 %.
^{1}H NMR (lock/solvent CD_3CN, 400 MHz), δ, ppm: 8.8 s (CH); 7.5 s (2CH); 6.1 m (CH); 5.5 m (CH_2); 4.7 s (CH_2); 3.9 s (CH_3).

1–Allyl–3–methylimidazolium bis[bis(pentafluoroethyl)phosphinyl]imide, $[C_7H_{11}N_2][\{(C_2F_5)_2P(O)\}_2N]$ (7d)

Salt **6d** (1.84 g, 11.6 mmol) was dissolved in water (10 mL) and $HN[P(O)(C_2F_5)_2]_2$ (6.83 g, 11.7 mmol) aqueous solution (in 10 mL of water) was added at room temperature. After 1 h stirring the water insoluble material was extracted with CH_2Cl_2 and washed few times with water containing a few mg of K_2CO_3. After evaporation of CH_2Cl_2 the residue was dried 20 h in vacuum at 60 °C. 6.5 g of a liquid material was obtained. Yield: 79%.
^{1}H NMR (lock/solvent CD_3CN, 400 MHz), δ, ppm: 8.4 s (CH); 7.4 quint ($^3J_{H,H}$ = 1.8 Hz, 2CH); 6.0 t,t,d,d (CH, J_{trans} = 27.3 Hz, J_{cis} = 12.9 Hz, $^3J_{H,H}$ = 6.3 Hz); 5.4 m (CH_2); 4.8 d,t (CH_2, $^3J_{H,H}$ = 6.3 Hz); 3.8 s (CH_3).
^{13}C NMR (lock/solvent CD_3CN, 100.6 MHz), δ, ppm: 136.9 (N*C*N); 131.6 (CH_2=*C*HCH$_2$N); 124.8 (N*C*H); 123.3 (*C*H$_2$=CHCH$_2$N); 121.7 (*C*HN); 52.4 (N*C*H$_2$); 36.8 (N*C*H$_3$) (the signals for anion are not detected).
^{19}F NMR (lock/solvent CD_3CN, 376.4 MHz), δ, ppm: –80.7 s ($4CF_3$); –123.4 m ($4CF_a$); –126.6 m ($4CF_b$); $^2J_{P,F}$ = 67 Hz; $^2J_{P,F}$ = 89 Hz; $^2J_{Fa,Fb}$ = 314 Hz.
^{31}P NMR (lock/solvent CD_3CN, 161.9 MHz), δ, ppm: –9.4 quin,m (2P; $^2J_{P,F}$ = 78.6 Hz).
Elemental analysis calcd. (%) for $C_{15}H_{11}F_{20}N_3O_2P_2$ (*M* = 707.18 g/mol): C 25.48, H 1.57, N 5.94; found: C 25.23, H 1.37, N 5.74.

1–n–Butyl–2,3–dimethylimidazolium bis[bis(pentafluoroethyl)phosphinyl]imide $[C_9H_{17}N_2][\{(C_2F_5)_2P(O)\}_2N]$ (8d)

A solution of $HN[P(O)(C_2F_5)_2]_2$, (5.80 g, 9.9 mmol) in 10 mL water was added at room temperature to a stirred solution of $[C_9H_{17}N_2]Cl$ (1.82 g, 9.6 mmol) in 5 mL water. After 30 min the liquid phase at the bottom was extracted with CH_2Cl_2 and washed few times with water. The residue was dried under vacuum at 80 °C for 12 h. 6.1 g of a solid material (**8d**) was obtained. Yield: 86%. Mp: 42 °C.

^{1}H NMR (lock/solvent CD_3CN, 400 MHz), δ, ppm: 7.24 d (CH, $^3J_{H,H}$ = 2 Hz); 7.22 d (CH, $^3J_{H,H}$ = 2 Hz); 4.01 t (CH_2, $^3J_{H,H}$ = 7.4 Hz); 3.67 s (CH_3); 2.48 s (CH_3); 1.72 t,t (CH_2, $^3J_{H,H}$ = 7.5 Hz); 1.33 q,t (CH_2, $^3J_{H,H}$ = 7.5 Hz); 0.93 t (CH_3, $^3J_{H,H}$ = 7.4 Hz).
^{19}F NMR (lock/solvent CD_3CN, 376.4 MHz), δ, ppm: –81.1 s ($4CF_3$); –123.7 m, ($4CF_a$); –126.8 m, ($4CF_b$); $^2J_{P,Fa}$ = 75 Hz; $^2J_{P,Fb}$ = 85 Hz; $^2J_{Fa,Fb}$ = 326 Hz.
^{31}P NMR (lock/solvent CD_3CN, 161.9 MHz), δ, ppm: –8.2 quin,m (2P; $^2J_{P,F}$ = 80 Hz).
Elemental analysis calcd. (%) for $C_{17}H_{17}F_{20}N_3O_2P_2$ (*M* = 737.25 g/mol): C 27.70, H 2.32, N 5.7; found: C 27.69, H 2.25, N 5.78.

1–n–Butylpyridinium bis[bis(pentafluoroethyl)phosphinyl]imide, $[C_9H_{14}N][\{(C_2F_5)_2P(O)\}_2N]$ (9d)

A solution of $[C_9H_{14}N]Cl$ (2.0 g, 11.8 mmol) in 5 mL water was added to a vigorously stirred solution of $HN[P(O)(C_2F_5)_2]_2$ (7.0 g, 11.9 mmol) in 10 mL water. The reaction mixture was diluted with 25 mL of water and stirred additionally 30 min. The resulting solid precipitate was collected by filtration and washed three times with water until pH 6 to 7 and the test for chloride with $AgNO_3$ was negative. After drying in vacuum for 18 h at 80 °C, a white solid material (8 g) was obtained. Yield: 94%. Mp: 49 °C.
^{1}H NMR (lock/solvent CD_3CN, 400 MHz), δ, ppm: 8.67 d (2CH, $^3J_{H,H}$ = 6.1 Hz); 8.48 t (CH, $^3J_{H,H}$ = 7.8 Hz); 8.00 t (2CH, $^3J_{H,H}$ = 6.6 Hz); 4.50 t (CH_2, $^3J_{H,H}$ = 7.6 Hz); 1.92 m (CH_2); 1.35 q,t (CH_2, $^3J_{H,H}$ = 7.4 Hz); 0.94 t (CH_3, $^3J_{H,H}$ = 7.4 Hz).
^{19}F NMR (lock/solvent CD_3CN, 376.4 MHz), δ, ppm: –81.1 s ($4CF_3$); –123.7 m ($4CF_a$); –126.8 m ($4CF_b$); $^2J_{P,Fa}$ = 69 Hz; $^2J_{P,Fb}$ = 79 Hz; $^2J_{Fa,Fb}$ = 314 Hz.
^{31}P NMR (lock/solvent CD_3CN, 161.9 MHz), δ, ppm: –8.2 quin,m (2P; $^2J_{P,F}$ = 80 Hz).
Elemental analysis calcd. (%) for $C_{17}H_{17}F_{20}N_3O_2P_2$ (*M* = 737.25 g/mol): C 28.35, H 1.96, N 3.89; found: C 27.91, H 1.82, N 3.88.
% MS (ESI$^+$) {m/z calcd./m/z found [rel. int.(%)]}: [C_4Py] {136.11/136.11 [100]}; [C_5H_6N] {80.05/80.04 [18]}
% MS (ESI$^-$) {m/z calcd./m/z found [rel. int.(%)]}: [FPI] {583.90/583.90 [100]}.

1–n–Butyl–3,5–dimethylpyridinium bis[bis(pentafluoroethyl)phosphinyl]imide, $[C_{11}H_{18}N][\{(C_2F_5)_2P(O)\}_2N]$ (10d)

To the stirred solution of $[C_{11}H_{18}N]Cl$ (2.11 g, 10.5 mmol) in 5 mL of water, 6.20 g (10.6 mmol) of $HN[P(O)(C_2F_5)_2]_2$ in 10 mL of water was added at room temperature.

After 10 min two phases were formed. The reaction mixture was stirred for 30 min. The upper phase, containing unreacted starting material and HCl was removed from the mixture. The bottom phase was collected and approximately equal volume of CH_2Cl_2 was added. This solution was transferred to a separatory funnel and washed several times with water. The CH_2Cl_2 solvent was evaporated and the residue was dried for 18 h in vacuum at 60 °C resulting in a liquid material (6.90 g). Yield: 88%.
^{1}H NMR (lock/solvent CD_3CN, 400 MHz), δ, ppm: 8.35 s (2CH); 8.11 s (CH); 4.39 t (CH_2, $^3J_{H,H}$ = 7.6 Hz); 2.45 s ($2CH_3$); 1.92 m (CH_2); 1.34 q,t (CH_2, $^3J_{H,H}$ = 7.4 Hz); 0.94 t (CH_3, $^3J_{H,H}$ = 7.4 Hz).
^{19}F NMR (lock/solvent CD_3CN, 376.4 MHz), δ, ppm: –81.1 s ($4CF_3$); –123.7 m ($4CF_a$); –126.8 m ($4CF_b$); $^2J_{P,Fa}$ = 74 Hz; $^2J_{P,Fb}$ = 83 Hz; $^2J_{Fa,Fb}$ = 314 Hz.
^{31}P NMR (lock/solvent CD_3CN, 161.9 MHz), δ, ppm: –8.2 quin,m (2P; $^2J_{P,F}$ = 80 Hz).
Elemental analysis calcd. (%) for $C_{19}H_{18}F_{20}N_2O_2P_2$ (*M* = 748.27 g/mol): C 30.50, H 2.42, N 3.74; found: C 29.90, H 2.24, N 3.72.

Tetramethylammonium bis[bis(pentafluoroethyl)phosphinyl]imide, $[(CH_3)_4N][\{(C_2F_5)_2P(O)\}_2N]$ (11d)

To a solution of 0.3 g (2.7 mmol) of $[(CH_3)_4N]Cl$ in water (5 mL) a solution of 1.6 g (2.7 mmol) of $HN[P(O)(C_2F_5)_2]_2$ in 5 mL water was added by stirring at room temperature. The mixture was left stirring for 20 minute and the white precipitate was filtered off and washed four times with 20 mL of water until the test for chloride was negative. The product was dried in vacuum at 50 °C for 3 h. 1.68 g of **11d** was obtained. Single crystals were obtained from recrystallization in isopropanole/H_2O solution. Yield: 93 %. Mp: 100 °C.
^{1}H NMR (lock/solvent CD_3CN, 400 MHz), δ, ppm: 3.06 s (CH_3).
^{19}F NMR (lock/solvent CD_3CN, 376.4 MHz), δ, ppm: –79.9 s ($4CF_3$); –122.9 m ($4CF_a$); –126 m ($4CF_b$); $^2J_{P,Fa}$ = 73 Hz; $^2J_{P,Fb}$ = 82 Hz; $^2J_{Fa,Fb}$ = 325 Hz.
^{31}P NMR (lock/solvent CD_3CN, 161.9 MHz), δ, ppm: –9.0 quin,m (2P; $^2J_{P,F}$ = 78 Hz).
Elemental analysis calcd. (%) for $C_{12}H_{12}F_{20}N_2O_2P_2$ (*M* = 685.15 g/mol): C 21.90, H 1.84, N 4.26; found: C 21.89, H 1.80, N 4.09.

Tetraethylammonium bis[bis(pentafluoroethyl)phosphinyl]imide, $[(C_2H_5)_4N][\{(C_2F_5)_2P(O)\}_2N]$ (12d)

A 20% aqueous solution of Et_4NOH (5.55 g, 7.53 mmol) was slowly added to the solution of $HN[P(O)(C_2F_5)_2]_2$ (4.41 g, 7.53 mmol) in 15 mL water by stirring and cooling of the reaction mixture with an ice water bath until the reaction mixture was neutral. The reaction mixture was stirred additionally 30 minute at room temperature. The resulting mixture was concentrated by rotary evaporator. The residue was dissolved and stirred in 10 mL dioxane for 30 min. After the dioxane was distilled off, a very hygroscopic colourless solid remains in the reaction flask. The product (5 g, yield 94%) was dried at 60 °C in vacuum for ca. 12 hours. It contains 12 ppm of water was measured by Karl–Fischer titration. Mp: 46 – 47 °C.

^{1}H NMR (lock/solvent CD_3CN, 400 MHz), δ, ppm: 3.15 q ($4CH_2$, $^3J_{H,H}$ = 7.1 Hz); 1.19 t,m ($4CH_3$, $^3J_{H,H}$ = 7.1 Hz).

^{19}F NMR (lock/solvent CD_3CN, 376.4 MHz), δ, ppm: –81.1 s ($4CF_3$); –123.7 m ($4CF_a$); –126.8 m ($4CF_b$); $^2J_{P,Fa}$ = 81 Hz; $^2J_{P,Fb}$ = 87 Hz; $^2J_{Fa,Fb}$ = 320 Hz.

^{31}P NMR (lock/solvent CD_3CN, 161.9 MHz), δ, ppm: –8.2 quin,m (2P; $^2J_{P,F}$ = 80 Hz).

Elemental analysis calcd. (%) for $C_{16}H_{20}F_{20}N_2O_2P_2$ (M = 714.26 g/mol): C 26.91, H 2.82, N 3.92; found: C 26.92, H 2.76, N 3.98.

Tetra(n–butyl)ammonium bis[bis(pentafluoroethyl)phosphinyl]imide, $[(C_4H_9)_4N][\{(C_2F_5)_2P(O)\}_2N]$ (13d)

To the solution of $[(C_4H_9)_4N]Br$ (1.23 g, 3.8 mmol) in 5 mL of water was slowly added a solution of $HN[P(O)(C_2F_5)_2]_2$ (2.23 g, 3.8 mmol) in 5 mL of water under stirring at room temperature. The mixture was left stirring for 30 minute and the liquid bottom phase was extracted with 10 mL of CH_2Cl_2. The extract was washed four times with 40 mL of water until the test for bromide with $AgNO_3$ was negative. The CH_2Cl_2 solvent was evaporated and the residue was dried 18 h in vacuum ($<10^{-3}$ mbar) at 60 °C. Yield: 87%. Mp: 150 – 151 °C.

^{1}H NMR (lock/solvent CD_3CN, 400 MHz), δ, ppm: 3.07 m ($4CH_2$); 1.59 m ($4CH_2$); 1.34 q,t ($4CH_2$, $^3J_{H,H}$ = 7.3 Hz); 0.95 t ($4CH_3$, $^3J_{H,H}$ = 7.4 Hz).

^{19}F NMR (lock/solvent CD_3CN, 376.4 MHz), δ, ppm: –81.2 s ($4CF_3$); –123.7 m ($4CF_a$); –126.8 m ($4CF_b$); $^2J_{P,Fa}$ = 76 Hz; $^2J_{P,Fb}$ = 82 Hz; $^2J_{Fa,Fb}$ = 330 Hz.

^{31}P NMR (lock/solvent CD_3CN, 161.9 MHz), δ, ppm: –8.4 quin,m (2P; $^2J_{P,F}$ = 79 Hz).

Elemental analysis calcd. (%) for $C_{24}H_{36}F_{20}N_2O_2P_2$ (*M* = 826.47 g/mol): C 34.88, H 4.39, N 3.39; found: C 34.95, H 4.55, N 3.34.
% MS (ESI$^+$) {m/z calcd./m/z found [rel. int.(%)]}: [Bu_4N] {242.28/282.28 [100]}; [$C_{12}H_{28}N$] {186.22/186.22} [0.5]
% MS (ESI$^-$) {m/z calcd./m/z found [rel. int.(%)]}: [FPI] 583.90/583.91 [100].
IR (KBr pellet): ν (cm^{-1}) = 3050 (w); 2972 (vw); 1628 (br. w); 1495 (s); 1420 (br. m); 1380 (s); 1307 (s); 1263 (vs); 1231 (br. vs); 1210 (vs);1150 (vs); 991 (s); 952 (m); 773 (w); 753 (m); 629 (m); 597 (m); 564 (s); 511 (s); 477 (s); 426 (m).

1–n–Butyl–1–methylpyrrolidinium bis[bis(pentafluoroethyl)phosphinyl]imide [$C_9H_{20}N$][{$(C_2F_5)_2P(O)$}$_2$N] (14d)

To the stirred solution of [$C_9H_{20}N$]Cl (1.46 g, 8.2 mmol) in 4 mL of water was slowly added a solution of $HN[P(O)(C_2F_5)_2]_2$ (4.83 g, 8.2 mmol) in 10 mL of water. The reaction proceeds within few minutes. The water insoluble material was extracted with CH_2Cl_2 and washed three times with water. After drying, 5 g of liquid material (**14d**) was obtained. Yield: 84 %.
^{1}H NMR (lock/solvent CD_3CN, 400 MHz), δ, ppm: 3.38 m (2CH_2); 3.21 m (CH_2); 2.92 s (CH_3); 2.13 m (2CH_2); 1.70 m (CH_2); 1.35 q,t (CH_2, $^3J_{H,H}$ = 7.4 Hz); 0.95.t (CH_3, $^3J_{H,H}$ = 7.3 Hz).
^{19}F NMR (lock/solvent CD_3CN, 376.4 MHz), δ, ppm: –81.0 s (4CF_3); –123.7 m (4CF_a); –126.8 m (4CF_b); $^2J_{P,Fa}$ = 78 Hz; $^2J_{P,Fb}$ = 89 Hz; $^2J_{Fa,Fb}$ = 318 Hz.
^{31}P NMR (lock/solvent CD_3CN, 161.9 MHz), δ, ppm: –7.9 quin,m (2P; $^2J_{P,F}$ = 81 Hz).
Elemental analysis calcd. (%) for $C_{17}H_{20}F_{20}N_2O_2P_2$ (*M* = 726.27 g/mol): C 28.11, H 2.78, N 3.86; found: C 28.15, H 2.25, N 4.22.
% MS (ESI$^+$) {m/z calcd./m/z found [rel. int.(%)]}: [bmpl] {142.15/142.15 [100]}; [$C_5H_{12}N$] {86.09/86.09 [3]}
% MS (ESI$^-$) {m/z calcd./m/z found [rel. int.(%)]}: [FPI] {583.90/583.90 [100]}.

N–(2–hydroxyethyl)–N–methylpyrrolidinium bis[bis(pentafluoroethyl)phosphinyl]imide [$C_7H_{16}NO$][{$(C_2F_5)_2P(O)$}$_2$N] (15d)

N–(acetyloxy)ethyl N–methylpyrrolidinium bromide (3.02 g, 11.9 mmol) was dissolved in approximately 15 mL of water. An equimolar amount of $HN[P(O)(C_2F_5)_2]_2$ (7.01 g, 11.9 mmol) in 10 mL water was added at RT. After few minutes a viscous liquid phase was formed on the bottom of the flask. The aqueous phase containing HBr was removed and the residue was washed with water two times. The separation becomes more difficult and the water turned cloudy. Then, a white product precipitates. The precipitation was accelerated under cooling with ice. The resulting white product was filtered off and dried for 18 h in vacuum. The further purification was done by crystallization from ethanol and water at 0 °C. Yield: 60%. Mp: 76 °C.

^{1}H NMR (lock/solvent $CDCl_3$, 400 MHz), δ, ppm: 3.9 m (CH_2); 3.5 m (CH_2); 3.4 t ($2CH_2$, $^3J_{H,H}$ = 4.9 Hz); 3 s (CH_3); 2.1 br.s (OH); 1.9 q ($2CH_2$, $^3J_{H,H}$ = 2.4 Hz).

^{13}C NMR (lock/solvent $CDCl_3$, 100.6 MHz), δ, ppm: 64.92 (NCH_2CH_2OH); 64.94 (CH_2CH_2OH); 55.78 (NCH_2CH_2); 48.23 (NCH_3); 20.73 (CH_2–Ar).

^{19}F NMR (lock/solvent $CDCl_3$, 376.4 MHz), δ, ppm: –81.1 s ($4CF_3$); –123.7 m ($4CF_a$); –126.8 m ($4CF_b$); $^2J_{P,Fa}$ = 74 Hz; $^2J_{P,Fb}$ = 79 Hz; $^2J_{Fa,Fb}$ = 322 Hz.

^{31}P NMR (lock/solvent $CDCl_3$, 161.9 MHz), δ, ppm: –8.0 quin,m (2P;$^2J_{P,F}$ = 79 Hz).

Elemental analysis calcd. (%) for $C_{15}H_{16}F_{20}N_2O_3P_2$ (mol. mass 714.21): C 25.22, H 2.26, N 3.92; found: C 25.37, H 2.26, N 3.80.

N–(3–ethoxy–3-oxopropy)–N–methylpyrrolidinium bis[bis(pentafluoroethyl)phosphinyl]imide [$C_{10}H_{20}NO_2$][{(C_2F_5)$_2$P(O)}$_2$N] (16d)

A solution of [$C_{10}H_{20}NO_2$][CF_3SO_2] (4 g, 11.9 mmol) in 10 mL of water was added to the solution of $HN[P(O)(C_2F_5)_2]_2$ (7 g, 11.9 mmol) in 10 mL of water at room temperature. After 40 min stirring the water insoluble material was extracted with CH_2Cl_2 and washed few times with water containing of few mg of K_2CO_3. After evaporation of CH_2Cl_2 the residue was dissolved and stirred in 30 mL ethanol for 30 min. The ethanol was distilled off and a very viscous yellow material (6.6 g) was obtained. Yield: 72%.

^{1}H NMR (lock/solvent CD_3CN, 400 MHz), δ, ppm: 4.2 q (CH_2; $^3J_{H,H}$ = 7.2 Hz); 3.6 t (CH_2; $^3J_{H,H}$ = 7.4 Hz); 3.4 m ($2CH_2$); 2.9 s (CH_3); 2.9 t (CH_2; $^3J_{H,H}$ = 7.5 Hz); 2.9 s ($2CH_2$); 1.2 t (CH_3; $^3J_{H,H}$ = 7 Hz).

^{13}C NMR (lock/solvent CD_3CN, 100.6 MHz), δ, ppm: 169.8 (CH_2COO); 64.3 (OCH_2CH_3); 61.2 (NCH_2CH_2); 59.2 (NCH_2CH_2); 28.3 (CH_2CH_2O); 20.9 (CH_2–Ar); 12.92 (CH_2CH_3) (the signals for anion are not detected).

^{19}F NMR (lock/solvent CD_3CN, 376.4 MHz), δ, ppm: –81.1 s ($4CF_3$); –123.7 m ($4CF_a$); –126.8 m ($4CF_b$); $^2J_{P,Fa}$ = 73 Hz; $^2J_{P,Fb}$ = 83 Hz; $^2J_{Fa,Fb}$ = 318 Hz.

^{31}P NMR (lock/solvent CD_3CN, 161.9 MHz), δ, ppm: –8.0 quin,m (2P;$^{2}J_{P,F}$ = 78 Hz).

Guanidinium bis[bis(pentafluoroethyl)phosphinyl]imide, $[(NH_2)_3C][\{(C_2F_5)_2P(O)\}_2N]$ (17d)

To the stirred solution of $HN[P(O)(C_2F_5)_2]_2$ (1.80 g, 3.1 mmol) in 5 mL water, solid $[(NH_2)_3C]_2[CO_3]$ (0.28 g, 1.5 mmol) was slowly added at 0 °C. The reaction mixture was stirred at this temperature for 20 min and left to warm up to room temperature. After 30 min stirring at room temperature the precipitate was separated by filtration and washed with cold water several times. After drying in vacuum, 1.68 g of a very hygroscopic white solid material was obtained. Yield: 84 %. Mp: 52 °C.

^{1}H NMR (lock/solvent CD_3CN, 400 MHz), δ, ppm: 5.92 br.s ($3NH_2$).

^{19}F NMR (lock/solvent CD_3CN, 376.4 MHz), δ, ppm: –81.2 s ($4CF_3$); –123.9 m ($4CF_a$); –126.8 m ($4CF_b$); $^{2}J_{P,Fa}$ = 86 Hz; $^{2}J_{P,Fb}$ = 81 Hz; $^{2}J_{Fa,Fb}$ = 316 Hz.

^{31}P NMR (lock/solvent CD_3CN, 161.9 MHz), δ, ppm: –6.5 quin,m (2P; $^{2}J_{P,F}$ = 82 Hz).

Elemental analysis calcd. (%) for $C_9H_6F_{20}N_4O_2P_2$ (*M* = 644.09 g/mol): C 16.78, H 0.94, N 8.7; found: C 16.83, H 0.86, N 8.54.

Tetra(n–butyl)phosphonium bis[bis(pentafluoroethyl)phosphinyl]imide, $[(C_4H_9)_4P][\{(C_2F_5)_2P(O)\}_2N]$ (18d)

A solution of $[(C_4H_9)_4P]Br$ (1.15 g, 3.38 mmol) in 10 mL of water was slowly added to the stirred solution of $HN[P(O)(C_2F_5)_2]_2$ (1.99 g, 3.4 mmol) in 10 mL of water at room temperature. The mixture was left stirring for 30 minute and the white precipitate was filtered off and washed three times with 30 mL of water. After drying, 2.47 g of a white solid material was obtained. Yield: 86%. Mp: 143 – 145 °C.

^{1}H NMR (lock/solvent CD_3CN, 400 MHz), δ, ppm: 2.00 to 2.10 m ($4CH_2$); 1.47 m ($8CH_2$); 0.93 t ($4CH_3$, $^{3}J_{H,H}$ = 7.1Hz).

^{19}F NMR (lock/solvent CD_3CN, 376.4 MHz), δ, ppm: –81.1 s ($4CF_3$); –123.7 m ($4CF_a$); –126.8 m ($4CF_b$); $^{2}J_{P,Fa}$ = 79 Hz; $^{2}J_{P,Fb}$ = 89 Hz; $^{2}J_{Fa,Fb}$ = 322 Hz.

^{31}P NMR (lock/solvent CD_3CN, 161.9 MHz), δ, ppm: 34.9 m (1P); –8.3 quin,m (2P; $^{2}J_{P,F}$ = 80 Hz).

Elemental analysis calcd. (%) for $C_{24}H_{39}F_{20}NO_2P_3$ (*M* = 843.44 g/mol): C 34.18, H 4.30, N 1.66; found: C 34.42, H 4.71, N 1.65.

IR (KBr pellet): ν (cm^{-1}) = 2976 (m); 2946 (m); 2885 (m); 1470 (s); 1427 (br. s); 1391 (s); 1309 (br. s); 1271 (vs); 1237 (vs); 1217 (vs);1192 (s); 1147 (br. vs); 1139 (br. vs); 1119 (s); 980 (s); 973 (br. s); 923 (m); 911 (m); 816 (br. m); 762 (w); 753 (m); 722 (br. w); 632 (m); 596 (m); 563 (s); 510 (br. s); 501 (s); 482 (s); 429 (m).

Benzyl(triphenyl)phosphonium bis[bis(pentafluoroethyl)phosphinyl]imide, $[(C_6H_5)_3P(CH_2C_6H_5)][\{(C_2F_5)_2P(O)\}_2N]$ (19d)

To the stirred solution of $[(C_6H_5)_3P(CH_2C_6H_5)]Cl$ (0.83 g, 2.1 mmol) in 5 mL of water, a solution of $HN[P(O)(C_2F_5)_2]_2$ (1.25 g, 2.1 mmol) in 5 mL of water was slowly added at room temperature. The mixture was kept stirring for one hour at room temperature. The water insoluble material was extracted with CH_2Cl_2 and washed with water two times. After evaporation of CH_2Cl_2 and drying, 1.48 g of a pure white solid (**19d**) was obtained. Yield: 75 %. Mp: 110 °C.

^{1}H NMR (lock/solvent CD_3CN, 400 MHz), δ, ppm: 7.9 m (3CH, $^3J_{H,H}$ = 7.6 Hz); 7.6 m (6CH); 7.5 m (6CH); 7.3 m (CH); 7.2 t (2CH, $^3J_{H,H}$ = 7.6 Hz); 6.9 d, m (2CH, $^3J_{H,H}$ = 7.1 Hz); 4.61 d (CH_2P; $^2J_{P,H}$ =14.7 Hz).

^{19}F NMR (lock/solvent CD_3CN, 376.4 MHz), δ, ppm: –81.1 s ($4CF_3$); –123.7 m ($4CF_a$); –126.8 m ($4CF_b$); $^2J_{P,Fa}$ = 78 Hz; $^2J_{P,Fb}$ = 85 Hz; $^2J_{Fa,Fb}$ = 320 Hz.

^{31}P NMR (lock/solvent CD_3CN, 161.9 MHz), δ, ppm: 23.7 s (1P); –8.3 quin,m (2P; $^2J_{P,F}$ = 80 Hz).

Elemental analysis calcd. (%) for $C_{33}H_{22}F_{20}NO_2P_3$ (*M* = 937.42 g/mol): C 42.28, H 2.37, N 1.49; found: C 42.55, H 0.56, N 1.50.

Trihexyl(tetradecyl)phosphonium bis[bis(pentafluoroethyl)phosphinyl]imide, $[(C_6H_{13})_3P(C_{14}H_{29})][\{(C_2F_5)_2P(O)\}_2N]$ (20d)

To the stirred solution of $[(C_6H_{13})_3P(C_{14}H_{29})]Cl$ (4.11 g, 7.9 mmol) in 13 mL of ethanol, 4.62 g (7.9 mmol) of $HN[P(O)(C_2F_5)_2]_2$ in 20 mL of water was added. The mixture was kept stirring for 1 hour. After the ethanol was distilled off in vacuum, the liquid material was washed with water three times. After drying, 7.24 g of a liquid material was obtained. Yield: 86 %.

^{1}H NMR (lock/solvent CD_3CN, 400 MHz), δ, ppm: 2.01 to 2.08 m ($4CH_2$); 1.38 to 1.54 m ($8CH_2$); 1.28 to 1.33 m ($16CH_2$); 0.86 to 0.91 m ($4CH_3$).

^{19}F NMR (lock/solvent CD_3CN, 376.4 MHz), δ, ppm: –81.0 s ($4CF_3$); –123.6 m ($4CF_a$); –126.7 m ($4CF_b$); $^2J_{P,Fa}$ = 74 Hz; $^2J_{P,Fb}$ = 80 Hz; $^2J_{Fa,Fb}$ = 318 Hz.
^{31}P NMR (lock/solvent CD_3CN, 161.9 MHz), δ, ppm: 34.7 m (1P); –8.3 quin,m (2P; $^2J_{P,F}$ = 80 Hz).
Elemental analysis calcd. (%) for $C_{40}H_{68}F_{20}NO_2P_3$ (*M* = 1067.86 g/mol): C 44.83, H 5.88, N 1.62; found: C 44.99, H 6.42, N 1.31.
IR (ATR_IR/neat liquid): ν (cm^{-1}) = 2958 (br. m); 2931 (m); 2859 (m); 1387 (s); 1304 (s); 1267 (s); 1216 (vs); 1143 (vs); 1121 (br. m); 985 (s); 874 (br. w); 827 (br. w); 751 (w); 721 (br. w); 627 (m); 595 (m); 563 (s); 507 (br. s); 477 (br. s); 427 (m).

N–ethylbenzothiazolium bis[bis(pentafluoroethyl)phosphinyl]imide, [(C_6H_4)SCHNC_2H_5][{(C_2F_5)$_2$P(O)}$_2$N] (21d)

A solution of [(C_6H_4)SCHNC_2H_5]Br (0.21 g, 0.85 mmol) in 5 mL of water was slowly added to the stirred solution of HN[P(O)(C_2F_5)$_2$]$_2$ (0.5 g, 0.85 mmol) in 5 mL of water at room temperature. The mixture was left stirring for 30 minutes. The water phase turned cloudy and a white precipitate formation was accelerated by cooling of the reaction mixture with ice bath. The product was washed three times with water and then dissolved in 30 mL of ethanol and stirred for 30 min. The ethanol was distilled off and 0.6 g of a white material (**21d**) was obtained. Yield: 94%. Mp: 68 °C.
^{1}H NMR (lock/solvent $CDCl_3$, 400 MHz), δ, ppm: 11.1 s (CH); 8.2 d (CH, $^3J_{H,H}$ = 7.5 Hz); 8.0 d (CH, $^3J_{H,H}$ = 7.5 Hz); 7.9 t (CH, $^3J_{H,H}$ = 7.2 Hz); 7.8 t ($^3J_{H,H}$ = 8.2 Hz, CH); 4.9 q (CH_2, $^3J_{H,H}$ = 7.3 Hz); 1.7 t (CH_3, $^3J_{H,H}$ = 7.3 Hz).
^{13}C NMR (lock/solvent $CDCl_3$, 100.6 MHz), δ, ppm: 164.5 (NCS); 139.7, 130.3, 129.3, 124.6, 116.1 (C–Ar); 48.9 ($\mathit{C}H_2CH_3$); 14.5 ($CH_2\mathit{C}H_3$).
^{19}F NMR (lock/solvent $CDCl_3$, 376.4 MHz), δ, ppm: –79.9 s ($4CF_3$); –123.0 m ($4CF_a$); –125.4 m ($4CF_b$); $^2J_{P,Fa}$ = 79 Hz; $^2J_{P,Fb}$ = 88 Hz; $^2J_{Fa,Fb}$ = 324 Hz.
^{31}P NMR (lock/solvent $CDCl_3$, 161.9 MHz), δ, ppm: –3.1 quin,m (2P;$^2J_{P,F}$ = 80 Hz).
Elemental analysis calcd. (%) for $C_{17}H_{10}F_{20}NO_2P_2S$ (*M* = 747.96 g/mol): C 27.29, H 1.35, N 3.74, S 4.29; found: C 27.25, H 1.76, N 3.66, S 3.79.

Chapter 5

5. Ionic liquids with the [bis(pentafluoroethyl)phosphinyl–(trifluoromethyl)sulfonyl]imide (PSI) anion

There are only two reports about ILs composed by an asymmetrical imide anions: $[(CF_3SO_2)(CF_3CO)N]^-$ [160], $[(CF_3SO_2)(C_2F_5SO_2)N]^-$ and $[(FSO_2)(CF_3SO_2)N]^-$ [161]. Quaternary ammonium salts with these anions afford low melting points ILs possessing low viscosities.

Therefore, synthesis and characterization of ILs with an asymmetrical [bis(pentafluoroethyl)phosphinyl–(trifluoromethyl)sulfonyl]imide anion, $[\{(C_2F_5)_2P(O)\}N\{S(O)_2CF_3\}]$ (PSI) was an interesting goal [162].

5.1 Synthesis of $H[\{(C_2F_5)_2P(O)\}N\{S(O)_2CF_3\}]$ – HPSI

The synthesis of $H[\{(C_2F_5)_2P(O)\}N\{S(O)_2CF_3\}]$ (named HPSI) was performed analogue to the synthesis of HFPI [48], shown in equation 5.1 and 5.2. Two equivalents of Et_3N and 1 equivalent of $(C_2F_5)_2P(O)Cl$ was added to 1 equivalent of $CF_3SO_2NH_2$ diluted in dry diethyl ether at –30 °C. After warming up the reaction mixture to room temperature, the liquid product mixture was analyzed by NMR spectroscopy. The product $[Et_3NH][\{(C_2F_5)_2P(O)\}N\{S(O)_2CF_3\}]$ (**1e**) and traces of $[NH_4][(C_2F_5)_2PO_2]$ (**3b**) were detected. The solid material of $[Et_3NH]Cl$ was filtered off and traces of (**3b**) were removed by washing with cold water several times. The desired pure acid HPSI (**2e**) was isolated by heating the salt (**1e**) with sulphuric acid (100 %) in vacuum (equation 5.2) (yield 96%). During of this process, if small traces of water are present, fast hydrolysis occurred due to the protonation of P=O and formation of $(C_2F_5)_2P(O)OH$ (**1a**) as identified by NMR measurements.

$$(C_2F_5)_2P(O)Cl + CF_3SO_2NH_2 + 2\ Et_3N \xrightarrow[-30\ °C]{Et_2O}$$

$$\longrightarrow [Et_3NH][\{(C_2F_5)_2P(O)\}N\{S(O)_2CF_3\}] + [Et_3NH]Cl\downarrow \qquad (5.1)$$

(**1e**)

$$[Et_3NH][\{(C_2F_5)_2P(O)\}N\{S(O)_2CF_3\}] + H_2SO_4 \longrightarrow$$

$$\longrightarrow H[\{(C_2F_5)_2P(O)\}N\{S(O)_2CF_3\}] + [Et_3NH]HSO_4 \qquad (5.2)$$

(**2e**)

The acid, $H[\{(C_2F_5)_2P(O)\}N\{S(O)_2CF_3\}]$ is a colourless very hygroscopic solid. It is soluble in acetonitrile, acetone, and chloroform. In very dry solvents like DMSO, ethanol (or methanol) and acetonitrile at room temperature the acid is stable for more then 4 days.

In aqueous solution, after 4 days at room temperature, in the ^{19}F NMR and ^{31}P spectra, a small signal was observed which belongs to the hydrolysis product (**1a**). The hydrolysis is accelerated at higher temperature. After 4 days at 40 °C, the hydrolysis product (**1a**) was formed in nearly 30 % yield and H_3PO_4 in 5% yield. After 10 days the content of (**1a**) was increased to 50 %.

The thermal behaviour of HPSI was characterized by DSC measurements. The sample (25 – 40 mg) in a DSC Al pan was heated in inert atmosphere (N_2) at the rate of 10 $°C{\cdot}min^{-1}$. The Figure 5.1 shows the thermal effects of the HPSI. An endothermic peak at about 175 °C was observed which probably belongs to the sublimation of the HPSI and/or decomposition of product. In order to study the decomposition of HPSI, a few mg of this acid were heated into NMR tube at 110 °C for 5 min. Sublimation was observed also in NMR tube. After separation of the crystals from the residue, in the ^{19}F NMR spectrum, a signal of the $CF_3SO_2NH–$ moiety was observed.

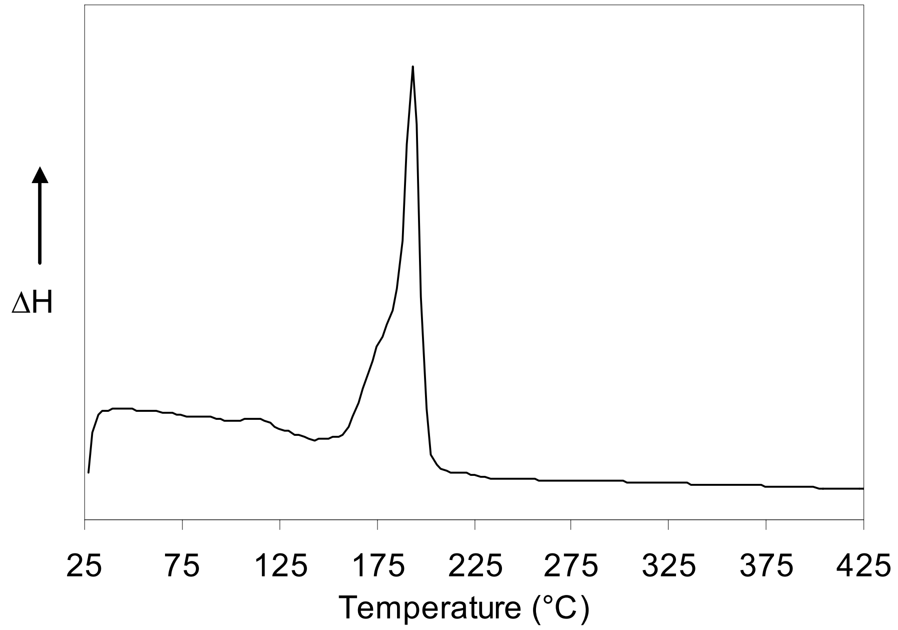

Figure 5.1 DSC diagram of H[{(C_2F_5)$_2$P(O)}N{S(O)$_2$CF$_3$}] (**2e**).

5.1.1 Vibrational spectroscopy

Infrared and Raman spectra of (**1e**) and (**2e**) were recorded at room temperature using ATR–IR accessory (**HARRICK, MVP Star^{TM}**) with a diamond as the ATR crystal and a Bruker (**EQUINOX 55**) FT Raman spectrometer. The spectra of (**1e**) are depicted in Figure 5.2.

The bands at 3050 cm^{-1} are attributed to ν(NH), the bands at 3000 – 2800 cm^{-1} to CH stretching vibrations and 1480 – 1400 cm^{-1} to the deformation vibrations of CH_3 and CH_2 groups of the cation in **1e**. All fundamental vibrations of the PSI anion are below 1400 cm^{-1} and 66 internal vibrations are in principle allowed. According to literature data on similar systems [44], the antisymmetric stretching mode of the SO_2 groups, $\nu_{as}(SO_2)$, is expected between 1350 and 1300 cm^{-1} and the symmetrical one, $\nu_s(SO_2)$, between 1160 and 1120 cm^{-1}. In the case of **1e** were found the bands at 1331 cm^{-1} of $\nu_{as}(SO_2)$ and 1203 cm^{-1} and 1144 cm^{-1} of $\nu_s(SO_2)$. There are also very intense absorption assigned to C_2F_5 and P=O between 1330 and 1100 cm^{-1}. Some stretching modes are overlapping each other as can be seen by comparison of observed and calculated band positions in Table 5.1. The strongest Raman band at 746 cm^{-1} is attributed to the symmetric CF_3 deformations. Altogether, the vibrational spectra are suitable for fingerprint identification.

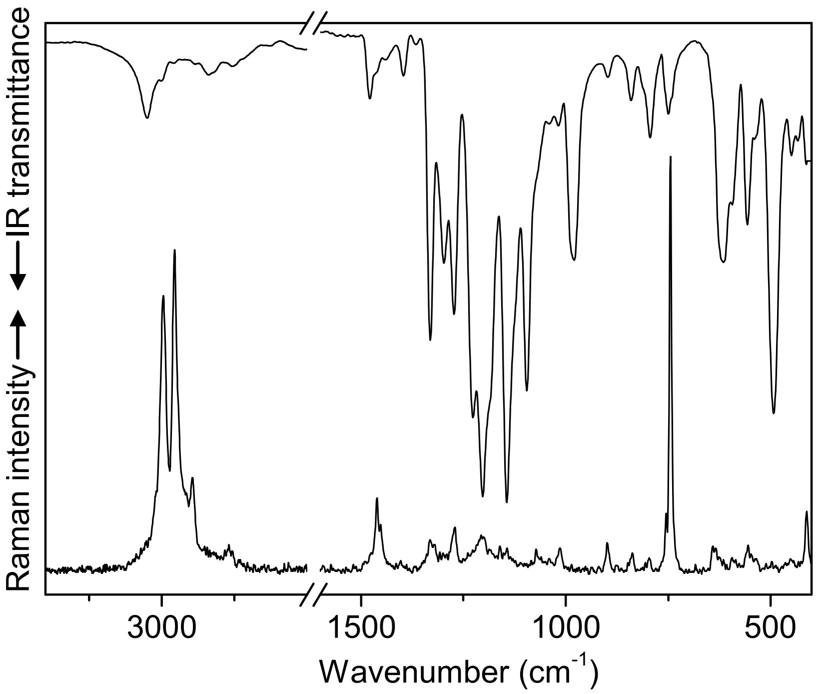

Figure 5.2 Infrared and Raman spectra of solid $[Et_3NH][\{(C_2F_5)_2P(O)\}N\{S(O)_2CF_3\}]$ (**1e**) recorded as neat compound.

The infrared spectra for HPSI do not exhibit a typical sharp ν(N–H) band as it was observed in some cases [32], maybe due to the very hygroscopic/deliquescent nature of the compound. The vibrational spectra of the HPSI (**2e**) are quite similar to that of the (**1e**) anion. Some additional bands between 700 and 665 cm^{-1} were observed.

Table 5.1 Observed and calculated band positions (cm^{-1}) and infrared band intensities of the $[\{(C_2F_5)_2P(O)\}N\{S(O)_2CF_3\}]^-$ anion in **1e**.

IR[a]	Raman[b]	$\nu_{calcd.}$[c]	Assignment
–	1324 m	1316 (30)	ν_1 $\nu_{as}(SO_2)$
1298 s	–	1292 (270)	ν_2 $\nu(CC)$
1273 vs	1274 w	1280 (900)	ν_3/ν_4 $\nu(CC)/\nu_s(CF_3)$
1226 vs	1208 w	1206 (550)	ν_5/ν_6 $\nu_{as}(CF_3)$
1203 vs	1203 w	1197 (250)	ν_7 $\nu_{as}(PO)$
1183 s	1164 w	1170 (1060)	$\nu_8 - \nu_{11}$ $\nu_{as}(CF_3)/\nu_s(SO_2)$
1144 vs	1146 w	1147 (330)	ν_{12}/ν_{13} $\nu_s(CF_2)/\nu_s(SO_2)$
1095 vs	1076 w	1091 (220)	$\nu_{14} - \nu_{16}$ $\nu_s(CF_2)/\nu(CN)$
1018 w	1016 w	1010 (380)	$\nu_{17} - \nu_{18}$ $\nu(CC)/\nu(PC)$
979 s	–	960 (80)	ν_{19} $\nu(PC)$
750 w	759 m	754 (20)	ν_{20} $\nu_s(PN)$

741 w	741 vw	737 (30)	$\nu_{21} - \nu_{23}$ $\delta(CF_3)$
615 s	644 w	615 (20)	ν_{24}/ν_{25} $\delta(SO_2)/\delta(SN)$
595 m	594 vw	590 (240)	$\nu_{26} - \nu_{28}$ $\delta(SO_2)$
557 m	559 w	538 (40)	ν_{29}/ν_{30} $\delta(CF_3)$
538 w	–	536 (20)	ν_{31}/ν_{32} $\rho(CH_2)$
495 vs	–	492 (80)	ν_{33}/ν_{34}
449 w		476 (100)	ν_{35}
433		436 (9)	ν_{36}
413 w	417 m	406 (20)	ν_{37}/ν_{38}
	368 m	360 (4)	ν_{39}
	324 m	340 (6)	ν_{40}/ν_{41}
	304 m	306 (5)	$\nu_{42} - \nu_{44}$
	270 m	278 (3)	$\nu_{45} - \nu_{46}$
	260 m	230 (11)	$\nu_{47} - \nu_{49}$
	176 m	208 (17)	$\nu_{50} - \nu_{54}$
	157 vw	120 (2)	$\nu_{55} - \nu_{57}$
	88 m	86 (3)	$\nu_{58} - \nu_{66}$

[a] Solid/[b] Solid neat compound – s = strong, m = medium, w = weak, v = very.
[c] B3LYP/6–31+G(d), IR intensities in parentheses (km·mol^{-1}).

5.1.2 NMR spectroscopy

NMR spectra of HPSI (**2e**) were measured in dry CD_3CN solution. A sharp singlet at 11.7 ppm in the ^{1}H NMR corresponds to a strong acidic N–H band. The compound possesses non–equivalent trifluoromethyl groups as well as two types of fluorine atoms. The ^{19}F NMR spectrum shows a singlet at –81 ppm (two CF_3 groups) and at –81.7 (one CF_3 group) and a multiplet at –125 ppm (CF_2 groups) in a relative intensity ratio of 6:3:4. As a consequence of asymmetry of the anion, the F atoms in the CF_2 group are not equivalent and form an AA'X spin system.

In the ^{31}P NMR spectrum a triplet of triplet was observed between –6 at –7 ppm due to coupling with the two nearly identical ^{19}F nuclear of the two CF_2 groups.

5.2 Synthesis of new ionic liquids with the PSI anion

Six starting materials with different cations were used for the syntheses of ILs with the PSI anion (Table 5.2). The metathesis reactions were performed according to the equation 5.3. The acid and the cation–precursors were dissolved in a minimum quantity of cold water and mixed together at low temperature for 1 hour and the resulting yields are shown in Table 5.2.

$$\mathrm{Cat^{+}A^{-}} + \mathrm{H[\{(C_2F_5)_2P(O)\}N\{S(O)_2CF_3\}]} \longrightarrow \xrightarrow[\text{ice / 1 h}]{\text{water}} \mathrm{Cat^{+}[\{(C_2F_5)_2P(O)\}N\{S(O)_2CF_3\}]^{-}} + \mathrm{HA}$$

A = Cl, Br, OH (5.3)

Table 5.2 Structures and yields of ILs with $[\{(C_2F_5)_2P(O)\}N\{S(O)_2CF_3\}]^-$ anion.

Cation	**Compound**	**R**	**R_1**	**yield, %**
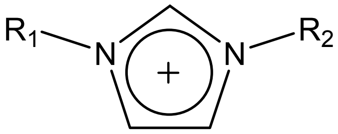	**3e**	CH_3	C_2H_5	74
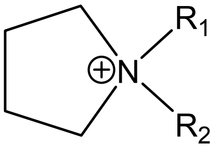	**4e**	C_4H_9	CH_3	78
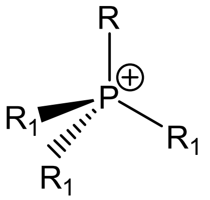	**5e**	C_6H_{13}	$C_{14}H_{29}$	78
	6e	C_6H_5	$CH_2C_6H_5$	86
	7e	C_4H_9	C_4H_9	73
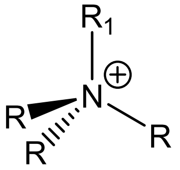	**8e**	C_4H_9	C_4H_9	85

The products were characterised by ^{1}H, ^{19}F, ^{31}P NMR, IR, mass spectroscopy and elemental analysis.

5.3 Physical and chemical properties of ionic liquids with the asymmetrical PSI anion

All six ionic liquids with the PSI anion obtained in this work are hygroscopic and take up water from air. The water content was measured by Karl Fischer titration (in ppm):

3e (34); **4e** (20); **5e** (35). The chloride content measured by ion chromatography in ppm is: **3e** (26); **4e** (5); **5e** (78); **6e** (5). For **5e** the chloride content could not be reduced less than 78 ppm. Nevertheless, the viscosity for **5e** was 343 mPa·s with 173 ppm of chloride and 346 mPa·s with 78 ppm of chloride, which indicate a not significant influence on the viscosity.

5.3.1 Viscosity and density

The viscosity of ILs is strongly dependent to the type of the anion and the coordinating ability and the symmetry of the ions [56]. As can be seen in Table 5.3 low anion weight and low symmetry is necessary to obtain ILs with low viscosity.

Table 5.3 The influence of the anion weight and symmetry on the viscosity of [emim] ILs.

[emim]	**$[(C_2F_5)_2P(O)]_2N^-$**	152 mPa·s (20 °C) (this work)
	$[C_2F_5SO_2]_2N^-$	61 mPa·s (26 °C)[a]
	$[CF_3SO_2]_2N^-$	41 mPa·s (20 °C)[b]
	$[CH_3SO_2]_2N^-$	787 mPa·s (20 °C)[c]
	$[\{(C_2F_5)_2P(O)\}N\{S(O)_2CF_3\}]^-$	127 mPa·s (20 °C) (this work)
	$[CF_3CO]N[CF_3S(O)_2]^-$	25 mPa·s (25 °C)[b]

[a] Ref. [163]; [b] Ref. [164]; [c] Ref. [165]

Figure 5.2 presents the viscosity of different PSI ILs plotted as a function of temperature. The viscosity decrease with introduction of CF_3SO_2 group as was presented in Table 5.4.

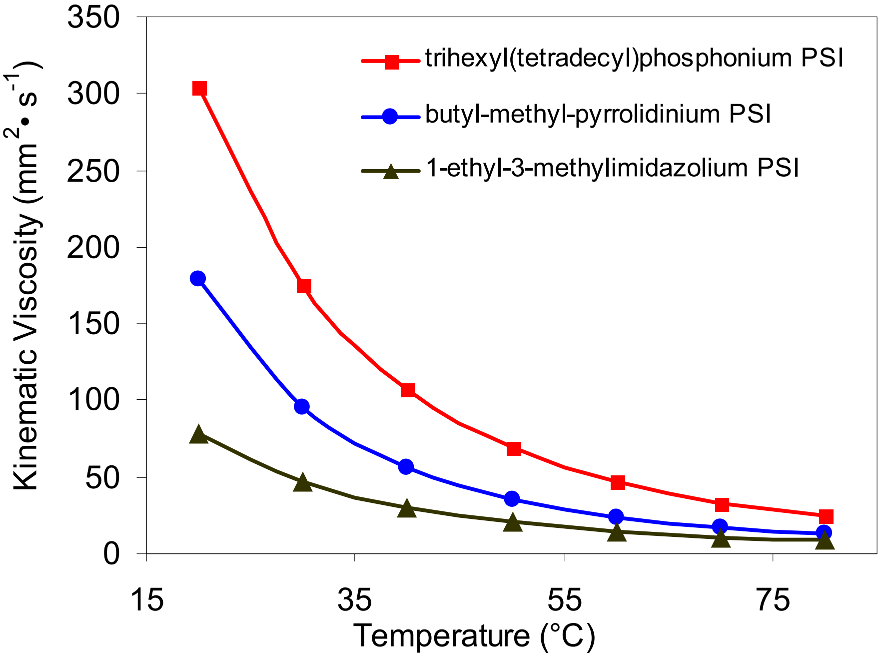

Figure 5.3 Viscosity of different PSI ILs as a function of temperature.

Table 5.4 Dynamic and kinematic viscosity and density of ILs with the PSI anion.

Ionic liquid	**Dynamic viscosity η/mPa·s (20 °C)**	**Kinematic viscosity ν/mm^2·s^{-1} (20 °C)**	**Density ρ/g·cm^{-3}**
[emim]FPI	171	102	1.68
[emim][TFSI]	41	27	1.52[a]
[emim]PSI	**127**	**79**	**1.61**
[bmpl]FPI	325	206	1.58
[bmpl][TFSI]	184	131	1.40[b]
[bmpl]PSI	**268**	**179**	**1.49**
[p(h3)t]FPI	536	443	1.21
[p(h3)t][TFSI]	148	141	1.05[a]
[p(h3)t]PSI	**346**	**304**	**1.14**

[a] Ref. [164]; [b] Ref. [166]

The densities of [emim]FPI, [emim]FAP, [emim]TFSI and [emim]PSI are shown as a function of temperature in Figure 5.4. Densities of these ILs decrease slightly with increasing of temperature. All ILs studied exhibited a similar degree of volume expansion with temperature. The density of [emim]PSI is in between densities value of [emim]FPI and [emim]TFSI respectively.

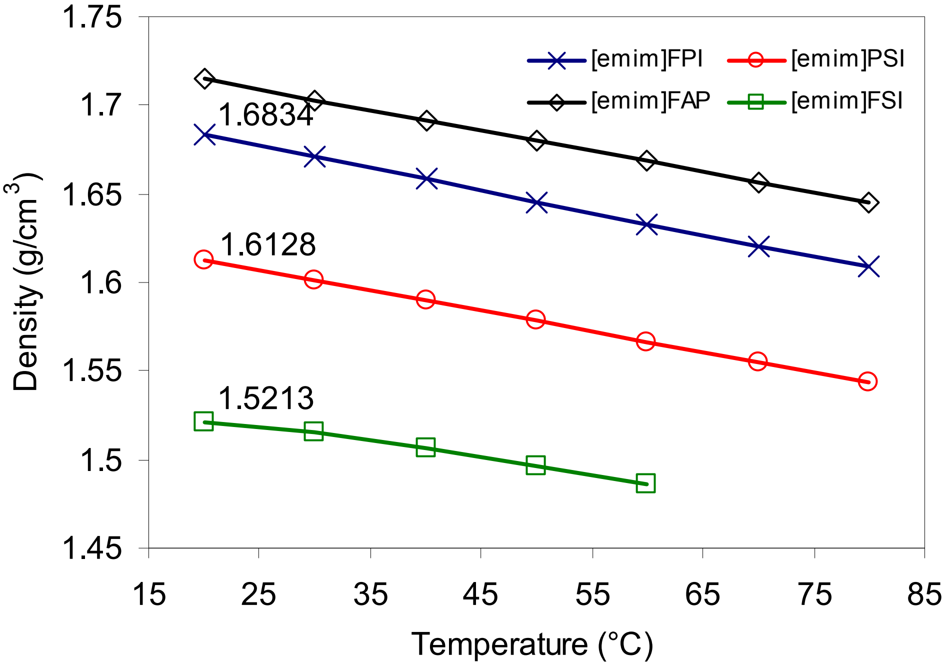

Figure 5.4 Densities of a series of [emim] ILs as a function of temperature.

5.3.2 Melting point and glass transition temperature

The thermal behaviour of the ILs with PSI was examined visually and by DSC and TGA measurements with a **Netzsch DSC**, model **204** and a **Netzsch STA** thermal gravimetric analyzer, model **409**.

There are only two publications dealing with the preparation of lower melting points ILs with asymmetrical amide anion [160, 161]. In this thesis is presented preparation of six new room temperature ILs with different cations and the PSI anion (Figure 5.2). Surprisingly, the [Bu_4P]PSI (**7e**) is liquid at room temperature, while [Bu_4P]FPI (**18d**) has a melting point of 145 °C. The melting point of [Bu_4N]PSI (**8e**) (36 °C) is much lower than that of [Bu_4N]FPI (**13d**) (151 °C) and lower than [Bu_4N]TFSI (90 °C) [128]. Not only the symmetrical ammonium or phosphonium cations, but also a big asymmetrical cation, [$(C_6H_5)_3P(CH_2C_6H_5)$], forms low melting point IL (**6e**) (73 °C). [Et_3NH]PSI has melting point at 43 °C. These data show that the PSI anion forms salts with much lower melting point on compararison to FPI salts.

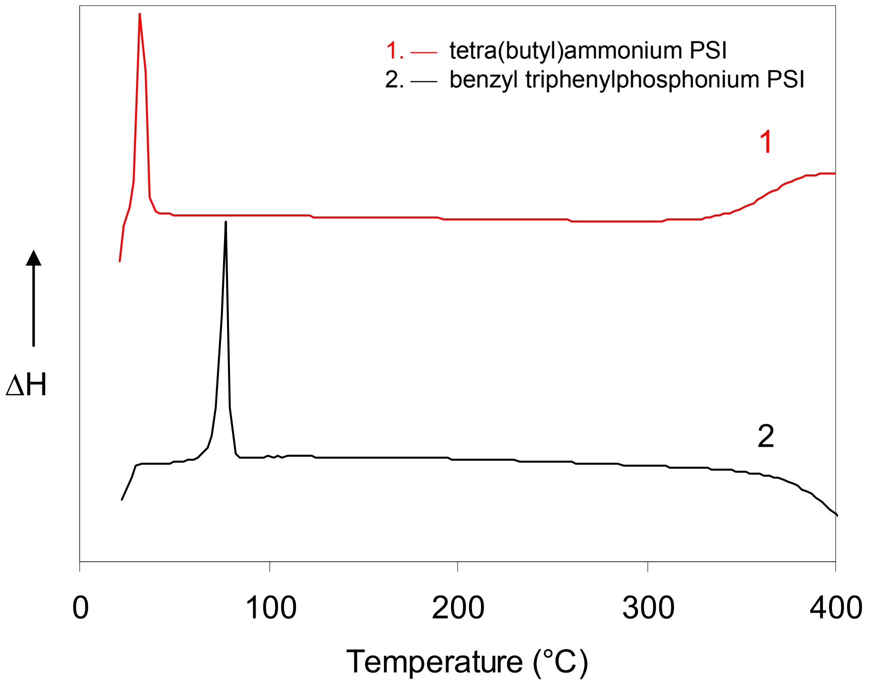

Figure 5.5 DSC diagrams for two ILs: $[Bu_4N]PSI$ (T_m = 36 °C) and $[(C_6H_5)_3P(CH_2C_6H_5)]PSI$ (T_m = 73 °C).

The DSC diagrams of the room temperature ILs with PSI anion show no melting point, only glass transition at –81 °C for (**5e**), –77 °C (**4e**) and –80 °C (**3e**). The DSC representations of two ILs are displayed in Figure 5.6.

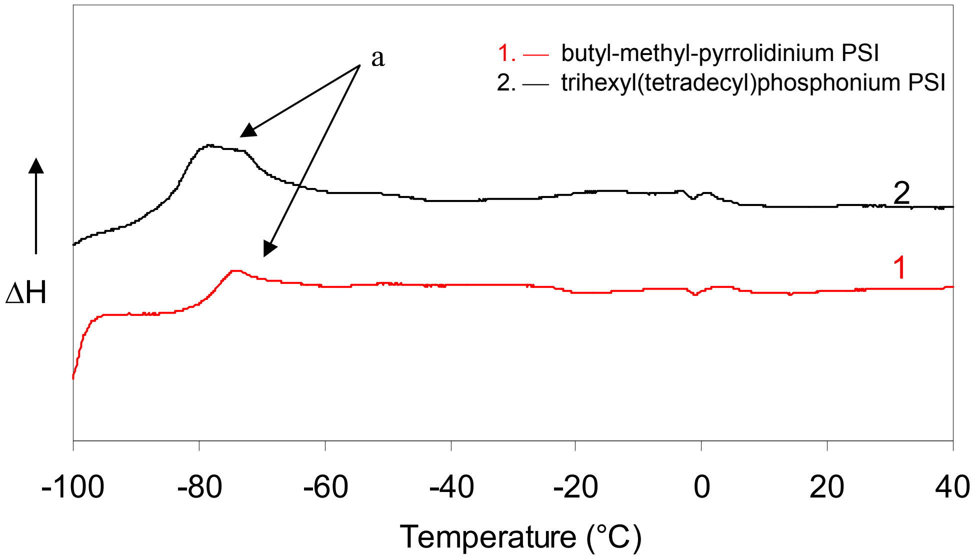

Figure 5.6 DSC diagrams for [bmpl]PSI (1) and [p(h3)t]PSI (2); (a) glass transition temperature (–77 °C and -81°C).

5.3.3 Thermal stability

The thermogravimetric analyses of two ILs with PSI anion are displayed in Figure 5.7. The well dried compounds show no weight loss until at least 300 °C, providing a large, stable liquid range. The thermal stabilities (T_{onset}, TGA) of the ILs with PSI decrease in the series:

6e (360 °C) > **4e** (350 °C) > **7e** (320 °C) > **3e** (300 °C) > **1e** (260 °C)

[Et_3NH]PSI (**1e**) is less thermally stable and decomposes at 260 °C. For [p(h3)te3]PSI (**5e**), the weight loss (3.5 %), in the 90 – 140 °C range, corresponds to the loss of some volatile impurities.

In conclusion, the thermal stability of ILs with PSI anion is high and comparable with FPI anion.

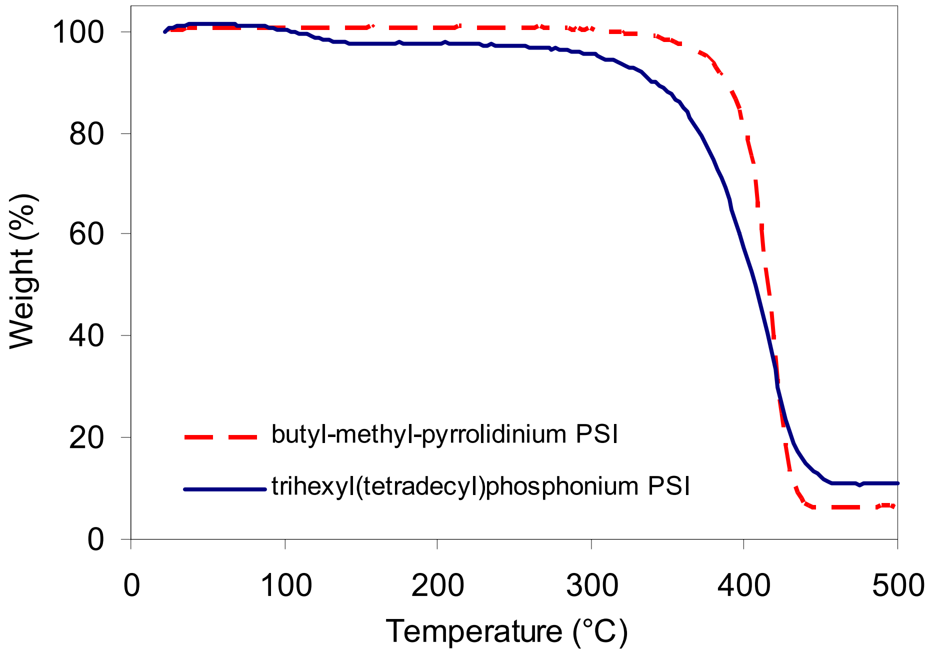

Figure 5.7 TGA for two ILs (**4e** and **5e**) with the PSI anion.

5.4 Crystal structure of $[Et_3NH][\{(C_2F_5)_2P(O)\}N\{S(O)_2CF_3\}]$

Single crystals of $[Et_3NH]PSI$ (**1e**) suitable for X–ray diffractometry were obtained by crystallization from an Et_2O/water solution by slow evaporation. A **Kappa CCD** diffractometer (**Bruker AXS**) was used for measurements at 100 K with Mo–K_α radiation (λ = 0.71073 Å) and a graphite monochromator. The crystal structure of (**1e**) was solved by direct methods using SHELXS–97 and full–matrix least–squares refinement on F^2 was performed with SHELXL–97 [155]. Diffracted intensities were corrected for absorption based on indexed crystal faces, T_{min}, and T_{max}: 0.90 and 0.98, respectively. The parameters obtained for (**1e**) are listed in Table 5.5 and the angle and distance in Appendix 1. The crystal structure was determined in space group $P2_1$ (Table 5.6) with two independent formula units per unit cell, which are depicted in Figure 5.8.

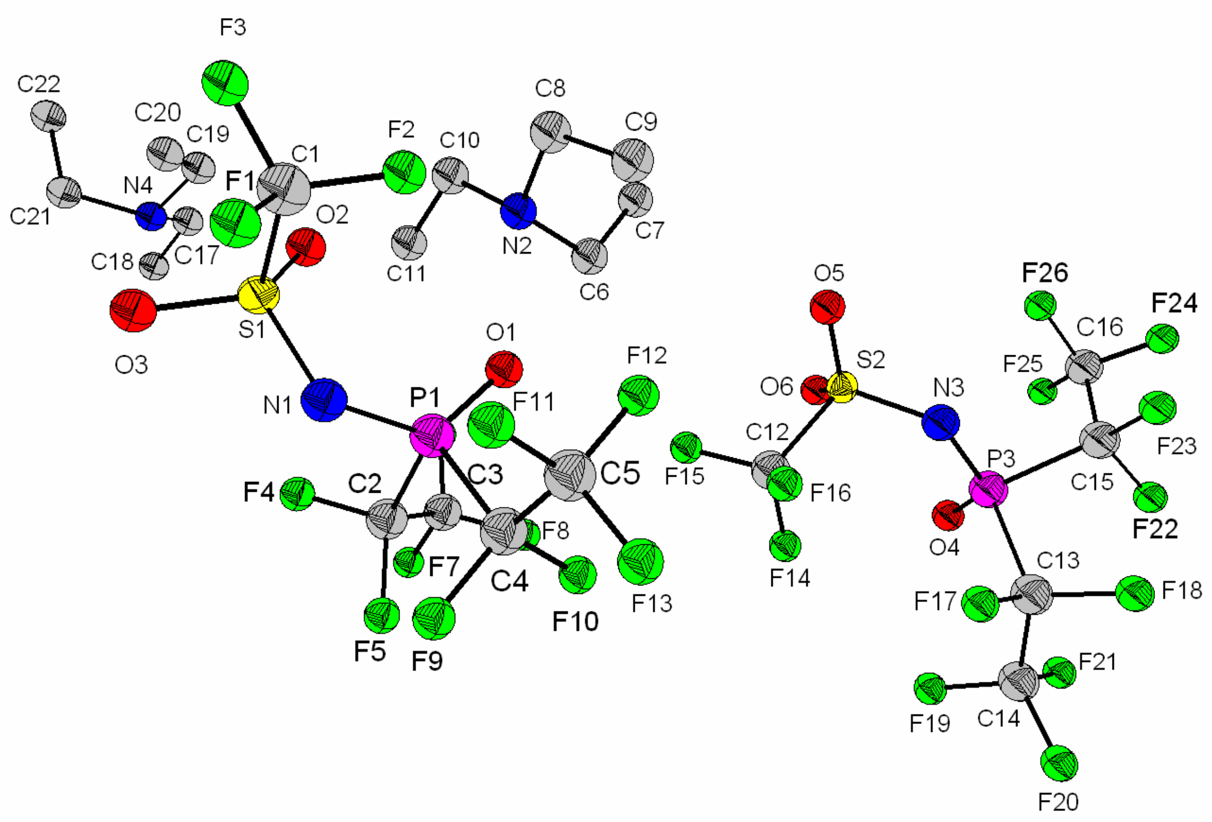

Figure 5.8 Molecular structure of two formula unit of $[Et_3NH]PSI$ in the unit cell.

The PNS skeleton of both PSI anions shows approx. C_2 symmetry. Average values of selected bond lengths and angles for the anion are collected in Table 5.5, which show a good agreement between experimental and calculated data for two different anions: $[\{(C_2F_5)_2P(O)\}_2N]^-$ and $[(CF_3SO_2)_2N]^-$ [44]. The P–N and S–N bond distance are shorter than that for corresponding acids: 1.588 Å in PSI compared to 1.670(1) Å in $iPr_2P(O)NHP(O)iPr_2$ [157] and 1.561 Å for PSI compared to 1.660 Å in $(CF_3SO_2)_2NH$ [44]. That probably reflects the differencies in electron–withdrawing properties of these groups.

Table 5.5 Observed/calculated[a] average bond lengths (Å) and angles (deg.) for the PSI anion in the $[Et_3NH]PSI$ salt.

bond/angle	obs. (this work)	calc[a]./obs[ref].
P=O	1.47	1.49/1.47[b]
P–N	1.58	1.59/1.56[b]
P–C	1.87	1.92/1.88[b]
C–C	1.52	1.55/1.53[b]
CF_2–F	1.33	1.35/1.33[b]
CF–F	1.34	1.37/1.36[b]
CF_2–F (–SO_2)	1.34	1.31/1.30[c]
C–S	1.82	1.82/1.81[c]
S=O	1.43	1.43/1.41[c]
S–N	1.56	1.57[c] and 1.64[d]
P–N–S	126.4	-

[a] B3LYP/6–31+G(d); [b] for $[\{(C_2F_5)_2P(O)\}_2N]^-$; [c] for $[(CF_3SO_2)_2N]^-$ ref. [44];
[d] for $[(CF_3SO_2)_2N]^-$ ref. [167].

The X–ray structure (Figure 5.8) shows that the hydrogen bonding between the O donor from anions and the H acceptor from the cation is shorter than usually: P_1–O_1…H_2–N_2 (1.942 Å) and P_4–O_4…H_4–N_4 (2.258 Å).

Table 5.6 Crystalographic and refinement data for **1e**.

Crystalographic data	$[(C_2H_5)_3NH]$PSI (**1e**)
Empirical formula	$C_{11}H_{16}F_{13}N_2O_3PS$
Colour	colourless
Formula weight	534.29 g·mol^{-1}
Temperature	100 K
Wavelength	0.71073 Å
Crystal system	Monoclinic
Space group	**P2$_1$, (no. 4)**
Unit cell dimensions	a = 10.8058(3) Å α= 90° b = 11.1886(3) Å β = 91.628(1)° c = 15.6646(5) Å γ = 90°
Volume	2013.97(10) Å^3
Z	4
Density (calculated)	1.762 mg·m^{-3}
Absorption coefficient	0.374 mm^{-1}
F(000)	1072 e
Crystal size	0.30 x 0.26 x 0.05 mm^3
θ range for data collection	2.91 to 33.31°
Index ranges	$-16 \le h \le 16$, $-17\le k \le 17$,$-25 \le l \le 25$
Reflections collected	40674
Independent reflections	15368 [R_{int} = 0.0514]
Reflections with I>2σ(I)	12704
Completeness to	(= 33.31°) 99.0 %
Absorption correction	Gaussian
Max. / min. transmission	0.98179 and 0.90756
Refinement method	Full-matrix least-squares on F^2
Data/restraints/parameters	15368/1/565
Goodness-of-fit on F^2	1.098
Final R indices [I>2σ(I)]^a	R_1 = 0.0656 wR^2 = 0.1823
R indices (all data)^b	R_1 = 0.0804 wR^2 = 0.1926
Absolute structure parameter	0.02(8)
Largest diff. peak and hole	1.096 and -0.816 e Å^{-3}

5.5 Experimental part

Triethylammonium [bis(pentafluoroethyl)phosphinyl – (trifluoromethyl)sulfonyl)]imide, $[Et_3NH][\{(C_2F_5)_2P(O)\}N\{S(O)_2CF_3\}]$ (1e)

A 250 mL, three neck, round–bottomed flask was fitted with stirrer and a combined inlet–outlet assembly connected to an argon source and a bubbler. The flask was charged with 9.83 g (65.9 mmol) of $CF_3SO_2NH_2$ and 13.50 g (133.0 mmol) of Et_3N in 20 mL of dry Et_2O. The mixture was cooled with bath at –30 °C (ethanol/dry ice) while 21.66 g (65.9 mmol) of $(C_2F_5)_2P(O)Cl$ was added slowly under vigorous stirring. After an exothermic process, the reaction mixture was stirred and allowed to warm up to room temperature. The white deposit of NH_4Cl was filtered off and washed three times with 30 mL Et_2O. After removing the solvent, a brown–yellow liquid product was obtained. The impurities from raw product were removed by washing several times with cold water. 33.68 g (62.9 mmol) of the desired product (yellowish) was obtained after drying in high vacuum (10^{-3} mbar). Yield: 95.5 %. Mp: 43 °C.

^{1}H NMR (lock/solvent CD_3CN, 400MHz), δ, ppm: 3.11 to 3.04 m ($3CH_2$, $^3J_{H,H}$ = 7.2 Hz); 1.18 t ($3CH_3$, $^3J_{H,H}$ = 7.2 Hz).

^{19}F NMR (lock/solvent CD_3CN, 376.4 MHz), δ, ppm: –81.1 s ($2CF_3$); –81.2 s (CF_3); –123.8 m ($2CF_a$); –126.6 m ($2CF_b$); $^2J_{P,Fa}$ = 74 Hz; $^2J_{P,Fb}$ = 84 Hz; $^2J_{Fa,Fb}$ = 317 Hz.

^{31}P NMR (lock/solvent CD_3CN, 161.9 MHz), δ, ppm: –6.8 t,t (1P; $^2J_{P,Fa}$ = 73 Hz; $^2J_{P,Fb}$ = 84 Hz).

Elemental analysis calcd. (%) for $C_{11}H_{16}F_{13}N_2O_3PS$ (*M* = 543.27 g/mol): C 24.73, H 3.02, N 5.24, S 6.00; found: C 24.80, H 2.69, N 5.10, S 5.86.

MS – CI for $[Et_3NH]^+\{[(C_2F_5)_2P(O)]N[S(O)_2CF_3]\}^-$: m/z 301 $(C_2H_5)_2P(O)NH_2)$; 149 $(CF_3SO_2NH_2)$.

Bis[(pentafluoroethyl)phosphinyl–(trifluoromethyl)sulfonyl]imide $H[\{(C_2F_5)_2P(O)\}N\{S(O)_2CF_3\}]$ (2e)

6.7 g of concentrated sulphuric acid was added to 9.4 g (17.5 mmol) of (**1e**) salt and heated under vacuum (10^{-3} mbar) to 40 – 50 °C. The desired pure product was obtained by sublimation onto a cold–finger condenser cooled with dry ice and ethanol. The white solid of **2e** is very hygroscopic and must be handled under argon. Yield: 97%.

^1H NMR (lock/solvent CD_3CN, 400MHz), δ, ppm: 11.69 s (NH).
^{19}F NMR (lock/solvent CD_3CN, 376.4 MHz), δ, ppm: –80.9 s ($2CF_3$); –81.7 s (CF_3); —123.7 m ($2CF_a$); –126 m ($2CF_b$); $^2J_{P,Fa}$ = 79 Hz; $^2J_{P,Fb}$ = 91 Hz; $^2J_{Fa,Fb}$ = 318 Hz.
^{31}P NMR (lock/solvent CD_3CN, 161.9 MHz), δ, ppm: –7.4 t,t (1P; $^2J_{P,Fa}$ = 79 Hz; $^2J_{P,Fb}$ = 87 Hz).
Elemental analysis calcd. (%) for $C_5HF_{13}NO_3PS$ (*M* = 433.09 g/mol): C 13.87, H 0.23, N 3.23, S 7.40; found: C 13.98, H 0.60, N 3.01, S 7.29.

1–Ethyl–3–methylimidazolium [bis(pentafluoroethyl)phosphinyl – (trifluoromethyl)sulfonyl)]imide, $[C_6H_{11}N_2][\{(C_2F_5)_2P(O)\}N\{S(O)_2CF_3\}]$ (3e)

A solution of $[C_6H_{11}N_2]Cl$ (2.53 g, 17.2 mmol) in water (5 mL) was added slowly to a cooled solution of $H[\{(C_2F_5)_2P(O)\}N\{S(O)_2CF_3\}]$ (7.50 g, 17.3 mmol) in water (5 mL), under vigorous stirring. The product precipitated as a viscous liquid. It was collected by separation, dissolved in CH_2Cl_2 and washed several times with water. After evaporation of the solvent the residue was dried in high vacuum (10^{-3} mbar) for 22 h at 60 °C. 6.91 g of product **3e** was obtained. Yield: 74%.
^1H NMR (lock/solvent CD_3CN, 400MHz), δ, ppm: 8.42 s (CH); 7.38 s (CH); 7.31 s (CH); 4.14 q (CH_2, $^3J_{H,H}$ = 7.3 Hz); 3.80 s (CH_3); 1.43 t (CH_3, $^3J_{H,H}$ = 7.1 Hz).
^{19}F NMR (lock/solvent CD_3CN, 376.4 MHz), δ, ppm: –81.1 s ($2CF_3$); –81.8 s (CF_3); –123.8 m ($2CF_a$); –126.6 m ($2CF_b$); $^2J_{P,Fa}$ = 72 Hz; $^2J_{P,Fb}$ = 85 Hz; $^2J_{Fa,Fb}$ = 312 Hz.
^{31}P NMR (lock/solvent CD_3CN, 161.9 MHz), δ, ppm: –6.9 t,t (1P; $^2J_{P,Fa}$ = 74 Hz; $^2J_{P,Fb}$ = 83 Hz).
Elemental analysis calcd. (%) for $C_{11}H_{11}F_{13}N_3O_3PS$ (*M* = 543.01 g/mol): C 24.32, H 2.04, N 7.74, S 5.90; found: C 23.68, H 2.18, N 7.89, S 5.53.

1–n–Butyl–1–methylpyrrolidinium [bis(pentafluoroethyl)phosphinyl – (trifluoromethyl)sulfonyl)]imide, $[C_9H_{20}N][\{(C_2F_5)_2P(O)\}N\{S(O)_2CF_3\}]$ (4e)

A slight excess of freshly prepared $H[\{(C_2F_5)_2P(O)\}N\{S(O)_2CF_3\}]$ (7.30 g, 16.8 mmol) in water (or methanol) (5 mL) was added to a cooled aqueous solution of $[C_9H_{20}N]Cl$ (2.92 g, 16.4 mmol) and reaction mixture was left stirred for approximately 1 h. The precipitated product, as a viscous liquid, was collected by separation and was washed several times with water. For a good separation was dissolved in dichloromethane and washed again two times with water. The organic layer was collected; the solvent was distilled off and the residue was dried in high vacuum (10^{-3} mbar) for 36 h at 60 °C. 7.34 g of **4e** was obtained. Yield: 78%.

^{1}H NMR (lock/solvent CD_3CN, 400MHz), δ, ppm: 3.38 m ($2CH_2$); 3.21 m (CH_2); 2.92 s (CH_3); 2.13 m ($2CH_2$); 1.70 m (CH_2); 1.35 q,t (CH_2, $^{3}J_{H,H}$ = 7.5 Hz); 0.99.t (CH_3, $^{3}J_{H,H}$ = 7.3 Hz).

^{19}F NMR (lock/solvent CD_3CN, 376.4 MHz), δ, ppm: –81.0 s ($2CF_3$); –81.7 s (CF_3); –123.7 m ($2CF_a$); –126.5 m ($2CF_b$); $^{2}J_{P,Fa}$ = 78 Hz; $^{2}J_{P,Fb}$ = 83 Hz; $^{2}J_{Fa,Fb}$ = 316 Hz.

^{31}P NMR (lock/solvent CD_3CN, 161.9 MHz), δ, ppm: –8.4 t,t (1P; $^{2}J_{P,Fa}$ = 73 Hz; $^{2}J_{P,Fb}$ = 84 Hz).

Elemental analysis calcd. (%) for $C_{14}H_{20}F_{13}N_2O_3PS$ (*M* = 574.34 g/mol): C 29.28, H 3.51, N 4.88, S 5.58; found: C 29.04, H 3.68, N 4.9, S 4.94.

Trihexyl(tetradecyl)phosphonium [bis(pentafluoroethyl)phosphinyl – (trifluoromethyl)sulfonyl)]imide, $[(C_6H_{13})_3PC_{14}H_{29}][\{(C_2F_5)_2P(O)\}N\{S(O)_2CF_3\}]$ (5e)

To a stirred solution of 6.94 g (13.36 mmol) $[(C_6H_{13})_3PC_{14}H_{29}]Cl$ in 20 mL of ethanol was added 5.80 g (13.39 mmol) of $H[\{(C_2F_5)_2P(O)\}N\{S(O)_2CF_3\}]$ in 8 mL of water at 0 °C. The mixture was kept stirring for 1 h at room temperature. The ethanol was distilled off in vacuum and then the residue was washed several times with water, dissolved in dichloromethane and washed again with water several times. The organic layer was collected; the solvent distilled off the residue dried in high vacuum (10^{-3} mbar) for 36 h at 60 °C. 9.52 g of a liquid material was obtained. Yield : 78 %.

^{1}H NMR (lock/solvent CD_3CN, 400MHz), δ, ppm: 2.10 to 2.02 m ($4CH_2$); 1.57 to 1.41 m ($8CH_2$); 1.38 to 1.28 m ($16CH_2$); 0.95 to 0.89 m ($4CH_3$).

^{19}F NMR (lock/solvent CD_3CN, 376.4 MHz), δ, ppm: –81.0 s ($2CF_3$); –81.6 s (CF_3); –123.6 m ($2CF_a$); –126.5 m ($2CF_b$); $^{2}J_{P,Fa}$ = 72 Hz; $^{2}J_{P,Fb}$ = 84 Hz; $^{2}J_{Fa,Fb}$ = 322 Hz.

^{31}P NMR (lock/solvent CD_3CN, 161.9 MHz), δ, ppm: 33.6 m (1P); –8.5 t,t (1P; $^{2}J_{P,Fa}$ = 72 Hz; $^{2}J_{P,Fb}$ = 83 Hz).

Elemental analysis calcd. (%) for $C_{37}H_{68}F_{13}NO_3P_2S$ (*M* = 915.93 g/mol): C 48.52, H 7.48, N 1.53, S 3.50; found: C 48.88, H 7.84, N 1.45, S 2.73.

Benzyl(triphenyl)phosphonium

[bis(pentafluoroethyl)phosphinyl – (trifluoromethyl)sulfonyl)]imide,

$[(C_6H_5)_3P(CH_2C_6H_5)][\{(C_2F_5)_2P(O)\}N\{S(O)_2CF_3\}]$ (6e)

To the stirred solution of $[(C_6H_5)_3P(CH_2C_6H_5)]^+Cl^-$ (0.35 g, 0.9 mmol) in 2 mL of water, a solution of $H[\{(C_2F_5)_2P(O)\}N\{S(O)_2CF_3\}]$ (0.40 g, 0.9 mmol) in 3 mL of water was slowly added at room temperature. The mixture was kept stirring for 1 h at room temperature. The colloid mixture cannot be separated by filtration. The desired product (**6e**) was extracted with Et_2O. The extract was washed two times with 20 mL of water until the test for bromide with $AgNO_3$ was negative. After evaporation of solvent and drying, 0.62 g of a pure white solid was obtained. Yield: 86%. Mp: 73 °C.

^{1}H NMR (lock/solvent CD_3CN, 400MHz), δ, ppm: 7.9 m (3CH); 7.7 m (6CH); 7.6 m (6CH); 7.4 m (CH); 7.2 t (2CH, $^3J_{H,H}$ = 7.7 Hz); 6.9 d,m (2CH); 4.6 d (CH_2P, $^2J_{P,H}$ =14.4 Hz).

^{19}F NMR (lock/solvent CD_3CN, 376.4 MHz), δ, ppm: –81.1 s ($2CF_3$); –81.7 s (CF_3); –123.6 m ($2CF_a$); –126.5 m ($2CF_b$); $^2J_{P,Fa}$ = 72 Hz; $^2J_{P,Fb}$ = 84 Hz; $^2J_{Fa,Fb}$ = 316 Hz.

^{31}P NMR (lock/solvent CD_3CN, 161.9 MHz), δ, ppm: 22.5 s (1P); –6.8 t,t (1P; $^2J_{P,Fa}$ = 72 Hz; $^2J_{P,Fb}$ = 83 Hz).

Tetra(n–butyl)phosphonium

[bis(pentafluoroethyl)phosphinyl – (trifluoromethyl)sulfonyl)]imide,

$[(C_4H_9)_4N][\{(C_2F_5)_2P(O)\}N\{S(O)_2CF_3\}]$ (7e)

A solution of $[(C_4H_9)_4P]Br$ (0.5 g, 1.4 mmol) in 3 mL of water was slowly added to the stirred solution of $H[\{(C_2F_5)_2P(O)\}N\{S(O)_2CF_3\}]$ (0.6 g, 1.4 mmol) in 4 mL of water at room temperature. The mixture was left stirring for 30 minutes. The precipitated viscous liquid was washed several times with water. After drying, 0.7 g of a liquid material was obtained. Yield: 73%.

^{1}H NMR (lock/solvent CD_3CN, 400 MHz), δ, ppm: 2.11 to 2.04 m ($4CH_2$); 1.50 m ($8CH_2$); 0.97 t ($4CH_3$, $^3J_{H,H}$ = 7.1Hz).

^{19}F NMR (lock/solvent CD_3CN, 376.4 MHz), δ, ppm: –81.0 s ($2CF_3$); –81.7 s (CF_3); –123.6 m ($4CF_a$); –126.5 m ($4CF_b$); $^2J_{P,Fa}$ = 73 Hz; $^2J_{P,Fb}$ = 82 Hz; $^2J_{Fa,Fb}$ = 315 Hz.

^{31}P NMR (lock/solvent CD_3CN, 161.9 MHz), δ, ppm: 33.6 m (1P); –8.5 quin,m (2P; $^2J_{P,Fa}$ = 72 Hz; $^2J_{P,Fb}$ = 84 Hz).

Elemental analysis calcd. (%) for $C_{21}H_{36}F_{13}NO_3P_2S$ (*M* = 691.5 g/mol): C 36.47, H 5.25, N 2.03, S 4.64; found: C 36.39, H 5.17, N 1.96, S 4.74.

Tetra(n–butyl)ammonium [bis(pentafluoroethyl)phosphinyl – (trifluoromethyl)sulfonyl)]imide, $[(C_4H_9)_4N][\{(C_2F_5)_2P(O)\}N\{S(O)_2CF_3\}]$ (8e)

A solution of $[(C_4H_9)_4N]OH$ (1 M, 1.1 mL) in ethanol was slowly added at room temperature to the stirred solution of $H[\{(C_2F_5)_2P(O)\}N\{S(O)_2CF_3\}]$ (0.5 g, 1.1 mmol) in 3 mL of water. The mixture was left stirring for 30 minute. The product was extracted with 10 mL of Et_2O. The solvent was evaporated and the residue was dried 8 h in vacuum (<10^{-3} mbar) at room temperature. Yield: 85%. Mp: 36 °C.

^{1}H NMR (lock/solvent CD_3CN, 400MHz), δ, ppm: 3.10 m ($4CH_2$); 1.64 m ($4CH_2$); 1.39 q,t ($4CH_2$, $^3J_{H,H}$ = 7.3 Hz); 1.0 t ($4CH_3$, $^3J_{H,H}$ = 7.3 Hz).

^{19}F NMR (lock/solvent CD_3CN, 376.4 MHz), δ, ppm: : –81.0 s ($2CF_3$); –81.7 s (CF_3); –123.6 m ($4CF_a$); –126.5 m ($4CF_b$); $^2J_{P,Fa}$ = 73 Hz; $^2J_{P,Fb}$ = 82 Hz; $^2J_{Fa,Fb}$ = 315 Hz.

^{31}P NMR (lock/solvent CD_3CN, 161.9 MHz), δ, ppm: –8.5 t,t (1P; $^2J_{P,Fa}$ = 72 Hz; $^2J_{P,Fb}$ = 83 Hz).

Elemental analysis calcd. (%) for $C_{21}H_{36}F_{13}N_2O_3PS$ (*M* = 674.54 g/mol): C 37.39, H 5.38, N 4.15, S 4.75; found: C 37.37, H 5.24, N 4.01, S 4.51.

Chapter 6

6. HFPI – an efficient catalyst for acylation reactions

Protection of alcohols, phenols, thiols and amides with acyl group is one of the frequently used protocol in organic chemistry and is usually achieved through acylation with anhydrides or acetyl chloride [168]. The various catalysts are developed for acylation, for example Lewis acids (metal halides, metal triflates, and metal triflimide) or acids themself. Recently, ILs were also used as catalyst and medium in acylation processes. The application of $HN[P(O)(C_2F_5)_2]_2$ (HFPI) in organic synthesis and its use as catalyst for efficient acylation of phenols, amines and thiols are reported in this chapter [169].

6.1 Acylation of – OH, – NH, and – SH functional groups with HFPI

Despite the great number of reported acylation procedures, new and more efficient methodologies are still demanded. Various acids and bases were tested as catalysts, but the applications of many of them are limited due to the instability of reactants or products under the reaction conditions or difficult workup (long reaction times, stringent conditions, use of hazardous materials). For example, many Lewis acids, such as scandium triflate, $Sc(OTf)_3$ [170], cerium triflate $Ce(OTf)_3$ [171], magnesium bromide, $MgBr_2$ [172], tantalum chloride, $TaCl_5$ [173], trimethylsilyl triflate Me_3SiOTf [174], copper triflate, $Cu(OTf)_2$ [175], indium triflate $In(OTf)_3$ [176], aluminium triflate

$Al(OTf)_3$ [177], or bismuth triflate, $Bi(OTf)_3$ [178] have been used as catalysts for acylation processes. In general metal triflates are very expensive. Some of them are moisture sensitive and cannot be used for acylation of acid–sensitive alcohols. Recently, Alleti *et al.* (2005) have been reported the application of $Gd(OTf)_3$ as a mild catalyst in acetylation of alcohols and amides [179]. Further improvement was achieved by using of some metal imide (e.g. LiTFSI, $Mg(TFSI)_2$, $Sc(TFSI)_2$) as very stable and mild catalyst [180, 60].

In this work was found that HFPI is an efficient catalyst in acylation reactions according to equation 6.1.

$$\mathrm{R(Ar)XH} + (\mathrm{CH_3CO})_2\mathrm{O} \xrightarrow[\mathrm{RT}]{\text{cat.: HFPI}} \mathrm{R(Ar)XCOCH_3} + \mathrm{CH_3COOH} \qquad (6.1)$$

X = O, NH, S

Various phenols were subjected to acylation according to this protocol, i.e. 1–naphtol, 2–naphtol, catechol, 4–nitrophenol and 4–methoxyphenol. Most of the reactions were carried out with 1.2 equiv. of acetic anhydride, under solvent free conditions at room temperature in the presence of 1 mol % of catalysts (HFPI), unless otherwise stated. The results are summarized in the Table 6.1. The reactions proceeded fast, within ca. 30 min. The products were isolated mostly in excellent yields after sample work–up, using the procedures described in the experimental part. The product yields were influenced by the nature of the substrates (steric and electronic factors). Very small difference in the yield of 2– and 1– naphtyl acetate (entry 2 and 5) was observed. Good results were also obtained with phenols having electron–withdrawing substituent, such as NO_2 (entry 14). 4–methoxyphenol was acylated smoothly and the –OMe group remained intact by this protocol. Dihydroxy aromatic compond afforded the diacetates in excellent yield. The isolated products were characterized with typical analytical procedure and the data were in full agreement with authentic samples (Mp, NMR, MS).

Exploration of the catalytic activity of HFPI for acylation of diverse phenols was completed by studies with another acid, HTFSI as catalyst. Its comparable acidity was presented in Chapter 2. HFPI and HTFSI are equally effective in the acylation reactions.

Table 6.1 Acylation of O–substrates with Ac_2O in the presence of HFPI and HTFSI as catalysts[b].

Entry	Substrate[a]	Product	Catalyst[b] (mol %)	Time (min)	Temp. (°C)	Solv.	Yield (%)
1 – 2.	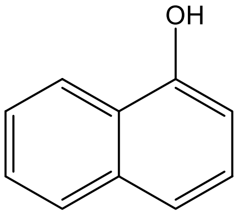	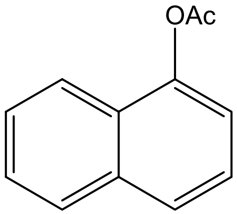	HFPI (1 %)	30	RT	CH_2Cl_2 (2 mL)	91
			HFPI (1 %)	30	RT	–	98
3 – 8.	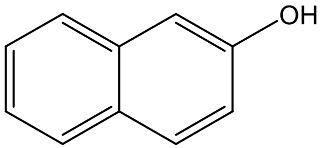	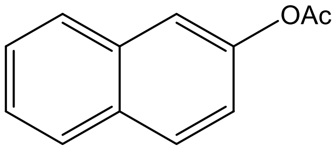	HFPI (1 %)	10	RT	CH_2Cl_2 (2 mL)	74
			HFPI (1 %)	30	RT	CH_2Cl_2 (2 mL)	97
			HFPI (1 %)	30	RT	–	99
			HFPI (0.1 %)	**30**	**RT**	**–**	**95**
			HTFSI (1 %)	30	RT	–	95–96
			HTFSI (1.5 %)	30	RT	–	95

Entry (contd.)	Substrate[a]	Product	Catalyst[b] (mol %)	Time (min)	Temp. (°C)	Solv.	Yield (%)
9 – 13.	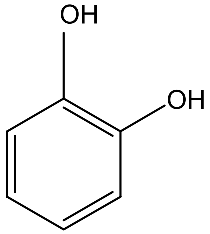	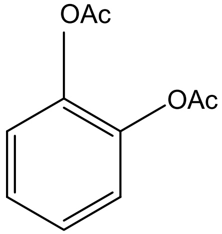	HFPI (1 %)	10	RT	–	63
			HFPI (1 %)	20	RT	–	79
			HFPI (1 %)	30	RT	–	96–97
			HFPI (0.1 %)	**30**	**RT**	**–**	**92–93**
			HTFSI (1.5 %)	30	RT	–	97
14 – 15.	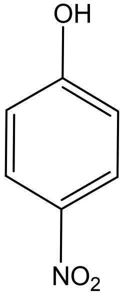	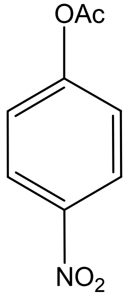	HFPI (1 %)	25	RT	–	93–94
			HTFSI (2 %)	30	RT	–	89
16 – 17.	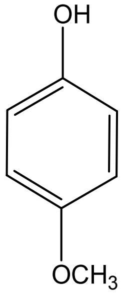	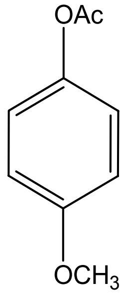	HFPI (1 %)	30	RT	–	97
			HTFSI (1 %)	30	RT	–	87–89

[a] The substrate was treated with Ac_2O (1.2 equiv.) in the presence of the catalyst under neat conditions at room temperature.
[b] Molar equiv of the catalyst used with respect to the substrate.

The influence of the reaction time of O–substrate with acetic anhydride was studied as well. When acetic anhydride was used as reagent and as a solvent, the higher yield of the desired product was obtained. On the other hand, in CH_2Cl_2, the catalyst was not completely dissolved and the yield of the acylation product was less (entries 1 and 3 – 4). Recovery of the catalyst, HFPI, is possible but not necessary because only 0.1 mol % of the catalyst was used (entry 6 and 12).

Further, the catalytic activity of various FPI salts in acylation process was compared. The catalytic activity of AgFPI, $Mg(FPI)_2$ and $Zn([FPI)_2$ was investigated. The results are summerised in Table 6.2. The corresponding acetates were formed in relatively good yields, except the cases that $Mg(FPI)_2$ and $MgCl_2$ were used as catalysts (entries 3, 4 and 7).

Table 6.2 Acylation of catechol[a] with Ac_2O in the presence of different catalysts.

Entry	**Catalyst[b] (mol %)**	**Pyrocatechol diacetate – Yield (%)**			
		Time (min)	**Temp. (°C)**	**Solv.**	**Yield (%)**
1.	AgFPI (2 %)	30	RT	-	75
2.	AgFPI (5 %)	30	RT	-	78
3.	$Mg(FPI)_2$ (1 %)	30	RT	-	43-45
4.	$Mg(FPI)_2$ (1 %)	30	RT	CH_2Cl_2	25
5.	$Zn(FPI)_2$ (1 %)	30	RT	-	84
6.	$Mg[TFSI]_2$ (1 %)	20	RT	-	92
		15	RT	-	86[c]
7.	$MgCl_2$ (5 %)	60	RT	-	27

[a] The catechol was treated with Ac_2O (1.2 equiv.) in the presence of the catalyst under neat conditions at room temperature.

[b] Molar equiv of the catalyst used with respect to the substrate; [c] ref. [180].

It is known that lanthanide (III) salts are active Lewis acid catalysts. Therefore, lanthanide bis[bis(pentafluoroethyl)phosphinyl]imide, such as $La(FPI)_3$, $Yb(FPI)_3$, $Ce(FPI)_3$, have been used as efficient catalysts in acylation with acetic anhydride (Table 6.3). Catechol was chosen as a model substrat. All lanthanide FPI salts were effective in acylation, however, the activity of $La(FPI)_3$ was relatively low (entries 1 – 3) compared to the FPI acid, as catalyst, due to the heterogeneous conditions of the process. High yield, was obtained when ionic liquid, [emim]FPI (0.2 g, three drops), was choosed as solvent in this reaction (entry 4). The pure pyrocatechol diacetate was separated by sublimation in vacuum at 60 – 80 °C.

The N–acylation of amino groups is an important functionalization in organic chemisty [168]. Usually, acetic anhydride as a N–acylation reagent and a basic catalysts such as pyridine, 4–pyrrolidinopyridine, 4–dialkylaminopyridine, and ammonium acetate are used [181]. A variety of other catalysts, for instance as $Cu(OTf)_2$ [175], $In(OTf)_2$ [176], or zeolite H–FER [181] were also employed in these reactions. Here, a convenient procedure with HFPI as catalyst was developed for the N–acylation of aniline and its derivatives (Table 6.4). The reaction time was longer than in the case of O–acylation. N–benzyl–acetamide was easily isolated by crystallization (ether or CH_2Cl_2/hexane) from the crude product in good yield (entries 3 – 4). *p*–Br–aniline undergo acylation at the same conditions (entry 6) resulting in a good yield of product. N–acylated products were characterized by comparison of their NMR, MS spectra and melting points with those of authentic samples.

S–acylation was carried out with two different thiols: thiophenol and octane–1–thiol. The products were obtained in good yields (entry 7 and 8).

In conclusion, HFPI and the corresponding lanthanide salts are efficient catalyst for acetylation of phenols, thiols and amines [169]. The reactions proceed at room temperature, in solvent free conditions, resulting in a high yield of acetylated product.

Table 6.3 Acylation of substrates[a] with Ac_2O in the presence of different catalysts[b].

Entry	Substrate[a]	Product	Time (min)	Catalyst[b] (mol %)	Solv.	Temp. (°C)	Yield (%)
1.	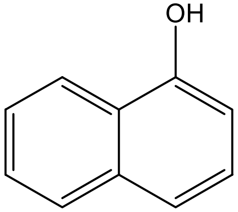	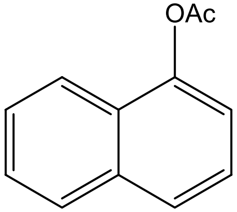	30	$La(FPI)_3$ (1 %)	–	RT	82
2.	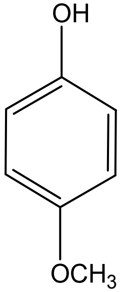	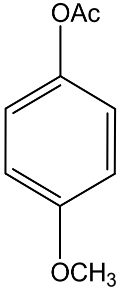	30	$La(FPI)_3$ (1 %)	–	RT	95
3 – 6.	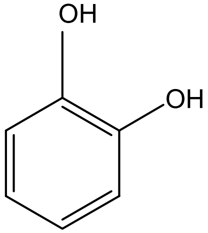	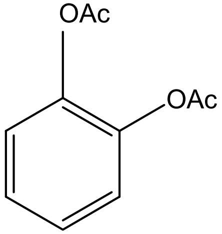	30	$La(FPI)_3$ (1 %)	–	RT	81–84
			30	**$La(FPI)_3$ (1 %)**	**IL[c]**	**RT**	**96**
			39	$Ce(FPI)_3$ (1 %)	–	RT	89
			30	$Yb(FPI)_3$ (1 %)	–	RT	79

[a] The substrate was treated with Ac_2O (1.2 equiv.) in the presence of the catalyst under neat conditions at room temperature.

[b] Molar equiv of the catalyst used with respect to the substrate.

[c] The reaction was carried out in [emim]FPI (0.2 g).

Table 6.4 Acylation of N, S – substrates[a] with Ac_2O in the presence of HFPI as catalysts[b].

Entry	Substrate[a]	Product	Catalyst[b] (mol %)	Time (min)	Temp. (°C)	Yield (%)
1 – 2.	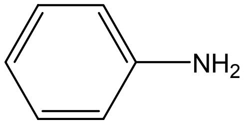	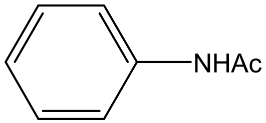	HFPI (0.8 %)	180	50	91
			HFPI (1%)	180	RT	90
3 – 4.	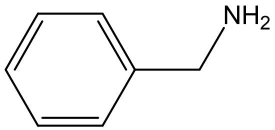	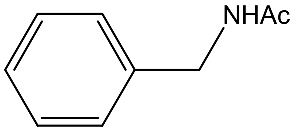	HFPI (1 %)	180	50	94–96
			HFPI (1 %)	70	RT	70
5	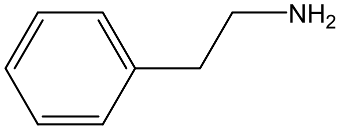	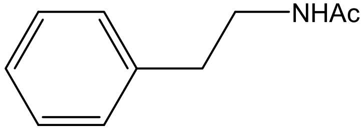	HFPI (1.25 %)	180	50	96
6.	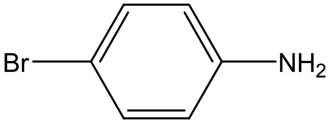	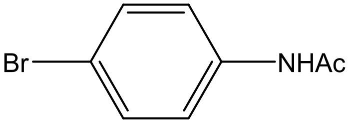	HFPI (1 %)	15	RT	95
7.	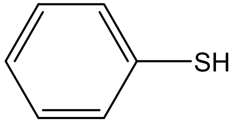	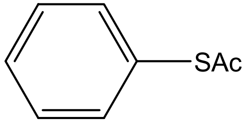	HFPI (1 %)	180	RT	93
8.	$CH_3(CH_2)_7SH$	$CH_3(CH_2)_7SAc$	HFPI (1.2 %)	180	RT	89

[a] The substrate was treated with Ac_2O (1.2 equiv.) in the presence of the catalyst at different temperature.
[b] Molar equiv of the catalyst used with respect to the substrate.

6.2 Acylation of – OH groups with other Brønsted acids as catalysts

Recently, it has been shown that $(C_2F_5)_2P(O)OH$ and $(C_4F_9)_2P(O)OH$ are efficient catalysts for acylation of 2–naphtol [13]. The acylation was carried out using variable amounts of catalyst with and without solvent. Addition of 1 mol % of $(C_2F_5)_2P(O)OH$ to a CH_2Cl_2 solution of 2–naphtol and acetic anhydride resulted in the formation of ester (**2f**) in high yield (96 %, entry 1), after 30 minutes. With 10 mol % of $(C_2F_5)_2P(O)OH$ as catalyst, under solvent free conditions, at room temperature, the product is formed in 94 – 95 % yield (entry 2). Triflic acid is also an active catalyst for acylation of 2–naphtol (entry 4). These observations suggested that the catalytic activities of these acids are comparable. Without catalyst (entry 5) the yield of the acylated product was lower than 10 %.

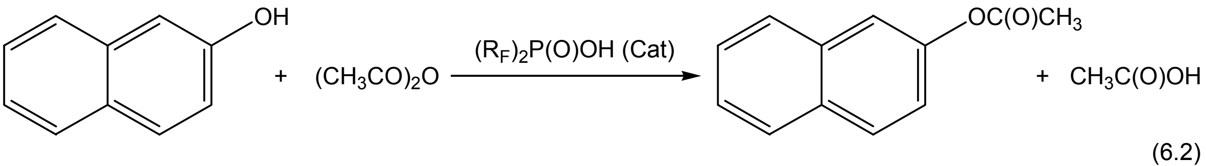

(**2f**)

(6.2)

Table 6.5 Acylation of 2–naphtol[a] with Ac_2O in the presence of different catalysts[b].

Entry	Catalyst[b] (mol %)	Time (min)	Solv.	Temp. (°C)	Yield (%)
1.	$(C_2F_5)_2P(O)OH$ (1 %)	30	CH_2Cl_2	RT	96
2.	$(C_2F_5)_2P(O)OH$ (10 %)	30	–	RT	94–95
3.	$(C_4F_9)_2P(O)OH$ (1 %)	30	CH_2Cl_2	RT	97
4.	CF_3SO_3H (1 %)	30	CH_2Cl_2	RT	95
5.	–	30	CH_2Cl_2	RT	< 10%

[a] The substrate was treated with Ac_2O (1.2 equiv.) in the presence of the catalyst at room temperature.
[b] Molar equiv of the catalyst used with respect to the substrate.

6.4 Experimental part

General procedure for the O – acetylation of 1–naphtol and 2–naphtol:

A mixture of the substrate, 2–naphtol (6.00 g, 41.6 mmol), acetic anhydride (5.09 g, 49.9 mmol, 1.2 equiv.) and HFPI (0.024 g, 0.1 mol % – related on substrate), was stirred at room temperature, under solvent free conditions, for 30 min. Then 15 mL of water was added to the reaction mixture and extracted with Et_2O (3 x 15 mL). The organic phase was washed successively with 2% aqueous NaOH (15 mL) and saturated NaCl solution (15 mL). After drying with $MgSO_4$, filtration and evaporation of the solvent at reduced pressure, the solid product was isolated and analyzed; **(Table 6.1, entry 6)**.

1–Naphtyl acetate (1f): white powder; Mp: 48 – 49 °C (lit. 48 – 49 °C [182]).
^{1}H NMR (lock/solvent $CDCl_3$, 400 MHz), δ, ppm: 7.90 – 7.89 m (CH; 2 x Ar); 7.78 d (CH; $^3J_{H,H}$ = 7.9 Hz); 7.57 – 7.53 m (CH; 3 x Ar); 7.29 m (CH; $^3J_{H,H}$ = 7.53 Hz); 2.50 s (CH_3).
^{13}C NMR (lock/solvent $CDCl_3$, 100.6 MHz), δ, ppm: 169.5 ($CH_3C(O)$); 146.5 (CH); 134.6 (CH); 128.0 (CH); 126.7 (CH); 126.4 (2 x *C*H); 126.0 (CH); 125.3 (CH); 121.1 (CH); 118.0 (CH); 20.9 ($C(O)CH_3$).
MS (ESI$^+$): 187 (M$^+$ + 1).
2–Naphtyl acetate (2f): yellowish powder; Mp: 70 °C (lit. 71 °C [182])
^{1}H NMR (lock/solvent $CDCl_3$, 400 MHz), δ, ppm: 7.89 – 7.86 m (CH; 2 x Ar); 7.84 – 7.83 d (CH; $^3J_{H,H}$ = 7.9 Hz); 7.61 d (CH; $^3J_{H,H}$ = 2.3 Hz); 7.51 m (CH; 2 x Ar); 7.27 d,d (CH; $^3J_{H,H}$ = 9.03 Hz); 2.38 s (CH_3).
^{13}C NMR (lock/solvent CD_3CN, 100.6 MHz), δ, ppm: 169.6 ($CH_3C(O)$); 148.3 (CH); 133.7 (CH); 131.4 (CH); 129.3 (CH); 127.7 (*C*H); 127.6 (CH); 126.5 (CH); 125.6 (CH); 121.1 (CH); 118.5 (CH); 21.1 ($C(O)CH_3$).
MS (ESI$^+$): m/z 187 (M$^+$ + 1).

General procedure for the O – acetylation of catechol and 4–nitrophenol:

A. In a round–bottom flask 4–nitrophenol (0.50 g, 3.5 mmol) was treated with acetic anhydride (0.44 g, 4.3 mmol,1.2 equiv) in the presence of HFPI (0.021 g, 0.035 mmol, 1 mol %). After 30 min stirring at room temperature 10 mL of water was added to the reaction mixture. The solid material was separated by filtration. Then Et_2O (10 mL) and 2% aqueous NaOH (10 mL) was added, and organic and aqueous layers were separated. The aqueous layer was extracted with Et_2O three times, and the organic layers were combined and dried over $MgSO_4$ and filtered. The solvent was removed under reduce pressure and yellowish solid product was obtained; **(Table 6.1, entry 14)**.

B. A mixture of $La(FPI)_3$ (0.17 g, 0.089 mmol, 1 mol %), [emim]FPI (0.2 g), catechol (1 g, 9.09 mmol) and acetic anhydride (2.22 g, 21.6 mmol, 1.2 equiv.) was stirred at room temperature for 30 min. The reaction mixture was washed with water (2 x 10 mL). The water was removed using Pasteur pipette and from the solid residue, pure pyrocatechol diacetate was obtained by sublimation in vacuum at 60 – 80 °C; **(Table 6.3, entry 4)**.

Pyrocatechol diacetate (3f): white crystals; Mp: 62 °C (lit. 62 – 63 °C [182]).

^{1}H NMR (lock/solvent $CDCl_3$, 400 MHz), δ, ppm: 7.22 – 7.20 m (CH; 2 x Ar); 7.29 – 7.26 m (CH; 2 x Ar); 2.31 s (CH_3).

^{13}C NMR (lock/solvent $CDCl_3$, 100.6 MHz), δ, ppm: 168.2 (2 x $CH_3C(O)$); 142.1 (2 x *C*H); 126.5 (2 x *C*H); 123.4 (2 x O*C*CH); 20.5 (2 x $C(O)CH_3$).

4–Nitrophenol acetate (4f): yellowish powder; Mp: 82 °C (lit. 82 °C [182]).

^{1}H NMR (lock/solvent $CDCl_3$, 400 MHz), δ, ppm: 8.28 d (CH; 2 x Ar; $^3J_{H,H}$ = 9.03 Hz); 7.30 d (CH; 2 x Ar; $^3J_{H,H}$ = 9.03 Hz); 2.36 s (CH_3).

^{13}C NMR (lock/solvent $CDCl_3$, 100.6 MHz), δ, ppm: 168.3 ($CH_3C(O)$); 155.3 (CH*C*C(O)); 145.3 (CH*C*NO_2); 124.1 (2 x *C*H); 122.3 (2 x *C*H); 21.0 ($C(O)CH_3$).

General procedure for the O–acetylation of 4–methoxyphenol:

A mixture of 4–methoxyphenol (0.60 g, 4.8 mmol), acetic anhydride (0.59 g, 5,7 mmol, 1.2 equiv) and catalyst (e.g. HFPI, 0.028 g, 1 mol %) was stirred at room temperature, under solvent free conditions. After 30 min, Et_2O (10 mL) and 2% aqueous NaOH (10 mL) was added, and organic and aqueous layers were separated. The aqueous layer was extracted with Et_2O three times; the organic layers were combined; dried over $MgSO_4$ and filtered. To isolate the product, the solvent was removed under reduce pressure; **(Table 6.1, entry 16)**.

<u>4–Methoxyphenyl acetate (5f)</u>: yellowish powder; Mp: 32-36 °C (lit. 32 °C, [183]).
^{1}H NMR (lock/solvent CDCl$_3$, 400 MHz), δ, ppm: 7.02 d,m (CH; 2 x Ar; $^3J_{H,H}$ = 9.4 Hz); 6.91 d,m (CH; 2 x Ar; $^3J_{H,H}$ = 9.03 Hz); 3.81 s (CH$_3$); 2.36 s (CH$_3$).
^{3}C NMR (lock/solvent CDCl$_3$, 100.6 MHz), δ, ppm: 169.9 (CH$_3$*C*(O)); 157.2 (CH*C*OC(O)CH$_3$); 144.1 (CH*C*OCH$_3$); 122.2 (2 x *C*H); 114.4 (2 x *C*H); 55.5 (O*C*H$_3$); 21.0 (C(O)*C*H$_3$).
MS (ESI$^+$): m/z 136 (M$^+$ - 2CH$_3$); 108 [M$^+$ - (C(O)CH$_3$ + CH$_3$)].

General procedure for the N–acetylation and S–acylation (Table 6.4):

To the mixture of HFPI (0.054 g, 1 mol %) and acetic anhydride (1.14 g, 11.1 mmol, 1.2 equiv), the substrate, N–benzylamine (1 g, 9.3 mmol), was added and the reaction mixture stirred at 50 °C for 3 hours. The volatile compounds were removed from the reaction mixture under vacuum. The reaction mixture was neutralized with 2% aqueous NaOH (10 mL) and extracted with CH$_2$Cl$_2$ (3 x 10 mL). The combined organic extracts were washed with cold water and dried over MgSO$_4$. To isolate the product, the solvent was removed under reduced pressure. The residue was recrystallized from ether or DCM/hexane **(Table 6.4, entry 3)**.

<u>N–Phenyl–acetamide (6f)</u>: white powder, Mp: 118 °C (lit. 117.5 °C [184]).
^{1}H NMR (lock/solvent CDCl$_3$, 400 MHz), δ, ppm: 7.67 br. s (NH); 7.52 d (2CH; $^3J_{H,H}$ = 7.51 Hz); 7.32 t (2CH; $^3J_{H,H}$ = 7.91 Hz); 7.12 t (CH; $^3J_{H,H}$ = 7.53 Hz); 2.18 s (CH$_3$).
^{13}C NMR (lock/solvent CDCl$_3$, 100.6 MHz), δ, ppm: 168.6 (CH$_3$*C*(O)); 137.8 (CH*C*HNH); 128.9 (2 x *C*H); 124.2 (2 x *C*H); 119.9 (*C*H); 24.4 (C(O)*C*H$_3$).
MS (ESI$^+$): m/z 136 (M$^+$+1); 137 (M$^+$+1/^{13}C).
<u>N–Benzyl–acetamide (7f)</u>: white crystals; Mp: 62 °C (lit. 62 °C [185]).
^{1}H NMR (lock/solvent CDCl$_3$, 400 MHz), δ, ppm: 7.34 m (CH; 2 x Ar); 7.29 m (CH; 3 x Ar); 6.76 br. s (NH); 4.43 d (CH$_2$; $^3J_{H,H}$ = 4.9 Hz); 2.07 s (CH$_3$).
^{13}C NMR (lock/solvent CDCl$_3$, 100.6 MHz), δ, ppm: 170.7 (CH$_3$*C*(O)); 137.7 (CH*C*HNH); 128.7 (2 x *C*H); 127.8 (2 x *C*H); 127.6 (*C*H); 43.9 (*C*H$_2$NH); 22.6 (C(O)*C*H$_3$).
MS (ESI$^+$): m/z 150 (M$^+$+1); 151 (M$^+$+1/^{13}C); 106 (M$^+$–C(O)CH$_3$); 91 (M$^+$–HC(O)CH$_3$).
<u>N–Phenethyl–acetamide (8f)</u>: white powder; Mp: 53 °C (lit. 52 °C [184]).

^{1}H NMR (lock/solvent $CDCl_3$, 400MHz), δ, ppm: 7.31 m (CH; 2 x Ar); 7.24 m (CH; Ar); 7.21 m (CH; 2 x Ar); 6.27 br. s (NH); 3.52 m (CH_2); 2.84 t (CH_2;$^3J_{H,H}$ = 7.1 Hz); 1.97 s (CH_3).

^{13}C NMR (lock/solvent $CDCl_3$, 100.6 MHz), δ, ppm: 170.5 (CH_3*C*(O)); 138.7 (CH*C*HNH); 128.6 (2 x *C*H); 128.5 (2 x *C*H); 126.4 (*C*H); 40.8 (*C*H_2CH_2NH); 35.4 (*C*H_2NH); 22.8 (C(O)*C*H_3).

MS (ESI$^+$): m/z 164 (M^++1); 165 (M^++1/^{13}C); 105 (M^+–NHC(O)CH_3).

N–(4–bromophenyl)–acetamide (9f): white solid, Mp: 169 °C (lit. 167-169 °C [186])

^{1}H NMR (lock/solvent $CDCl_3$, 400 MHz), δ, ppm: 8.13 br. s (NH); 7.38 m (2CH); 7.31 m (2CH); 2.05 s (CH_3).

^{13}C NMR (lock/solvent $CDCl_3$, 100.6 MHz), δ, ppm: 168.6 (CH_3*C*(O)); 137.3 (CH*C*HNH); 131.2 (2 x *C*H); 120.9 (2 x *C*H); 116.6 (*C*HBr); 23.7 (C(O)*C*H_3).

S–Phenyl–thioacetate (10f): white liquid; Mp: 18 - 20 °C (lit. 18 – 19 °C [187])

^{1}H NMR (lock/solvent $CDCl_3$, 400 MHz), δ, ppm: 2.45 s (CH_3); 7.45–7.43 m (CH; 5 x Ar).

^{13}C NMR (lock/solvent $CDCl_3$, 100.6 MHz), δ, ppm: 193.9 (CH_3*C*(O)); 134.4 (2 x *C*H); 129.3 (CH*C*S); 129.1 (2 x *C*H); 127.9 (*C*H); 30.1 (C(O)*C*H_3).

S–Octyl–thioacetate (11f): white liquid; Mp: - 19 to - 18 °C.

^{1}H NMR (lock/solvent $CDCl_3$, 400 MHz), δ, ppm: 2.88 t (CH_2; $^3J_{H,H}$ = 7.4 Hz); 2.31 s (CH_3); 1.58 quin (CH_2; $^3J_{H,H}$ = 7.4 Hz); 1.35 to1.39 m (CH_2); 1.26 to1.33 m (4CH_2); 0.92 t (CH_3).

^{13}C NMR (lock/solvent $CDCl_3$, 100.6 MHz), δ, ppm: 196.0 (CH_3*C*(O)); 31.7 (*C*H); 30.6 (*C*H); 29.4 (*C*H); 29.2 (*C*H); 29.1 (*C*H); 29.0 (*C*H); 28.8 (*C*H); 22.6 (*C*H); 14.0 (C(O)*C*H_3).

Chapter 7

7. Bis(pentafluoroethyl)phosphinic acid amides and acid hydrazides

Bis(perfluoroalkyl)phosphinic acid amides and acid hydrazides are very interesting compounds for several possible applications, for example in the synthesis of organic compounds having a $(R_F)_2P(O)$– moiety or as phase–transfer catalyst, surfactants (tensides), lubrificants, plasticizers, flame retardants, foams forming agents, antioxidants, or additives to electrolytes in electrochemical cells.

In the following chapter the recent developments in the synthesis of bis(pentafluoroethyl)phosphinic acid amides and acid hydrazides are highlighted [188].

7.1 Bis(pentafluoroethyl)phosphinic acid amides

Only few fluorinated phosphinic acid amides are described in the literature. Their syntheses are based on interaction of phosphinic acid chloride with amines [16]. For example, bis(perfluoroalkyl)phosphinic acid amide $(C_nF_{2n+2})_2P(O)NHR$ were prepared in moderate yield by the reaction of $(C_nF_{2n+1})_2P(O)Cl$ (n =3, 4) with aliphatic and aromatic amines [18, 47, 189].

Tris(perfluoroalkyl)phosphine oxides are also possible starting material for the synthesis of bis(perfluoroalkyl)phosphinic acid amides: (i) Burg and Sarkis (1969) reported a quantitative reaction of bis(trifluoromethyl)phosphine oxide with dimethyl amine [190] and (ii) Mahmood *et al.* (1988) have found that reaction of bis(nonafluorobutyl)phosphine oxide with dimethyl amine results in the formation of complex mixture of products but they failed in their separation [191].

Here, the aminolysis of tris(pentafluroethyl)phosphine oxides with ammonia, aliphatic and aromatic amines are presented, according to equation 7.1. These reactions occur at low temperature (–30 to 0 °C) giving the products in good yields as it is shown in Table 7.1.

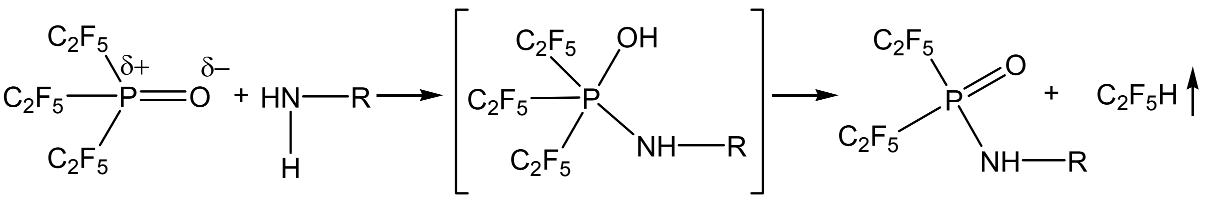

(**1b** and **1-3 g**) (7.1)

Table 7.1 Structures, melting points and yields of bis(pentafluoroethyl)phosphinic acid amides.

Compound	R	Mp (°C)	yield, %
1b	H	96 – 98	86
1g	$CH_2C_6H_5$	93 – 94	89
2g	$CH_2CH_2C_6H_5$	109 – 110	84
3g	$CH_2CH(C_2H_5)(CH_2)_3CH_3$	76	92

$(C_2F_5)_2P(O)NH_2$ (**1b**) as a precursor for the synthesis of HFPI acid is described in chapter 2. $(C_2F_5)_2P(O)NH_2$ is hydrolytically unstable compound. It is slowly converted to an ammonium salt when is disolved in wet solvents. The amides having longer alkyl chain attached to the nitrogen (**1g** – **3g**) are more stable against hydrolysis.

The IR and Raman spectra of $(C_2F_5)_2P(O)NH_2$ (**1b**) are shown in Figure 7.1. The bands attributed to ν(N–H) are at 3360 cm^{-1} and other fundamental vibrations are below 1400 cm^{-1}. Between 1300 and 997 cm^{-1} there are intense absorption assigned to CF_3, CF_2, P–N and P=O. The strongest Raman band at 754 cm^{-1} is attributed to the symmetric CF_3 deformations.

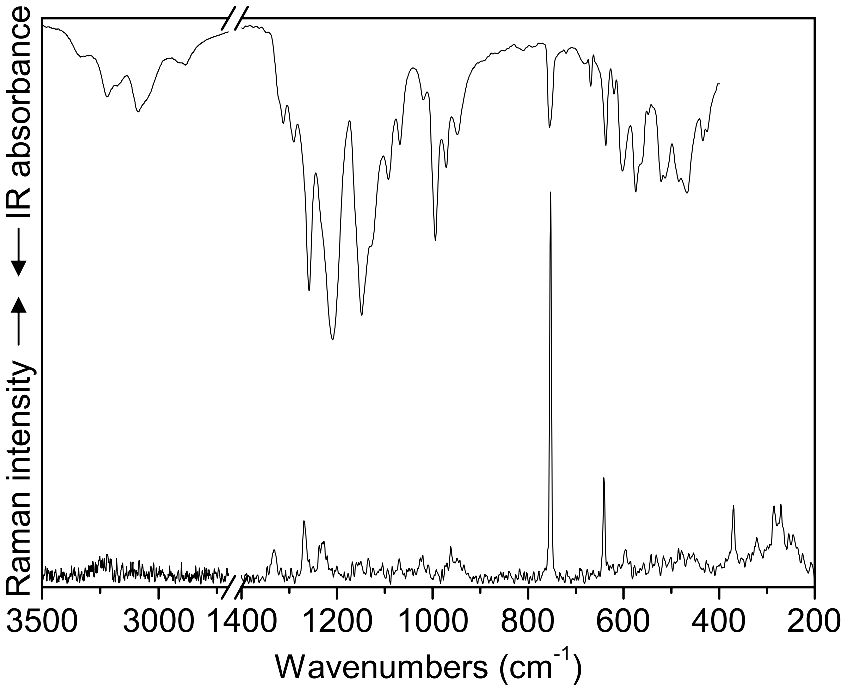

Figure 7.1 Infrared and Raman spectra of solid $(C_2F_5)_2P(O)NH_2$ recorded as neat compound.

All products were characterized by ^{1}H, ^{19}F, ^{31}P NMR spectroscopy (see experimental part). The NMR spectra were measured in dry CD_3CN solution. In the ^{1}H NMR – spectrum for (**1b**) the NH is a broad singlet at 5.3 ppm and for (**1g** – **3g**) is a broad dublet at 5.7, 5.3 and 5.08 ppm, respectively. The ^{19}F NMR spectrum of the C_2F_5 group is complicate and shows a singlet at –81 and a multiplett at –125 ppm in a relative ratio of 3:2. In the ^{31}P NMR spectrum of (**1b**) only a quintet of multiples is observed at 12.9 ppm. The ^{31}P NMR spectrum of (**1g** – **3g**) showed overlapping triplet of triplet of doublet of triplet as depicted in Figure 7.2, due to the P–H spin–coupling ($^2J_{PH}$ = 20 Hz and $^3J_{PH}$ = 11 Hz). In the ^{31}P{^{1}H} an overlapping triplet of triplet is observed due to the coupling with the four ^{19}F nuclear of the two CF_2 groups.

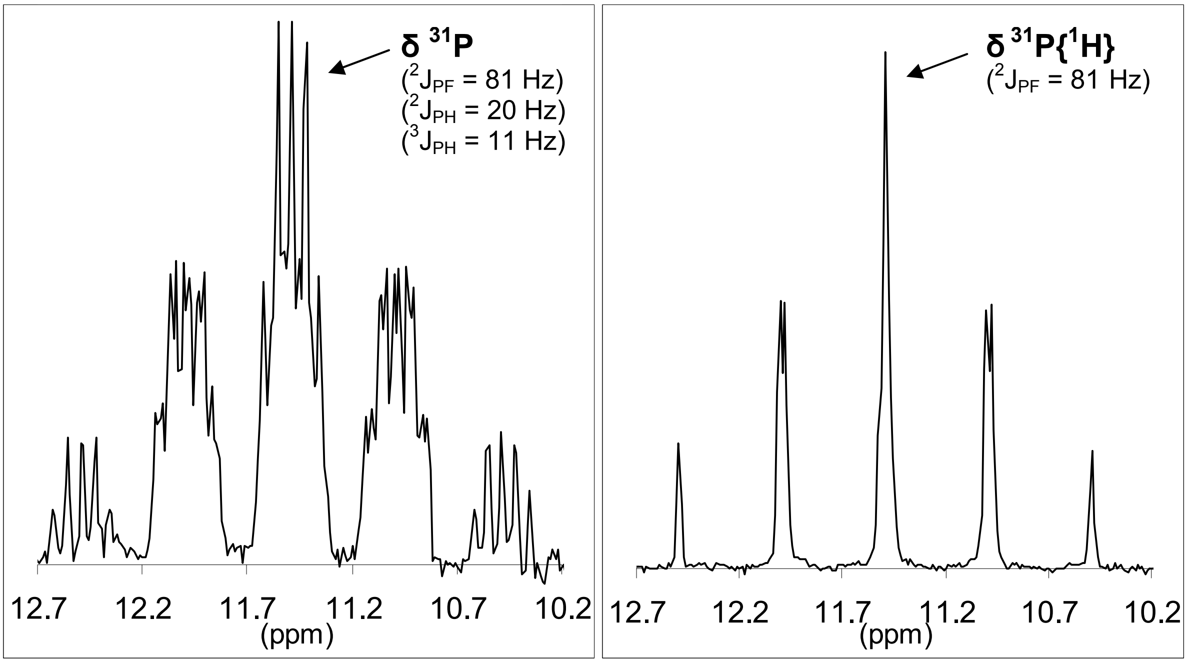

Figure 7.2 ^{31}P and $^{31}P\{^1H\}$ NMR spectra of $(C_2F_5)_2P(O)NHCH_2C_6H_5$ (**1g**) in acetonitrile–D_3.

7.2 Bis(pentafluoroethyl)phosphinic acid hydrazide

Acetylhydrazides are well known building block in organic chemistry [192]. They play an important role as reagents in the synthesis of heterocyclic compounds: which are of interest as drugs, dyes or initiators for polymerization. There are few reports on the preparation of phosphinic acid hydrazides: (i) $(CH_3)_2P(O)NHNHPh$ and $Ph_2P(O)NHNHPh$ [193]; (ii) $(CH_3)_2P(O)NHNH_2$ [194]; (iii) $(C_2H_5)_2P(O)NHNH(t\text{–}C_4H_9)$ [195] and (iv) $Ph_2P(O)NHNH_2$ and $Ph_2P(O)NHNH(CH_3)_2$ [196]. All these compounds were prepared by reaction of phosphinic acid chlorides, $R_2P(O)Cl$ with corresponding hydrazines. No fluorinated phosphinyl hydrazides are described in the literature.

Bis(pentafluoroethyl)phosphinic acid hydrazides, $(C_2F_5)_2P(O)NHNHR$ are unknown compounds and are investigated for the first time. Results based on the synthesis of the acid hydrazides having C_2F_5 groups attached to the phosphorus will be reported also in the patent application by Ignatiev *et al.*, (2010) [188]. These hydrazides can be synthesized not only from bis(pentafluoroethyl)phosphinic acid chlorides, but also from less reactive tris(pentafluoroethyl)phosphine oxides, as shown in equations 7.2, and 7.4. In the preparation of the acid hydrazides from bis(pentafluoroethyl)phoshinic acid chlorides, CaH_2 was used as scavenger of HCl in order to avoid the formation of [NH_2NRR']Cl as side product (equation 7.3). The melting points and yields of hydrazides are presented in Table 7.2.

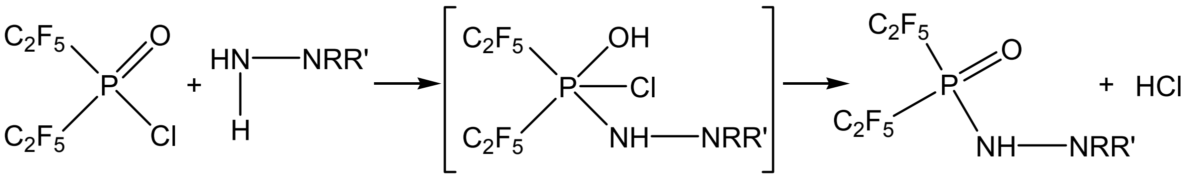

(**4 - 5 g**) (7.2)

$$2HCl + CaH_2 \longrightarrow CaCl_2 + H_2\uparrow \qquad (7.3)$$

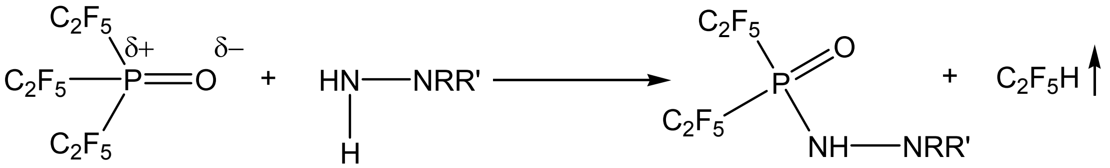

(**4 - 6 g**) (7.4)

Table 7.2 Structures, melting points and yields of bis(pentafluoroethyl)phosphinic acid hydrazides.

Compound	R	R'	Mp (°C)	yield, %
4g	H	CH_3	72	84
	H	CH_3	72	<75
5g	H	C_6H_5	88	81
	H	C_6H_5	88	77
6g	CH_3	CH_3	71	82

These hydrazides are moisture sensitive compounds. All reactions were carried out in glass flasks equipped with a glass valve with PTFE piston (Young, London) attached to the vacuum line. Manipulations of non–volatile compounds were carried out in glove box.

Bis(pentafluoroethyl)phosphinic acid hydrazide were characterized by ^1H, ^{19}F, ^{31}P NMR spectroscopy (see experimental part). The NMR spectra were measured in dry CD_3CN solution. The ^{19}F NMR spectrum of the C_2F_5 group is complicated as a consequence of non–equivalent F atoms in the CF_2 group. The experimental ^{19}F NMR parameters were used as input for simulation (**gNMR 4.1** program) of the ^{19}F

NMR spectrum of **5g** as a AA'X spin system. The observed and simulated AA' part is depicted in Figure 7.3. The ^{31}P NMR spectrum of $(C_2F_5)_2P(O)NHNHC_6H_5$ (**5g**) shows an overlapping triplet of triplet of doublet of doublet as depicted in Figure 7.4, due to the P–H spin–coupling ($^2J_{PH}$ = 44 Hz and $^3J_{PH}$ = 4 Hz).

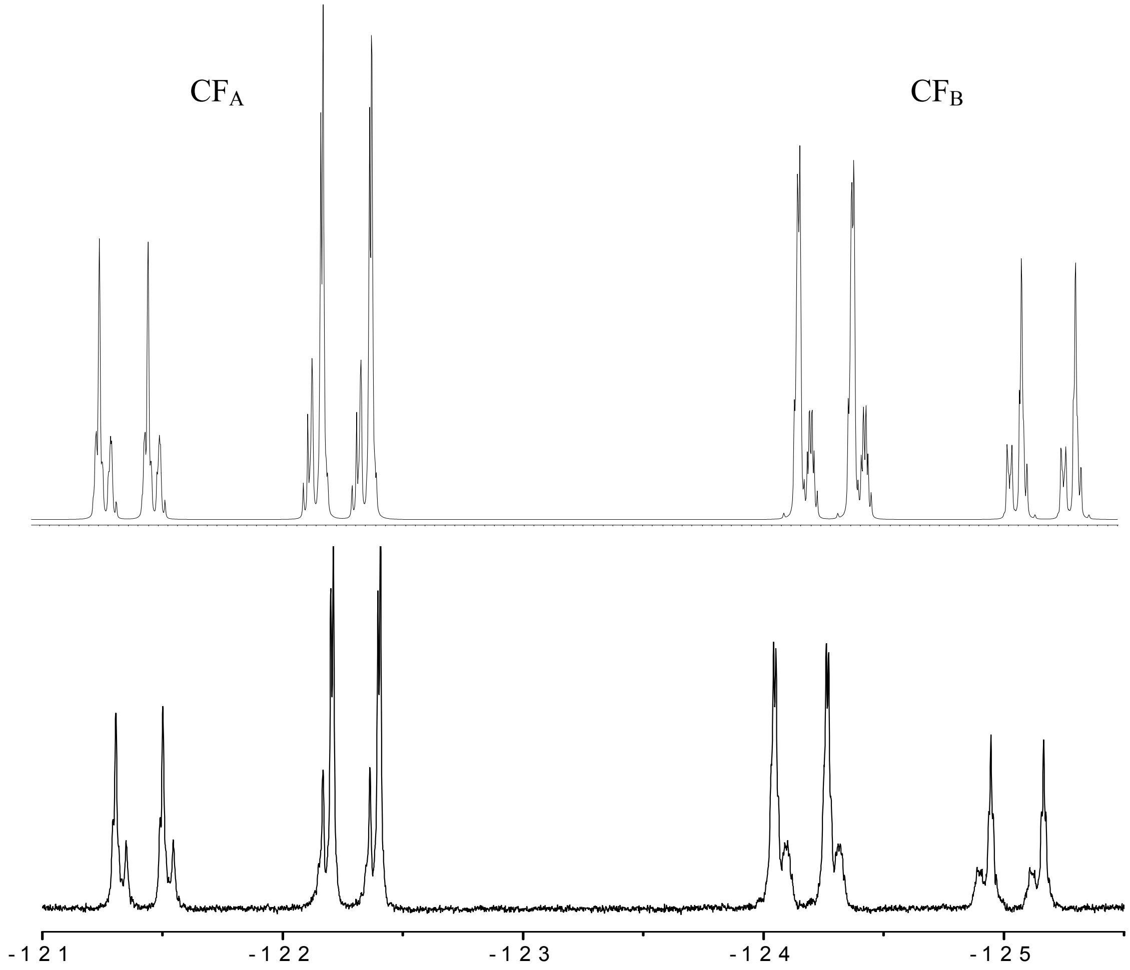

Figure 7.3 Simulated (top) and observed (bottom) spectrum of the CF_2 resonances in acetonitrile–D_3.

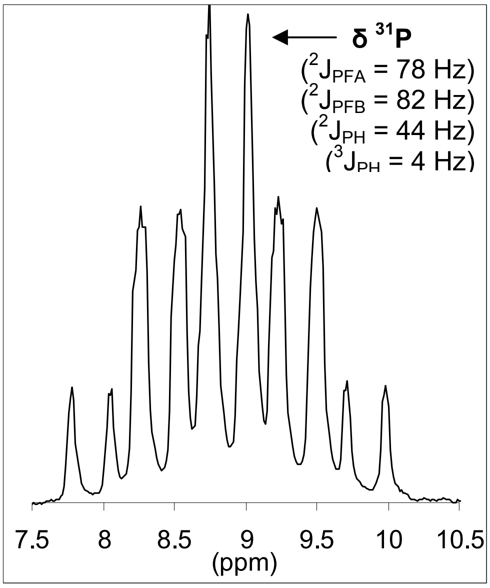

Figure 7.4 ^{31}P NMR spectra of $(C_2F_5)_2P(O)NHNHC_6H_5$ (**5g**) in acetonitrile–D_3.

7.3 Crystal structure of $(C_2F_5)_2P(O)NH_2$

Single crystals of $(C_2F_5)_2P(O)NH_2$ were obtained after aminolysis of $[(C_2F_5)_2P(O)]_2O$ with NH_3 and evaporation of the solvent at low temperature, as well as by recrystallisation from a mixture of benzene and hexane (1:2).

A **Gemini E Ultra –Diffractometer** (Oxford) was used for measurements at 150 K with Mo–Kα radiation (λ = 0.717073 Å). The crystal structures were solved by direct methods using SHELXS–97. Full–matrix least–squares of refinement on F^2 was perfomed with WinGX V1.6405 (SHELXL–97) [155].

The parameters obtained for $(C_2F_5)_2P(O)NH_2$ are listed in Table 7.3. The angles and distances are given in Appendix 1. Figure 7.5 presents two independent formula units.

Phosphorus atom is tetrahedral coordinated. The angle O–P–N (116°) is larger than in $P(O)(NH_2)_3$ (119.09, 108.91 and 109.09°, respectively) [197] and C–P–C angle (101.9°) is smaller than in $[\{(C_2F_5)_2P(O)\}_2N]^-$ (102.4 or 104.8°). The angles of nitrogen atom are P–N–H_1 (114.5°), P–N–H_2 (112.5°) and H_2–N–H_1 (124.7°) close to average 120°.

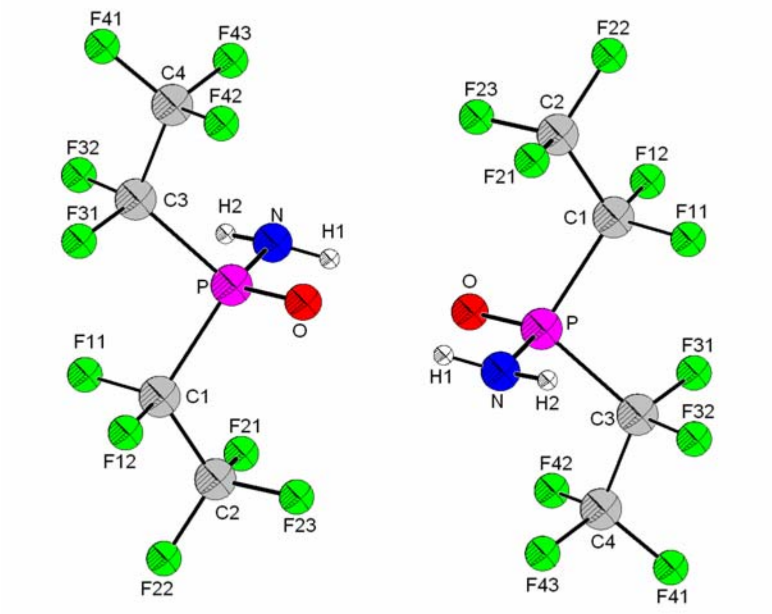

Figure 7.5 Molecular structure of two formula unit of $(C_2F_5)_2P(O)NH_2$ in the unit cell.

The P=O bond in phosphinic acid amide (1.476 Å) is longer that in phosphoryl compounds such as $POCl_3$ (1.45 Å) [198], but similar in length to that in molecules as $H[\{(C_2F_5)_2P(O)\}N\{S(O)_2CF_3\}]$ (1.472 Å) and $H[\{(C_2F_5)_2P(O)\}_2N]$ (1.474 Å). The bonds: P–N (1.594 Å), $N–H_1$ (0.889 Å) and $N–H_2$ (0.885 Å) are quite similar than the length usually accepted. After refinement the hydrogen bond are $N–H_1…O$ (2.089 Å) and $N–H_2…O$ (2.258 Å).

The mesomeric and tautomeric structures of **1a** (Figure 7.6) can be used to rationalize the crystal structure of $(C_2F_5)_2P(O)NH_2$, were the sp^2 hybridization for N atom was clearly marked.

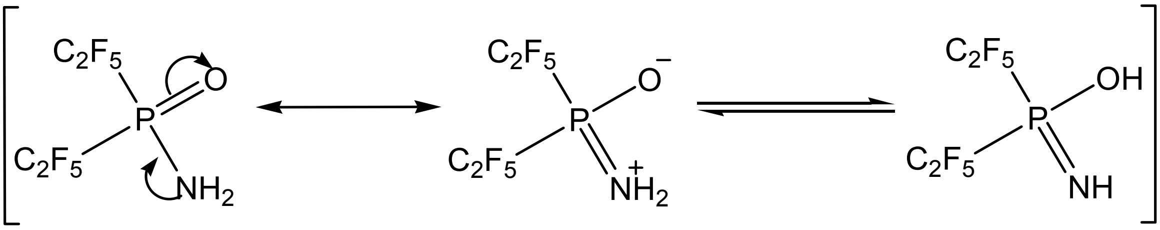

Figure 7.6 Mesomeric and tautomeric structures of $(C_2F_5)_2P(O)NH_2$.

Table 7.3 Crystalographic and refinement data for **1e**.

Crystalographic data	$(C_2F_5)_2P(O)NH_2$ (**1b**)
Empirical formula	$C_4H_2F_{10}NOP$
Colour	colorless
Formula weight	301.04 g·mol^{-1}
Temperature	150 K
Wavelength	0.71073 Å
Crystal system	Monoclinic
Space group	**$P2_1$, (no. 14)**
Unit cell dimensions	a = 5.4103(6) Å α= 90° b = 15.5309(18) Å β = 95.538(12)° c = 11.6353(16) Å γ = 90°
Volume	973.1(2) Å^3
Z	4
Density (calculated)	2.055 mg·m^{-3}
Absorption coefficient	0.421 mm^{-1}
F(000)	584 e
Crystal size	0.56 x 0.13 x 0.04 mm^3
θ range for data collection	3.16 to 29.01°
Index ranges	$-3 \le h \le 7$, $-20 \le k \le 19$,$-15 \le l \le 15$
Reflections collected	4305
Independent reflections	2190 [R_{int} = 0.0412]
Reflections with $I>2\sigma(I)$	6920
Completeness to	(= 29.01°) 84.6 %
Absorption correction	Numerical
Refinement method	Full-matrix least-squares on F^2
Data/restraints/parameters	2190/2/161
Goodness-of-fit on F^2	1.025
Final R indices $[I>2\sigma(I)]^a$	R_1 = 0.0836 wR^2 = 0.2147
R indices (all data)^b	R_1 = 0.1093 wR^2 = 0.2284
Largest diff. peak and hole	0.895 and -0.580 e Å^{-3}

7.4 Experimental part

Bis(pentafluoroethyl)phosphinyl–N–(benzyl)amide, $(C_2F_5)_2P(O)NHCH_2C_6H_5$ (1g)

A 10 mL flask, equipped with a magnetic stirring bar, septum and drying tube filled with sicapent, was charged under nitrogen with $(C_2F_5)_3PO$ (3.22 g, 7.9 mmol). The benzyl amine (0.85 g, 7.9 mmol) was slowly added under good stirring at 0 °C. The reaction is exothermic and was let to warm up at room temperature to liberate C_2F_5H. The flask was connected to the membrane vacuum for 5 minutes to remove not reacted $(C_2F_5)_3PO$. The resultant solid was solved in benzene and transferred to a separator funnel and washed 3 times with water. The solvent was distilled off under reduced pressure (< 0.05 mbar). After drying under vacuum, 2.76 g of white solid material was obtained. Yield: 89%. Mp: 93 – 94 °C.

^{1}H NMR (lock/solvent CD_3CN, 400 MHz), δ, ppm: 7.39–7.29 m (5CH); 5.7 br.d (NH); 4.31 d,d (CH_2); $^2J_{P,H}$ = 20 Hz; $^3J_{H,H}$ = 7.1 Hz.

^{19}F NMR (lock/solvent CD_3CN, 376.4 MHz), δ, ppm: –81.1 m ($2CF_3$); –124.6 d,d,m ($2CF_a$); –126.6 d,d,m ($2CF_b$); $^2J_{P,Fa}$ = 80 Hz; $^2J_{P,Fb}$ = 87 Hz; $^2J_{Fa,Fb}$ = 319 Hz.

^{31}P NMR (lock/solvent CD_3CN, 161.9 MHz), δ, ppm: 12.7 t,t,d,t (1P); $^2J_{P,H}$ = 20 Hz; $^3J_{P,H}$ = 11 Hz, $^2J_{P,F}$ = 81 Hz.

Bis(pentafluoroethyl)phosphinyl–N–(2–phenyl–ethyl)amide, $(C_2F_5)_2P(O)NHCH_2CH_2C_6H_5$ (2g)

Under an inert atmosphere of nitrogen 2.29 g (17.7 mmol) of 2–phenyl–ethyl amine was added slowly to $(C_2F_5)_3PO$ (7.15 g, 17.7 mmol) at 0 °C with a good stirring. During this time the reaction mixture turned into a white solid. Then the same procedure was followed as that described above. 6.12 g of white solid was obtained. Yield: 84%. Mp: 109 – 110 °C.

^{1}H NMR (lock/solvent CD_3CN, 400 MHz), δ, ppm: 7.34–7.26 m (5CH); 5.3 br.d (NH); 3.37 quin (CH_2); 2.84 t (CH_2); $^2J_{P,H}$ = 20 Hz; $^3J_{H,H}$ = 7.1 Hz.

^{19}F NMR (lock/solvent CD_3CN, 376.4 MHz), δ, ppm: –81.4 m ($2CF_3$); –124.6 m ($2CF_a$); –126.7 m ($2CF_b$); $^2J_{P,Fa}$ = 81 Hz; $^2J_{P,Fb}$ = 88 Hz; $^2J_{Fa,Fb}$ = 319 Hz.

^{31}P NMR (lock/solvent CD_3CN, 161.9 MHz), δ, ppm: 11.2 t,t,d,t (1P); $^2J_{P,F}$ = 81 Hz.

Bis(pentafluoroethyl)phosphinyl–N–(2–ethylhexyl)amide, $(C_2F_5)_2P(O)NHCH_2CH(C_2H_5)(CH_2)_3CH_3$ (3g)

The same procedure as described above. The 2–ethylhexyl amine (2.19 g, 16.9 mmol) was added slowly to $(C_2F_5)_3PO$ (6.8 g, 16.9 mmol) at 0 °C with a good stirring. The product **3g** was obtained as a white solid (glue) (6.45 g). Yield: 92%. Mp: 76 °C.
^{1}H NMR (lock/solvent CD_3CN, 400 MHz), δ, ppm: 5.08 br.d (NH); 3.05 t,d (CH); 1.35 m ($5CH_2$), 0.88 t (CH_3), 0.85 t (CH_3); $^2J_{P,H}$ = 20 Hz; $^3J_{P,H}$ = 10 Hz, $^3J_{H,H}$ = 6.8 Hz.
^{19}F NMR (lock/solvent CD_3CN, 376.4 MHz), δ, ppm: –81.2 m ($2CF_3$); –124.6 m ($2CF_a$); –126.6 m ($2CF_b$); $^2J_{P,Fa}$ = 76 Hz; $^2J_{P,Fb}$ = 81 Hz; $^2J_{Fa,Fb}$ = 332 Hz.
^{31}P NMR (lock/solvent CD_3CN, 161.9 MHz), δ, ppm: 11.2 t,t,d,t (1P); $^2J_{P,H}$ = 20 Hz; $^3J_{P,H}$ = 10 Hz $^2J_{P,F}$ = 81 Hz.

Bis(pentafluoroethyl)phosphinyl–N–(methyl)hydrazide, $(C_2F_5)_2P(O)NHNHCH_3$ (4g)

A dry 25 mL flask, equipped with a glass valve with PTFE piston (Young), was charged in a vacuum line with 0.10 g (2.1 mmol) of methylhydrazine, 1 mL of dry acetonitrile and 1.3 g (3.2 mmol) of $(C_2F_5)_3PO$. The reaction mixture was left stirring at room temperature for 16 h and then all volatile products were removed under vacuum (10^{-3} mbar). 0.58 g of a white solid product was obtained. **4g** was handled in a dry–box for NMR and melting point measuring. Yield: 84 %. Mp: 72 °C.
^{1}H NMR (lock/solvent CD_3CN, 400 MHz), δ, ppm: 6.75 br.d (NH); 4.12 br.s (NH); 2.57 s (CH_3); $^2J_{P,H}$ = 40 Hz .
^{19}F NMR (lock/solvent CD_3CN, 376.4 MHz), δ, ppm: : –81.4 m ($2CF_3$); –122.4 m ($2CF_a$); –124.6 m ($2CF_b$); $^2J_{P,Fa}$ = 73 Hz; $^2J_{P,Fb}$ = 80 Hz; $^2J_{Fa,Fb}$ = 322 Hz.
^{31}P NMR (lock/solvent CD_3CN, 161.9 MHz), δ, ppm: 9.0 m (1P).
Elemental analysis calcd. (%) for $C_5H_5F_{10}N_2OP$ (M = 330.06 g/mol): C 18.19, H 1.53, N 8.49; found: C 17.93, H 1.94, N 9.28.

Bis(pentafluoroethyl)phosphinyl–N–(phenyl)hydrazide, $(C_2F_5)_2P(O)NHNHC_6H_5$ (5g)

A. A dry 25 mL flask, equipped with a glass valve with PTFE piston (Young), was charged in a vacuum line with 0.47 g (4.3 mmol) of phenylhydrazine, 1 mL of dry acetonitrile and 1.9 g (4.7 mmol) of $(C_2F_5)_3P(O)$. After one hour stirring at room temperature a homogeneous solution was formed. To complete the reaction, the mixture was left stirring at room temperature for 20 hours and then all volatile products were removed under vacuum (10^{-3} mbar). The resulting slightly yellow solid material (1.37 g) was purified by sublimation in high vacuum at 82 °C. Yield: 81%. Mp = 88 °C.

^{1}H NMR (lock/solvent CD_3CN, 400 MHz), δ, ppm: 7.46 br.d (NH); 7.24 – 7.31 m (2H); 7.00 – 6.92 m (3H); 6.47 d (NH); $^2J_{P,H}$ = 44 Hz; $^3J_{P,H}$ = 4 Hz.

^{19}F NMR (lock/solvent CD_3CN, 376.4 MHz), δ, ppm: –81.2 m ($2CF_3$); –121.9 m ($2CF_a$); –124.6 m ($2CF_b$); $^2J_{P,Fa}$ = 74 Hz; $^2J_{P,Fb}$ = 83 Hz; $^2J_{Fa,Fb}$ = 340 Hz.

^{31}P NMR (lock/solvent CD_3CN, 161.9 MHz), δ, ppm: 8.9 t,t,d,d (1 P); $^2J_{P,H}$ = 44 Hz; $^3J_{P,H}$ = 4 Hz; $^2J_{P,Fa}$ = 78 Hz; $^2J_{P,Fb}$ = 82 Hz.

Elemental analysis calcd. (%) for $C_{10}H_7F_{10}N_2OP$ (M = 392.13 g/mol): C 30.63, H 1.80, N 7.14; found: C 30.76, H 2.13, N 7.47.

B. A dry 25 mL flask, equipped with a glass valve with PTFE piston (Young), was charged with 0.15 g CaH_2, 0.34 g (3.1 mmol) of phenylhydrazine, 1 mL of dry acetonitrile. At a vacuum line 1.5 g (4.6 mmol) of $(C_2F_5)_2P(O)Cl$ were condensed to the reaction mixture. After warming up to room temperature, the reaction mixture was left stirring for 20 h and filtered. Subsequently all volatile material were removed under vacuum (10^{-3} mbar). The resulting yellow crystalline solid product (0.94 g) was handled only in a dry–box. Yield: 77%. Mp = 88 °C.

Bis(pentafluoroethyl)phosphinyl–N,N–di(methyl)hydrazide, $(C_2F_5)_2P(O)NHN(CH_3)_2$

A dry 25 mL flask, equipped with a glass valve with PTFE piston (Young), was charged at a vacuum line with 0.23 g (3.8 mmol) of 1,1–dimethylhydrazine, 1 mL of dry acetonitrile and 1.78g (4.4 mmol) of $(C_2F_5)_3P(O)$. At room temperature the exothermic reaction started and the reaction mixture became homogeneous. The reaction mixture was left stirring at room temperature for 15 hours and then all volatile materials were removed under vacuum (10^{-3} mbar). The white solid product (1.45 g) was handled only in a dry–box. Yield: 82%. Mp = 71 °C.

^{1}H NMR (lock/solvent CD_3CN, 400 MHz), δ, ppm: 6.90 br.d (NH); 2.61 (CH_3); 6.47 d (NH); $^2J_{P,H}$ = 42 Hz.

^{19}F NMR (lock/solvent CD_3CN, 376.4 MHz), δ, ppm: –81.2 m ($2CF_3$); –121.4 m ($2CF_a$); –124.9 m ($2CF_b$); $^2J_{P,Fa}$ = 72 Hz; $^2J_{P,Fb}$ = 82 Hz; $^2J_{Fa,Fb}$ = 338 Hz.

^{31}P NMR (lock/solvent CD_3CN, 161.9 MHz), δ, ppm: 6.5 t,t,d(1P); $^2J_{P,H}$ = 42 Hz; $^3J_{P,H}$ = 4 Hz; $^2J_{P,F(A)}$ = 74 Hz; $^2J_{P,F(B)}$ = 82 Hz;

Elemental analysis calcd. (%) for $C_6H_7F_{10}N_2OP$ (*M* = 344.09 g/mol): C 20.94, H 2.05, N 8.14; found: C 21.25, H 2.58, N 8.87.

Instrumental

The reactions were carried out usually in cylindrical or round bottom flasks. The special equipments made from FEP (tetrafluoroethylen-hexafluoropropylene), PFA (perfluoroalkyl–perfluoralkoxycopolymer) or PTFE (polytetrafluoroethylene) container and connections were used for working with HF solution (Figure 8.1).

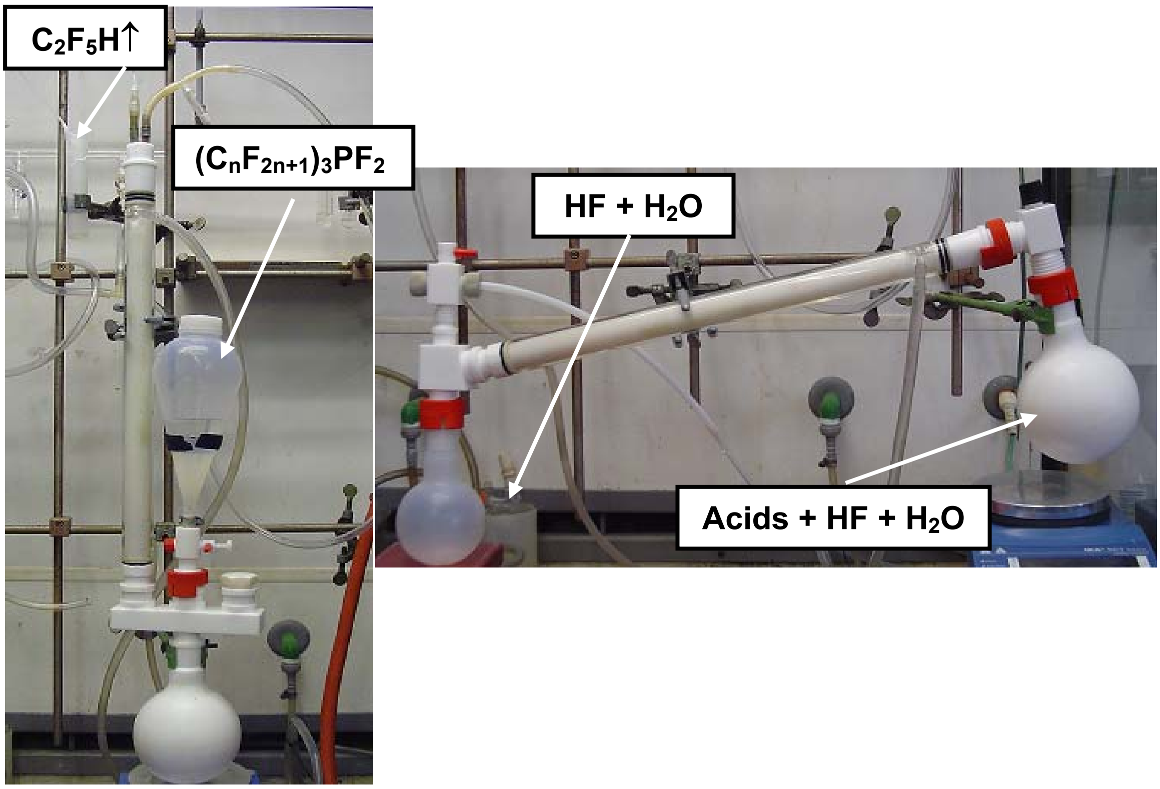

Figure 8.1 Laboratory set–up for preparation of bis(perfluoroalkyl)phosphinic and perfluoroalkylphosphonic acids.

The commercial solvents and reagents were obtained from various sources. For drying and purification, the solvents were distilled following standard procedures and stored over molecular sieves. For handling and storage non volatile air sensitive compounds a glovebox (**mBraun**, **Siemens SIMATIC OP7**) with residual water (H_2O < 2 ppm) and ($O_2 < 2$ ppm) was used. Air and moist-sensitive reactions or manipulations were conducted under nitrogen or argon atmosphere into flasks equipped with a glass valve with PTFE piston (Young, London).

1. Analytical procedures: Elemental analysis was performed using a **HEKATECH EA 3000** (Wegberg, Germany) elemental analyser and the **Callidus** software.

2. NMR spectroscopy: NMR spectra of all compounds were recorded on a **Bruker Avance DRX-400 MHz** (^{1}H, 400.13 MHz; ^{19}F, 376.49 MHz; ^{13}C, 100.61 MHz; ^{31}P, 161.97 MHz) and **Bruker Avance DRX-600 MHz** (^{1}H, 600.13 MHz; ^{13}C, 150.9 MHz; ^{31}P, 242.9 MHz) spectrometer. For simulation a **gNMR 4.1** program was used.

The spectra were recorded at room temperature. The chemical shifts are reported in parts per million (ppm) relative to external TMS (^{1}H), $CFCl_3$ (^{19}F) and H_3PO_4 (^{31}P). The coupling constants (*J*) are reported in Hertz (Hz). Usually approximatively 100 – 150 mg of samples dissolved in 0.7 – 1 mL solvent were introduced in 5 mm NMR tubes (528-PP, **Wilmad-Labglass**). For perfluorinated compound or solution of HF, spectra were recorded using FEP sample tube inside a 5 mm thin walled NMR tube (537–PPT, **Wilmad**) with an acetonitrile-D_3 film as an external lock.

3. Vibrational spectroscopy: Infrared spectra were recorded at room temperature on a FTIR spectrometer **TENSOR 27** (Bruker, Karsruhe, Germany) equipped with a DTGS detector and a KBr/Ge beam splitter operating in the region 4000 – 400 cm^{-1}. For each spectrum of the solid samples as KBr pellets, 64 scans were added with a resolution of 2 cm^{-1}. For solutions the IR spectra were recorded with an adjustable path length IR cell (**Glenrothes RIIK**) with KRS–5 windows on the **TENSOR 27** (Bruker, Karsruhe, Germany) equipped with a DTGS detector.

Also, an ATR_IR accessory (**HARRICK, MVP Star^{TM}**) with a diamond as the ATR crystal was used to obtain IR spectra, which were measured on a **TENSOR 27** (Bruker, Karsruhe, Germany) equipped with a DTGS detector.

Raman spectra were recorded at room temperature on a **Bruker EQUINOX 55** FT Raman spectrometer using the 9394.8 cm^{-1} exciting line (500 mW) of a Nd: YAG laser. Solid samples were placed in melting point capillaries and used for recording spectra in the region 3000 – 50 cm^{-1} with a resolution of 2 cm^{-1}. For each spectrum, between 32–500 scans were added.

4. Theoretical calculations: Starting from the experimental geometry of the anion (FPI or PSI), the structure was fully optimized at the **B3LYP/6-31+G(d)** level using the **Gaussian 03W** program package (version 6.0, revision B.04). The vibrational frequencies and the IR intensities for the anion have been calculated at the energy-minimized structure of *C_1* symmetry for which no imaginary vibrational frequency was found.

5. Water content: Water content in the ILs was measured using a **Metrohm Instrument Coulometric Karl Fisher Titrator**, **Model 831** which was calibrated using a **Hydranal–Coulomat AD Water Standard** (Riedel–de Haen). Samples ranging from 50 – 100 mg were injected into the titrator using a syringe with a steel needle. To study the absorption of water by the ILs at room temperature, 2 mL of sample was placed into a glass vial and exposed to the humid atmosphere for various time intervals. Then the water content was measured.

6. Halide content: Chloride or bromide mas measured by ion-chromatography (**Methrom Advanced IC System with Metrosep A Supp 5–150**). About 50 – 80 mg of ionic liquids was solved in 25 ml acetonitrile and automatically injected using an autosampler.

7. Viscosities and densities: Viscosities and densities of ILs were measured using the **Viscosimeter SVM 3000 Anton Paar**. About 3–3.5 mL of ILs were placed into a seringe (bubble free) and measured in the temperature range 20 to 80 °C.

8. Electrochemical measurements: The electrochemical potential windows of the salts with FPI were measured at 23.8 °C using an **Autolab PGSTAT 30** (Eco Chemie). Cyclic voltamogramms were recorded for different solutions in acetonitril. A glass carbon (gc) (Ø 3 mm; surface area: 7.065×10^{-2} cm^2) electrode was used as the working electrode, $Ag/AgNO_3$ (CH_3CN) electrode served as the reference electrode and Pt wire as a counter electrode. The potential's values were normalized to E° of ferrocene (E_p^{ox} ferrocene = 0.425 V).

9. Conductivity: Conductivity data were obtained using a **Conductometer 703** (**Knick**). The conductivity of the ILs was measured at –20, –10, 0, 20, 40, 60, 80 °C. The cell constant of the electrode was calibrated by measuring the conductance of several standard solutions of potassium chloride with concentration ranging from 0.1 mol/L to 0.01 mol/L at room temperature.

10. Thermal analysis: The **Schmelzpunkt SMP 10 – STUART** apparatus was used for visual determinations of the melting point in glass capillaries (Ø 2 mm).

Thermo–analytical measurements were performed with a **DSC Netzsch 204** and a **TG Netzsch STA 409** instrument. Temperature and sensitivity calibrations in the temperature range of 30 – 600 °C were carried out with naphthalene, benzoic acid, KNO_3, $AgNO_3$, $LiNO_3$ and CsCl. About 25 – 40 mg of solid samples were weighed and sealed in a DSC aluminium crucible or placed in ceramic pans for TG measurements. The temperature range used for measurements was between –120 to 600 °C with a heating rate of 10 °C min^{-1}, under an atmosphere of dry nitrogen. The data were processed with the **Netzsch Protens 4.2** software.

11. MS: Mass spectra were recorded on a **Brucker micrOTOF** coupled to a **Agilent 1200 Series** with a Coloum and **Perfect Sil Target ODS-3HD** 5μm.

12. Single crystal X–ray diffraction: Two single–crystal diffraction data were collected on a **Kappa CCD diffractometer** (**Bruker AXS**) using Mo–K_α radiation (λ = 0.71073 Å) and a graphite monochromator and the others with a **Gemini E Ultra – Diffractometer** (Oxford). The crystal structures were solved by direct methods using SHELXS–97 and full–matrix least–squares refinement on F^2 was performed with SHELXL–97.

Appendix I

I.1 Crystal structure of $Ca[(C_2F_5)_2PO_2]_2 \cdot 2H_2O$

Table I.1.1 Atomic coordinates and equivalent isotropic displacement parameters($Å^2$). U_{eq} is defined as one third of the trace of the orthogonalized U_{ij} tensor for $Ca[(C_2F_5)_2PO_2]_2 \cdot 2H_2O$.

	x	**y**	**z**	**U(eq)**
P	1207(1)	1207(1)	0	21(1)
O(1)	786(1)	907(1)	-2234(2)	30(1)
C(1)	2566(2)	1077(2)	-198(4)	36(1)
F(11)	3011(1)	1749(1)	1149(3)	58(1)
F(12)	2858(1)	1234(2)	-2425(3)	76(1)
C(2)	2962(2)	79(2)	523(5)	46(1)
F(21)	3890(1)	-14(1)	-60(3)	78(1)
F(22)	2459(1)	-620(1)	-450(4)	71(1)
F(23)	2904(1)	-28(1)	2806(2)	51(1)
Ca	0	0	-5000	17(1)
O(2)	-1214(1)	1214(1)	-5000	38(1)

Table I.1.2 Selected bond lengths [Å] and angles [°] in $Ca[(C_2F_5)_2PO_2]_2 \cdot 2H_2O$.

P-O(1)	1.4664(12)	F(12)-C(1)-C(2)	107.0(2)
P-O(1)*1	1.4664(12)	F(11)-C(1)-P	110.48(17)
P-C(1)	1.879(2)	F(12)-C(1)-P	109.58(15)
P-C(1)*1	1.879(2)	C(2)-C(1)-P	114.93(15)
O(1)-Ca	2.2890(12)	F(22)-C(2)-F(21)	109.2(2)
C(1)-F(11)	1.351(3)	F(22)-C(2)-F(23)	108.1(2)
C(1)-F(12)	1.357(3)	F(21)-C(2)-F(23)	107.4(2)
C(1)-C(2)	1.531(3)	F(22)-C(2)-C(1)	110.7(2)
C(2)-F(22)	1.308(3)	F(21)-C(2)-C(1)	111.1(2)
C(2)-F(21)	1.323(3)	F(23)-C(2)-C(1)	110.3(2)
C(2)-F(23)	1.323(3)	O(1)-Ca-O(1)*2	174.16(9)
Ca-O(1)*2	2.2890(12)	O(1)-Ca-O(1)*3	92.08(6)
Ca-O(1)*3	2.2890(12)	O(1)*2-Ca-O(1)*3	88.22(6)
Ca-O(1)*4	2.2890(12)	O(1)-Ca-O(1)*4	88.22(6)
Ca-O(2)	2.357(2)	O(1)*2-Ca-O(1)*4	92.08(6)
Ca-O(2)*3	2.357(2)	O(1)*3-Ca-O(1)*4	174.16(9)
O(2)-H	0.76(4)	O(1)-Ca-O(2)	87.08(4)
O(1)-P-O(1)*1	123.05(11)	O(1)*2-Ca-O(2)	87.08(4)
O(1)-P-C(1)	108.13(10)	O(1)*3-Ca-O(2)	92.92(4)
O(1)*1-P-C(1)	107.15(10)	O(1)*4-Ca-O(2)	92.92(4)
O(1)-P-C(1)*1	107.15(10)	O(1)-Ca-O(2)*3	92.92(4)
O(1)*1-P-C(1)*1	108.13(10)	O(1)*2-Ca-O(2)*3	92.92(4)
C(1)-P-C(1)*1	101.09(14)	O(1)*3-Ca-O(2)*3	87.08(4)
P-O(1)-Ca	161.07(9)	O(1)*4-Ca-O(2)*3	87.08(4)

F(11)-C(1)-F(12)	107.34(18)	O(2)-Ca-O(2)*3	180.00(5)
F(11)-C(1)-C(2)	107.19(18)	Ca-O(2)-H	118(3)

Symmetry transformations used to generate equivalent atoms:
*1 y,x,-z ; *2 -y,-x,-z-1; *3 -x,-y,z; *4 y,x,-z-1.

Table I.1.3 Anisotropic displacement parameters (Å^2).

	U11	**U22**	**U33**	**U23**	**U13**	**U12**
P	21(1)	21(1)	19(1)	0(1)	0(1)	-7(1)
O(1)	33(1)	34(1)	24(1)	-5(1)	-5(1)	-5(1)
C(1)	24(1)	47(1)	37(1)	10(1)	0(1)	-9(1)
F(11)	40(1)	39(1)	96(1)	13(1)	-34(1)	-18(1)
F(12)	37(1)	138(2)	53(1)	40(1)	21(1)	4(1)
C(2)	27(1)	51(2)	59(2)	-7(1)	-1(1)	4(1)
F(21)	33(1)	106(2)	93(1)	9(2)	12(1)	22(1)
F(22)	62(1)	48(1)	103(2)	-36(1)	-22(1)	14(1)
F(23)	49(1)	50(1)	55(1)	18(1)	-8(1)	6(1)
Ca	18(1)	18(1)	16(1)	0	0	0(1)
O(2)	31(1)	31(1)	52(1)	-5(1)	-5(1)	9(1)

The anisotropic displacement factor exponent takes the form:
$-2\pi^2[h^2a^{*2}U_{11} + ..+2hka^*b^*U_{12}]$

Table I.1.4 Hydrogen coordinates and isotropic displacement parameters.

	x	**y**	**z**	**U(eq)**
H	-1110(30)	1680(30)	-4330(80)	140(20)

I.2 Crystal structure of $[H_3O][(C_4F_9)_2PO_2]$

Table I.2.1 Atomic coordinates and equivalent isotropic displacement parameters (Å^2). U_{eq} is defined as one third of the trace of the orthogonalized U_{ij} tensor for $[H_3O][(C_4F_9)_2PO_2]$.

	x	**y**	**z**	**U(eq)**
P(1)	1142(2)	4885(1)	3421(1)	35(1)
O(1)	-1119(5)	4616(3)	3392(2)	41(1)
O(2)	2317(5)	4668(3)	2762(2)	39(1)
C(1)	1590(7)	6302(4)	3919(3)	42(1)
F(1)	1483(5)	6447(3)	4608(2)	52(1)
F(2)	3525(5)	6616(3)	3797(2)	53(1)
C(2)	5(8)	7007(5)	3700(3)	47(1)
F(3)	-1833(5)	6884(3)	3977(2)	59(1)
F(4)	-273(5)	6665(3)	2997(2)	54(1)
C(3)	620(11)	8179(5)	3921(3)	58(2)
F(5)	1475(7)	8464(3)	4576(2)	75(1)
F(6)	2006(7)	8339(3)	3484(3)	80(1)
C(4)	-1201(13)	8915(5)	3923(4)	69(2)
F(7)	-2443(9)	8946(4)	4437(3)	94(2)
F(8)	-2306(8)	8580(4)	3324(2)	88(1)
F(9)	-457(10)	9866(4)	3998(3)	101(2)
C(5)	2516(7)	4236(4)	4006(2)	42(1)

F(11)	4357(5)	4760(3)	4237(2)	63(1)
F(12)	1372(6)	4276(3)	4563(2)	62(1)
C(6)	2975(8)	3085(5)	3648(3)	45(1)
F(13)	1388(6)	2649(3)	3203(2)	71(1)
F(14)	4661(6)	3080(3)	3251(2)	71(1)
C(7)	3485(11)	2423(6)	4128(3)	63(2)
F(15)	4481(6)	2992(3)	4712(2)	69(1)
F(16)	1571(7)	2114(4)	4329(2)	75(1)
C(8)	4579(14)	1423(7)	3819(5)	79(2)
F(17)	6588(9)	1661(5)	3750(4)	123(2)
F(18)	3810(9)	904(4)	3199(3)	98(2)
F(19)	4631(10)	834(4)	4228(3)	109(2)
P(2)	5801(2)	2694(1)	883(1)	41(1)
O(3)	3536(6)	2781(4)	864(2)	69(1)
O(4)	7161(5)	3546(3)	1356(2)	38(1)
C(11)	6762(8)	2405(4)	-21(3)	44(1)
F(21)	6514(6)	1381(3)	-361(2)	57(1)
F(22)	8840(5)	2665(3)	16(2)	59(1)
C(12)	5648(10)	3015(5)	-450(3)	53(1)
F(23)	3688(6)	2627(4)	-615(2)	71(1)
F(24)	5586(8)	4007(3)	-41(2)	76(1)
C(13)	6692(14)	3017(6)	-1136(4)	69(2)
F(25)	7171(11)	2047(4)	-1479(3)	109(2)
F(26)	8433(9)	3606(5)	-983(3)	111(2)
C(14)	5360(16)	3429(7)	-1630(4)	83(2)
F(27)	3766(12)	2790(5)	-1907(3)	128(2)
F(28)	4713(12)	4358(4)	-1303(3)	117(2)
F(29)	6410(12)	3491(5)	-2162(3)	124(2)
C(15)	6221(15)	1487(6)	1166(3)	77(2)
F(31)	5185(8)	666(3)	719(2)	82(1)
F(32)	5327(12)	1728(4)	1817(3)	124(3)
C(16)	8393(18)	1243(6)	1308(5)	92(3)
F(33)	9435(8)	1261(4)	737(3)	95(2)
F(34)	9311(12)	1960(4)	1840(3)	136(3)
C(17)	9240(20)	155(10)	1378(7)	57(4)
C(17A)	7860(40)	182(16)	1499(13)	85(8)
F(35)	8544(11)	-584(4)	802(3)	108(2)
F(36)	11353(6)	187(4)	1559(3)	95(2)
C(18)	8290(30)	-145(11)	1977(7)	67(5)
C(18A)	9640(30)	-81(17)	1858(17)	98(10)
F(37)	6158(7)	-204(4)	1812(3)	101(2)
F(38)	8869(12)	611(5)	2586(3)	126(2)
F(39)	9296(10)	-984(5)	2002(4)	126(2)
O(5)	6237(5)	4840(3)	2553(2)	38(1)
O(6)	1070(5)	4105(3)	1452(2)	44(1)

Table I.2.2 Selected bond lengths [Å] and angles [°] in $[H_3O][(C_4F_9)_2PO_2]$.

P(1)-O(1)	1.488(3)	O(4)-P(2)-C(15)	107.0(3)
P(1)-O(2)	1.504(3)	C(11)-P(2)-C(15)	106.7(3)

P(1)-C(5)	1.875(5)	P(2)-O(3)-O(6)	135.5(3)
P(1)-C(1)	1.885(6)	P(2)-O(4)-O(5)	127.4(2)
C(1)-F(1)	1.342(6)	F(21)-C(11)-F(22)	107.9(4)
C(1)-F(2)	1.362(6)	F(21)-C(11)-C(12)	109.0(4)
C(1)-C(2)	1.553(8)	F(22)-C(11)-C(12)	107.7(5)
C(2)-F(4)	1.352(6)	F(21)-C(11)-P(2)	110.1(4)
C(2)-F(3)	1.354(7)	F(22)-C(11)-P(2)	109.4(4)
C(2)-C(3)	1.549(8)	C(12)-C(11)-P(2)	112.6(4)
C(3)-F(6)	1.333(8)	F(23)-C(12)-F(24)	108.8(5)
C(3)-F(5)	1.348(7)	F(23)-C(12)-C(11)	109.0(5)
C(3)-C(4)	1.556(10)	F(24)-C(12)-C(11)	107.3(5)
C(4)-F(7)	1.320(9)	F(23)-C(12)-C(13)	108.4(5)
C(4)-F(9)	1.325(9)	F(24)-C(12)-C(13)	107.9(5)
C(4)-F(8)	1.325(9)	C(11)-C(12)-C(13)	115.4(5)
C(5)-F(12)	1.351(6)	F(26)-C(13)-F(25)	108.7(7)
C(5)-F(11)	1.360(6)	F(26)-C(13)-C(14)	106.8(6)
C(5)-C(6)	1.546(8)	F(25)-C(13)-C(14)	108.0(7)
C(6)-F(13)	1.335(6)	F(26)-C(13)-C(12)	109.7(6)
C(6)-F(14)	1.371(6)	F(25)-C(13)-C(12)	108.7(5)
C(6)-C(7)	1.532(8)	C(14)-C(13)-C(12)	114.8(7)
C(7)-F(15)	1.328(7)	F(29)-C(14)-F(28)	108.4(7)
C(7)-F(16)	1.404(9)	F(29)-C(14)-F(27)	105.1(7)
C(7)-C(8)	1.511(10)	F(28)-C(14)-F(27)	110.4(9)
C(8)-F(18)	1.304(10)	F(29)-C(14)-C(13)	111.0(8)
C(8)-F(19)	1.305(9)	F(28)-C(14)-C(13)	110.6(6)
C(8)-F(17)	1.349(11)	F(27)-C(14)-C(13)	111.2(7)
P(2)-O(3)	1.467(4)	F(31)-C(15)-F(32)	109.4(6)
P(2)-O(4)	1.495(3)	F(31)-C(15)-C(16)	111.6(7)
P(2)-C(11)	1.871(6)	F(32)-C(15)-C(16)	104.4(7)
P(2)-C(15)	1.905(8)	F(31)-C(15)-P(2)	109.9(6)
C(11)-F(21)	1.350(6)	F(32)-C(15)-P(2)	103.4(6)
C(11)-F(22)	1.370(6)	C(16)-C(15)-P(2)	117.4(6)
C(11)-C(12)	1.533(8)	F(34)-C(16)-F(33)	106.1(9)
C(12)-F(23)	1.347(7)	F(34)-C(16)-C(15)	112.5(8)
C(12)-F(24)	1.348(7)	F(33)-C(16)-C(15)	105.6(6)
C(12)-C(13)	1.555(10)	F(34)-C(16)-C(17A)	112.0(11)
C(13)-F(26)	1.332(9)	F(33)-C(16)-C(17A)	123.1(11)
C(13)-F(25)	1.335(8)	C(15)-C(16)-C(17A)	97.0(11)
C(13)-C(14)	1.526(11)	F(34)-C(16)-C(17)	104.5(7)
C(14)-F(29)	1.308(10)	F(33)-C(16)-C(17)	97.7(9)
C(14)-F(28)	1.315(10)	C(15)-C(16)-C(17)	127.7(9)
C(14)-F(27)	1.319(10)	C(17A)-C(16)-C(17)	33.3(8)
C(15)-F(31)	1.344(7)	C(17A)-C(17)-C(18A)	88(2)
C(15)-F(32)	1.398(9)	C(17A)-C(17)-F(35)	84.6(19)
C(15)-C(16)	1.483(14)	C(18A)-C(17)-F(35)	117.9(18)
C(16)-F(34)	1.317(9)	C(17A)-C(17)-F(36)	151(2)
C(16)-F(33)	1.357(11)	C(18A)-C(17)-F(36)	64.9(15)
C(16)-C(17A)	1.62(2)	F(35)-C(17)-F(36)	117.5(11)
C(16)-C(17)	1.626(15)	C(17A)-C(17)-C(18)	51.8(17)

C(17)-C(17A)	0.93(2)	C(18A)-C(17)-C(18)	36.8(12)
C(17)-C(18A)	1.13(3)	F(35)-C(17)-C(18)	104.6(11)
C(17)-F(35)	1.337(14)	F(36)-C(17)-C(18)	101.5(11)
C(17)-F(36)	1.391(14)	C(17A)-C(17)-C(16)	73.3(15)
C(17)-C(18)	1.53(2)	C(18A)-C(17)-C(16)	130.1(19)
C(17A)-C(18)	1.20(2)	F(35)-C(17)-C(16)	106.4(9)
C(17A)-C(18A)	1.44(3)	F(36)-C(17)-C(16)	114.1(9)
C(17A)-F(37)	1.45(2)	C(18)-C(17)-C(16)	112.3(12)
C(17A)-F(35)	1.56(3)	C(17)-C(17A)-C(18)	90(2)
F(36)-C(18A)	1.37(2)	C(17)-C(17A)-C(18A)	51.3(19)
C(18)-C(18A)	0.92(2)	C(18)-C(17A)-C(18A)	39.4(12)
C(18)-F(39)	1.332(15)	C(17)-C(17A)-F(37)	150(2)
C(18)-F(38)	1.370(16)	C(18)-C(17A)-F(37)	62.9(16)
C(18)-F(37)	1.397(19)	C(18A)-C(17A)-F(37)	101.9(18)
C(18A)-F(39)	1.35(2)	C(17)-C(17A)-F(35)	58.8(16)
C(18A)-F(38)	1.58(3)	C(18)-C(17A)-F(35)	110.0(17)
O(2)-O(5)	2.592(5)	C(18A)-C(17A)-F(35)	90(2)
O(4)-O(5)	2.611(5)	F(37)-C(17A)-F(35)	114.5(15)
O(5)-O(1)*1	2.441(5)	C(17)-C(17A)-C(16)	73.4(16)
O(5)-H(51)	0.84(2)	C(18)-C(17A)-C(16)	135(2)
O(5)-H(52)	0.84(2)	C(18A)-C(17A)-C(16)	109.3(19)
O(5)-H(53)	0.85(2)	F(37)-C(17A)-C(16)	135.7(17)
O(2)-O(6)	2.600(5)	F(35)-C(17A)-C(16)	96.7(14)
O(3)-O(6)	2.474(6)	C(17)-F(35)-C(17A)	36.6(8)
O(6)-O(4)*2	2.596(5)	C(18A)-F(36)-C(17)	48.1(11)
O(6)-H(61)	0.84(2)	C(18A)-C(18)-C(17A)	85(2)
O(6)-H(62)	0.84(2)	C(18A)-C(18)-F(39)	71.1(16)
O(6)-H(63)	0.85(2)	C(17A)-C(18)-F(39)	131.3(18)
O(1)-P(1)-O(2)	120.66(19)	C(18A)-C(18)-F(38)	85(3)
O(1)-P(1)-C(5)	108.5(2)	C(17A)-C(18)-F(38)	113.9(16)
O(2)-P(1)-C(5)	107.4(2)	F(39)-C(18)-F(38)	105.6(11)
O(1)-P(1)-C(1)	108.9(2)	C(18A)-C(18)-F(37)	150(2)
O(2)-P(1)-C(1)	107.7(2)	C(17A)-C(18)-F(37)	67.2(17)
C(5)-P(1)-C(1)	102.1(2)	F(39)-C(18)-F(37)	120.9(13)
P(1)-O(2)-O(5)	131.83(19)	F(38)-C(18)-F(37)	113.7(12)
P(1)-O(2)-O(6)	131.76(19)	C(18A)-C(18)-C(17)	47.2(18)
O(5)-O(2)-O(6)	96.32(15)	C(17A)-C(18)-C(17)	37.7(13)
F(1)-C(1)-F(2)	108.2(4)	F(39)-C(18)-C(17)	104.2(13)
F(1)-C(1)-C(2)	108.6(4)	F(38)-C(18)-C(17)	107.7(12)
F(2)-C(1)-C(2)	107.6(5)	F(37)-C(18)-C(17)	103.7(11)
F(1)-C(1)-P(1)	110.2(4)	C(18)-C(18A)-C(17)	96(2)
F(2)-C(1)-P(1)	109.1(3)	C(18)-C(18A)-F(39)	68.9(16)
C(2)-C(1)-P(1)	112.9(4)	C(17)-C(18A)-F(39)	131(3)
F(4)-C(2)-F(3)	107.8(4)	C(18)-C(18A)-F(36)	162(3)
F(4)-C(2)-C(3)	108.4(5)	C(17)-C(18A)-F(36)	67.0(17)
F(3)-C(2)-C(3)	108.7(5)	F(39)-C(18A)-F(36)	126.3(17)
F(4)-C(2)-C(1)	107.9(4)	C(18)-C(18A)-C(17A)	56.0(18)
F(3)-C(2)-C(1)	108.0(5)	C(17)-C(18A)-C(17A)	40.3(13)
C(3)-C(2)-C(1)	115.8(5)	F(39)-C(18A)-C(17A)	111.4(19)

F(6)-C(3)-F(5)	109.5(6)	F(36)-C(18A)-C(17A)	106(2)
F(6)-C(3)-C(2)	108.6(5)	C(18)-C(18A)-F(38)	59(2)
F(5)-C(3)-C(2)	109.1(5)	C(17)-C(18A)-F(38)	118.4(18)
F(6)-C(3)-C(4)	107.6(6)	F(39)-C(18A)-F(38)	93.9(17)
F(5)-C(3)-C(4)	106.6(5)	F(36)-C(18A)-F(38)	122.5(19)
C(2)-C(3)-C(4)	115.3(6)	C(17A)-C(18A)-F(38)	90.7(18)
F(7)-C(4)-F(9)	108.9(6)	C(18)-F(37)-C(17A)	49.9(10)
F(7)-C(4)-F(8)	108.4(7)	C(18)-F(38)-C(18A)	35.3(9)
F(9)-C(4)-F(8)	108.9(6)	C(18)-F(39)-C(18A)	40.1(9)
F(7)-C(4)-C(3)	111.1(6)	O(1)*1-O(5)-O(2)	120.94(18)
F(9)-C(4)-C(3)	109.9(7)	O(1)*1-O(5)-O(4)	105.02(17)
F(8)-C(4)-C(3)	109.7(6)	O(2)-O(5)-O(4)	110.59(16)
F(12)-C(5)-F(11)	108.7(4)	O(1)*1-O(5)-H(51)	19(5)
F(12)-C(5)-C(6)	107.5(5)	O(2)-O(5)-H(51)	112(5)
F(11)-C(5)-C(6)	108.0(4)	O(4)-O(5)-H(51)	124(5)
F(12)-C(5)-P(1)	110.1(3)	O(1)*1-O(5)-H(52)	118(5)
F(11)-C(5)-P(1)	108.1(4)	O(2)-O(5)-H(52)	4(5)
C(6)-C(5)-P(1)	114.3(3)	O(4)-O(5)-H(52)	111(5)
F(13)-C(6)-F(14)	106.4(5)	H(51)-O(5)-H(52)	109(6)
F(13)-C(6)-C(7)	110.3(5)	O(1)*1-O(5)-H(53)	122(5)
F(14)-C(6)-C(7)	107.3(5)	O(2)-O(5)-H(53)	105(4)
F(13)-C(6)-C(5)	108.7(4)	O(4)-O(5)-H(53)	19(5)
F(14)-C(6)-C(5)	106.7(5)	H(51)-O(5)-H(53)	139(6)
C(7)-C(6)-C(5)	117.0(5)	H(52)-O(5)-H(53)	107(6)
F(15)-C(7)-F(16)	106.0(6)	O(3)-O(6)-O(4)*2	117.5(2)
F(15)-C(7)-C(8)	110.5(6)	O(3)-O(6)-O(2)	104.56(19)
F(16)-C(7)-C(8)	104.7(6)	O(4)*2-O(6)-O(2)	108.66(17)
F(15)-C(7)-C(6)	110.7(6)	O(3)-O(6)-H(61)	108(5)
F(16)-C(7)-C(6)	106.3(5)	O(4)*2-O(6)-H(61)	105(4)
C(8)-C(7)-C(6)	117.8(6)	O(2)-O(6)-H(61)	4(5)
F(18)-C(8)-F(19)	110.6(8)	O(3)-O(6)-H(62)	4(5)
F(18)-C(8)-F(17)	107.3(7)	O(4)*2-O(6)-H(62)	117(5)
F(19)-C(8)-F(17)	105.0(7)	O(2)-O(6)-H(62)	101(5)
F(18)-C(8)-C(7)	112.4(6)	H(61)-O(6)-H(62)	105(6)
F(19)-C(8)-C(7)	113.0(7)	O(3)-O(6)-H(63)	102(5)
F(17)-C(8)-C(7)	108.1(7)	O(4)*2-O(6)-H(63)	16(5)
O(3)-P(2)-O(4)	120.5(2)	O(2)-O(6)-H(63)	111(5)
O(3)-P(2)-C(11)	109.8(3)	H(61)-O(6)-H(63)	108(6)
O(4)-P(2)-C(11)	108.0(2)	H(62)-O(6)-H(63)	102(6)
O(3)-P(2)-C(15)	104.0(4)		

Symmetry transformations used to generate equivalent atoms:
*1 x+1,y,z; *2 x-1,y,z.

Table I.2.3 Anisotropic displacement parameters (Å^2).

	U11	**U22**	**U33**	**U23**	**U13**	**U12**
P(1)	22(1)	51(1)	30(1)	6(1)	-4(1)	2(1)
O(1)	22(2)	57(2)	44(2)	14(2)	-3(1)	-1(1)
O(2)	25(2)	60(2)	27(2)	5(2)	-3(1)	1(1)

C(1)	27(2)	54(3)	40(3)	7(2)	-2(2)	2(2)
F(1)	55(2)	60(2)	34(2)	3(1)	-5(1)	5(2)
F(2)	35(2)	62(2)	56(2)	9(2)	-4(1)	-10(1)
C(2)	42(3)	50(3)	45(3)	10(2)	-4(2)	4(2)
F(3)	37(2)	62(2)	75(2)	17(2)	7(2)	12(2)
F(4)	58(2)	54(2)	44(2)	9(1)	-12(1)	4(2)
C(3)	71(4)	47(3)	49(3)	6(3)	-3(3)	-2(3)
F(5)	92(3)	54(2)	65(2)	-2(2)	-25(2)	0(2)
F(6)	84(3)	60(3)	92(3)	19(2)	14(2)	-9(2)
C(4)	93(5)	49(4)	65(5)	16(3)	-4(4)	16(3)
F(7)	110(4)	87(3)	89(3)	27(3)	22(3)	48(3)
F(8)	113(4)	72(3)	75(3)	15(2)	-21(3)	27(3)
F(9)	146(5)	50(3)	104(4)	19(2)	-6(3)	14(3)
C(5)	29(2)	61(3)	27(2)	2(2)	-6(2)	2(2)
F(11)	43(2)	66(2)	70(2)	10(2)	-30(2)	-4(2)
F(12)	72(2)	79(3)	38(2)	21(2)	14(2)	27(2)
C(6)	39(3)	56(3)	34(3)	7(2)	-5(2)	4(2)
F(13)	76(3)	61(2)	66(2)	8(2)	-32(2)	-1(2)
F(14)	71(3)	75(3)	69(3)	21(2)	27(2)	22(2)
C(7)	70(4)	65(4)	50(4)	13(3)	-14(3)	16(3)
F(15)	69(2)	81(3)	56(2)	21(2)	-26(2)	7(2)
F(16)	66(2)	84(3)	85(3)	40(2)	10(2)	4(2)
C(8)	89(6)	74(5)	78(5)	29(4)	3(4)	36(4)
F(17)	79(4)	148(6)	157(6)	64(5)	26(4)	57(4)
F(18)	143(5)	65(3)	76(3)	6(2)	-4(3)	36(3)
F(19)	145(5)	88(4)	110(4)	49(3)	5(3)	58(3)
P(2)	30(1)	50(1)	34(1)	2(1)	-3(1)	-6(1)
O(3)	29(2)	94(4)	56(3)	-17(2)	2(2)	-10(2)
O(4)	29(2)	42(2)	38(2)	4(1)	-5(1)	-2(1)
C(11)	40(3)	39(3)	47(3)	6(2)	3(2)	2(2)
F(21)	76(2)	44(2)	46(2)	6(1)	4(2)	4(2)
F(22)	36(2)	75(2)	66(2)	20(2)	7(2)	5(2)
C(12)	62(4)	39(3)	51(3)	5(2)	-4(3)	5(3)
F(23)	55(2)	96(3)	60(2)	22(2)	-15(2)	3(2)
F(24)	116(3)	45(2)	60(2)	6(2)	-8(2)	26(2)
C(13)	100(6)	52(4)	59(4)	20(3)	11(4)	9(4)
F(25)	190(6)	76(3)	75(3)	33(3)	62(3)	56(3)
F(26)	100(4)	137(5)	122(5)	82(4)	-1(3)	-23(4)
C(14)	127(8)	66(5)	55(4)	16(4)	-10(4)	-3(5)
F(27)	187(7)	120(5)	77(3)	41(3)	-57(4)	-43(4)
F(28)	216(7)	70(3)	67(3)	23(2)	-10(3)	48(4)
F(29)	210(7)	116(5)	69(3)	57(3)	40(4)	49(4)
C(15)	127(7)	56(4)	40(3)	5(3)	-6(4)	-39(4)
F(31)	116(4)	58(2)	58(2)	0(2)	4(2)	-41(2)
F(32)	226(7)	79(3)	64(3)	13(2)	56(4)	-30(4)
C(16)	153(9)	52(4)	67(5)	19(4)	-51(5)	-4(5)
F(33)	81(3)	88(4)	132(5)	61(3)	-20(3)	2(3)
F(34)	197(6)	57(3)	141(5)	23(3)	-113(5)	-9(3)
C(17)	39(8)	59(7)	80(9)	32(6)	8(5)	7(5)

C(17A)	71(17)	68(12)	130(20)	54(12)	13(12)	14(9)
F(35)	168(6)	55(3)	90(4)	4(2)	26(4)	-5(3)
F(36)	49(2)	86(3)	166(5)	62(3)	17(3)	15(2)
C(18)	80(13)	65(8)	69(9)	36(7)	15(7)	15(7)
C(18A)	51(12)	84(14)	200(30)	94(17)	29(14)	22(9)
F(37)	62(3)	104(4)	126(4)	17(3)	24(3)	-10(3)
F(38)	187(7)	128(5)	72(4)	43(4)	1(4)	-30(5)
F(39)	132(5)	90(4)	190(7)	90(4)	9(4)	34(3)
O(5)	24(2)	50(2)	37(2)	8(2)	-4(1)	0(1)
O(6)	31(2)	62(3)	35(2)	8(2)	-6(1)	-8(2)

The anisotropic displacement factor exponent takes the form: $-2\pi^2[h^2a^{*2}U_{11}+ ..+2hka^*b^*U_{12}]$

Table I.2.4 Hydrogen coordinates and isotropic displacement parameters.

	x	**y**	**z**	**U(eq)**
H(51)	6970(90)	4950(50)	2920(20)	56(8)
H(52)	4980(40)	4750(50)	2640(30)	56(8)
H(53)	6350(100)	4580(50)	2118(12)	56(8)
H(61)	1390(100)	4300(50)	1884(12)	56(8)
H(62)	1920(80)	3640(40)	1280(30)	56(8)
H(63)	-60(60)	3750(40)	1390(30)	56(8)

I.3 Crystal structure of $[Me_4N][\{(C_2F_5)_2P(O)\}_2N]$

Table I.3.1 Atomic coordinates and equivalent isotropic displacement parameters ($Å^2$). U_{eq} is defined as one third of the trace of the orthogonalized U_{ij} tensor for $[Me_4N][\{(C_2F_5)_2P(O)\}_2N]$.

	x	**y**	**z**	**U(eq)**
C(1)	0.3210(2)	0.0662(2)	0.5477(2)	0.025(1)
C(2)	0.4218(2)	0.0499(2)	0.5654(2)	0.030(1)
C(3)	0.2637(2)	-0.0694(2)	0.4376(2)	0.025(1)
C(4)	0.1907(2)	-0.1113(2)	0.3751(2)	0.032(1)
C(5)	0.2133(2)	0.2697(2)	0.3652(2)	0.032(1)
C(6)	0.1505(3)	0.3279(2)	0.3080(2)	0.034(1)
C(7)	0.3408(2)	0.1721(2)	0.3162(2)	0.030(1)
C(8)	0.3613(3)	0.0987(3)	0.2729(2)	0.038(1)
C(9)	0.3134(2)	-0.1323(2)	0.9117(2)	0.030(1)
C(10)	0.3302(3)	-0.2180(3)	0.8826(2)	0.047(1)
C(11)	0.3618(2)	-0.0107(2)	0.8151(2)	0.029(1)
C(12)	0.3530(3)	0.0794(2)	0.7828(2)	0.036(1)
C(13)	0.2768(2)	0.1477(2)	1.0003(2)	0.026(1)
C(14)	0.3631(2)	0.1024(2)	1.0449(2)	0.033(1)
C(15)	0.1324(2)	0.1696(2)	0.8675(2)	0.030(1)
C(16)	0.0431(2)	0.1411(2)	0.8132(2)	0.035(1)
F(1)	0.3122(1)	0.1522(1)	0.5580(1)	0.036(1)
F(2)	0.2953(1)	0.0243(1)	0.5972(1)	0.037(1)
F(3)	0.4675(1)	0.0816(1)	0.6287(1)	0.038(1)
F(4)	0.4382(1)	-0.0338(1)	0.5663(1)	0.046(1)

F(5)	0.4521(1)	0.0874(2)	0.5190(1)	0.043(1)
F(6)	0.2731(1)	-0.1203(1)	0.4950(1)	0.034(1)
F(7)	0.3421(1)	-0.0737(1)	0.4240(1)	0.034(1)
F(8)	0.1166(1)	-0.1275(1)	0.3908(1)	0.047(1)
F(9)	0.1693(2)	-0.0604(1)	0.3195(1)	0.044(1)
F(10)	0.2202(1)	-0.1852(1)	0.3582(1)	0.040(1)
F(11)	0.1729(2)	0.2608(1)	0.4153(1)	0.044(1)
F(12)	0.2910(2)	0.3132(1)	0.3948(1)	0.046(1)
F(13)	0.0681(1)	0.2939(1)	0.2831(1)	0.043(1)
F(14)	0.1434(2)	0.4047(1)	0.3341(1)	0.054(1)
F(15)	0.1814(1)	0.3383(1)	0.2548(1)	0.039(1)
F(16)	0.3343(1)	0.2450(1)	0.2771(1)	0.042(1)
F(17)	0.4141(1)	0.1816(1)	0.3749(1)	0.039(1)
F(18)	0.3007(2)	0.0966(2)	0.2086(1)	0.051(1)
F(19)	0.3589(2)	0.0238(1)	0.3041(1)	0.046(1)
F(20)	0.4420(2)	0.1074(2)	0.2670(1)	0.055(1)
F(21)	0.2506(1)	-0.1465(1)	0.9433(1)	0.037(1)
F(22)	0.3902(1)	-0.1095(1)	0.9634(1)	0.046(1)
F(23)	0.3902(2)	-0.2090(2)	0.8501(2)	0.085(1)
F(24)	0.3623(2)	-0.2758(1)	0.9334(1)	0.060(1)
F(25)	0.2552(2)	-0.2496(1)	0.8380(1)	0.067(1)
F(26)	0.4428(1)	-0.0145(1)	0.8666(1)	0.043(1)
F(27)	0.3637(1)	-0.0659(1)	0.7634(1)	0.042(1)
F(28)	0.3710(2)	0.1402(1)	0.8320(1)	0.048(1)
F(29)	0.2693(2)	0.0913(1)	0.7386(1)	0.049(1)
F(30)	0.4097(2)	0.0897(1)	0.7471(1)	0.049(1)
F(31)	0.2339(1)	0.1747(1)	1.0452(1)	0.041(1)
F(32)	0.3022(1)	0.2197(1)	0.9735(1)	0.037(1)
F(33)	0.4053(1)	0.1492(1)	1.1019(1)	0.046(1)
F(34)	0.4191(1)	0.0921(1)	1.0091(1)	0.043(1)
F(35)	0.3437(2)	0.0266(1)	1.0658(1)	0.050(1)
F(36)	0.1127(1)	0.2337(1)	0.9059(1)	0.043(1)
F(37)	0.1823(1)	0.2045(1)	0.8308(1)	0.040(1)
F(38)	0.0557(1)	0.0696(1)	0.7808(1)	0.048(1)
F(39)	-0.0184(1)	0.1240(1)	0.8433(1)	0.044(1)
F(40)	0.0100(1)	0.2008(1)	0.7643(1)	0.044(1)
N(3)	0.2673(2)	0.1044(2)	0.4083(1)	0.028(1)
N(4)	0.2595(2)	0.0373(2)	0.8935(1)	0.026(1)
P(1)	0.2371(1)	0.0435(1)	0.4575(1)	0.024(1)
P(2)	0.2350(1)	0.1575(1)	0.3381(1)	0.024(1)
P(3)	0.1960(1)	0.0815(1)	0.9285(1)	0.024(1)
P(4)	0.2667(1)	-0.0418(1)	0.8475(1)	0.023(1)
O(1)	0.1468(1)	0.0422(1)	0.4645(1)	0.029(1)
O(2)	0.1601(2)	0.1330(1)	0.2748(1)	0.028(1)
O(3)	0.1315(2)	0.0364(1)	0.9550(1)	0.030(1)
O(4)	0.1907(1)	-0.0757(1)	0.7891(1)	0.028(1)
N(1)	0.9173(2)	0.1111(2)	0.3898(1)	0.025(1)
N(2)	0.9820(2)	0.8512(2)	0.9047(1)	0.026(1)
C(91)	0.9184(2)	0.7765(2)	0.8882(2)	0.031(1)

C(92)	1.0472(2)	0.8427(2)	0.9781(2)	0.036(1)
C(93)	0.9295(2)	0.9328(2)	0.8985(2)	0.032(1)
C(94)	1.0324(2)	0.8534(2)	0.8535(2)	0.031(1)
C(95)	0.8227(2)	0.1443(2)	0.3644(2)	0.030(1)
C(96)	0.9700(2)	0.1519(2)	0.3489(2)	0.034(1)
C(97)	0.9170(2)	0.0156(2)	0.3798(2)	0.033(1)
C(98)	0.9601(2)	0.1318(3)	0.4664(2)	0.039(1)

Table I.3.2 Selected bond lengths [Å] and angles [°] in $[Me_4N][\{(C_2F_5)_2P(O)\}_2N]$.

C(1)-F(2)	1.360(4)	F(14)-C(6)-F(13)	107.9(3)
C(1)-F(1)	1.367(4)	F(15)-C(6)-F(13)	108.5(3)
C(1)-C(2)	1.525(5)	F(14)-C(6)-C(5)	110.6(3)
C(1)-P(1)	1.888(3)	F(15)-C(6)-C(5)	111.1(3)
C(2)-F(5)	1.320(4)	F(13)-C(6)-C(5)	110.5(3)
C(2)-F(4)	1.325(4)	F(17)-C(7)-F(16)	106.9(3)
C(2)-F(3)	1.331(4)	F(17)-C(7)-C(8)	107.3(3)
C(3)-F(7)	1.352(3)	F(16)-C(7)-C(8)	106.4(3)
C(3)-F(6)	1.367(3)	F(17)-C(7)-P(2)	111.8(2)
C(3)-C(4)	1.538(5)	F(16)-C(7)-P(2)	109.6(2)
C(3)-P(1)	1.878(3)	C(8)-C(7)-P(2)	114.5(2)
C(4)-F(9)	1.321(4)	F(20)-C(8)-F(18)	108.4(3)
C(4)-F(10)	1.326(4)	F(20)-C(8)-F(19)	108.2(3)
C(4)-F(8)	1.329(4)	F(18)-C(8)-F(19)	108.4(3)
C(5)-F(12)	1.350(4)	F(20)-C(8)-C(7)	111.4(3)
C(5)-F(11)	1.367(4)	F(18)-C(8)-C(7)	110.6(3)
C(5)-C(6)	1.537(5)	F(19)-C(8)-C(7)	109.8(3)
C(5)-P(2)	1.893(3)	F(22)-C(9)-F(21)	106.4(3)
C(6)-F(14)	1.324(4)	F(22)-C(9)-C(10)	107.6(3)
C(6)-F(15)	1.327(4)	F(21)-C(9)-C(10)	106.6(3)
C(6)-F(13)	1.333(4)	F(22)-C(9)-P(4)	112.0(2)
C(7)-F(17)	1.358(4)	F(21)-C(9)-P(4)	105.3(2)
C(7)-F(16)	1.364(4)	C(10)-C(9)-P(4)	118.2(3)
C(7)-C(8)	1.534(5)	F(25)-C(10)-F(23)	109.1(4)
C(7)-P(2)	1.873(3)	F(25)-C(10)-F(24)	107.3(3)
C(8)-F(20)	1.321(4)	F(23)-C(10)-F(24)	107.6(3)
C(8)-F(18)	1.328(4)	F(25)-C(10)-C(9)	111.0(3)
C(8)-F(19)	1.330(4)	F(23)-C(10)-C(9)	110.0(3)
C(9)-F(22)	1.354(4)	F(24)-C(10)-C(9)	111.7(3)
C(9)-F(21)	1.360(4)	F(26)-C(11)-F(27)	107.7(3)
C(9)-C(10)	1.513(5)	F(26)-C(11)-C(12)	107.2(3)
C(9)-P(4)	1.886(3)	F(27)-C(11)-C(12)	106.0(3)
C(10)-F(25)	1.317(5)	F(26)-C(11)-P(4)	112.2(2)
C(10)-F(23)	1.323(4)	F(27)-C(11)-P(4)	109.1(2)
C(10)-F(24)	1.327(4)	C(12)-C(11)-P(4)	114.3(2)
C(11)-F(26)	1.350(4)	F(28)-C(12)-F(30)	107.5(3)
C(11)-F(27)	1.359(4)	F(28)-C(12)-F(29)	108.4(3)
C(11)-C(12)	1.531(5)	F(30)-C(12)-F(29)	108.3(3)
C(11)-P(4)	1.883(3)	F(28)-C(12)-C(11)	111.6(3)
C(12)-F(28)	1.329(4)	F(30)-C(12)-C(11)	111.0(3)

C(12)-F(30)	1.329(4)	F(29)-C(12)-C(11)	109.9(3)
C(12)-F(29)	1.333(4)	F(32)-C(13)-F(31)	106.7(3)
C(13)-F(32)	1.358(4)	F(32)-C(13)-C(14)	107.0(3)
C(13)-F(31)	1.361(3)	F(32)-C(13)-C(14)	107.0(3)
C(13)-C(14)	1.528(5)	F(32)-C(13)-P(3)	111.0(2)
C(13)-P(3)	1.883(3)	F(31)-C(13)-P(3)	108.7(2)
C(14)-F(34)	1.321(4)	C(14)-C(13)-P(3)	116.1(2)
C(14)-F(35)	1.321(4)	F(34)-C(14)-F(35)	109.4(3)
C(14)-F(33)	1.333(4)	F(34)-C(14)-F(33)	107.7(3)
C(15)-F(37)	1.357(4)	F(35)-C(14)-F(33)	108.4(3)
C(15)-F(36)	1.359(4)	F(34)-C(14)-C(13)	111.1(3)
C(15)-C(16)	1.530(5)	F(35)-C(14)-C(13)	110.1(3)
C(15)-P(3)	1.888(4)	F(33)-C(14)-C(13)	110.2(3)
C(16)-F(40)	1.327(4)	F(37)-C(15)-F(36)	107.4(3)
C(16)-F(39)	1.329(4)	F(37)-C(15)-C(16)	106.7(3)
C(16)-F(38)	1.337(4)	F(36)-C(15)-C(16)	106.8(3)
N(3)-P(1)	1.554(3)	F(37)-C(15)-P(3)	111.5(2)
N(3)-P(2)	1.568(3)	F(36)-C(15)-P(3)	109.5(2)
N(4)-P(3)	1.560(3)	C(16)-C(15)-P(3)	114.6(2)
N(4)-P(4)	1.566(3)	F(40)-C(16)-F(39)	108.2(3)
P(1)-O(1)	1.474(2)	F(40)-C(16)-F(38)	107.8(3)
P(2)-O(2)	1.468(2)	F(39)-C(16)-F(38)	107.7(3)
P(3)-O(3)	1.473(2)	F(40)-C(16)-C(15)	111.6(3)
P(4)-O(4)	1.468(2)	F(39)-C(16)-C(15)	111.5(3)
N(1)-C(96)	1.492(4)	F(38)-C(16)-C(15)	109.8(3)
N(1)-C(95)	1.495(4)	P(1)-N(3)-P(2)	145.02(19)
N(1)-C(98)	1.497(4)	P(3)-N(4)-P(4)	142.77(19)
N(1)-C(97)	1.498(4)	O(1)-P(1)-N(3)	125.32(14)
N(2)-C(93)	1.496(4)	O(1)-P(1)-C(3)	107.25(14)
N(2)-C(91)	1.496(4)	N(3)-P(1)-C(3)	107.32(14)
N(2)-C(92)	1.496(4)	O(1)-P(1)-C(1)	107.30(14)
N(2)-C(94)	1.496(4)	N(3)-P(1)-C(1)	103.61(15)
F(2)-C(1)-F(1)	106.6(2)	C(3)-P(1)-C(1)	104.21(15)
F(2)-C(1)-C(2)	106.7(3)	O(2)-P(2)-N(3)	124.85(14)
F(1)-C(1)-C(2)	106.1(3)	O(2)-P(2)-C(7)	110.22(14)
F(2)-C(1)-P(1)	109.4(2)	N(3)-P(2)-C(7)	103.29(15)
F(1)-C(1)-P(1)	104.8(2)	O(2)-P(2)-C(5)	108.65(15)
C(2)-C(1)-P(1)	122.2(2)	N(3)-P(2)-C(5)	105.10(15)
F(5)-C(2)-F(4)	109.1(3)	C(7)-P(2)-C(5)	102.48(16)
F(5)-C(2)-F(3)	107.8(3)	O(3)-P(3)-N(4)	125.17(14)
F(4)-C(2)-F(3)	108.1(3)	O(3)-P(3)-C(13)	110.63(14)
F(5)-C(2)-C(1)	110.7(3)	N(4)-P(3)-C(13)	102.58(14)
F(4)-C(2)-C(1)	110.5(3)	O(3)-P(3)-C(15)	107.57(14)
F(3)-C(2)-C(1)	110.5(3)	N(4)-P(3)-C(15)	107.81(15)
F(7)-C(3)-F(6)	107.1(2)	C(13)-P(3)-C(15)	100.30(15)
F(7)-C(3)-C(4)	107.2(3)	O(4)-P(4)-N(4)	123.80(14)
F(6)-C(3)-C(4)	106.7(3)	O(4)-P(4)-C(11)	110.06(14)
F(7)-C(3)-P(1)	111.8(2)	N(4)-P(4)-C(11)	103.05(15)
F(6)-C(3)-P(1)	109.3(2)	O(4)-P(4)-C(9)	107.89(14)

C(4)-C(3)-P(1)	114.3(2)	N(4)-P(4)-C(9)	105.68(15)
F(9)-C(4)-F(10)	108.4(3)	C(11)-P(4)-C(9)	104.83(15)
F(9)-C(4)-F(8)	108.6(3)	C(96)-N(1)-C(95)	109.7(2)
F(10)-C(4)-F(8)	107.8(3)	C(96)-N(1)-C(98)	109.5(3)
F(9)-C(4)-C(3)	110.5(3)	C(95)-N(1)-C(98)	109.5(2)
F(10)-C(4)-C(3)	110.4(3)	C(96)-N(1)-C(97)	108.9(3)
F(8)-C(4)-C(3)	111.1(3)	C(95)-N(1)-C(97)	109.8(3)
F(12)-C(5)-F(11)	107.4(3)	C(98)-N(1)-C(97)	109.4(3)
F(12)-C(5)-C(6)	107.3(3)	C(93)-N(2)-C(91)	109.3(2)
F(11)-C(5)-C(6)	105.8(3)	C(93)-N(2)-C(92)	109.6(3)
F(12)-C(5)-P(2)	111.4(2)	C(91)-N(2)-C(92)	109.9(3)
F(11)-C(5)-P(2)	107.1(2)	C(93)-N(2)-C(94)	109.0(3)
C(6)-C(5)-P(2)	117.4(2)	C(91)-N(2)-C(94)	109.4(2)
F(14)-C(6)-F(15)	108.2(3)	C(92)-N(2)-C(94)	109.6(3)

Table I.3.3 Anisotropic displacement parameters (Å^2).

	U11	**U22**	**U33**	**U23**	**U13**	**U12**
C(1)	0.027(2)	0.030(2)	0.021(2)	0.000(2)	0.010(2)	-0.002(2)
C(2)	0.028(2)	0.035(2)	0.024(2)	-0.002(2)	0.007(2)	-0.001(2)
C(3)	0.025(2)	0.029(2)	0.024(2)	0.006(2)	0.012(2)	0.002(2)
C(4)	0.039(2)	0.027(2)	0.031(2)	0.001(2)	0.012(2)	0.002(2)
C(5)	0.040(2)	0.029(2)	0.024(2)	-0.002(2)	0.007(2)	-0.003(2)
C(6)	0.046(2)	0.025(2)	0.029(2)	-0.003(2)	0.008(2)	0.006(2)
C(7)	0.026(2)	0.036(2)	0.025(2)	0.011(2)	0.005(2)	-0.002(2)
C(8)	0.032(2)	0.047(2)	0.040(2)	0.010(2)	0.018(2)	0.007(2)
C(9)	0.018(2)	0.038(2)	0.030(2)	0.005(2)	0.004(2)	-0.002(2)
C(10)	0.056(3)	0.034(2)	0.056(3)	0.007(2)	0.027(2)	0.009(2)
C(11)	0.028(2)	0.034(2)	0.029(2)	-0.007(2)	0.013(2)	-0.002(2)
C(12)	0.036(2)	0.040(2)	0.038(2)	-0.002(2)	0.019(2)	-0.008(2)
C(13)	0.027(2)	0.029(2)	0.025(2)	-0.004(2)	0.012(2)	-0.004(2)
C(14)	0.030(2)	0.039(2)	0.024(2)	0.000(2)	0.003(2)	-0.005(2)
C(15)	0.026(2)	0.030(2)	0.034(2)	0.001(2)	0.011(2)	0.000(2)
C(16)	0.028(2)	0.037(2)	0.038(2)	-0.002(2)	0.009(2)	0.004(2)
F(1)	0.036(1)	0.032(1)	0.037(1)	-0.009(1)	0.008(1)	0.004(1)
F(2)	0.034(1)	0.053(1)	0.024(1)	0.003(1)	0.011(1)	-0.009(1)
F(3)	0.031(1)	0.051(1)	0.026(1)	-0.002(1)	0.004(1)	-0.004(1)
F(4)	0.037(1)	0.040(1)	0.048(1)	-0.004(1)	-0.001(1)	0.013(1)
F(5)	0.026(1)	0.076(2)	0.030(1)	0.007(1)	0.012(1)	-0.002(1)
F(6)	0.049(1)	0.026(1)	0.025(1)	0.006(1)	0.010(1)	-0.001(1)
F(7)	0.031(1)	0.035(1)	0.038(1)	0.001(1)	0.015(1)	0.007(1)
F(8)	0.041(1)	0.052(1)	0.051(1)	-0.019(1)	0.018(1)	-0.017(1)
F(9)	0.058(2)	0.036(1)	0.027(1)	0.004(1)	-0.001(1)	-0.002(1)
F(10)	0.057(1)	0.029(1)	0.032(1)	-0.005(1)	0.012(1)	0.004(1)
F(11)	0.065(2)	0.040(1)	0.030(1)	0.001(1)	0.019(1)	0.013(1)
F(12)	0.051(1)	0.033(1)	0.038(1)	-0.004(1)	-0.005(1)	-0.008(1)
F(13)	0.035(1)	0.042(1)	0.049(1)	0.004(1)	0.007(1)	0.011(1)
F(14)	0.084(2)	0.029(1)	0.044(1)	-0.007(1)	0.013(1)	0.017(1)
F(15)	0.049(1)	0.034(1)	0.032(1)	0.008(1)	0.012(1)	0.004(1)

F(16)	0.038(1)	0.042(1)	0.047(1)	0.019(1)	0.015(1)	-0.001(1)
F(17)	0.023(1)	0.049(1)	0.037(1)	0.006(1)	0.001(1)	-0.007(1)
F(18)	0.047(1)	0.079(2)	0.029(1)	-0.004(1)	0.012(1)	0.012(1)
F(19)	0.057(2)	0.038(1)	0.052(1)	0.005(1)	0.029(1)	0.009(1)
F(20)	0.039(1)	0.076(2)	0.059(2)	0.013(1)	0.029(1)	0.011(1)
F(21)	0.035(1)	0.042(1)	0.036(1)	0.012(1)	0.016(1)	0.003(1)
F(22)	0.031(1)	0.050(1)	0.047(1)	0.014(1)	-0.002(1)	-0.002(1)
F(23)	0.121(3)	0.044(2)	0.135(3)	0.015(2)	0.102(2)	0.025(2)
F(24)	0.056(2)	0.039(1)	0.086(2)	0.027(1)	0.025(1)	0.017(1)
F(25)	0.099(2)	0.028(1)	0.059(2)	-0.005(1)	0.008(2)	0.001(1)
F(26)	0.023(1)	0.061(1)	0.042(1)	0.004(1)	0.008(1)	-0.003(1)
F(27)	0.048(1)	0.041(1)	0.049(1)	-0.014(1)	0.032(1)	-0.007(1)
F(28)	0.066(2)	0.033(1)	0.057(2)	-0.012(1)	0.035(1)	-0.016(1)
F(29)	0.045(1)	0.053(1)	0.047(1)	0.021(1)	0.012(1)	-0.001(1)
F(30)	0.054(2)	0.054(1)	0.052(1)	-0.004(1)	0.034(1)	-0.019(1)
F(31)	0.036(1)	0.053(1)	0.038(1)	-0.020(1)	0.019(1)	-0.007(1)
F(32)	0.040(1)	0.029(1)	0.038(1)	0.002(1)	0.009(1)	-0.010(1)
F(33)	0.043(1)	0.056(1)	0.030(1)	-0.008(1)	0.001(1)	-0.006(1)
F(34)	0.026(1)	0.061(2)	0.041(1)	-0.007(1)	0.009(1)	0.003(1)
F(35)	0.056(2)	0.041(1)	0.041(1)	0.014(1)	0.001(1)	-0.006(1)
F(36)	0.042(1)	0.034(1)	0.046(1)	-0.008(1)	0.008(1)	0.010(1)
F(37)	0.032(1)	0.043(1)	0.044(1)	0.015(1)	0.010(1)	-0.002(1)
F(38)	0.037(1)	0.046(1)	0.047(1)	-0.016(1)	-0.003(1)	0.007(1)
F(39)	0.025(1)	0.053(1)	0.051(1)	0.009(1)	0.009(1)	0.002(1)
F(40)	0.035(1)	0.051(1)	0.040(1)	0.013(1)	0.004(1)	0.010(1)
N(3)	0.022(2)	0.029(2)	0.029(2)	0.001(1)	0.007(1)	-0.001(1)
N(4)	0.023(2)	0.028(2)	0.026(2)	-0.001(1)	0.008(1)	0.001(1)
P(1)	0.022(1)	0.025(1)	0.024(1)	0.001(1)	0.007(1)	0.002(1)
P(2)	0.024(1)	0.023(1)	0.023(1)	0.002(1)	0.005(1)	0.000(1)
P(3)	0.023(1)	0.026(1)	0.023(1)	-0.002(1)	0.008(1)	-0.003(1)
P(4)	0.022(1)	0.025(1)	0.024(1)	0.000(1)	0.009(1)	0.001(1)
O(1)	0.023(1)	0.033(1)	0.030(1)	-0.002(1)	0.008(1)	0.000(1)
O(2)	0.028(1)	0.027(1)	0.025(1)	-0.002(1)	0.004(1)	-0.002(1)
O(3)	0.028(1)	0.033(1)	0.031(1)	-0.004(1)	0.010(1)	-0.007(1)
O(4)	0.027(1)	0.031(1)	0.026(1)	-0.003(1)	0.007(1)	0.000(1)
N(1)	0.024(2)	0.030(2)	0.020(2)	0.000(1)	0.007(1)	0.003(1)
N(2)	0.023(2)	0.033(2)	0.022(2)	-0.001(1)	0.007(1)	-0.002(1)
C(91)	0.029(2)	0.029(2)	0.036(2)	-0.006(2)	0.012(2)	-0.005(2)
C(92)	0.038(2)	0.044(2)	0.022(2)	0.001(2)	0.004(2)	-0.002(2)
C(93)	0.029(2)	0.031(2)	0.034(2)	-0.006(2)	0.010(2)	-0.002(2)
C(94)	0.025(2)	0.044(2)	0.028(2)	-0.003(2)	0.012(2)	-0.002(2)
C(95)	0.027(2)	0.036(2)	0.027(2)	-0.001(2)	0.010(2)	0.007(2)
C(96)	0.027(2)	0.039(2)	0.037(2)	0.007(2)	0.015(2)	0.002(2)
C(97)	0.032(2)	0.029(2)	0.038(2)	0.002(2)	0.011(2)	0.001(2)
C(98)	0.031(2)	0.057(3)	0.025(2)	-0.008(2)	0.003(2)	0.009(2)

The anisotropic displacement factor exponent takes the form:
$-2\pi^2[h^2a^{*2}U_{11}+ ..+2hka^*b^*U_{12}]$

I.4 Crystal structure of [$C_7H_{16}NO$]FPI

Table I.4.1 Atomic coordinates and equivalent isotropic displacement parameters (Å^2). U_{eq} is defined as one third of the trace of the orthogonalized U_{ij} tensor for [$C_7H_{16}NO$]FPI.

	x	**y**	**z**	**U(eq)**
P(1)	500(1)	3426(1)	3994(1)	40(1)
O(1)	1708(3)	2559(3)	4183(1)	52(1)
C(11)	-588(5)	3888(6)	4527(2)	53(1)
F(111)	-1398(3)	4979(3)	4418(1)	61(1)
F(112)	-1521(3)	2857(3)	4647(1)	69(1)
C(12)	291(6)	4160(7)	4998(2)	68(2)
F(124)	1286(3)	5100(4)	4892(1)	72(1)
F(122)	972(3)	3073(4)	5181(1)	73(1)
F(123)	-504(3)	4588(4)	5344(1)	76(1)
C(13)	-942(5)	2449(5)	3617(2)	49(1)
F(131)	-2211(3)	3108(3)	3591(1)	60(1)
F(134)	-1141(3)	1264(3)	3843(1)	64(1)
C(14)	-635(6)	2116(6)	3090(2)	60(1)
F(141)	-1622(4)	1303(4)	2884(1)	78(1)
F(145)	-645(4)	3198(4)	2819(1)	74(1)
F(146)	652(3)	1533(5)	3102(1)	87(1)
N(1)	541(11)	4650(10)	3650(5)	32(2)
P(2)	1762(6)	5648(4)	3552(2)	29(1)
O(2)	2595(18)	6475(18)	3925(8)	39(2)
C(21)	3037(10)	4811(8)	3157(3)	52(3)
F(213)	3174(6)	3494(5)	3304(2)	68(2)
F(214)	2520(20)	4886(14)	2676(3)	62(2)
C(22)	4598(13)	5274(11)	3212(4)	52(2)
F(223)	5160(7)	5054(12)	3674(2)	77(2)
F(225)	4659(7)	6574(7)	3125(3)	83(2)
F(226)	5470(20)	4700(30)	2915(10)	62(2)
C(23)	711(11)	6737(10)	3090(4)	52(3)
F(232)	1627(6)	7568(7)	2879(2)	70(2)
F(233)	-39(19)	5971(8)	2728(4)	60(2)
C(24)	-435(10)	7632(10)	3284(3)	48(3)
F(241)	-1137(8)	8338(8)	2926(3)	71(2)
F(243)	207(9)	8443(8)	3623(3)	96(2)
F(245)	-1460(12)	6918(12)	3483(4)	83(3)
N(1A)	803(12)	4757(9)	3721(5)	32(2)
P(2A)	1625(6)	6059(4)	3588(2)	29(1)
O(2A)	2425(18)	6842(18)	3978(8)	39(2)
C(21A)	2893(10)	5621(9)	3112(3)	46(2)
F(211)	2430(20)	4589(13)	2812(3)	62(2)
F(212)	3123(8)	6677(7)	2819(2)	81(2)
C(22A)	4392(13)	5149(10)	3316(4)	52(2)
F(221)	5100(20)	4630(30)	2956(10)	62(2)
F(222)	4251(8)	4208(7)	3657(2)	68(2)

F(224)	5137(7)	6139(9)	3553(3)	74(2)
C(23A)	378(11)	7115(9)	3172(4)	52(3)
F(231)	964(8)	8336(6)	3127(3)	73(2)
F(234)	24(19)	6552(8)	2711(4)	60(2)
C(24A)	-1107(12)	7340(10)	3358(3)	65(5)
F(242)	-1864(9)	8249(9)	3093(4)	88(3)
F(244)	-902(10)	7713(10)	3828(2)	95(3)
F(246)	-1882(8)	6227(8)	3291(3)	76(2)
P(3)	4553(1)	8725(1)	1038(1)	37(1)
O(3)	3311(3)	7895(4)	860(1)	52(1)
C(31)	5633(4)	9087(6)	496(2)	46(1)
F(311)	6479(3)	10178(3)	584(1)	63(1)
F(312)	6502(3)	8054(4)	393(1)	72(1)
C(32)	4701(5)	9382(7)	22(2)	57(1)
F(321)	5501(3)	9760(4)	-337(1)	74(1)
F(322)	3748(3)	10321(4)	105(1)	70(1)
F(323)	3995(3)	8293(4)	-148(1)	71(1)
C(33)	5967(5)	7751(5)	1423(2)	52(1)
F(331)	7261(3)	8358(3)	1435(1)	58(1)
F(332)	6117(4)	6525(3)	1212(1)	70(1)
C(34)	5670(6)	7497(7)	1957(2)	66(2)
F(341)	4338(4)	7012(5)	1954(1)	104(1)
F(342)	5775(4)	8575(4)	2215(1)	79(1)
F(343)	6602(4)	6618(4)	2161(1)	86(1)
N(3)	4450(3)	10032(4)	1333(1)	39(1)
P(4)	3532(1)	11299(1)	1406(1)	41(1)
O(4)	2746(3)	12028(4)	997(1)	48(1)
C(41)	2231(5)	10964(7)	1879(2)	59(2)
F(411)	2085(5)	12080(5)	2170(2)	107(1)
F(412)	2717(3)	9992(4)	2192(1)	86(1)
C(42)	756(6)	10605(6)	1694(2)	62(1)
F(421)	804(4)	9683(4)	1345(1)	79(1)
F(422)	80(3)	11678(4)	1460(2)	92(1)
F(423)	-49(3)	10173(4)	2039(1)	81(1)
C(43)	4822(6)	12434(6)	1788(2)	68(2)
F(431)	5099(4)	11901(5)	2282(1)	87(1)
F(432)	4202(4)	13663(4)	1818(1)	90(1)
C(44)	6281(8)	12604(8)	1626(3)	92(2)
F(441)	6080(5)	12960(5)	1159(1)	116(2)
F(442)	6962(5)	13564(4)	1917(2)	116(2)
F(443)	7059(3)	11506(4)	1714(2)	92(1)
N(2)	432(3)	5479(4)	754(1)	33(1)
C(51)	1016(4)	5541(5)	254(1)	39(1)
C(52)	-77(4)	5685(6)	-185(1)	50(1)
O(52)	-840(3)	6887(4)	-156(1)	55(1)
C(53)	-72(5)	6776(5)	938(2)	51(1)
C(54)	-60(7)	6452(7)	1509(2)	77(2)
C(55)	1080(5)	5403(6)	1623(2)	58(1)
C(56)	1637(4)	5108(5)	1134(1)	43(1)

C(57)	-745(5)	4475(6)	764(2)	61(1)
N(4)	4631(17)	35(12)	4241(7)	31(2)
C(61)	4000(20)	-20(20)	4725(6)	34(2)
C(62)	5020(20)	348(17)	5178(8)	44(3)
O(62)	5821(17)	1546(17)	5149(6)	46(2)
C(63)	5752(18)	-1031(12)	4230(5)	49(2)
C(66)	3400(20)	-280(20)	3859(6)	45(3)
C(65)	3945(13)	49(16)	3366(6)	50(3)
C(68)	5140(12)	1080(10)	3486(3)	57(3)
C(67)	5152(17)	1320(11)	4043(3)	38(2)
N(4A)	4580(18)	305(12)	4203(7)	31(2)
C(61A)	3980(20)	190(20)	4693(6)	34(2)
C(62A)	5090(20)	42(16)	5140(8)	44(3)
O(62A)	5512(17)	1390(16)	5249(6)	46(2)
C(67A)	5097(16)	1703(11)	4167(4)	38(2)
C(63A)	5758(18)	-638(13)	4094(4)	49(2)
C(64)	5816(8)	-688(10)	3541(3)	49(2)
C(65A)	4343(11)	-150(17)	3345(6)	50(3)
C(66A)	3450(20)	40(20)	3781(6)	45(3)

Table I.4.2 Selected bond lengths [Å] and angles [°] in [C$_7$H$_{16}$NO]FPI.

P(1)-O(1)	1.476(3)	F(211)-C(21A)-C(22A)	102.1(10)
P(1)-N(1)	1.550(4)	F(212)-C(21A)-P(2A)	111.4(6)
P(1)-N(1A)	1.571(4)	F(211)-C(21A)-P(2A)	113.9(9)
P(1)-C(13)	1.887(5)	C(22A)-C(21A)-P(2A)	115.5(7)
P(1)-C(11)	1.904(5)	F(221)-C(22A)-F(222)	108.6(16)
C(11)-F(111)	1.349(6)	F(221)-C(22A)-F(224)	111.9(15)
C(11)-F(112)	1.411(6)	F(222)-C(22A)-F(224)	105.8(9)
C(11)-C(12)	1.482(7)	F(221)-C(22A)-C(21A)	110.4(14)
C(12)-F(123)	1.323(6)	F(222)-C(22A)-C(21A)	109.1(9)
C(12)-F(122)	1.337(7)	F(224)-C(22A)-C(21A)	110.8(9)
C(12)-F(124)	1.373(7)	F(231)-C(23A)-F(234)	110.5(9)
C(13)-F(131)	1.349(5)	F(231)-C(23A)-C(24A)	106.1(9)
C(13)-F(134)	1.363(6)	F(234)-C(23A)-C(24A)	102.4(10)
C(13)-C(14)	1.526(7)	F(231)-C(23A)-P(2A)	109.8(7)
C(14)-F(145)	1.316(7)	F(234)-C(23A)-P(2A)	113.3(9)
C(14)-F(141)	1.316(6)	C(24A)-C(23A)-P(2A)	114.2(7)
C(14)-F(146)	1.330(6)	F(242)-C(24A)-F(244)	110.5(9)
N(1)-P(2)	1.558(5)	F(242)-C(24A)-F(246)	104.6(9)
P(2)-O(2)	1.475(8)	F(244)-C(24A)-F(246)	113.2(10)
P(2)-C(23)	1.874(8)	F(242)-C(24A)-C(23A)	111.8(9)
P(2)-C(21)	1.874(7)	F(244)-C(24A)-C(23A)	107.9(9)
C(21)-F(214)	1.357(8)	F(246)-C(24A)-C(23A)	108.8(8)
C(21)-F(213)	1.387(8)	O(3)-P(3)-N(3)	124.66(19)
C(21)-C(22)	1.518(9)	O(3)-P(3)-C(33)	111.9(2)
C(22)-F(226)	1.331(9)	N(3)-P(3)-C(33)	103.1(2)
C(22)-F(225)	1.332(9)	O(3)-P(3)-C(31)	108.08(19)
C(22)-F(223)	1.336(9)	N(3)-P(3)-C(31)	107.7(2)
C(23)-F(232)	1.358(9)	C(33)-P(3)-C(31)	98.1(2)

C(23)-F(233)	1.387(9)	F(311)-C(31)-F(312)	108.0(3)
C(23)-C(24)	1.527(9)	F(311)-C(31)-C(32)	105.4(4)
C(24)-F(241)	1.328(8)	F(312)-C(31)-C(32)	106.0(4)
C(24)-F(243)	1.331(8)	F(311)-C(31)-P(3)	111.0(3)
C(24)-F(245)	1.348(9)	F(312)-C(31)-P(3)	112.5(3)
N(1A)-P(2A)	1.576(4)	C(32)-C(31)-P(3)	113.5(3)
P(2A)-O(2A)	1.469(8)	F(322)-C(32)-F(321)	110.3(5)
P(2A)-C(23A)	1.873(8)	F(322)-C(32)-F(323)	109.1(4)
P(2A)-C(21A)	1.884(7)	F(321)-C(32)-F(323)	105.6(4)
C(21A)-F(212)	1.358(8)	F(322)-C(32)-C(31)	109.4(4)
C(21A)-F(211)	1.367(9)	F(321)-C(32)-C(31)	111.5(4)
C(21A)-C(22A)	1.528(9)	F(323)-C(32)-C(31)	110.9(5)
C(22A)-F(221)	1.339(9)	F(331)-C(33)-F(332)	107.0(4)
C(22A)-F(222)	1.340(9)	F(331)-C(33)-C(34)	107.0(4)
C(22A)-F(224)	1.344(9)	F(332)-C(33)-C(34)	106.4(5)
C(23A)-F(231)	1.355(9)	F(331)-C(33)-P(3)	110.7(3)
C(23A)-F(234)	1.389(9)	F(332)-C(33)-P(3)	109.2(3)
C(23A)-C(24A)	1.531(9)	C(34)-C(33)-P(3)	116.1(4)
C(24A)-F(242)	1.327(9)	F(342)-C(34)-F(343)	108.6(5)
C(24A)-F(244)	1.331(9)	F(342)-C(34)-F(341)	109.5(5)
C(24A)-F(246)	1.335(9)	F(343)-C(34)-F(341)	109.2(5)
P(3)-O(3)	1.470(3)	F(342)-C(34)-C(33)	111.6(5)
P(3)-N(3)	1.549(4)	F(343)-C(34)-C(33)	110.0(5)
P(3)-C(33)	1.880(5)	F(341)-C(34)-C(33)	107.9(5)
P(3)-C(31)	1.896(4)	P(3)-N(3)-P(4)	145.4(2)
C(31)-F(311)	1.360(6)	O(4)-P(4)-N(3)	123.41(18)
C(31)-F(312)	1.362(6)	O(4)-P(4)-C(41)	107.6(2)
C(31)-C(32)	1.517(6)	N(3)-P(4)-C(41)	109.7(2)
C(32)-F(322)	1.330(6)	O(4)-P(4)-C(43)	111.0(2)
C(32)-F(321)	1.337(5)	N(3)-P(4)-C(43)	103.8(2)
C(32)-F(323)	1.338(7)	C(41)-P(4)-C(43)	98.4(3)
C(33)-F(331)	1.347(6)	F(412)-C(41)-F(411)	105.7(4)
C(33)-F(332)	1.372(6)	F(412)-C(41)-C(42)	106.6(5)
C(33)-C(34)	1.528(7)	F(411)-C(41)-C(42)	105.0(4)
C(34)-F(342)	1.291(7)	F(412)-C(41)-P(4)	111.5(3)
C(34)-F(343)	1.324(7)	F(411)-C(41)-P(4)	110.5(4)
C(34)-F(341)	1.330(7)	C(42)-C(41)-P(4)	116.8(3)
N(3)-P(4)	1.559(4)	F(423)-C(42)-F(421)	109.6(5)
P(4)-O(4)	1.470(3)	F(423)-C(42)-F(422)	108.8(4)
P(4)-C(41)	1.879(5)	F(421)-C(42)-F(422)	105.0(4)
P(4)-C(43)	1.895(5)	F(423)-C(42)-C(41)	114.2(5)
C(41)-F(412)	1.348(6)	F(421)-C(42)-C(41)	109.0(4)
C(41)-F(411)	1.388(7)	F(422)-C(42)-C(41)	109.8(5)
C(41)-C(42)	1.462(7)	F(432)-C(43)-F(431)	108.5(4)
C(42)-F(423)	1.328(6)	F(432)-C(43)-C(44)	108.5(6)
C(42)-F(421)	1.334(6)	F(431)-C(43)-C(44)	103.4(4)
C(42)-F(422)	1.376(7)	F(432)-C(43)-P(4)	109.2(3)
C(43)-F(432)	1.370(6)	F(431)-C(43)-P(4)	109.5(4)
C(43)-F(431)	1.451(7)	C(44)-C(43)-P(4)	117.3(4)

C(43)-C(44)	1.475(10)	F(441)-C(44)-F(443)	115.2(8)
C(44)-F(441)	1.318(7)	F(441)-C(44)-F(442)	112.5(6)
C(44)-F(443)	1.330(9)	F(443)-C(44)-F(442)	105.6(5)
C(44)-F(442)	1.366(7)	F(441)-C(44)-C(43)	105.6(5)
N(2)-C(53)	1.490(6)	F(443)-C(44)-C(43)	110.4(6)
N(2)-C(57)	1.491(6)	F(442)-C(44)-C(43)	107.3(7)
N(2)-C(56)	1.501(4)	C(53)-N(2)-C(57)	109.5(3)
N(2)-C(51)	1.514(4)	C(53)-N(2)-C(56)	102.9(3)
C(51)-C(52)	1.502(5)	C(57)-N(2)-C(56)	108.7(3)
C(51)-H(51A)	0.99	C(53)-N(2)-C(51)	114.7(3)
C(51)-H(51B)	0.99	C(57)-N(2)-C(51)	111.7(3)
C(52)-O(52)	1.408(6)	C(56)-N(2)-C(51)	108.9(3)
C(52)-H(52A)	0.99	C(52)-C(51)-N(2)	116.6(3)
C(52)-H(52B)	0.99	C(52)-C(51)-H(51A)	108.1
O(52)-H(52)	0.84	N(2)-C(51)-H(51A)	108.1
C(53)-C(54)	1.589(7)	C(52)-C(51)-H(51B)	108.1
C(53)-H(53A)	0.99	N(2)-C(51)-H(51B)	108.1
C(53)-H(53B)	0.99	H(51A)-C(51)-H(51B)	107.3
C(54)-C(55)	1.507(8)	O(52)-C(52)-C(51)	110.2(4)
C(54)-H(54A)	0.99	O(52)-C(52)-H(52A)	109.6
C(54)-H(54B)	0.99	C(51)-C(52)-H(52A)	109.6
C(55)-C(56)	1.504(6)	O(52)-C(52)-H(52B)	109.6
C(55)-H(55A)	0.99	C(51)-C(52)-H(52B)	109.6
C(55)-H(55B)	0.99	H(52A)-C(52)-H(52B)	108.1
C(56)-H(56A)	0.99	C(52)-O(52)-H(52)	109.5
C(56)-H(56B)	0.99	N(2)-C(53)-C(54)	100.2(4)
C(57)-H(57A)	0.98	N(2)-C(53)-H(53A)	111.7
C(57)-H(57B)	0.98	C(54)-C(53)-H(53A)	111.7
C(57)-H(57C)	0.98	N(2)-C(53)-H(53B)	111.7
N(4)-C(61)	1.496(8)	C(54)-C(53)-H(53B)	111.7
N(4)-C(63)	1.498(9)	H(53A)-C(53)-H(53B)	109.5
N(4)-C(67)	1.499(9)	C(55)-C(54)-C(53)	106.6(4)
N(4)-C(66)	1.507(8)	C(55)-C(54)-H(54A)	110.4
C(61)-C(62)	1.529(9)	C(53)-C(54)-H(54A)	110.4
C(61)-H(61A)	0.99	C(55)-C(54)-H(54B)	110.4
C(61)-H(61B)	0.99	C(53)-C(54)-H(54B)	110.4
C(62)-O(62)	1.424(9)	H(54A)-C(54)-H(54B)	108.6
C(62)-H(62A)	0.99	C(56)-C(55)-C(54)	104.5(4)
C(62)-H(62B)	0.99	C(56)-C(55)-H(55A)	110.9
O(62)-H(62)	0.84	C(54)-C(55)-H(55A)	110.9
C(63)-H(63A)	0.98	C(56)-C(55)-H(55B)	110.9
C(63)-H(63B)	0.98	C(54)-C(55)-H(55B)	110.9
C(63)-H(63C)	0.98	H(55A)-C(55)-H(55B)	108.9
C(66)-C(65)	1.519(9)	N(2)-C(56)-C(55)	105.4(3)
C(66)-H(66A)	0.99	N(2)-C(56)-H(56A)	110.7
C(66)-H(66B)	0.99	C(55)-C(56)-H(56A)	110.7
C(65)-C(68)	1.533(10)	N(2)-C(56)-H(56B)	110.7
C(65)-H(65A)	0.99	C(55)-C(56)-H(56B)	110.7
C(65)-H(65B)	0.99	H(56A)-C(56)-H(56B)	108.8

C(68)-C(67)	1.536(8)	N(2)-C(57)-H(57A)	109.5
C(68)-H(68A)	0.99	N(2)-C(57)-H(57B)	109.5
C(68)-H(68B)	0.99	H(57A)-C(57)-H(57B)	109.5
C(67)-H(67A)	0.99	N(2)-C(57)-H(57C)	109.5
C(67)-H(67B)	0.99	H(57A)-C(57)-H(57C)	109.5
N(4A)-C(67A)	1.493(9)	H(57B)-C(57)-H(57C)	109.5
N(4A)-C(61A)	1.500(8)	C(61)-N(4)-C(63)	109.0(14)
N(4A)-C(63A)	1.501(9)	C(61)-N(4)-C(67)	121.1(13)
N(4A)-C(66A)	1.507(8)	C(63)-N(4)-C(67)	111.2(11)
C(61A)-C(62A)	1.531(9)	C(61)-N(4)-C(66)	105.3(13)
C(61A)-H(61C)	0.99	C(63)-N(4)-C(66)	108.5(15)
C(61A)-H(61D)	0.99	C(67)-N(4)-C(66)	100.6(13)
C(62A)-O(62A)	1.435(9)	N(4)-C(61)-C(62)	115.8(19)
C(62A)-H(62C)	0.99	N(4)-C(61)-H(61A)	108.3
C(62A)-H(62D)	0.99	C(62)-C(61)-H(61A)	108.3
O(62A)-H(62E)	0.84	N(4)-C(61)-H(61B)	108.3
C(67A)-H(67C)	0.98	C(62)-C(61)-H(61B)	108.3
C(67A)-H(67D)	0.98	H(61A)-C(61)-H(61B)	107.4
C(67A)-H(67E)	0.98	O(62)-C(62)-C(61)	116.7(17)
C(63A)-C(64)	1.514(9)	O(62)-C(62)-H(62A)	108.1
C(63A)-H(63D)	0.99	C(61)-C(62)-H(62A)	108.1
C(63A)-H(63E)	0.99	O(62)-C(62)-H(62B)	108.1
C(64)-C(65A)	1.522(9)	C(61)-C(62)-H(62B)	108.1
C(64)-H(64A)	0.99	H(62A)-C(62)-H(62B)	107.3
C(64)-H(64B)	0.99	N(4)-C(63)-H(63A)	109.5
C(65A)-C(66A)	1.524(9)	N(4)-C(63)-H(63B)	109.5
C(65A)-H(65C)	0.99	H(63A)-C(63)-H(63B)	109.5
C(65A)-H(65D)	0.99	N(4)-C(63)-H(63C)	109.5
C(66A)-H(66C)	0.99	H(63A)-C(63)-H(63C)	109.5
C(66A)-H(66D)	0.99	H(63B)-C(63)-H(63C)	109.5
O(1)-P(1)-N(1)	128.3(5)	N(4)-C(66)-C(65)	105.7(15)
O(1)-P(1)-N(1A)	120.3(5)	N(4)-C(66)-H(66A)	110.6
N(1)-P(1)-N(1A)	11.6(7)	C(65)-C(66)-H(66A)	110.6
O(1)-P(1)-C(13)	111.2(2)	N(4)-C(66)-H(66B)	110.6
N(1)-P(1)-C(13)	98.1(4)	C(65)-C(66)-H(66B)	110.6
N(1A)-P(1)-C(13)	109.7(4)	H(66A)-C(66)-H(66B)	108.7
O(1)-P(1)-C(11)	108.59(19)	C(66)-C(65)-C(68)	104.7(12)
N(1)-P(1)-C(11)	108.2(6)	C(66)-C(65)-H(65A)	110.8
N(1A)-P(1)-C(11)	106.5(6)	C(68)-C(65)-H(65A)	110.8
C(13)-P(1)-C(11)	98.2(2)	C(66)-C(65)-H(65B)	110.8
F(111)-C(11)-F(112)	107.9(4)	C(68)-C(65)-H(65B)	110.8
F(111)-C(11)-C(12)	106.9(5)	H(65A)-C(65)-H(65B)	108.9
F(112)-C(11)-C(12)	103.6(4)	C(65)-C(68)-C(67)	104.8(10)
F(111)-C(11)-P(1)	110.9(3)	C(65)-C(68)-H(68A)	110.8
F(112)-C(11)-P(1)	112.3(4)	C(67)-C(68)-H(68A)	110.8
C(12)-C(11)-P(1)	114.7(3)	C(65)-C(68)-H(68B)	110.8
F(123)-C(12)-F(122)	106.1(5)	C(67)-C(68)-H(68B)	110.8
F(123)-C(12)-F(124)	111.0(5)	H(68A)-C(68)-H(68B)	108.9
F(122)-C(12)-F(124)	109.8(4)	N(4)-C(67)-C(68)	104.3(10)

F(123)-C(12)-C(11)	112.2(4)	N(4)-C(67)-H(67A)	110.9
F(122)-C(12)-C(11)	112.0(5)	C(68)-C(67)-H(67A)	110.9
F(124)-C(12)-C(11)	105.8(4)	N(4)-C(67)-H(67B)	110.9
F(131)-C(13)-F(134)	107.4(4)	C(68)-C(67)-H(67B)	110.9
F(131)-C(13)-C(14)	107.4(4)	H(67A)-C(67)-H(67B)	108.9
F(134)-C(13)-C(14)	106.1(4)	C(67A)-N(4A)-C(61A)	106.1(13)
F(131)-C(13)-P(1)	110.2(3)	C(67A)-N(4A)-C(63A)	109.7(11)
F(134)-C(13)-P(1)	109.2(3)	C(61A)-N(4A)-C(63A)	118.0(14)
C(14)-C(13)-P(1)	116.1(3)	C(67A)-N(4A)-C(66A)	108.9(13)
F(145)-C(14)-F(141)	107.9(4)	C(61A)-N(4A)-C(66A)	112.0(13)
F(145)-C(14)-F(146)	109.7(4)	C(63A)-N(4A)-C(66A)	101.9(14)
F(141)-C(14)-F(146)	109.0(5)	N(4A)-C(61A)-C(62A)	115.8(19)
F(145)-C(14)-C(13)	110.7(5)	N(4A)-C(61A)-H(61C)	108.3
F(141)-C(14)-C(13)	110.7(4)	C(62A)-C(61A)-H(61C)	108.3
F(146)-C(14)-C(13)	108.8(4)	N(4A)-C(61A)-H(61D)	108.3
P(1)-N(1)-P(2)	132.6(6)	C(62A)-C(61A)-H(61D)	108.3
O(2)-P(2)-N(1)	126.1(13)	H(61C)-C(61A)-H(61D)	107.4
O(2)-P(2)-C(23)	109.9(9)	O(62A)-C(62A)-C(61A)	102.7(16)
N(1)-P(2)-C(23)	98.7(5)	O(62A)-C(62A)-H(62C)	111.2
O(2)-P(2)-C(21)	109.2(8)	C(61A)-C(62A)-H(62C)	111.2
N(1)-P(2)-C(21)	108.6(7)	O(62A)-C(62A)-H(62D)	111.2
C(23)-P(2)-C(21)	101.3(5)	C(61A)-C(62A)-H(62D)	111.2
F(214)-C(21)-F(213)	110.2(9)	H(62C)-C(62A)-H(62D)	109.1
F(214)-C(21)-C(22)	109.1(10)	C(62A)-O(62A)-H(62E)	109.5
F(213)-C(21)-C(22)	101.8(7)	N(4A)-C(67A)-H(67C)	109.5
F(214)-C(21)-P(2)	110.1(10)	N(4A)-C(67A)-H(67D)	109.5
F(213)-C(21)-P(2)	108.1(5)	H(67C)-C(67A)-H(67D)	109.5
C(22)-C(21)-P(2)	117.1(8)	N(4A)-C(67A)-H(67E)	109.5
F(226)-C(22)-F(225)	106.3(18)	H(67C)-C(67A)-H(67E)	109.5
F(226)-C(22)-F(223)	107.2(17)	H(67D)-C(67A)-H(67E)	109.5
F(225)-C(22)-F(223)	108.1(10)	N(4A)-C(63A)-C(64)	108.2(11)
F(226)-C(22)-C(21)	115.9(11)	N(4A)-C(63A)-H(63D)	110
F(225)-C(22)-C(21)	109.9(9)	C(64)-C(63A)-H(63D)	110.1
F(223)-C(22)-C(21)	109.2(9)	N(4A)-C(63A)-H(63E)	110
F(232)-C(23)-F(233)	109.6(9)	C(64)-C(63A)-H(63E)	110.1
F(232)-C(23)-C(24)	105.6(8)	H(63D)-C(63A)-H(63E)	108.4
F(233)-C(23)-C(24)	104.7(10)	C(63A)-C(64)-C(65A)	102.9(10)
F(232)-C(23)-P(2)	109.6(7)	C(63A)-C(64)-H(64A)	111.2
F(233)-C(23)-P(2)	110.4(8)	C(65A)-C(64)-H(64A)	111.2
C(24)-C(23)-P(2)	116.7(7)	C(63A)-C(64)-H(64B)	111.2
F(241)-C(24)-F(243)	109.9(9)	C(65A)-C(64)-H(64B)	111.2
F(241)-C(24)-F(245)	105.3(8)	H(64A)-C(64)-H(64B)	109.1
F(243)-C(24)-F(245)	109.6(12)	C(64)-C(65A)-C(66A)	108.0(13)
F(241)-C(24)-C(23)	111.8(8)	C(64)-C(65A)-H(65C)	110.1
F(243)-C(24)-C(23)	108.7(8)	C(66A)-C(65A)-H(65C)	110.1
F(245)-C(24)-C(23)	111.6(9)	C(64)-C(65A)-H(65D)	110.1
P(1)-N(1A)-P(2A)	158.6(7)	C(66A)-C(65A)-H(65D)	110.1
O(2A)-P(2A)-N(1A)	120.2(13)	H(65C)-C(65A)-H(65D)	108.4
O(2A)-P(2A)-C(23A)	112.1(9)	N(4A)-C(66A)-C(65A)	103.0(15)

N(1A)-P(2A)-C(23A)	109.0(5)	N(4A)-C(66A)-H(66C)	111.2
O(2A)-P(2A)-C(21A)	108.5(10)	C(65A)-C(66A)-H(66C)	111.2
N(1A)-P(2A)-C(21A)	108.2(7)	N(4A)-C(66A)-H(66D)	111.2
C(23A)-P(2A)-C(21A)	96.2(5)	C(65A)-C(66A)-H(66D)	111.2
F(212)-C(21A)-F(211)	107.6(7)	H(66C)-C(66A)-H(66D)	109.1
F(212)-C(21A)-C(22A)	105.6(7)		

Table I.4.3 Anisotropic displacement parameters (Å^2).

	U11	U22	U33	U23	U13	U12
P(1)	41(1)	46(1)	32(1)	7(1)	4(1)	13(1)
O(1)	48(2)	58(2)	49(2)	7(2)	5(1)	21(2)
C(11)	51(3)	65(4)	42(2)	10(2)	4(2)	6(3)
F(111)	58(2)	65(2)	61(2)	6(2)	13(1)	33(2)
F(112)	56(2)	72(2)	81(2)	-6(2)	22(1)	-29(2)
C(12)	63(3)	91(5)	51(3)	-5(3)	11(2)	21(3)
F(124)	47(2)	85(2)	85(2)	-24(2)	17(1)	-32(2)
F(122)	64(2)	108(3)	46(2)	22(2)	-2(1)	25(2)
F(123)	53(2)	136(3)	41(1)	-26(2)	9(1)	8(2)
C(13)	45(2)	48(3)	56(3)	16(2)	13(2)	0(2)
F(131)	38(1)	67(2)	75(2)	6(2)	6(1)	7(1)
F(134)	75(2)	49(2)	68(2)	13(1)	9(1)	-6(2)
C(14)	60(3)	76(4)	45(3)	-4(3)	0(2)	-10(3)
F(141)	85(2)	79(2)	70(2)	-13(2)	-1(2)	-25(2)
F(145)	92(2)	83(3)	45(2)	12(2)	-4(1)	-29(2)
F(146)	63(2)	130(3)	67(2)	-23(2)	10(2)	21(2)
N(1)	26(3)	38(2)	28(3)	1(2)	-12(2)	-1(2)
P(2)	35(1)	20(2)	30(1)	-4(2)	-3(1)	7(2)
O(2)	44(4)	28(9)	43(4)	-9(4)	-5(3)	12(4)
C(21)	71(7)	40(7)	49(6)	27(5)	26(5)	15(6)
F(213)	69(4)	36(3)	106(5)	19(3)	43(3)	10(3)
F(214)	79(3)	85(6)	21(4)	-2(4)	-9(5)	5(4)
C(22)	46(4)	64(4)	45(5)	-5(3)	4(4)	6(3)
F(223)	50(4)	134(8)	47(3)	-9(4)	0(3)	30(5)
F(225)	79(4)	49(4)	128(6)	4(4)	46(4)	-27(4)
F(226)	37(8)	91(4)	64(4)	-8(3)	32(5)	-8(7)
C(23)	60(6)	45(7)	47(4)	14(5)	-14(4)	-15(5)
F(232)	59(4)	69(5)	81(4)	45(4)	-1(3)	-17(3)
F(233)	81(2)	57(7)	39(2)	-2(5)	-6(2)	5(7)
C(24)	32(6)	58(8)	54(6)	10(5)	-3(5)	-2(6)
F(241)	62(5)	54(4)	98(5)	31(4)	7(4)	30(4)
F(243)	92(4)	73(5)	115(5)	-48(4)	-44(4)	39(4)
F(245)	62(5)	86(7)	105(7)	25(6)	29(5)	33(5)
N(1A)	26(3)	38(2)	28(3)	1(2)	-12(2)	-1(2)
P(2A)	35(1)	20(2)	30(1)	-4(2)	-3(1)	7(2)
O(2A)	44(4)	28(9)	43(4)	-9(4)	-5(3)	12(4)
C(21A)	61(6)	39(6)	36(5)	-1(4)	-5(4)	-6(6)
F(211)	79(3)	85(6)	21(4)	-2(4)	-9(5)	5(4)
F(212)	99(5)	89(5)	56(3)	39(4)	16(3)	4(4)

C(22A)	46(4)	64(4)	45(5)	-5(3)	4(4)	6(3)
F(221)	37(8)	91(4)	64(4)	-8(3)	32(5)	-8(7)
F(222)	70(4)	70(5)	66(4)	18(3)	13(3)	9(4)
F(224)	58(4)	88(6)	75(5)	-12(4)	0(3)	-30(4)
C(23A)	60(6)	45(7)	47(4)	14(5)	-14(4)	-15(5)
F(231)	76(4)	40(4)	94(5)	13(3)	-34(4)	-10(3)
F(234)	81(2)	57(7)	39(2)	-2(5)	-6(2)	5(7)
C(24A)	52(12)	82(14)	56(9)	16(8)	-11(8)	15(10)
F(242)	73(5)	71(6)	112(7)	18(5)	-28(5)	35(5)
F(244)	102(6)	127(8)	52(4)	-9(4)	-18(4)	51(6)
F(246)	50(4)	68(6)	105(6)	4(4)	-15(4)	-3(4)
P(3)	33(1)	44(1)	35(1)	-3(1)	4(1)	-1(1)
O(3)	38(2)	61(2)	59(2)	0(2)	6(1)	-12(2)
C(31)	30(2)	64(3)	46(2)	-8(2)	5(2)	1(2)
F(311)	51(2)	84(2)	55(2)	-7(2)	12(1)	-28(2)
F(312)	59(2)	92(3)	66(2)	-3(2)	13(1)	37(2)
C(32)	43(3)	86(4)	44(2)	3(3)	7(2)	-7(3)
F(321)	52(2)	136(3)	35(1)	12(2)	7(1)	-7(2)
F(322)	50(2)	90(3)	71(2)	17(2)	14(1)	28(2)
F(323)	61(2)	110(3)	42(1)	-22(2)	0(1)	-22(2)
C(33)	51(3)	49(3)	56(3)	-2(2)	5(2)	8(2)
F(331)	37(1)	66(2)	70(2)	1(2)	4(1)	8(1)
F(332)	87(2)	46(2)	75(2)	-7(2)	1(2)	18(2)
C(34)	60(3)	80(5)	58(3)	14(3)	8(3)	8(3)
F(341)	72(2)	159(4)	81(2)	49(2)	7(2)	-21(2)
F(342)	95(2)	96(3)	45(2)	1(2)	-1(1)	40(2)
F(343)	96(2)	83(3)	79(2)	30(2)	1(2)	32(2)
N(3)	39(2)	43(2)	33(2)	-4(2)	1(1)	9(2)
P(4)	35(1)	52(1)	34(1)	-8(1)	-5(1)	9(1)
O(4)	42(2)	55(2)	45(2)	-6(2)	-11(1)	3(2)
C(41)	44(2)	95(5)	38(2)	-6(3)	6(2)	21(3)
F(411)	117(3)	117(3)	93(2)	-55(2)	36(2)	-9(3)
F(412)	63(2)	129(3)	66(2)	43(2)	4(2)	20(2)
C(42)	57(3)	68(4)	62(3)	-4(3)	8(2)	6(3)
F(421)	93(2)	75(3)	71(2)	-19(2)	16(2)	-26(2)
F(422)	54(2)	102(3)	122(3)	21(3)	14(2)	28(2)
F(423)	59(2)	113(3)	74(2)	-8(2)	28(2)	1(2)
C(43)	67(3)	63(4)	67(3)	-29(3)	-25(3)	26(3)
F(431)	91(2)	123(3)	47(2)	-7(2)	7(2)	-22(2)
F(432)	79(2)	69(2)	112(3)	-42(2)	-43(2)	26(2)
C(44)	83(5)	90(6)	92(5)	18(4)	-44(4)	-35(4)
F(441)	130(3)	147(4)	65(2)	20(2)	-16(2)	-53(3)
F(442)	102(3)	77(3)	156(4)	-23(3)	-52(3)	-18(2)
F(443)	47(2)	90(3)	136(3)	-20(3)	-2(2)	12(2)
N(2)	26(2)	44(2)	29(1)	-2(1)	1(1)	4(2)
C(51)	28(2)	58(3)	31(2)	-2(2)	6(1)	6(2)
C(52)	35(2)	84(4)	32(2)	-13(2)	0(2)	1(2)
O(52)	46(2)	58(2)	56(2)	14(2)	-21(1)	1(2)
C(53)	40(2)	56(3)	56(3)	-12(2)	7(2)	16(2)

C(54)	92(4)	91(5)	49(3)	-9(3)	15(3)	30(4)
C(55)	62(3)	78(4)	34(2)	8(2)	0(2)	27(3)
C(56)	31(2)	54(3)	40(2)	11(2)	-6(2)	8(2)
C(57)	34(2)	71(4)	78(3)	12(3)	7(2)	-7(2)
N(4)	25(2)	33(4)	36(3)	1(3)	1(2)	2(3)
C(61)	29(2)	34(4)	39(2)	10(2)	4(2)	-3(3)
C(62)	41(3)	49(6)	41(3)	12(4)	-1(2)	0(4)
O(62)	45(5)	47(4)	43(5)	4(3)	-9(3)	-11(3)
C(63)	37(2)	40(6)	71(5)	9(4)	8(4)	11(4)
C(66)	36(2)	53(7)	44(4)	-9(4)	-5(3)	-1(4)
C(65)	54(5)	59(5)	36(2)	-6(3)	-2(4)	-2(4)
C(68)	75(6)	47(6)	52(5)	-5(4)	18(4)	3(5)
C(67)	49(2)	34(5)	31(4)	-7(3)	11(3)	-5(4)
N(4A)	25(2)	33(4)	36(3)	1(3)	1(2)	2(3)
C(61A)	29(2)	34(4)	39(2)	10(2)	4(2)	-3(3)
C(62A)	41(3)	49(6)	41(3)	12(4)	-1(2)	0(4)
O(62A)	45(5)	47(4)	43(5)	4(3)	-9(3)	-11(3)
C(67A)	49(2)	34(5)	31(4)	-7(3)	11(3)	-5(4)
C(63A)	37(2)	40(6)	71(5)	9(4)	8(4)	11(4)
C(64)	45(4)	48(5)	57(5)	-21(4)	12(4)	-6(4)
C(65A)	54(5)	59(5)	36(2)	-6(3)	-2(4)	-2(4)
C(66A)	36(2)	53(7)	44(4)	-9(4)	-5(3)	-1(4)

The anisotropic displacement factor exponent takes the form: $-2\pi^2[h^2a^{*2}U_{11}+ ..+2hka^*b^*U_{12}]$

Table I.4.4 Hydrogen coordinates and isotropic displacement parameters.

	x	**y**	**z**	**U(eq)**
H(51A)	1695	6298	255	47
H(51B)	1579	4721	211	47
H(52A)	419	5671	-491	60
H(52B)	-762	4930	-196	60
H(52)	-1379	7001	-418	83
H(53A)	-1054	7002	789	61
H(53B)	602	7506	877	61
H(54A)	174	7260	1708	92
H(54B)	-1017	6120	1585	92
H(55A)	1864	5740	1862	70
H(55B)	658	4598	1761	70
H(56A)	2512	5639	1091	51
H(56B)	1879	4154	1109	51
H(57A)	-1617	4805	572	91
H(57B)	-951	4321	1105	91
H(57C)	-439	3641	620	91
H(61A)	3632	-929	4772	41
H(61B)	3155	589	4709	41
H(62A)	4440	415	5465	53
H(62B)	5710	-391	5245	53
H(62)	6227	1733	5429	69

H(63A)	6621	-771	4439	74
H(63B)	5995	-1155	3890	74
H(63C)	5374	-1864	4352	74
H(66A)	2541	259	3913	54
H(66B)	3138	-1234	3874	54
H(65A)	3159	422	3136	60
H(65B)	4335	-753	3214	60
H(68A)	4924	1912	3300	69
H(68B)	6085	735	3404	69
H(67A)	6139	1532	4191	45
H(67B)	4497	2060	4111	45
H(61C)	3318	-579	4683	41
H(61D)	3392	997	4742	41
H(62C)	4656	-372	5421	53
H(62D)	5925	-499	5059	53
H(62E)	6208	1398	5469	69
H(67C)	5358	1872	3833	56
H(67D)	5945	1839	4404	56
H(67E)	4328	2315	4242	56
H(63D)	5559	-1534	4221	59
H(63E)	6697	-330	4256	59
H(64A)	5954	-1609	3427	59
H(64B)	6605	-123	3437	59
H(65C)	3855	-782	3106	60
H(65D)	4454	709	3175	60
H(66C)	2779	799	3726	54
H(66D)	2888	-771	3841	54

I.5 Crystal structure of $[Et_3NH][\{(C_2F_5)_2P(O)\}N\{S(O)_2CF_3\}]$

Table I.5.1 Atomic coordinates and equivalent isotropic displacement parameters (Å^2). U_{eq} is defined as one third of the trace of the orthogonalized U_{ij} tensor for $[Et_3NH][\{(C_2F_5)_2P(O)\}N\{S(O)_2CF_3\}]$.

	x	**y**	**z**	**U(eq)**
C(1)	0.8085(3)	0.8835(4)	0.1511(2)	0.031(1)
C(2)	0.4364(3)	0.8579(3)	0.3498(2)	0.028(1)
C(3)	0.4134(3)	0.7715(4)	0.4189(2)	0.031(1)
C(4)	0.6196(3)	1.0515(3)	0.3753(2)	0.026(1)
C(5)	0.7515(4)	1.1060(3)	0.3709(3)	0.035(1)
C(6)	0.7951(4)	0.5867(3)	0.4596(2)	0.031(1)
C(7)	0.8792(4)	0.4920(4)	0.4986(3)	0.038(1)
C(8)	0.9391(3)	0.6392(3)	0.3491(2)	0.030(1)
C(9)	0.9857(4)	0.7480(4)	0.3940(3)	0.037(1)
C(10)	0.7745(3)	0.4921(3)	0.3223(2)	0.028(1)
C(11)	0.6383(4)	0.4611(4)	0.3260(3)	0.036(1)
C(12)	0.7413(4)	0.8836(4)	0.6320(2)	0.034(1)
C(13)	0.8289(3)	1.0856(3)	0.8328(2)	0.026(1)
C(14)	0.7123(3)	1.1146(3)	0.8807(2)	0.028(1)

C(15)	1.0171(3)	0.9223(3)	0.8974(2)	0.024(1)
C(16)	1.0740(3)	0.7956(3)	0.9125(2)	0.031(1)
C(17)	0.3007(3)	0.0194(3)	0.1632(2)	0.026(1)
C(18)	0.1660(4)	-0.0136(3)	0.1516(2)	0.031(1)
C(19)	0.4703(3)	0.1595(3)	0.1403(2)	0.030(1)
C(20)	0.5170(4)	0.2710(3)	0.1005(3)	0.035(1)
C(21)	0.3098(3)	0.1263(3)	0.0293(2)	0.027(1)
C(22)	0.3823(4)	0.0307(4)	-0.0135(2)	0.034(1)
F(1)	0.8035(3)	0.9932(3)	0.1230(2)	0.045(1)
F(2)	0.8829(2)	0.8808(3)	0.2159(2)	0.045(1)
F(3)	0.8568(3)	0.8136(3)	0.0954(2)	0.045(1)
F(4)	0.3887(2)	0.8052(3)	0.2823(1)	0.038(1)
F(5)	0.3685(2)	0.9579(2)	0.3628(2)	0.037(1)
F(6)	0.4680(3)	0.6675(2)	0.4056(2)	0.042(1)
F(7)	0.2935(2)	0.7524(3)	0.4245(2)	0.041(1)
F(8)	0.4560(2)	0.8172(3)	0.4874(1)	0.041(1)
F(9)	0.5423(3)	1.1303(2)	0.3388(2)	0.038(1)
F(10)	0.5914(2)	1.0459(2)	0.4536(1)	0.035(1)
F(11)	0.7816(4)	1.1230(3)	0.2964(2)	0.067(1)
F(12)	0.8337(3)	1.0365(3)	0.4077(3)	0.068(1)
F(13)	0.7547(3)	1.2111(2)	0.4076(2)	0.044(1)
F(14)	0.6575(2)	0.9160(3)	0.6840(2)	0.050(1)
F(15)	0.6854(3)	0.8137(4)	0.5770(2)	0.056(1)
F(16)	0.7802(3)	0.9831(3)	0.5955(2)	0.050(1)
F(17)	0.8066(2)	1.1235(2)	0.7570(2)	0.036(1)
F(18)	0.9225(2)	1.1533(2)	0.8642(2)	0.041(1)
F(19)	0.6142(2)	1.0629(2)	0.8465(2)	0.035(1)
F(20)	0.6941(2)	1.2322(2)	0.8814(2)	0.037(1)
F(21)	0.7260(3)	1.0766(2)	0.9560(2)	0.038(1)
F(22)	0.9918(2)	0.9673(2)	0.9697(1)	0.031(1)
F(23)	1.1087(2)	0.9888(2)	0.8659(1)	0.032(1)
F(24)	1.1733(2)	0.8046(3)	0.9610(2)	0.042(1)
F(25)	0.9938(3)	0.7239(2)	0.9468(2)	0.046(1)
F(26)	1.1088(3)	0.7475(3)	0.8443(2)	0.052(1)
N(1)	0.6124(3)	0.9196(2)	0.2385(2)	0.025(1)
N(2)	0.8105(3)	0.6003(2)	0.3713(2)	0.024(1)
N(3)	0.9205(3)	0.8975(3)	0.7437(2)	0.024(1)
N(4)	0.3365(3)	0.1315(2)	0.1185(2)	0.023(1)
O(1)	0.6848(2)	0.8140(2)	0.3786(2)	0.027(1)
O(2)	0.6776(3)	0.7097(2)	0.2052(2)	0.033(1)
O(3)	0.5825(3)	0.8400(3)	0.1013(2)	0.035(1)
O(4)	0.7776(2)	0.8497(2)	0.8712(2)	0.025(1)
O(5)	0.9560(3)	0.7857(3)	0.6199(2)	0.036(1)
O(6)	0.8112(3)	0.7023(3)	0.7164(2)	0.041(1)
P(1)	0.6052(1)	0.8972(1)	0.3322(1)	0.022(1)
P(3)	0.8731(1)	0.9212(1)	0.8317(1)	0.021(1)
S(1)	0.6540(1)	0.8275(1)	0.1748(1)	0.024(1)
S(2)	0.8693(1)	0.8041(1)	0.6816(1)	0.025(1)

Table I.5.2 Selected bond lengths [Å] and angles [°] in $[\mathrm{Et_3NH}][\{(\mathrm{C_2F_5})_2\mathrm{P(O)}\}\mathrm{N}\{\mathrm{S(O)_2CF_3}\}]$.

C(1)-F(1)	1.313(5)	F(10)-C(4)-C(5)	107.2(3)
C(1)-F(2)	1.328(5)	F(9)-C(4)-P(1)	112.7(2)
C(1)-F(3)	1.332(5)	F(10)-C(4)-P(1)	108.0(2)
C(1)-S(1)	1.836(4)	C(5)-C(4)-P(1)	114.1(2)
C(2)-F(4)	1.358(4)	F(11)-C(5)-F(12)	110.2(4)
C(2)-F(5)	1.359(4)	F(11)-C(5)-F(13)	107.8(4)
C(2)-C(3)	1.529(5)	F(12)-C(5)-F(13)	107.4(4)
C(2)-P(1)	1.907(4)	F(11)-C(5)-C(4)	110.9(3)
C(3)-F(7)	1.319(4)	F(12)-C(5)-C(4)	110.7(3)
C(3)-F(8)	1.322(5)	F(13)-C(5)-C(4)	109.8(3)
C(3)-F(6)	1.327(5)	N(2)-C(6)-C(7)	114.1(3)
C(4)-F(9)	1.347(4)	C(9)-C(8)-N(2)	114.0(3)
C(4)-F(10)	1.350(4)	N(2)-C(10)-C(11)	113.5(3)
C(4)-C(5)	1.554(5)	F(14)-C(12)-F(15)	107.8(3)
C(4)-P(1)	1.874(3)	F(14)-C(12)-F(16)	107.4(4)
C(5)-F(11)	1.306(5)	F(15)-C(12)-F(16)	108.4(4)
C(5)-F(12)	1.319(5)	F(14)-C(12)-S(2)	111.2(3)
C(5)-F(13)	1.326(4)	F(15)-C(12)-S(2)	110.4(3)
C(6)-N(2)	1.494(5)	F(16)-C(12)-S(2)	111.5(3)
C(6)-C(7)	1.529(5)	F(17)-C(13)-F(18)	107.3(3)
C(8)-C(9)	1.508(5)	F(17)-C(13)-C(14)	106.9(3)
C(8)-N(2)	1.513(4)	F(18)-C(13)-C(14)	107.1(3)
C(10)-N(2)	1.505(4)	F(17)-C(13)-P(3)	109.5(2)
C(10)-C(11)	1.515(5)	F(18)-C(13)-P(3)	111.1(2)
C(12)-F(14)	1.323(5)	C(14)-C(13)-P(3)	114.7(2)
C(12)-F(15)	1.335(5)	F(19)-C(14)-F(21)	109.5(3)
C(12)-F(16)	1.343(5)	F(19)-C(14)-F(20)	108.7(3)
C(12)-S(2)	1.823(4)	F(21)-C(14)-F(20)	108.7(3)
C(13)-F(17)	1.348(4)	F(19)-C(14)-C(13)	109.9(3)
C(13)-F(18)	1.356(4)	F(21)-C(14)-C(13)	110.5(3)
C(13)-C(14)	1.545(5)	F(20)-C(14)-C(13)	109.6(3)
C(13)-P(3)	1.901(3)	F(22)-C(15)-F(23)	108.1(3)
C(14)-F(19)	1.322(4)	F(22)-C(15)-C(16)	106.6(3)
C(14)-F(21)	1.329(4)	F(23)-C(15)-C(16)	105.8(3)
C(14)-F(20)	1.330(4)	F(22)-C(15)-P(3)	109.9(2)
C(15)-F(22)	1.341(4)	F(23)-C(15)-P(3)	112.3(2)
C(15)-F(23)	1.356(4)	C(16)-C(15)-P(3)	113.8(2)
C(15)-C(16)	1.563(5)	F(26)-C(16)-F(25)	109.3(4)
C(15)-P(3)	1.878(3)	F(26)-C(16)-F(24)	108.1(3)
C(16)-F(26)	1.321(5)	F(25)-C(16)-F(24)	108.1(3)
C(16)-F(25)	1.322(5)	F(26)-C(16)-C(15)	110.6(3)
C(16)-F(24)	1.328(4)	F(25)-C(16)-C(15)	111.1(3)
C(17)-C(18)	1.509(5)	F(24)-C(16)-C(15)	109.6(3)
C(17)-N(4)	1.514(4)	C(18)-C(17)-N(4)	113.5(3)
C(19)-C(20)	1.507(5)	C(20)-C(19)-N(4)	113.3(3)
C(19)-N(4)	1.513(5)	N(4)-C(21)-C(22)	113.9(3)
C(21)-N(4)	1.508(4)	S(1)-N(1)-P(1)	126.24(18)

C(21)-C(22)	1.515(5)	C(6)-N(2)-C(10)	114.8(3)
N(1)-S(1)	1.555(3)	C(6)-N(2)-C(8)	113.5(3)
N(1)-P(1)	1.585(3)	C(10)-N(2)-C(8)	108.9(3)
N(3)-S(2)	1.561(3)	S(2)-N(3)-P(3)	127.29(18)
N(3)-P(3)	1.588(3)	C(21)-N(4)-C(19)	113.5(3)
O(1)-P(1)	1.472(2)	C(21)-N(4)-C(17)	114.1(3)
O(2)-S(1)	1.433(3)	C(19)-N(4)-C(17)	108.0(3)
O(3)-S(1)	1.436(3)	O(1)-P(1)-N(1)	124.93(14)
O(4)-P(3)	1.476(2)	O(1)-P(1)-C(4)	109.90(16)
O(5)-S(2)	1.426(3)	N(1)-P(1)-C(4)	103.07(15)
O(6)-S(2)	1.431(3)	O(1)-P(1)-C(2)	108.70(15)
F(1)-C(1)-F(2)	109.2(3)	N(1)-P(1)-C(2)	105.17(16)
F(1)-C(1)-F(3)	108.3(3)	C(4)-P(1)-C(2)	102.89(16)
F(2)-C(1)-F(3)	108.3(3)	O(4)-P(3)-N(3)	124.77(15)
F(1)-C(1)-S(1)	111.5(3)	O(4)-P(3)-C(15)	108.75(14)
F(2)-C(1)-S(1)	110.5(3)	N(3)-P(3)-C(15)	104.83(15)
F(3)-C(1)-S(1)	109.0(3)	O(4)-P(3)-C(13)	109.89(14)
F(4)-C(2)-F(5)	107.2(3)	N(3)-P(3)-C(13)	104.99(15)
F(4)-C(2)-C(3)	106.5(3)	C(15)-P(3)-C(13)	101.04(15)
F(5)-C(2)-C(3)	107.5(3)	O(2)-S(1)-O(3)	118.49(18)
F(4)-C(2)-P(1)	108.4(2)	O(2)-S(1)-N(1)	114.85(16)
F(5)-C(2)-P(1)	110.9(2)	O(3)-S(1)-N(1)	111.01(16)
C(3)-C(2)-P(1)	116.0(2)	O(2)-S(1)-C(1)	103.67(18)
F(7)-C(3)-F(8)	108.7(3)	O(3)-S(1)-C(1)	104.71(18)
F(7)-C(3)-F(6)	108.2(3)	N(1)-S(1)-C(1)	101.74(17)
F(8)-C(3)-F(6)	109.8(3)	O(5)-S(2)-O(6)	118.8(2)
F(7)-C(3)-C(2)	109.7(3)	O(5)-S(2)-N(3)	110.32(17)
F(8)-C(3)-C(2)	110.2(3)	O(6)-S(2)-N(3)	114.58(17)
F(6)-C(3)-C(2)	110.2(3)	O(5)-S(2)-C(12)	104.39(19)
F(9)-C(4)-F(10)	108.3(3)	O(6)-S(2)-C(12)	103.6(2)
F(9)-C(4)-C(5)	106.2(3)	N(3)-S(2)-C(12)	102.96(17)

Table I.5.3 Anisotropic displacement parameters (Å^2).

	U11	**U22**	**U33**	**U23**	**U13**	**U12**
C(1)	0.024(1)	0.039(2)	0.032(2)	-0.002(1)	0.006(1)	-0.005(1)
C(2)	0.027(1)	0.024(1)	0.031(2)	0.003(1)	-0.003(1)	0.002(1)
C(3)	0.028(2)	0.036(2)	0.031(2)	0.004(1)	0.003(1)	0.001(1)
C(4)	0.033(2)	0.019(1)	0.026(1)	-0.003(1)	-0.002(1)	0.004(1)
C(5)	0.038(2)	0.023(2)	0.043(2)	-0.005(1)	0.000(2)	-0.002(1)
C(6)	0.033(2)	0.029(2)	0.031(2)	0.002(1)	0.002(1)	0.008(1)
C(7)	0.041(2)	0.035(2)	0.039(2)	0.005(2)	-0.003(2)	0.005(2)
C(8)	0.023(1)	0.024(1)	0.041(2)	-0.002(1)	0.003(1)	0.000(1)
C(9)	0.028(2)	0.026(2)	0.058(3)	-0.004(2)	-0.002(2)	-0.001(1)
C(10)	0.028(2)	0.020(1)	0.036(2)	-0.003(1)	0.002(1)	0.000(1)
C(11)	0.029(2)	0.028(2)	0.050(2)	0.003(2)	-0.001(2)	-0.005(1)
C(12)	0.029(2)	0.038(2)	0.035(2)	-0.005(2)	-0.008(1)	0.002(1)
C(13)	0.025(1)	0.019(1)	0.032(2)	0.003(1)	0.001(1)	0.000(1)
C(14)	0.033(2)	0.019(1)	0.032(2)	0.001(1)	0.003(1)	0.003(1)
C(15)	0.023(1)	0.027(1)	0.023(1)	0.002(1)	-0.001(1)	-0.002(1)

C(16)	0.033(2)	0.031(2)	0.030(2)	0.002(1)	-0.005(1)	0.002(1)
C(17)	0.030(2)	0.017(1)	0.031(2)	0.004(1)	-0.001(1)	0.003(1)
C(18)	0.034(2)	0.023(1)	0.036(2)	0.000(1)	0.001(1)	-0.002(1)
C(19)	0.031(2)	0.020(1)	0.039(2)	0.004(1)	-0.008(1)	-0.001(1)
C(20)	0.028(2)	0.024(2)	0.052(2)	0.003(1)	0.002(2)	-0.006(1)
C(21)	0.031(2)	0.026(1)	0.024(1)	0.003(1)	-0.001(1)	0.003(1)
C(22)	0.038(2)	0.030(2)	0.033(2)	-0.004(1)	0.007(1)	0.002(1)
F(1)	0.055(2)	0.034(1)	0.047(2)	0.009(1)	0.010(1)	-0.010(1)
F(2)	0.030(1)	0.062(2)	0.042(1)	0.000(1)	-0.005(1)	-0.005(1)
F(3)	0.041(1)	0.051(2)	0.043(1)	-0.006(1)	0.015(1)	0.005(1)
F(4)	0.041(1)	0.044(1)	0.028(1)	-0.001(1)	-0.005(1)	-0.010(1)
F(5)	0.027(1)	0.031(1)	0.054(2)	0.005(1)	0.003(1)	0.011(1)
F(6)	0.044(1)	0.028(1)	0.054(2)	0.010(1)	0.013(1)	0.005(1)
F(7)	0.026(1)	0.049(2)	0.046(1)	0.007(1)	0.004(1)	-0.006(1)
F(8)	0.037(1)	0.058(2)	0.028(1)	0.003(1)	-0.001(1)	-0.004(1)
F(9)	0.048(1)	0.021(1)	0.043(1)	-0.001(1)	-0.008(1)	0.011(1)
F(10)	0.049(1)	0.028(1)	0.028(1)	-0.005(1)	0.005(1)	0.001(1)
F(11)	0.087(3)	0.063(2)	0.054(2)	-0.022(2)	0.032(2)	-0.045(2)
F(12)	0.033(1)	0.032(1)	0.137(4)	0.006(2)	-0.023(2)	-0.002(1)
F(13)	0.060(2)	0.023(1)	0.050(2)	-0.010(1)	-0.004(1)	-0.007(1)
F(14)	0.023(1)	0.070(2)	0.056(2)	-0.015(2)	-0.003(1)	0.007(1)
F(15)	0.047(2)	0.072(2)	0.048(2)	-0.018(2)	-0.020(1)	-0.002(2)
F(16)	0.061(2)	0.042(2)	0.044(1)	0.014(1)	-0.012(1)	0.010(1)
F(17)	0.043(1)	0.027(1)	0.037(1)	0.012(1)	0.007(1)	0.008(1)
F(18)	0.029(1)	0.018(1)	0.076(2)	-0.001(1)	-0.004(1)	-0.003(1)
F(19)	0.026(1)	0.028(1)	0.052(1)	-0.001(1)	0.002(1)	0.001(1)
F(20)	0.046(1)	0.017(1)	0.047(1)	0.000(1)	0.006(1)	0.006(1)
F(21)	0.057(2)	0.028(1)	0.030(1)	0.001(1)	0.007(1)	0.007(1)
F(22)	0.036(1)	0.030(1)	0.027(1)	-0.004(1)	-0.001(1)	-0.001(1)
F(23)	0.024(1)	0.032(1)	0.037(1)	0.004(1)	-0.001(1)	-0.007(1)
F(24)	0.035(1)	0.040(1)	0.049(1)	0.008(1)	-0.013(1)	0.002(1)
F(25)	0.036(1)	0.029(1)	0.072(2)	0.019(1)	-0.008(1)	-0.004(1)
F(26)	0.065(2)	0.045(2)	0.045(2)	-0.011(1)	-0.007(1)	0.032(1)
N(1)	0.028(1)	0.020(1)	0.026(1)	-0.001(1)	0.000(1)	0.005(1)
N(2)	0.024(1)	0.018(1)	0.031(1)	-0.001(1)	-0.001(1)	0.004(1)
N(3)	0.025(1)	0.021(1)	0.027(1)	0.002(1)	0.000(1)	-0.002(1)
N(4)	0.025(1)	0.017(1)	0.026(1)	0.001(1)	-0.001(1)	0.002(1)
O(1)	0.030(1)	0.021(1)	0.029(1)	0.003(1)	-0.001(1)	0.006(1)
O(2)	0.042(1)	0.019(1)	0.039(1)	-0.002(1)	0.007(1)	0.001(1)
O(3)	0.035(1)	0.038(2)	0.031(1)	-0.008(1)	-0.005(1)	0.003(1)
O(4)	0.025(1)	0.018(1)	0.032(1)	0.002(1)	0.002(1)	-0.001(1)
O(5)	0.034(1)	0.039(2)	0.035(1)	-0.008(1)	0.003(1)	0.005(1)
O(6)	0.056(2)	0.025(1)	0.041(2)	0.000(1)	-0.003(1)	-0.013(1)
P(1)	0.024(1)	0.017(1)	0.024(1)	0.001(1)	0.000(1)	0.003(1)
P(3)	0.022(1)	0.016(1)	0.025(1)	0.002(1)	0.000(1)	-0.001(1)
S(1)	0.026(1)	0.019(1)	0.025(1)	-0.002(1)	0.001(1)	0.001(1)
S(2)	0.027(1)	0.022(1)	0.027(1)	-0.001(1)	-0.001(1)	-0.001(1)

The anisotropic displacement factor exponent takes the form:
$-2\pi^2[h^2a^{*2}U_{11}+ ..+2hka^*b^*U_{12}]$

I.6 Crystal structure of $(C_2F_5)_2P(O)NH_2$

Table I.1.1 Atomic coordinates and equivalent isotropic displacement parameters (Å^2). U_{eq} is defined as one third of the trace of the orthogonalized U_{ij} tensor for $(C_2F_5)_2P(O)NH_2$.

	x	y	z	U(eq)
P	229(2)	1073(1)	8793(1)	24(1)
O	-2085(5)	735(2)	9199(3)	32(1)
N	2718(6)	885(3)	9603(4)	31(1)
C(1)	626(11)	692(4)	7289(5)	42(1)
F(11)	2506(10)	1122(3)	6879(4)	85(2)
F(12)	-1510(9)	850(3)	6609(4)	86(2)
C(2)	1151(11)	-267(4)	7168(6)	48(1)
F(21)	3354(8)	-450(3)	7698(5)	86(2)
F(22)	1134(9)	-503(3)	6088(4)	73(1)
F(23)	-461(10)	-731(3)	7684(5)	87(2)
C(3)	75(9)	2263(3)	8597(5)	33(1)
F(31)	-1534(9)	2466(2)	7694(4)	73(1)
F(32)	2345(7)	2565(2)	8377(4)	71(1)
C(4)	-697(10)	2769(3)	9626(5)	40(1)
F(41)	-695(7)	3600(2)	9458(4)	60(1)
F(42)	-2985(8)	2557(3)	9822(5)	91(2)
F(43)	714(11)	2592(3)	10558(4)	96(2)

Table I.6.2 Selected bond lengths [Å] and angles [°] in $(C_2F_5)_2P(O)NH_2$.

P-O	1.476(3)	H(1)-N-H(2)	124(7)
P-N	1.594(4)	F(11)-C(1)-F(12)	109.6(5)
P-C(3)	1.863(5)	F(11)-C(1)-C(2)	107.4(5)
P-C(1)	1.880(6)	F(12)-C(1)-C(2)	106.2(5)
N-H(1)	0.889(10)	F(11)-C(1)-P	109.4(4)
N-H(2)	0.885(10)	F(12)-C(1)-P	108.6(4)
C(1)-F(11)	1.342(7)	C(2)-C(1)-P	115.6(4)
C(1)-F(12)	1.358(7)	F(22)-C(2)-F(21)	108.1(5)
C(1)-C(2)	1.526(8)	F(22)-C(2)-F(23)	109.9(5)
C(2)-F(22)	1.309(7)	F(21)-C(2)-F(23)	106.1(6)
C(2)-F(21)	1.319(7)	F(22)-C(2)-C(1)	112.2(5)
C(2)-F(23)	1.320(7)	F(21)-C(2)-C(1)	109.6(5)
C(3)-F(31)	1.337(6)	F(23)-C(2)-C(1)	110.8(5)
C(3)-F(32)	1.361(6)	F(31)-C(3)-F(32)	107.5(5)
C(3)-C(4)	1.523(8)	F(31)-C(3)-C(4)	106.8(4)
C(4)-F(43)	1.294(7)	F(32)-C(3)-C(4)	106.9(4)
C(4)-F(41)	1.306(6)	F(31)-C(3)-P	110.4(3)
C(4)-F(42)	1.321(6)	F(32)-C(3)-P	109.5(3)
O-P-N	116.1(2)	C(4)-C(3)-P	115.3(4)
O-P-C(3)	111.3(2)	F(43)-C(4)-F(41)	109.0(5)
N-P-C(3)	106.2(2)	F(43)-C(4)-F(42)	106.8(6)
O-P-C(1)	111.2(2)	F(41)-C(4)-F(42)	106.6(5)
N-P-C(1)	109.1(2)	F(43)-C(4)-C(3)	111.4(5)

C(3)-P-C(1)	101.9(2)	F(41)-C(4)-C(3)	112.8(5)
P-N-H(1)	114(5)	F(42)-C(4)-C(3)	109.9(4)
P-N-H(2)	112(5)		

Table I.6.3 Anisotropic displacement parameters (Å^2).

	U11	U22	U33	U23	U13	U12
P	14(1)	23(1)	36(1)	6(1)	7(1)	1(1)
O	12(1)	33(2)	52(2)	10(2)	9(1)	-1(1)
N	12(2)	34(2)	48(2)	15(2)	6(2)	1(2)
C(1)	49(3)	40(3)	38(3)	0(2)	11(2)	8(2)
F(11)	129(4)	56(2)	81(3)	-6(2)	75(3)	-24(2)
F(12)	110(4)	93(3)	49(2)	-19(2)	-25(2)	64(3)
C(2)	48(3)	41(3)	58(4)	-13(3)	15(3)	3(3)
F(21)	71(3)	73(3)	108(4)	-34(3)	-23(3)	44(2)
F(22)	93(3)	67(3)	58(2)	-21(2)	9(2)	21(2)
F(23)	110(4)	42(2)	115(4)	-20(2)	45(3)	-21(2)
C(3)	32(2)	23(2)	43(3)	7(2)	8(2)	0(2)
F(31)	114(3)	40(2)	57(2)	-3(2)	-33(2)	31(2)
F(32)	62(2)	30(2)	130(4)	8(2)	63(3)	-10(2)
C(4)	39(3)	33(3)	49(3)	-5(2)	5(2)	-1(2)
F(41)	72(2)	29(2)	81(3)	-5(2)	12(2)	6(2)
F(42)	64(3)	70(3)	150(5)	-52(3)	63(3)	-24(2)
F(43)	146(5)	74(3)	59(3)	-28(2)	-41(3)	47(3)

The anisotropic displacement factor exponent takes the form: $-2\pi^2[h^2a^{*2}U_{11}+ ..+2hka^*b^*U_{12}]$

Table I.6.4 Hydrogen coordinates and isotropic displacement parameters.

	x	y	z	U(eq)
H(1)	2700(130)	400(30)	10000(50)	65(15)
H(2)	4040(80)	1090(40)	9300(60)	65(15)

References

[1] **Bennett, F. W., Emeleus, H. J. and Haszeldine, R. N. (1954)**
Organometallic and organometalloidal fluorine compounds. Part X. Trifluoromethyl-phosphonous and phosphonic acids, J. Chem. Soc., 34, 339-364.

[2] **Hierse, W. and Ignatyev, N. (2009)**
Fluorosurfactants, Patent, WO 2009/0171214 A2.

[3] **Hübner, G. and Huth, A. (2008)**
Verwendung von ionischen flüssigkeiten als electrolyte zur herstellung von brennstoffzellmembranen und brennstoffzellmembran-elektroden-einheiten (MEA), Patent, DE 10 2008/54737 A1.

[4] **Emeleus, H. J., Haszeldine, R. N. and Paul, R. C. (1955)**
Organometallic and organometalloidal fluorine compounds. Part XII. Bistrifluoromethyl phosphinic acid and related phosphorus oxyacids, J. Chem. Soc., 563-574.

[5] **Paul, R. C. (1955)**
The preparation of trifluoromethylphosphine oxide, J. Chem. Soc., 574-575.

[6] **Emeleus, H. J. and Smith, J. D. (1959)**
The heptafluoropropyliodophosphines and their derivatives, J. Chem. Soc., 375-381.

[7] **Mahmood, T. and Shreeve, J. M. (1986)**
New perfluoralkylphosphonic and bis(perfluoroalkyl)phosphinic acids and their precursors, Inorg. Chem., 25, 3128-3131.

[8] **Kovaleva, T. V., Martynyukh, E. G. and Semenii, V. Ya. (1989)**
Perfluoroalkylphosphonic acids and their derivatives, Zh. Obsch. Khim., 59, 2245-2248.

[9] **Ignatyev, N., Weiden, M., Weltz Biermann, U., Heider, U., Sartori, P., Kucheryna, A. and Willner, H. (2003)**
Method for the production of monohydro-perfluoroalkanes, bis(perfluoroalkyl)phosphinates and perfluoroalkylphosphonates, Patent, WO 03/087111 A1.

[10] **Weltz-Biermann, U., Ignatyev, N., Weiden, M., Heider, U., Kucheryna, A., Willner, H. And Sartori, P. (2003)**
Method for the production of bis(perfluoralkyl)phosphinic acids and salts thereof, Patent, WO 03/087110 A1.

[11] **Ignatyev, N., Schmidt, M., Kuehner, A., Hilarius, V., Heider, U., Kucheryna, A., Sartori, P. and Willner H. (2004)**
Novel strong acids, process for the preparation thereof, and uses thereof, Patent, US 2004/0171879 A1.

[12] **Singh, R. P. and Shreeve, J. M. (2000)**
C_6, C_7 and C_8 perfluoroalkyl – substituted phosphinic acids, Inorg. Chem., 39, 1787-1789.

[13] **Ignatyev, N., Bejan, D. and Willner, H. (2010)**
Process for preparing bis(fluoroalkyl)phosphinic acid or fluoroalkylphosphonic acids, Patent, WO 2010/012359 A1.

[14] **Ignat’ev, N. and Sartori, P. (2000)**
Electrochemical fluorination of trialkylphosphines, J. Fluorine Chem., 103, 57-61.

[15] **Burg, A. B. and Slota, P. J. (1956)**
Manufacturing phosphinoborines, Patent, US 2,877,272.

[16] **Corbridge, D. E. C. (1990)**
Posphorus an autline of its chemistry, biochemistry and technology (Fourth Edition), Elvesier, Amsterdam-Oxford-New York-Tokyo.

[17] **Griffiths, J. E. (1968)**

Trifluoromethylphosphonylchloride, $CF_3P(O)Cl_2$: preparation, properties, ^{19}F nuclear magnetic resonance and infrared absorption spectra, Spectrochim. Acta, Part 24A, 303-310.

[18] **Yagupol'skii, L. M., Pavlenko, N. V., Ignat'ev, N. V., Matyushecheva, G. I. and Semenii, V. Ya. (1984)**
Arylbis(heptafluoropropyl)phosphine oxides. Electron nature of the bis(heptafluoropropyl) phosphine oxide group, Zh. Obsch. Khim., 54(2), 334-339.

[19] **Ignatiev , N., Weltz-Biermann, U., Heckmeier, M., Bissky, G. and Willner, H. (2008)**
Low-viscosity ionic liquids, Patent, US 2008/0194831 A_1.

[20] **Michaelis, A. (1876)**
Ueber die verbinungen der elemente der stickstoffgruppe mit den radicalen der aromatischen reihe, Justus Liebigs Ann. Chem., 181, 322.

[21] **Lindner, J., Wirth, W. and Zaunbauer, B. (1937)**
Über aromatische halogenphoshine und ihre eignung zur maßanalylischen wasswerbesrimmung, Monatsh. Chem., 70, 1-19.

[22] **Hart, R. M. and Whitehead, M. A. (1971)**
Chlorine nuclear quadrupole resonance of phosphorus-chlorine compounds, J. Chem. Soc., A, 1738-1741.

[23] **Ignatyev, N., Aust, E. F., Bejan, D. and Willner, H. (2010)**
Method for producting bis(fluoroalkyl)phosphinic acid chlorides or fluoralkyl phosphonic acid chlorides, Patent, WO 2010/009791 A_1.

[24] **Corbridge, D. E. C. (1974)**
The structural chemistry of posphorus, Elvesier, Amsterdam-London-New York.

[25] **Glowiak, T. and Sawka-Dobrowolska, W. (1977)**
The crystal and molecular structure of α-aminomethylmethylphosphinic acid, Acta. Cryst., B33, 1522-1525.

[26] **Koppel, I. A., Taft, R. W., Anvia, F., Zhu, S. Z., Hu, L. Q., Sung, K. S.,DesMarteau, D. D., Yagupolskii, L. M., Yagupolskii, Y. L., Ignatiev , N., Kondratenko, N. V., Volkonskii, A. Y. Vlasov, M. V., Notario, R. and Maria, P. C. (1994)**
The gas-phase acidities of very strong neutral BrØnsted acids, J. Am. Chem. Soc., 116, 3047-3057.

[27] **DesMarteau, D. D. (2000)**
Superacids – It's a lot about anions, Science, 289, 72-73.

[28] **DesMarteau, D. D., Zhu, S. Z., Pennington, W. T., Gotoh, Y., Witz, M. and Zuberi, S., Singh S. (1989)**
Superacids of nitrogen and carbon, J. Fluorine Chem., 45, 24.

[29] **Hu, L. Q. and DesMarteau, D. D. (1993)**
Synthesis of perhaloalkanesulfonyl halides and their sulfonimide derivatives, Inorg. Chem., 32, 5007-5010.

[30] **Zhang, J. and DesMarteau, D. D. (2001)**
Synthesis and comparison of N-fluorobis[(perfluoroalkyl)sulfonyl]imides with different perfluoroalkyl groups, J. Fluorine Chem.,111, 253-257.

[31] **Hao, X.; Yoshida, A. and Nishikido, J. (2005)**
$Hf[N(SO_2C_8F_{17})_2]_4$-catalyzed Friedel–Crafts acylation in a fluorous biphase system, Tetrahedron Lett., 46, 2697-2700.

[32] **Foropoulos, J. J. and DesMarteau, D. D. (1984)**
Synthesis, properties, and reactions of bis((trifluoromethyl)sulfonyl)imide, $(CF_3SO_2)_2NH$, Inorg. Chem., 23, 3720-3723.

[33] **Herstedt, M., Smirnov, M., Jahansson, P., Chami, M., Grondin, J., Servant, L. and Lasseques, J. C. (2005)**
Spectroscopic characterization of the conformational states of the bis(trifluoromethanesulfonyl) imide anion ($TFSI^-$), J. Raman Spectrosc., 36, 762-770.

[34] **Fujii, K., Fujimori, T., Takamuku, T., Kanzaki, R., Umebayashi, Y. and Ishiguro, S. I. (2006)**
Conformational echilibrium of bis(trifluoromethanesulfonyl)imide anion of a room temperature ionic liquid: Raman spectroscopic study and DFT calculations, J. Phys. Chem. B, 110, 8179-8183.

[35] **DesMarteau, D. D. (1995)**
Novel perfluorinated ionomers and ionenes, J. Fluorine Chem., 72, 203-208.

[36] **Geiculescu, O. E., Xie, Y., Rajagopal, R., Creager, S. E. and DesMarteau, D. D. (2004)**
Dilithium bis[(perfluoroalkyl)sulfonyl]diimide salts as electrolytes for rechargeable lithium batteries, J. Fluorine Chem., 125, 1179-1185.

[37] **Thomas, H. B., Shafer, G., Ma, J. J., Tu, M. H. and DesMarteau, D. D. (2004)**
Synthesis of 3,6-dioxa-Δ^7-4-trifluoromethyl perfluorooctyl trifluoromethyl sulfonimide: bis[(perfluoroalkyl)sulfonyl] superacid monomer and polymer, J. Fluorine Chem., 125, 1231-1240.

[38] **Dzyuba, S. V. and Bartsch, R. A. (2002)**
Influence of structural variations in 1-alkyl(aralkyl)-3-methylimidazolium hexafluorophosphates and bis(trifluoromethylsulfonyl)imides and physical properties of the ionic liquids, Chem. Phy. Chem., 3, 161-166.

[39] **Holbrey, J. D., Reichert , W. M. and Rogers, R. D. (2004)**
Crystal structures of imidazolium bis(trifluoromethanesulfonyl)imide 'ionic liquid' salts: the first organic salts with a cis-TFSI anion conformation, Dalton Trans., 2267-2271.

[40] **Kobayashi, H., Nie, J. and Sonoda, T. (1995)**
Metal bis((perfluoroalkyl)sulfonyl)amides as novel Lewis acid catalysts in Diels-Alder reaction, Chem. Lett., 307-308.

[41] **Xue, L.; Padgett, C. W., DesMarteau, D. D.; Pennington, W. T. (2002)**
Synthesis and structures of alkali metal salts of bis[(trifluoromethyl)sulfonyl]imide, Solid State Sciences, 4, 1535-1545.

[42] **Wabnitz, T. C. and Spencer, J. B. (2003)**
A general, Brønsted acid catalyzed hetero-Michael addition of nitrogen, oxygen, and sulfur nucleophiles, Org. Lett., 5, 2141-2144.

[43] **Kawamura, M., Cui, D. M. and Shimada, S. (2006)**
Fluorous biphase catalytic Friedel-Crafts acylation: Ytterbium tris(perfluoroalkanesulfonyl) methide catalysts, Synlett, 6, 847-849.

[44] **Rey, I., Johansson, P., Lindengren, J., Lasseques, J. C., Grondin, J. and Servant, L. (1998)**
Spectroscopic and theoretical study of $(CF_3SO_2)_2N^-$ ($TFSI^-$) and $(CF_3SO_2)_2NH$ (HTFSI), J. Phys. Chem. A, 102, 3249-3258.

[45] **Tu, M. H. and DesMarteau, D. D. (2005)**
NMR and IR studies of bis((perfluoroalkyl)sulfonyl)imides, Spectrochim. Acta Part A, 61, 1701-1705.

[46] **Garlyauskayte, R., Chernega, A. N., Michot, C., Armand, M., Yagupolskii, Y. L. and Yagupolskii, L. M. (2005)**
Synthesis of new organic super acids-N-(trifluoromethylsulfonyl)imino derivatives of trifluoromethanesulfonic acid and bis(trifluoromethylsufonyl)imide, Org. Biomol. Chem., 3, 2239-2243.

[47] **Pavlenko, N. V., Matyushecheva, G. I., Semenii, V. Y. and Yagupol'skii, L. M. (1985)**
Nitrogenous derivatives of bis(heptafluoropropyl)phosphinic acid, Zh. Obsch. Khim., 55, 1586-1590.

[48] **Bejan, D., Willner, H., Ignatiev, N., Lehmann, C. (2008)**
Synthesis and characterisation of bis[bis(pentafluoroethyl)phosphinyl]imides, $M^+N[(C_2F_5)_2P(O)]_2^-$ M = H, Na, K, Cs, Ag, Me_4N, Inorg. Chem. 47, 9085-9089.

[49] **Semenii, V. Ya., Stepanov, V. A., Ignat’ev, N. V., Furin, G. G. and Yagupolskii, L. M. (1985)**

Tris(perfluoroalkyl)difluorophosphoranes, Zh. Obsch. Khim., 55, 2716-2720.

[50] **Farcasiu D. and Ghenciu, A. (1991)**
Carbodications. 3. The two dications derived from mesityloxide, J. Org. Chem., 56, 6050-6052.

[51] **Juhasz, M., Hoffmann, S., Stoyanov, E., Kim, K. C. and Reed, C. A. (2004)**
The strongest isolable acid, Angew. Chem. Int. Ed., 116, 5466-5469.

[52] **Juhasz, M., A. (2005)**
Carborane anions in superacidity and the stabilization of reactive cations, PhD thesis, University of California, Riverside.

[53] **Keder, W. E. and Burger, L. L. (1965)**
Proton magnetic resonance and infrared studies of hydrogen bonding in tri-n-octylammonium salt solutions, J. Phys. Chem., 69, 3075-3080.

[54] **Reed, C. A. (2005)**
Carborane acids. New "strong yet gentle" acids for organic and inorganic chemistry, Chem. Commun., 1669-1677.

[55] **Stoyanov, E. S., Kim, K. C. and Reed, C. A. (2006)**
An infrared ν NH scale for weakly basic anions. Implications for single-molecule acidity and superacidity, J. Am. Chem. Soc., 128, 8500-8508.

[56] **Ignat’ev, N. V., Willner, H. and Sartori, P. (2009)**
Electrochemical fluorination (Simons process)-A powerful tool for the acid preparation of new conducting salts, ionic liquids and strong Brønsted acids, J. Fluorine Chem., 130, 1183-1191.

[57] **Kobayashi, S. (1998)**
New types of Lewis acids used in organic synthesis, Pure & Appl. Chem. 70, 1019-1026.

[58] **Marko, I. E. and Evans, G. R. (1994)**
Efficient lanthanide catalysis in the Diels-Alder cycloaddition of electron-deficient 2- pyrones, Synlett, 6, 431-433.

[59] **Kobayashi, S. Hachiya, I., Takakori, T., Akida M. and Ishitani, H. (1992)**
Lanthanide trifluoromethanesulfonates as reusable catalysts Michael and Diels-Alder reactions, Tetrahedron Lett., 33, 6815.

[60] **Kawamura, M., Cui, D. M., Hayashi, T. and Shimada, S. (2003)**
Lewis acid-catalyzed Friedel- Crafts acylation reaction using carboxylic acids as acylating agents, Tetrahedron Lett., 44, 7715-7717.

[61] **Kawada, A., Mitamura, S. And Kobayashi, S. (1993)**
Lanthanide trifluoromethanesulfonates as reusable catalysts: catalytic Friedel-Crafts acylation, J. Chem. Soc., Chem. Commun., 1157-1158.

[62] **Kobayashi, S. and Hachiya, I. (1994)**
Lanthanide triflates as water-tolerant Lewis acids. Activation of commercial formaldehyde solution and use in the aldol reaction of silyl enol ethers with aldehydes in aqueous media, J. Org. Chem., 59, 3590-3596.

[63] **Hagiwara, R. and Ito, Y. (2000)**
Room temperature ionic liquids of alkylimidazolium cations and fluoroanions, J. Fluorine Chem., 105, 221-227.

[64] **Ray, P. C. and Rakshit, J. N. (1911)**
Nitrites of the alkylammnoium bases: ethylammonium nitrite, dimethylammonium nitrite and trimethylammonium nitrite, J. Chem. Soc., 1470-1475.

[65] **Walden P. (1914)**
Molecular weights and electrical conductivity of several fused salts, Bull. Acad. Imper. Sci., 1800, 405-422.

[66] **Hurley, F. H. and Jr. Wier, T. P. (1951)**
The electrodeposition of aluminium from nonaqueous solutions at room temperature, J. Electrochem. Soc., 98 (5), 207-212.

[67] **Hurley, F. H. and Jr. Wier, T. P. (1951)**
Electrodeposition of metals from fused quaternary ammonium salts, J. Electrochem. Soc., 98 (5), 203-206.

[68] **Swain, C. G., Ohno, A., Roe, D. K., Brawn R. and Maugh T. (1967)**
Tetrahexylammonium benzoate, a liquid salts at 25 degree., a solvent for kinetics or electrochemistry, J. Am. Chem. Soc., 89 (11), 2648-2649.

[69] **Hussey, C. L. and Laher, T. M. (1981)**
Electrochemical and spectroscopic stydies of cobalt (II) in molten aluminium chloride-N-n-butylpyridinium chloride, Inorg. Chem., 20, 4201-4206.

[70] **Wilkes, J. S. and Zaworotko, M. J. (1992)**
Air and water stable 1-ethyl-3methylimidazolium based ionic liquids, J. Chem. Soc., Chem. Commun., 965-967.

[71] **Lindstom, P., Tierney, J., Wathey, B. and Wetman L. (2001)**
Microwave assisted organic synthesis, Tetrahedron, 57, 9225-9283.

[72] **Assikkala, J. (2008)**
Application of ionic liquids and microwave activation in selected organic reactions, PhD thesis, University of Oulu, Finland.

[73] **Wasserscheid, P and Welton, T. (2008)**
Ionic liquids in synthesis, Second Edition, WILEY-VCH, Weinheim.

[74] **Wasserscheid, P (2006)**
Volatile times for ionic liquids, Nature, 439, 797.

[75] **Earle, M. J., Esperanca, J. M. S. S., Gilea, M. A., Canongia Lopes, J. N., Rebelo, L. P. N., Magee, J. W., Seddon, K. R. and Wildegren, J. A. (2006)**
The distillation and volatility of ionic liquids, Nature, 439, 831-834.

[76] **Welton, T (1999)**
Room temperature ionic liquids. Solvents for synthesis and catalysis, Chemical Rewiews, 99 (8), 2071-2084.

[77] **Fisher, T., Sethi, A., Welton, T. and Woolf J. (1999)**
Diels-Alder reactions in room temperature ionic liquids, Tetrahedron Lett., 40(4), 793-796.

[78] **Surette, J. K. D., Green, L. and Singer, R. D. (1996)**
1-Ethyl-3-methylimidazolium halogenoaluminate melts as reaction media for the Friedel–Crafts acylation of ferrocene, Chem Commun, 2753-2754.

[79] **Earle, M. J., Seddon, K. R., Adams, C. J. and Roberts, G. (1998)**
Friedel–Crafts reactions in room temperature ionic liquids, Chem. Commun., 2097-2098.

[80] **Deng, Y., Shi, F., Beng, J. and Qiao, K. (2001)**
Ionic liquid as a green catalytic reaction medium for esterifications, J. Mol. Catal A: Chem., 165, 33-36.

[81] **Chauvin, Y., Mussmann, L. and Olivier, H. (1996)**
A novel class of versatile solvents for two-phase catalysis: hydrogenation, isomerization, and hydroformylation of alkenes catalyzed by rhodium complexes in liquid 1,3-dialkylimidazolium salts, Angew. Chem. Int. Ed. Engl., 34, 2698-2700.

[82] **Kaufmann, D. E., Nouroozian, M. and Henze, H. (1996)**
Molten salts as an efficient medium for palladium catalyzed C-C coupling reactions, Synlett, 1091-1092.

[83] **Carmichael, A. J., Earle, M. J., Holbrey, J. D., McCormac, P. B. and Seddon, K. R. (1999)**
The Heck reaction in ionic liquids: A multiphasic catalyst system, Org. Lett. 7(1), 997-1000.

[84] **Song, C. E. and Roh, E. J. (2000)**
Practical method to recycle a chiral (salen) Mn epoxidation catalyst by using an ionic liquid, Chem. Commun., 837-838.

[85] **Wasserscheid, P. and Keim, W. (2000)**
Ionic liquids-new "solutions" for transition metal catalysis, Angew. Chem. Int. Ed. Engl., 39**,** 3772-3789.

[86] **Sheldon, R. (2001)**
Catalytic reactions in ionic liquids, Chem. Commun., 2399-2407.

[87] **Cull, S. G., Holbrey, J. D., Vargas-Mora, V., Seddon, K. R. and Lye, G. J. (2000)**
Room temperature ionic liquids as replacements for organic solvents in multiphase bioprocess operations, Biotechnol. Bioeng., 69, 227-233.

[88] **Pfründer, H., Amidjojo, M., Kragl, U. and Weuster-Botz, D. (2004)**
Efficient whole-cell biotransformation in a biphasic ionic liquid/water system, Angew. Chem. Int. Ed. Engl., 43**,** 4529-4531.

[89] **Armstrong, D. W, He, L. and Liu, Y. S. (1999)**
Examination of ionic liquids and their interaction with molecules, when used as stationary phases in gas chromatography, Anal. Chem., 71, 3873-3876.

[90] **Anderson, K. L. and Armstrong, D. W. (2003)**
High stability ionic liquids. A new class of stationary phases for gas chromatography, Anal. Chem., 75, 4851-4858.

[91] **Zhang, W., He, L., Gu, Y., Liu, X. and Jiang, S. (2003)**
Effect of ionic liquids as mobile phase additives on retation of catecholamines in revered-phase high-performance liquid chromatography, Anal. Lett., 36 (4), 827-838.

[92] **Mihkel, K. (2009)**
Ionic liquids in chemical analysis, CRC Press, Boca Raton, London, NewYork.

[93] **Yahnes, E. G, Gratz, S. R., Balwin, M. J., Robison, S. E. and Stalcup, A. M. (2001)**
Capillary electrophoretic application of 1-alkyl-3-methylimidazolium-based ionic liquids, Anal. Chem., 73, 3838-3844.

[94] www.aldrich.com

[95] **Zhao, D., Fei, Z., Geldbach, T. J., Scopelliti, R., Laurenczy, G. and Dyson, P. J. (2005**)
Allyl-functionalised ionic liquids: synthesis, characterization, and reactivity, Helv. Chim. Acta, 88, 665-675.

[96] **Schottenberger, H., Wurst, K., Horvath, U. E. I., Cronje, S., Lukasser, J., Polin, J., McKenzie, J. M. and Raubenheimer, G. (2003)**
Synthesis and characterization of organometallic imidazolium compounds that include a new organometallic ionic liquid, Dalton Trans., 22, 4275-4281.

[97] **Fei, Z, Zhao, D, Scopelliti, R and Dyson, P. J. (2004)**
Organometallic complexes derived from alkyne-functionalized imidazolium salts, Organometallics, 23, 1622-1628.

[98] **Zhao, D. (2006)**
Design, synthesis and applications of functionalized ionic liquids**,** PhD thesis, University of Lausanne, Switzerland

[99] **Fox, D. M., Gilman, J. W., De Long, H. C. and Trulove, P. C. (2005)**
TGA decomposition kinetics of butyl-2,3-dimethylimidazolium tetrafluoroborate and the thermal effects of contaminants, J. Chem. Thermodinamics, 37, 900-905.

[100] **Carpio, R., King, L., Lindstrom, R., Nardi, J. and Hussey, C. (1979)**.
Density, electric conductivity and viscosity of several N-alkylpyridinium halides and their mixtures with aluminum chloride, J. Electrochem. Soc., 126, 1644-1649.

[101] **Zhou, Z. B., Matsumoto, H. and Tatsumi, K. (2005**)
Low-melting, low-viscous, hydrophobic ionic liquids: aliphatic quaternary ammonium salts with perfluoroalkyltrifluoroborates, Chem. Eur. J., 11, 752-766.

[102] **Vega, J. A., Zhou, J. and Kohl, P. A. (2009)**

Electrochemical composition and deposition of litium and potasium from phosphonium- and ammonium –TFSI ionic liquids, J. Electrochem. Soc., 156 (4), A253-A259.

[103] **Weng, J., Wang, C, Li, H. and Wang, Y. (2006)**
Novel quaternary ammonium ionic liquids and their use as dual solvent-catalysts in the hydrolytic reaction, Green Chem., 8, 96-99.

[104] **Kulkarni, P. S., Branco, L. C., Crespo, J. G., Nunes, M. C., Raymundo, A. and Afonso, C. A. M. (2007)**
Comparison of physicochemical properties of new ionic liquids based on imidazolium, quaternary ammonium, and guanidinium cations, Chem. Eur. J., 13, 8478-8488.

[105] **Zhou, Q., Henderson, W. A., Appetecchi, G. B., Montanino, M. and Passerini, S. (2008**)
Physical and electrochemical properties of N-alkyl-N-methylpyrrolidinium bis(fluorosulfonyl) imide, ionic liquid: $PY_{13}FSI$ and $PY_{14}FSI$, J. Phys. Chem., 112, 13577-13580.

[106] **Baker, G. A., Pandey, S., Pandey, S. and Baker S. N. (2004)**
A new class of cationic surfactants inspired by N-alkyl-N-methyl pyrrolidinium ionic liquids, Analyst, 129, 890-892.

[107] **Burrell, A. K., DelSesto, R. E., Baker, S. N., McCleskey, M. and Baker, G. A. (2007)**
The large scale synthesis of pure imidazolium and pyrrolidinium ionic liquids, Green Chem., 9, 449-454.

[108] **Holbrey, J. D., Turner, M. B., Reichert, W. M. and Rogers, R. D. (2003)**
New ionic liquids containing an appended hydroxyl fuctionality from the atom-efficient, one-pot reaction of 1-metylimidazole and acid with propylene oxide, Green Chem., 5, 731-736.

[109] **Lee, J. S., Quan, N. D., Hwang, J. M., Bae, J. Y., Kim H., Chao, B. W., Kim, H. S. and Lee H. (2006)**
Ionic liquids containing an ester group as potential electrolytes, Electrochem. Commun., 8, 460-464.

[110] **Ramnial,T., Ingo, D. D. and Clyburne, J. A. C. (2005)**
Phosphonium ionic liquids as reaction media for strong bases, Chem. Commun., 325-327.

[111] **McNulty, J., Nair, J. J., Cheekoori, S., Larichev, V., Capretta, A. and Robertson, Al. J. (2006)**
Scope and mechanistic insight into the use of tetradecyl(trihexyl)phosphonium bistriflimide: a remarkably selective ionic liquid solvent for substitution reactions, Chem. Eur. J., 12, 9314-9322.

[112] **Bradaric, C. J., Downard, A., Kennedy, C. and Zhou, Y. (2003)**
Industrial preparation of phosphonium ionic liquids, Green Chem. 5, 143-152.

[113] **www. Iolitec.de (2006),** Ionic liquids today, Issue 3-06.

[114] **Dwan, J., Durant, D. and Ghandi, K. (2008)**
Nuclear magnetic resonance spectroscopic studies of the trihexyl(tetradecyl)phosphonium chloride ionic liquid mixtures with water, Cent. Eur. J. Chem., 6 (3), 347-358.

[115] **McNulty, J., Capretta, A., Wilson, J., Dyck, J., Abjabeng, G. and Robertson, A. J. (2002)**
Suzuki cross-coupling reactions of aryl halides in phosphonium salt ionic liquid under mild conditions, Chem. Commun., 17, 1986-1987.

[116] **Gerritsma, D. A., Robertson, A. J., McNulty, J. and Capretta, A. (2004)**
Heck reactions of aryl halides in phosphonium salt ionic liquids: library screening and applications, Tetrahedron Lett., 45, 7629-7631.

[117] **Kim, Y. J. and Varma, R. S (2005)**
Tetrahaloindate(III)-based ionic liquids in the coupling reaction of carbon dioxide and epoxides to generate cyclic carbonates: H-bonding and mechanistic studies, J. Org. Chem., 70, 7882-7891.

[118] **Suarez, P. A. S., Dullius, J. E. L., Einloft, S, C. A., De Souza, R. F and Dupont, J. (1996)**
The use of new ionic liquids in two phase catalytic hydrogenation reaction by rhodium complexes, Polyhedron, 15 (7), 1217-1219.

[119] **Dyson, P. J., Ellis, D. J., Parker, D. G. and Welton, T. (1999)**
Arene hydrogenation in a room temperature ionic liquids using a ruthenium cluster catalyst, Chem. Commun., 25-26.

[120] **Koenig, A., Stepanski, M., Kuszlik, A., Keil, P. and Weller, C (2008)**
Ultra-purification of ionic liquids by melt crystallization, Chem. Eng. Res. Des., 86 (7), 775-780.

[121] **Seddon, K. R., Stark, A. and Torres, M. J. (2000)**
Influence of chloride, water, and organic solvents on the physical properties of ionic liquids, Pure Appl. Chem., 72 (12), 2275-2287.

[122] **Rivera - Rubero, S. and Baldelli, S. (2004)**
Influence of water on the surface of hydrophilic and hydrophobic room temperature ionic liquids, J. Am. Chem. Soc., 126, 11788-11789.

[123] **Holbrey, J. D., and Seddon, K. R. (1999)**
Ionic liquids, J. Chem. Soc., Dalton Trans., 2133-2139.

[124] **Fuller, J., Carlin, R. T. and Osteryoung, R. A. (1997)**
The room temperature ionic liquid 1-ethyl-3-methylimidazolium tetrafluoroborate: electrochemical couples and physical properties, J. Electrochem. Soc., 144 (11), 3881-3886.

[125] **McEwen, A. B., Ngo, H. L., LeCompte, K. and Goldman, J. L. (1999)**
Electrochemical properties of imidazolium salt electrolytes for chemical capacitor applications, J. Electrochem. Soc., 146 (5), 1687-1695.

[126] **Noda, A. and Watanabe, M. (2000)**
Highly conductive polymer electrolytes prepared by in situ polymerization of vinyl monomers in room temperature molten salts, Electrochimica Acta, 45, 1265-1270.

[127] **Fredlake, P. C., Crosthwaite, J. M., Hert, D. G., Aki, S. N. V. K. and Brennecke, J. F. (2004)**
Thermophysical properties of imidazolium based ionic liquids, J. Chem. Eng. Data, 49, 954-964.

[128] **Ngo, L. H., LeCompte, K., Hargens, L. and McEwen, A. B. (2000)**
Thermal properties of imidazolium ionic liquids, Thermochimica Acta, 357-358, 97-102.

[129] **Lin, S. T., Ding, M. F., Chang, C. W. and Lue, S. S. (2004)**
Nuclear magnetic resonance spectroscopic study on ionic liquids of 1-alkyl-3-methylimidazolium salts, Tetrahedron, 60, 9441-9446.

[130] **Giernoth, R., Bankmann, D. and Schlorer, N. (2005)**
High performance NMR in ionic liquids, Green Chem., 7, 279-282.

[131] **Armstrong, D. W, Zhang, L. K., He, L. and Gross, M. L. (2001)**
Ionic liquids as matrixes for matrix-assisted laser desorption/ionization mass spectrometry, Anal. Chem., 73, 3679-3686.

[132] **Wasserscheid, P, Van Hal, R. and Bosmann, A. (2002)**
1-n-butyl-3-methylimidazolium([bmim])octylsulfate-an even “greener” ionic liquid, Green Chem., 4, 400-404.

[133] **Villagran, C, Deetlefs, M., Pitner, W. R. and Hardacre, C. (2004)**
Quantification of halide in ionic liquids using ion chromatography, Anal. Chem., 76, 2118-2123.

[134] **Villagran, C, Banks, C. E., Hardacre, C and Compton, R. G. (2004)**
Electroanalytical determination of trace chloride in room-temperature ionic liquids, Anal. Chem., 76, 1998-2003.

[135] **Cammarata, L., Kazarian, S. G, Salter, P. A. and Welton, T. (2001)**
Molecular states of water in room temperature ionic liquids, Phys. Chem. Chem. Phys., 3, 5192-5200.

[136] **Berg, R. W., Deetlefs, M., Seddon, K. R., Shim, I. and Thompson, J. M. (2005)**
Raman and ab initio studies of simple and binary 1-alkyl-3-methylimidazolium ionic liquids, J. Phys. Chem. B, 109, 19018-19025.

[137] **Ignatiev, N. V., Kucheryna, A., Bissky, G. and Willner, H. (2007)**

How to make ionic liquids more liquid, J. F. Brennecke, R. D. Rodgers and K. R. Seddon (Ed.), Ionic liquids IV, ACS Symposium Series 975, Washington DC, 320-334.

[138] **Ignat'ev, N. V., Weltz Biermann, Kucheryna, A., Bissky, G. and Willner, H. (2005)**
New ionic liquids with tris(perfluoroalkyl)trifluorophosphate (FAP) anions, J. Fluorine Chem., 126, 1150-1159.

[139] **Bejan, D., Ignat'ev, N. and Willner, H. (2010)**
New ionic liquids with the bis[bis(pentafluoroethyl)phosphinyl]imide anion, $[(C_2F_5)_2P(O)]_2N^-$ - Synthesis and characterization, J. Fluorine Chem., 131, 325-332.

[140] **Slattery, J. M., Daguenet, C., Dyson, P. J., Schubert, T. J. S. and Krossing, I. (2007)**
How to predict the physical properties of ionic liquids: A volume based approach, Angew. Chem. Int. Ed., 46, 5384-5388.

[141] **Jenkins, H. D. B., Roobottom, H. K., Passmore, J. and Glasser, L. (1999)**
Relationships among ionic lattice energies, molecular (formula unit) volumes, and thermochemical radii, Inorg. Chem., 38 ,3609-3620.

[142] **Palomar, J., Ferro, V. R., Torrecilla, J. S. and Rodriguez, F. (2007)**
Density and molar volume prediction usong COSMO-RS for ionic liquids. An approach to solvent design, Ind. Eng. Chem. Res. 46 (2007) 6041-6048.

[143] **Weingärtner, H. (2008)**
Understanding ionic liquids at the molecular level: facts, problems, and controversies, Angew. Chem. Int. Ed., 47, 654-670.

[144] **Kochin, D. A., Vashkov, V. I., Kiryutkin, G. V. and Svel'eva, A. R. (1964)**
Oxygen-containing organotin and organolead. V. Preparation and bactericidal activity of tin and lead organic derivatives and their mixtures with quaternary ammonium salts, Zh. Obsch. Khim., 34 (12), 4027-4029.

[145] **Sakizadeh, K., Olson, L. P., Cowdery-Corvan, P. J., Ishida, T. and Whitcomb, D. R. (2007)**
Termographic materials containing ioni liquids, Patent, US 7163786 B1

[146] **Corley, C. A. (2004)**
Proceedings-Electrochemical Society, Molten salts XIV, Proceedings, 24, 326-339.

[147] **Lapidus, A., Elissev, O., Bondarenko, T. and Stepin, N. (2006)**
Palladium catalysed hydroxycarbonylation of 1-phenylethanol in molten salt media, J. Mol. Catal. A: Chem., 252, 245-251.

[148] **Tolstikova, L. L. and Shainyan, B. A. (2006)**
Ionic liquids on the basis of 2,3,4,6,7,8,9,10-octahydropyrimido-[1,2-a]azepine(1,8-diazabicyclo [5.4.0]undec-7-ene), Zh. Obsch. Khim., 42, 1085-1091.

[149] **Vu, P. D., Boydston, A. J. And Bielawski, C. W. (2007)**
Ionic liquids via efficient, solvent-free anion metathesis, Green Chem., 9, 1158-1159.

[150] **Noda, A., Hayamizu, K. and Watanabe, M. (2001)**
Pulsed-gradient spin-echo H and F NMR ionic diffusion coefficient, viscosity, and ionic conductivity of non-chloroaluminate room-temperature ionic liquids, J. Phys. Chem. B, 105 (20), 4603-4610.

[151] **Muhammad, A., Abdul Mutalib, M. I., Wilfred, C. D., Murugesan, T. and Shafeeq, A. (2008)**
Thermophysical properties of 1-hexyl-3-methyl imidazolium based ionic liquids with tetrafluoroborat, hexafluorophosphate and bis(trifluorosulfonyl)imide, J. Chem. Therm., 40, 1433-1438.

[152] **Nishida, T., Tashiro, Y. and Yamamoto, M. (2003)**
Physical and electrochemical properties of 1-alkyl-3-methylimidazolium tetrafluoroborate for electrolyte, J. Fluorine Chem., 120, 135-141.

[153] **Ue, M., Ida, K. and Mori, S. (1994)**
Electrochemical properties of organic liquid electrolytes based on quaternary onium salts for electrochemical double-layer capacitors, J. Electrochem. Soc., 141, 2989-2996.

[154] **Matsumoto, H., Yanagida, M., Tanimoto, K., Nomura, M., Kitagawa, Y. and Miyazaki, Y. (2000)**
Highly conductive room temperature molten salts based on small trimethylalkylammonium cations and bis(trifluorometylsulfonyl)imide, Chem. Letters, 922-923.

[155] **Sheldrik, G. M. (1997)**
SHELX-97 Program package (SHELXS-97 - Program for crystal structure solution and SHELXL-97 - Program for crystal structure refinement) (Release 97-2); University of Göttingen**.**

[156] **Frisch, M. J et al. (2003)**
Gaussian 03W, Version 6.0, Rev. B04**.**

[157] **Cupertino, D., Birdsall, D. J., Slawin, A. M. Z. and Woollins, J. D. (1999)**
The preparation and coordination chemistry of ^{i}PrP(E)NHP(E$'$)^{i}Pr$_2$ (E, E$'$ = Se; E = Se, E$'$ = S; E = S, E$'$ = O; E, E$'$ =O), Inorg. Chim Acta, 290, 1-7.

[158] **Cruickshank, D. W. J. (1956)**
Errors in bond due to rotational oscillations of molecules, Acta Cryst., A, 9, 757-758.

[159] **Golding, J., Hamid, N., MacFarlane, D. R., Forsyth, M., Forsyth, C., Collins, C. and Huang, J. (2001)**
N-methyl-N-alkylpyrrolidinium hexafluorophosphate salts: novel molten salts and plastic crystal phases, Chem. Mater**.**, 13, 558-564.

[160] **Matsumoto, H., Kageyama, H. and Miyazaki, Y. (2002)**
Room temperature ionic liquids based on small aliphatic ammonium cations and asymmetric amide anions, Chem. Commun., 1726-1727.

[161] **Matsumoto, H., Teresawa, N., Umecky, T., Tsuzuki, S., Sakaebe, H., Asaka, K. and Tatsumi, K. (2008)**
Low melting and electrochemically stable ionic liquids based on asymmetric fluorosulfonyl(trifluoromethylsulfonyl)amide, Chem. Letters, 37, 1020-1021.

[162] **Ignatyev, N., Bejan, D. and Willner, H. (2010)**
Preparation of ionic liquids with an asymmetrical [bis(pentafluoroethyl)phosphinyl–(trifluoromethyl)sulfonyl]imide anion – [{(C_2F_5)$_2$P(O)}N{S(O)$_2$CF$_3$}] (PSI), Inventing report to Merck GmbH, Darmstadt, Germany.

[163] **Zhang, S., Sun, N., He, X., Lu, X. and Zhang, X. (2006)**
Physical properties of ionic liquids: database and evaluation, J. Phys. Chem. Ref. Data, 35, 1475-1517.

[164] **www.merck.de**

[165] **Pringle, J. M., Golding, J., Baranyai, K., Forsyth, C. M., Deacon, G. B., Scott, J. L. and MacFarlane, D. R. (2003)**
The effect of anion fluorination in ionic liquids-physical properties of a range of bis(methanesulfonyl)amide salts, New J. Chem., 27, 1504-1510.

[166] **Tokuda, H., Ishii, K., Hasan Susan, Md. A. B., Tsuzuki, S., Hayamizu, K. and Watanabe, M. (2006)**
Physicochemical properties and structures of room-temperature ionic liquids. 3. Variation of cationic structures, J. Phys. Chem. B., 110, 2833-2839.

[167] **Haas, A.; Klare, C.; Betz, P., Bruckmann, J., Kruger, C., Tsay, Y. H. and Aubke, F. (1996)**
Acyclic Sulfur-Nitrogen compounds. Synthesis and crystal and molecular structures of bis(trifluoromethyl)sulfonyl)amine ((CF_3SO_2)$_2$NH), Magnezium hexaaquo bis((trifluoromethyl)sulfonyl)amine dihydrate ([Mg(H_2O)$_6$][(CF_3SO_2)$_2$N]$_2$ ·2H_2O and bis(bis(trifluorosulfonyl)amino)sulfur ((FSO_2)$_2$NSN(SO_2F)$_2$), Inorg. Chem., 35, 1918-1925.

[168] **Greene, T. W. and Wuts, P. G. M. (1999)**
Protective groups in organic synthesis, John Wiley & Sons, New York.

[169] **Ignatyev, N., Bejan, D. and Willner, H. (2010)**
Bis[bis(pentafluoroethyl)phosphinyl] imide acid (HFPI) – an efficient catalyst for acylation reactions, Inventing report to Merck GmbH, Darmstadt, Germany.

[170] **Ishihara, K., Kubota, M., Kurihara, H. And Yamamoto, H. (1995)**
Scandium trifluromethanesulfate as an extremely active acylation catalyst, J. Am. Chem. Soc, 117, 4413-4414.

[171] **Dalpozzo, R., De Nino, A., Maiuolo, L., Procopio, A., Nardi, M., Bartoli, G. and Romeo, R. (2003)**
Highly efficient and versatile acetylation of alcohols catalyzed by cerium (III) triflate, Tetrahedron Lett., 44, 5621-5624.

[172] **Vedejs, E. and Daugulis, O. (1996)**
Dual activation in the esterification of hindered alcohols with anhydrides using $MgBr_2$ and a tertiary amine, J. Org. Chem., 61, 5702-5703

[173] **Chandrasekhar, S., Ramachander, T. and Takhi, M. (1998)**
Acylation of alcohols with acetic anhydride catalyzed by $TaCl_5$: some implications in kinetic resolution, Tetrahedron Lett., 39, 3263-3266.

[174] **Procopiou, P. A., Simon, S. P. D., Flack, S. S. and Inglis, G. G. A. (1998)**
An extremely powerful acylation reaction of alcohols with acid anhydrides catalyzed by trimethylsilyl trifluoromethanesulfonate, J. Org. Chem., 63, 2342-2347.

[175] **Saravanan, P. and Singh, V. K. (1999)**
An efficient method for acylation reactions, Tetrahedron Lett., 40, 2611-2614.

[176] **Chauhan, K. K., Forst, G. C., Love, I. and Waite, D. (1999)**
Indium triflate: an efficient catalyst for acylation reactions, Synlett, 11, 1743-1744

[177] **Kamal, A., Naseer, K. M. A., Reddy, K. S., Srikanth, Y. V. V. and Krishnaji, T. (2007)**
$Al(OTf)_3$ as a highly efficient catalyst for the rapid acetylation of alcohols, phenols, and thiophenols under solvent-free conditions, Tetrahedron Lett., 22, 3813-3818.

[178] **Carrigan, M. D., Eash, K. J., Oswald, M. C. and Mohan, R. S. (2001)**
An efficient method for the chemoselective synthesis of acylals from aromatic aldehydes using bismuth triflate, Tetrahedron Lett., 42, 8133-8135.

[179] **Alleti, R., Su Oh, W., Perambuduru, M., Afrasiabi, Z., Sinn, E. and Reddy V. P. (2005)**
Gadolinium triflate immobilized in imidazolium based ionic liquids: a recyclable catalyst and green solvent for acetylation of alcohols and amines, Green Chem., 7, 203-206.

[180] **Chakraborti, A. K. and Shivani (2006)**
Magnezium bistrifluoromethanesulfonimide as a new and efficient acylation catalyst, J. Org. Chem., 71, 5785-5788.

[181] **Prasad, H. S., Srinivasa, G. R. and Channe Gowda, D. (2005)**
Convenient, cost-effective, and mild method for the N-acetylation of anilines and secondary amines, Synthetic Commun., 35, 1189-1195.

[182] **Jin T. S., Zhao, Y., Liu, L. B., Chen. Z. and Li T. S. (2006)**
Rapid and efficient method for acetylation of alcohols and phenols with acetic anhydride catalyzed by silica sulphate, Synthetic Commun., 36, 1221-1227.

[183] **Hajipour, A. R. and Mazloumi, Gh. (2002)**
An efficient and simple procedure for preparation of esters and anhydrides from acid chlorides in the presence of 1,4-diazabicyclo[2.2.2]octane (DABCO) under solvent-free conditions, Synthetic Commun., 32, 23-30.

[184] **Kita, Y., Akai, S., Ajimura, N., Yoshigi, M., Tsugoshi, T., Yasuda, H. and Tamura, Y. (1986)**
Facile and efficient syntheses of carboxylic anhydrides and amides using (trimethylsilyl)ethoxyacetylene, J. Org. Chem., 51, 4150-4158.

[185] **Khan, A. T., Islam, S., Majee, A., Chattopadhyay, T. and Ghosh, S. (2005)**
Bromodimethylsulfonium bromide: A useful reagent for acylation of alcohols, phenols, amides, thiols, thiophenols and 1,1-diacylation of aldehydes under solvent fre conditions, J. Mol. Catal A: Chem., 239, 158-165.

[186] **Dlugosz, D., Pach, M., Zabrzenska, A., Zegar, M., Olksyn, B. J., Tluscik, J. K. and Ostrowska, K. (2008)**
Synthesis and reactivity of bis(cyclamidinium-2-yl)alkane bromide tribromides, brominating agents and tectons for molecular engineering, Monatsh. Chem., 139, 543-548.

[187] **Tarbell, D. S. and Herz, A. H. (1953)**
An attempted Fries reaction with thiolesters. The formation of trithioörthoesters, J. Am. Chem. Soc., 75, 1668-1672.

[188] **Ignatyev, N., Bejan, D., Dinoiu, V. and Willner, H. (2010)**
New bis(perfluoroalkyl)phosphinyl hydrazides, Patent Application Merck GmbH, Darmstadt, Germany.

[189] **Cavell, R. G., Charlton, T. L. and Sim W. (1971)**
Preparation and spectroscopic properties of methylamino derivatives of some difluoro- and bis(trifluoromethyl)phosphorus compounds, J. Am. Chem. Soc., 93, 1130-1131.

[190] **Burg, A. B. and Sarkis A. J. (1965)**
The quantitative synthesis and dimethylamine reaction of tris(trifluoromethyl)phosphine oxide, J. Am. Chem. Soc., 87, 238-241.

[191] **Mahmood, T., Bao, J. M., Kirchmeier, R. L. and Shreeve J. M. (1988)**
Comparative study of tris(trifluoromethyl)phosphine oxide, tris(nonafluorobutyl)phosphine oxide, and fluorobis(nonafluorobutyl)phosphine oxide with ammonia and amines, Inorg. Chem., 27, 2913-2916.

[192] **Teylor, E. C. and Wipf, P. (2004)**
The chemistry of heterocyclic compounds, John Wiley & Sons, Jersey.

[193] **Bock, H. and Baltin, E. (1965)**
Azo compounds. VI. Effect of substituents on phenylazophosphoric acid derivatives, Eberhard Chemische Berichte, 98, 2844-2854.

[194] **Steininger, E.(1966)**
Phosphinic acid hydrazides, Monatshefte fuer Chemie, 97, 383-390.

[195] **Negareche, M., Badrudin, Y., Berchadsky, Y., Friedmann, A. and Tordo P. (1986)**
Phosphinylhydrazyls $R_2NNP(0)L_2$, an ESR study. Influence of the captodative effect on the three-electron NN π Bond, J. Org. Chem., 51, 342-346

[196] **Nielsen, R. P. and Sisler, H. H. (1963)**
Hydrazinophosphorus compounds. I. Preparation of some substituted hydrazinophosphines, hydrazinophosphine oxides, and hydrazinophosphine sulfides, Inorg. Chem., 2 (4), 753-760.

[197] **Bullen, G. J., Stephenes, F. S. and Wade, R. J. (1969)**
Crystal structure of phosphoric triamide, J. Chem. Soc., A, 1804-1812.

[198] **Olie, K. (1971)**
Crystal structure of $POCl_3$, Acta Cryst., B27, 1459-1460.

List of scientific contributions:

Per-review articles:

1. **New ionic liquids with the bis[bis(pentafluoroethyl)phosphinyl]imide anion, $[(C_2F_5)_2P(O)]_2N^-$ – Synthesis and characterization**
   Bejan Dana, Ignat'ev Nikolai, Willner Helge.
   J. Fluorine Chem., **2010**, *131(3)*, 325–332.

2. **Synthesis and characterization of bis[bis(pentafluoroethyl)phosphinyl] imides, $M^+ N[(C_2F_5)_2P(O)]_2^-$, M = H, Na, K, Cs, Ag, Me_4N**
   Bejan Dana, Willner Helge, Ignatiev Nikolai, Lehmann Christian
   Inorg. Chem., **2008**, *47*, 9085–9089.

3. **Synthesis and physico-chemical characterization of some 4-styryl-coumarin derivatives**
   Nicolaescu Tatiana, Simion Catinca, Barabula Dana, Dorohoi Dana, Gradinaru Robert, *Annals of Univ. "Al. I. Cuza" Iasi,* **1998**, *6*, 23–28.

Patents:

1. **Process for preparing bis(fluoroalkyl)phosphinic acid or fluoroalkyl phosphonic acids**
   Ignatyev Nikolai, Bejan Dana and Willner Helge
   Patent, WO 2010/012359 A1, **2010**

2. **Method for producting bis(fluoroalkyl)phosphinic acid chlorides or fluoralkylphosphonic acid chlorides**
   Ignatyev Nikolai, Aust Emil Ferdinand, Bejan Dana and Willner Helge
   Patent, WO 2010/009791 A_1, **2010**

3. **New bis(perfluoroalkyl)phosphinyl hydrazides**
   Ignatyev Nikolai, Bejan Dana, Dinoiu Vasile and Willner Helge
   Patent Application Merck GmbH, Darmstadt, Germany, **2010**

4. **Preparation of ionic liquids with an asymmetrical [bis(pentafluoroethyl)phosphinyl–(trifluoromethyl)sulfonyl]imide anion – $[\{(C_2F_5)_2P(O)\}N\{S(O)_2CF_3\}]$ (PSI)**
   Ignatyev Nikolai, Bejan Dana and Willner Helge
   Inventing report to Merck GmbH, Darmstadt, Germany

5. **Bis[bis(pentafluoroethyl)phosphinyl] imide acid (HFPI) – an efficient catalyst for acylation reactions**
   Ignatyev Nikolai, Bejan Dana and Willner Helge
   Inventing report to Merck GmbH, Darmstadt, Germany

Posters and oral contributions:

1. **New perfluoroalkylphosphoric acids: synthesis, properties and perfluoroalkylphosphonic acids and their applications in catalysis (talk)**
   Ignat'ev Nikolai, Bejan Dana, Willner Helge,
   20th Winter Fluorine Conference, 9–14 January, 2011, St. Pete, Florida

2. **Convenient synthesis of bis(perfluoroalkyl)phosphinic and perfluoroalkylphosphonic acids and their applications in catalysis**
   Bejan Dana, Willner Helge, Ignat'ev Nikolai
   16th European Symposium on Fluorine Chemistry, 18–23 July, **2010**, Ljublijana, Slovenia

3. **Ionic liquids with the bis[(bis(pentafluoroethyl)phosphinyl]imido anion $[(C_2F_5)_2P(O)]_2N^-$ – Synthesis and characterization**
   Bejan Dana, Hübner Jane, Willner Helge, Ignatyev Nikolai V.
   11th JCF – Frühjarssymposium, 11–14 March, Essen, **2009,** Germany

4. **Ionic liquids with the bis[(bis(pentafluoroethyl)phosphinyl]imido anion $[(C_2F_5)_2P(O)]_2N^-$ – Synthesis and characterization**
   Bejan Dana, Hübner Jane, Willner Helge, Ignatyev Nikolai V.
   19th International Symposium on Fluorine Chemistry, 23–28 August, **2009**, Jackson Hole, Wyoming, USA

5. **New low viscosity ionic liquids: synthesis, properties and applications** (talk)
   Ignatyev Nikolai, Pitner William R., Schulte Michael, Schmidt Michael,
   Kirsch Peer, Aust Emil, Bejan Dana, Wenda André, Willner Helge
   19th International Symposium on Fluorine Chemistry, 23–28 August**, 2009**, Jackson Hole, Wyoming, USA

6. **Synthesis and characterisation of some ionic liquids with the bis[bis(pentafluoroethyl)phosphinyl]imido-anion: $[(C_2F_5)_2P(O)]_2N^-$**
   Bejan Dana, Willner Helge, Ignatiev Nikolai
   *10th Young Scientists Conference on Chemistry, 27-*29 March, **2008**, Rostock, Germany

7. **Synthesis and characterisation of some salts with the bis[bis(pentafluoroethyl)phosphinyl]imido-anion: $[(C_2F_5)_2P(O)]_2N^-$** (talk)
   Bejan Dana, Ignatiev Nikolai, Willner Helge
   *13. Deutscher Fluortag and 7th Regular German-Russian-Ukrainian Symposium on Fluorine Chemistry, 29 September–*2 Octombrie, **2008**, Schmitten, Germany

8. **Synthesis and characterisation of some salts with the bis[bis(pentafluoroethyl)phosphinyl]imido-anion: $[(C_2F_5)_2P(O)]_2N^-$** (talk)
   Bejan Dana, Willner Helge, Ignatiev Nikolai

1th Merck - Doktoranden/ PostDoc - Seminar Ionic Liquids, 2–3 September, **2008**, Darmstadt , Germany

9. **Synthesis and properties of $[(C_2F_5)_2P(O)]_2N^-$ salts** (talk)
   Bejan Dana, Ignatiev Nikolai, Willner Helge
   Frühjahrs Kolloquium, 17 May, **2007**, University of Wuppertal, Germany

10. **Synthesis and properties of bis[bis(pentafluoroethyl)phosphinyl]imido, $[(C_2F_5)_2P(O)]_2N^-$, salts**
    Bejan Dana, Willner Helge, Ignat'ev Nikolai
    15th European Symposium on Fluorine Chemistry, 15–20 July, **2007**, Prague, Czech Republic

Hiermit erkläre ich, dass ich die eingereichte Arbeit selbstständing verfasst habe und nur die angegebenen Hilfsmittel benutzt wurden. Desweiteren erkläre ich, dass die Disseration noch keinem andeeren Fachbereich einer wissenschaftlichen Hochschule vorgelegen hat.

....
(Dana Bejan)